Tailor Made Mixed-Metal Reagents for Metalation/C-C Bond Forming processes

Inaugural dissertation
of the Faculty of Science,
University of Bern

presented by

Pasquale Mastropierro

from Molfetta, Italy

Supervisor of the doctoral thesis:
Prof. Dr. Eva Hevia

Universität Bern

source: https://doi.org/10.48549/3660 | downloaded: 25.4.2024

This work is licensed under the Creative Commons Attribution-NonCommercial-NoDerivatives 4.0 International License. To view a copy of this license, visit http://creativecommons.org/licenses/by-nc-nd/4.0/ or send a letter to Creative Commons, PO Box 1866, Mountain View, CA 94042, USA

Tailor Made Mixed-Metal Reagents for Metalation/C-C Bond Forming processes

Inaugural dissertation
of the Faculty of Science,
University of Bern

presented by

Pasquale Mastropierro
from Molfetta, Italy

Supervisor of the doctoral thesis:
Prof. Dr. Eva Hevia
Universität Bern

Accepted by the Faculty of Science.

Bern, 21/3/2022

The Dean
Prof. Dr. Zoltan Balogh

.

Acknowledgments

I see this thesis as sum up of a 4 years and 5 months long journey of personal and scientific development. I hope I am at least a slightly better person and scientist than the disoriented boy who overcame the door of the Royal College Building in a cloudy day of the beginning of October. Many things happened during this time included a moving from Scotland to Switzerland, a global pandemic, a couple of papers and so on, but most importantly I met a lot of people that were important in this journey, and I therefore would like to thank

First of course there is the person who decided to let me start this journey, guided and supported me through, my amazing supervisor prof. Eva Hevia. I do not think I can thank you enough for the possibilities you gave me and for the constant support and encouragement during the whole PhD, despite my failures. Thank you for entrusting me your ideas, thank you for correcting my drafts, and thank you for the passion for science you share. I think you are a truly role-model for being a professor and a leader.

I would like to thank also the other academics I had the luck of meeting both in the University of Strathclyde and in University of Bern. Prof. Robert Mulvey, Dr. Charlie O' Hara and Dr. Stuart Robertson, your advice and your support were priceless. Prof. Martin Albrecht thank you for letting have a smooth Swiss move and thank you for letting us use your lab and your glovebox until the Hevia group had a new home.

To achieve the results described in this thesis I often needed the help of technician or expert of various experimental techniques. I am grateful to them for letting me use their experience and knowledge. Dr. Ilche Gjuroski (University of Bern) and Craig Irving (University of Strathclyde) for running the respective NMR services. I am also very indebting with the group of the crystallographers: Dr. Alan Kennedy in Scotland, PD Dr. Simon Grabowsky, Dr. Michal Andrzejewski and Dr. Lorraine Andrade Malaspina in Switzerland. The structures you provide me were always a reason to celebrate (except $MgBr_2$!). Also priceless was the help in running and understanding the EPR spectra provided by Dr. Ivana Borilovic and (for a short while without Dr.) Wowa Stroek. Whitout you I would feel even more blind working with manganese. Janie-Anne Pickrell is of course of the person to mention in those acknowledgments, her help was very important in let the laboratories in Scotland running smooth and in organizing our moving in Switzerland. A big thank is need to all the people that work in university as janitors, cleaner, secretary or any other non-scientific job, if we can focus only in research in university is also due to their effort.

During those years I had the opportunity in knowing a lot of colleagues in the Hevia group, and for me it was a pleasure work with them, get along with them and face various adventures inside and outside the lab, in rigorously random order: Andryj, Leonie, Andreu, Lewis (together with the adopted member Rachel), Sarah, Alessandra, Sophia, Florian, Jose, David, Andrew, Neil, Marzia, Martin, Xenia. A special mention is due to Lewis for having always an

answer to our questions, for the big effort in set up a brand-new lab and for improvement of our knowledge in the Schlenk technique. I can not wait to see your perish in lab work applied to coffee brewery. Alessandra, the Christmas enthusiast, it was a pleasure to share with you all those travels and the long stopover to reach home (and come back). I am sure in future we will keep talking each other in English even if surrounded by Italians. Thank you to Andryj for sharing with me an important part of our work, the glovebox.

I would like also to thank the member of Mulvey, O' Hara and Robertson group, for their friendship and for letting me discover Glasgow from the Ceilidh to the Sub-crawl. Speaking about friendship in University I can not forget to mention the people in the Albrecht's group, whom have special thanks to let us "invade" their laboratory and their facility at the beginning of our Swiss relocation, and the member of the Paradisi group, who kindly accepted my glassware in their freezer and let me obtain some interesting structure (that they keep storing). In Paradisi group the art (and the Italian language) seems to have an important role, in particular this is true for Valentina and Andrea who realized for me an amazing front cover.

A special thank is for two people I knew during my PhD and were for me incredibly important: Marina and Leonie. Marina took me under her wing from the very first moment guiding and training me to survive in this journey. Your kindness, patience, brightness, and wisdom brought me to consider you one of my dearest friends, almost like an elder sister. Leonie on the other hand is my best pal in the lab, always busy but always ready to help. Blessed with a considerably number of talents she is a truly multipurpose person: chemist, actress, dancer, singer (miss the karaoke time), performer, cleaning queen, incredible friend. Despite the facing hard times she carried most of the work in moving from Glasgow to Bern. I am blessed of knowing you and I owe you a lot (pyrimidine, just to mention one!).

A big thanks is from my friends and my family back in Italy (and in Austria). I may be physically far away from you, but I could feel your support and your care. You may not understand a lot of what I am doing and what is written in the next pages, but you built the person behind the lab-coat.

Last but not least thank you Lorraine. You were what I did not expect to find, but you truly made me happy. Thank you for the unconditional support and love you always provide. Having you on my side was fundamental to reach this goal and overcame all the troubles in this period.

Abstract

The thesis focusses on advancing the understanding on cooperative effects heterobimetallic compounds which combine an alkali-metal with a divalent metal such as magnesium, zinc and manganese. Through rational design, several alkali-metal ates have been prepared and structurally authenticated. Their applications towards two fundamental organic transformations, namely, deprotonative metallation and metal-halogen exchange have been investigated.

Chapter 2 discloses a new family of sodium zincates containing the bulky chelating silyl(bis) amide $\{Ph_2Si(NAr^*)_2\}^{2-}$ (Ar*= 2,6-diisopropylphenyl). Illustrating the enhanced kinetic basicity of Zn-N bonds versus Zn-C bonds, reacting $Ph_2Si(NHAr^*)_2$ (**1**) with an equimolar mixture of $NaCH_2SiMe_3$ and $Zn(HMDS)_2$ (HMDS= $N(SiMe_3)_2$) furnished alkyl sodium zincate $[\{(Ph_2Si(NAr^*)_2)Zn(CH_2SiMe_3)\}^-\{Na(THF)_6\}^+]$ (**3**). Contrastingly using a stepwise approach, by treating **1** first with $NaCH_2SiMe_3$ afforded sodium amide $[\{Ph_2Si(NHAr^*)(NAr^*)Na\}_2]$ (**5**), which can subsequently undergo co-complexation with $Zn(HMDS)_2$, favouring the metallation of the remaining NHAr* group to give heteroleptic tris(amido) zincate $[\{(Ph_2Si(NAr^*)_2)Zn(HMDS)\}^-\{Na(THF)_6\}^+]$ (**6**). The reactivity of sodium zincates **6, 3** and $[NaZn(CH_2SiMe_3)_3]$ (**4**) towards 2,4,6-trimethylacetophenone led to the isolation of enolate complexes $[\{(THF)NaZn(OC(=CH_2)Mes)_3\}_2]$ (**9**), $[\{(THF)NaZn(CH_2SiMe_3)(OC(=CH_2)Mes)_2\}_2]$ (**8**), and $[\{(THF)Na(OC(=CH_2)Mes)\}_4]$ (**10**) (Mes= 2,4,6 trimethylphenyl), respectively. These studies revealed that the chelating silyl(bis)amide $\{Ph_2Si(NAr^*)_2\}^{2-}$ far from being an innocent spectator is an effective base for the deprotonation of this ketone, showing an unexpected superior kinetic basicity than the CH_2SiMe_3 alkyl group when part of sodium heteroleptic zincate **3**. The bimetallic constitution of enolates **9** and **8** contrasts with that of all-sodium **10**, which is formed with concomitant elimination of $Zn(CH_2SiMe_3)_2$. Revealing the divergent behaviour of Mg versus Zn in these bimetallic systems, reaction of 2,4,6-trimethylacetophenone with the magnesium analogue of **3**, $[\{Ph_2Si(NAr^*)_2Mg(CH_2SiMe_3)\}^-\{Na(THF)_6\}^+]$ (**11**), produces magnesiate enolate $[\{Ph_2Si(NAr^*)_2Mg(O(=CH_2)Mes)(THF)\}^-\{Na(THF)_5\}^+]$ (**12**), where the chelating silyl(bis)amide ligand is retained and metalation of the ketone is actioned by the alkyl group.

Chapter 3 exploits the sequential deprotonative co-complexation approach developed in **Chapter 2** to access novel potassium metal(ates). Thus, monometallation of **1** is accomplished using potassium alkyl KCH_2SiMe_3 yielding $[\{Ph_2Si(NHAr^*)(NAr^*)K\}_\infty]$ (**13**), which, in turn, undergoes co-complexation with the relevant $M(CH_2SiMe_3)_2$ (M=Mg, Zn, Mn) enabling metallation of the remaining NHAr* group to furnish silylbis(amido) alkyl potassium metal(ates) $[\{Ph_2Si(NAr^*)_2M(THF)_x(CH_2SiMe_3)\}^-\{K(THF)_y\}^+]$ (M=Zn, x=0, y=4, **14**; M=Mg, x=1, y=3, **15**; and M=Mn, x=0, y=4, **16**). Reactivity studies of potassium manganate **16** with the amine HMDS(H) revealed the kinetic activation of the remaining alkyl group on Mn furnishing $[K(THF)_2\{Ph_2Si(NAr^*)_2\}Mn(HMDS)]$ (**18**). Similarly **16** reacts with phenyl acetylene to give $[\{Ph_2Si(NAr^*)_2Mn(THF)(C\equiv CPh)\}^-\{K(THF)_3\}^+]$ (**17**). The structures of

these bimetallic complexes along with that of the potassium precursor **13** have been established by X-ray crystallographic studies.

Chapter 4 introduces a new type of heterobimetallic base, the specially designed potassium zincate $[\{Ph_2Si(NAr^*)_2Zn(TMP)\}^-\{K(THF)_6^+]$ (**19**) which combines a sterically demanding silyl(bis)amide ligand with a kinetically activated terminal TMP amide group (TMP= 2,2,6,6-tetramethylpiperidide). Circumventing common limitations of conventional s-block metallating bases, **19** enables efficient and regioselective zincation of a broad range of substituted fluoroarenes including hypersensitive fluoronitrobenzene derivatives. Trapping and characterization of the organometallic species involved in these reactions $[\{Ph_2Si(NAr^*)_2Zn(Ar^F)\}^-\{K(THF)_x^+]$ (Ar^F =$C_6H_2F_3$, $C_6H_3F_2$, $C_6H_2Cl_3$, $C_6H_2F_2NO_2$, $C_6H_3FNO_2$, $C_{11}H_6F_2N$, C_5H_3FN, C_6F_5, C_6HF_4 and C_6F_4; x= 3-6) has provided informative mechanistic insights on how these direct zincation reactions may occur as well as shed light on the key role of the supporting silyl(bis)amido ligand. The first examples of directly metalated nitroarenes to be structurally characterised have been presented as well as the ability of this approach to promote polyzincations of fluoroarenes has been disclosed. Expanding the synthetic potential of this heterobimetallic approach it has been shown that these organometallic compounds can engage in onward C-C bond forming processes.

Chapter 5 explores the synthesis and reactivity of higher order manganates $[(TMEDA)_2AM_2Mn(CH_2SiMe_3)_4]$ (AM= Li, **37**; Na, **43**; K; TMEDA= N,N,N',N'-tetramethylethylenediamine) to promote Mn-I exchange /alkyne metallation reactions in tandem with oxidative homocoupling reactions. Lithium manganate **37** enables the efficient direct Mn–I exchange of aryliodides, affording transient (aryl)lithium manganate intermediates which in turn undergo spontaneous C−C homocoupling at room temperature to furnish symmetrical (bis)aryls in good yields under mild reaction conditions. The combination of EPR with X-ray crystallographic studies has revealed the mixed Li/Mn constitution of the organometallic intermediates involved in these reactions, including the homocoupling step which had previously been thought to occur via a single-metal Mn aryl species. These studies show Li and Mn working together in a synergistic manner to facilitate both the Mn–I exchange and the C−C bond-forming steps. Both steps are carefully synchronized, with the concomitant generation of the alkyliodide ICH_2SiMe_3 during the Mn–I exchange being essential to the aryl homocoupling process, wherein it serves as an in situ generated oxidant. Sodium manganate **43** reacts with 4 equivalents of phenylacetylene to give $[(THF)_4Na_4Mn_2(C{\equiv}CPh)_8]$ (**45)** which when exposed to dry air furnishes the relevant 1,3 enyne in a 97% yield.

Publications

1. *"Structurally Mapping Alkyl and Amide Basicity in Zincate Chemistry: Diversity in the Synthesis of Mixed Sodium–Zinc Complexes and Their Applications in Enolate Formation"* P. Mastropierro, Z. Livingstone, S. D. Robertson, A. R. Kennedy, E. Hevia,* *Organometallics* **2020**, 39, 4273-4281.
2. *"Exploiting Deprotonative Co-complexation to Access Potassium Metal(ates) Supported by a Bulky Silyl(bis)amide Ligand"* P. Mastropierro, A. R. Kennedy, E. Hevia,* *Eur. J. Inorg. Chem*. **2021**, 11, 1016-1022.
3. *"Tandem Mn-I Exchange and Homocoupling Process Mediated by a Synergistically Operative Lithium Manganate"* M. Uzelac,* P. Mastropierro, M. de Tullio, I. Borilovic, M. Tarrés, A. R. Kennedy, G. Aromí, E. Hevia,* *Angew. Chem. Int. Ed.* **2021**, 60, 3247-3253.
4. *"Metallation, Trapping and Stabilisation of Sensitive Fluoroarenes using a Potassium TMP-Zincate Supported a Silyl(bis)amido Ligand"* P.Mastropierro, A. R. Kennedy, E. Hevia,* *Chem. Commun.* manuscript submitted for publication

Conference Presentations

1. "*Direct Zincation of Fluoroarenes Using a Mixed Potassium-Zinc Base*" Poster Presentation at RSC Main Group Meeting, **2019** (London, UK)
2. "*Direct Zincation of Fluoroarenes Using a Mixed Potassium-Zinc Base*" Poster Presentation at RSC Twitter conference, **2020**
3. "*Direct Zincation of Fluoro-Arenes Using a Mixed Potassium-Zinc Base*" Poster Presentation at Swiss Chemical Society Fall Meeting, **2020** (Virtual Conference)
4. "*Tandem Mn-I Exchange and Homocoupling Processes Mediated by a Synergistically Operative Lithium Manganate*" Poster Presentation at RSC Twitter conference, **2021**
5. *"Tandem Mn-I exchange and homocoupling processes mediated by Li/Mn cooperativity"* Poster Presentation at Swiss Chemical Society Fall Meeting, **2021** (Virtual Conference)

List of Common Abbreviations

AM	Alkali metal
Ar*	2,6-Diisopropylphenyl
BDI*	HC{C(^{t}Bu)N[2,6-(3-pentyl)-phenyl]}$_2$
Bnz	Benzyl
C_6D_6	Deuterated benzene
$CDCl_3$	Deuterated chloroform
CIP	Contacted Ion Pair
COSY	Correlated Spectroscopy
Cy	Cyclohexane
D	Deuterium
D_8-THF	Deuterated tetrahydrofuran
Dipp	2,6-Diisopropylphenyl
^{Dipp}Nacnac	{(Ar*)NC(Me)}$_2$CH
dmpe	Bis(dimethylphosphino)ethane
D*o*M	Direct *ortho* metalation
DOSY	Diffusion Ordered Spectroscopy
E	Electrophile
EPR	Electron Paramagnetic Resonance
Eq.	Equivalents
Et	Ethyl
Et_2O	Diethyl ether
HMDS	-N(SiMe$_3$)$_2$
HMDS(H)	Hexamethyldisilazane
^{i}Pr	Isopropyl
KO^{t}Bu	Potassium tert-butoxide
LiC-KOR	Alkyllithium/potassium alkoxide Superbase
LiTMP	Lithium tetramethylpiperidide
m	*meta*
M	Metal
Me	Methyl
Mes	Mesityl or 2,4,6 trimethylphenyl
^{n}Bu	*normal* Butyl
^{n}BuLi	Butyl lithium
NHC	N-heterocyclic carbene
NMR	Nuclear Magnetic Resonance
NpLi	*neo*-Pentyllithium
o	*ortho*
p	*para*
Ph	Phenyl
PMDETA	N,N,N',N'',N''-Pentamethyldiethylenetriamine
R	-CH_2SiMe_3 or alkyl
R'	C(=CH2)Mes
RT	Room temperature (25 °C, 298 K)
SQUID	Superconducting Quantum Interference Device
SSIP	Solvent Separated Ion Pair
^{t}Bu	*tert*-Butyl

^{t}BuLi	*tert*-Butyllithium
THF	Tetrahydrofuran
TMEDA	N,N,N',N'-Tetramethylethylenediamine
TMP	2,2,6,6-Tetramethylpiperidide
TMP(H)	2,2,6,6-Tetramethylpiperidine
TMS	Tetramethylsilane
X	Halides

Table of Numbered Compounds

N°	Compound	N°	Compound
1	$Ph_2Si(NHAr^*)_2$	**2**	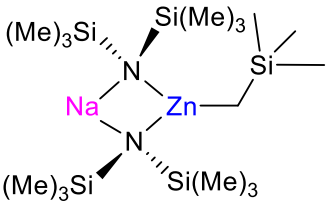
3	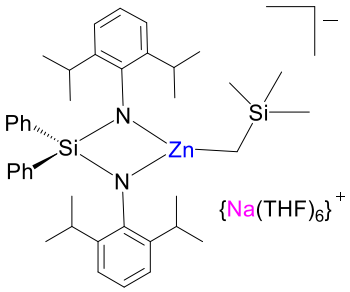	**4**	$[(TMEDA)NaZn(CH_2SiMe_3)_3]$
5	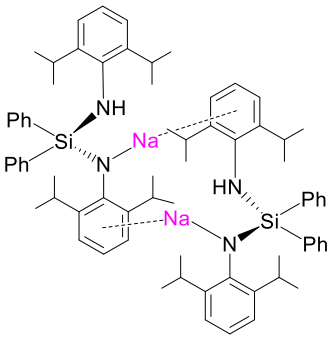	**6**	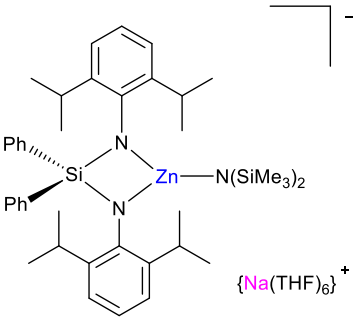
7	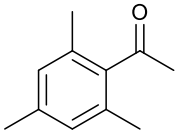	**8**	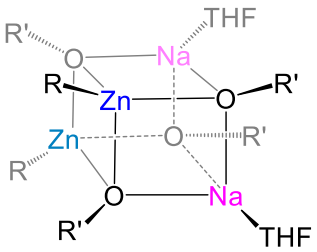
9	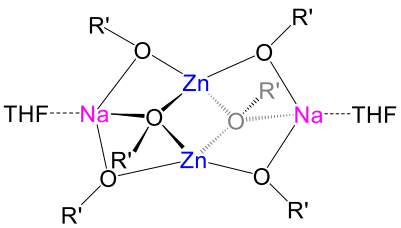	**10**	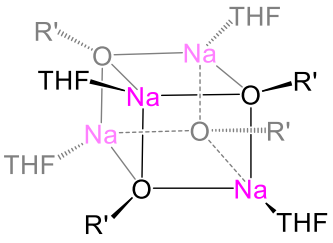
11	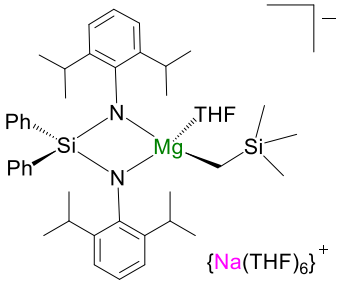	**12**	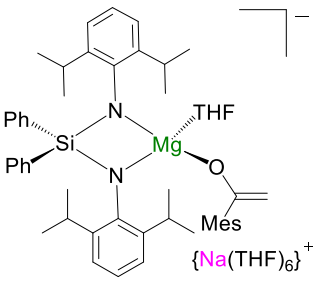

13

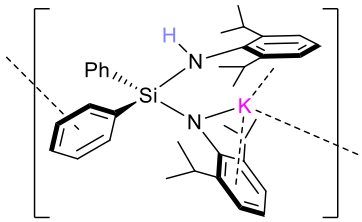

14

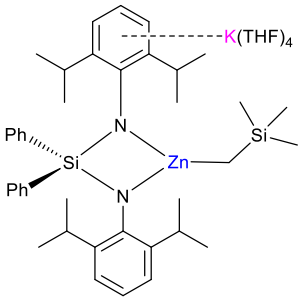

15

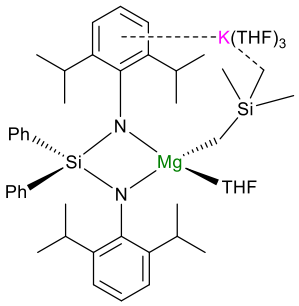

16

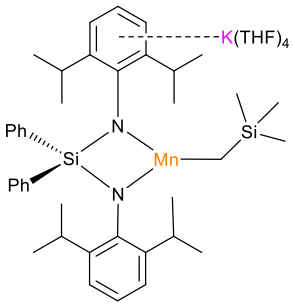

17

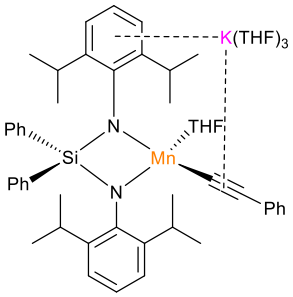

18

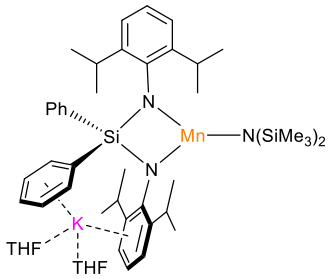

19

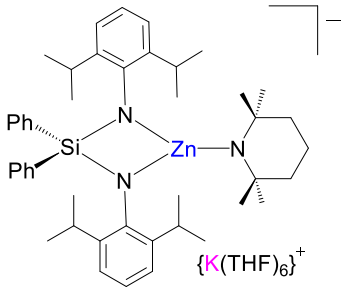

19b

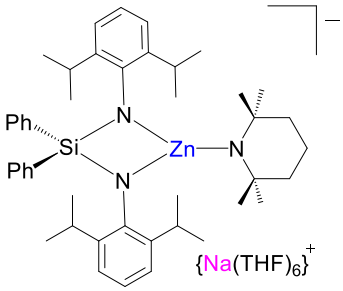

20

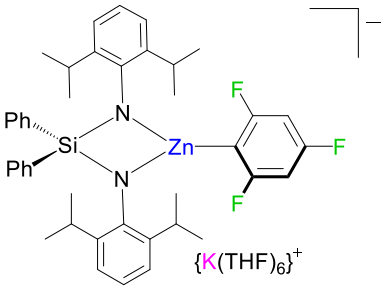

20b

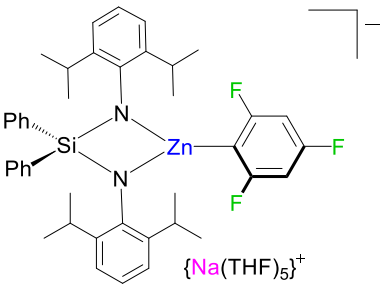

21

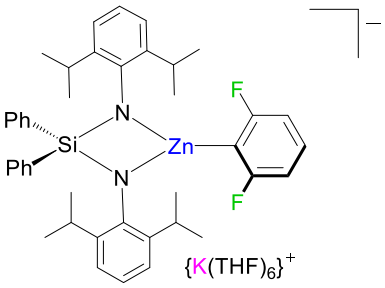

22

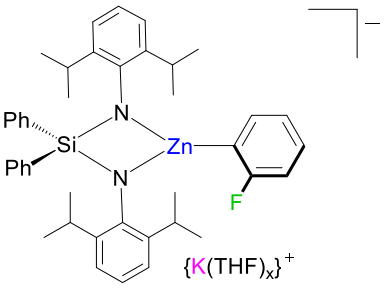

X

23

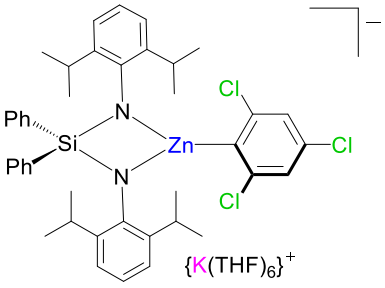

24

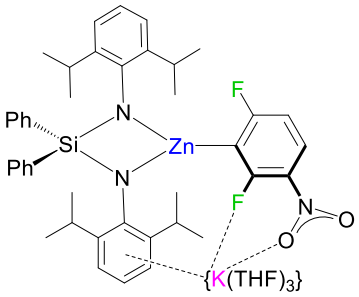

25

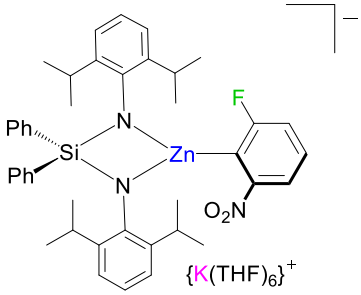

26

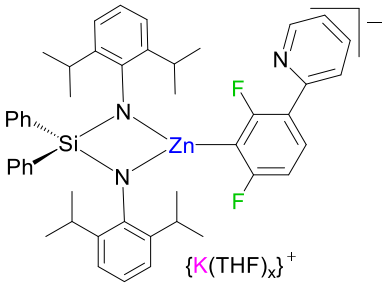

27

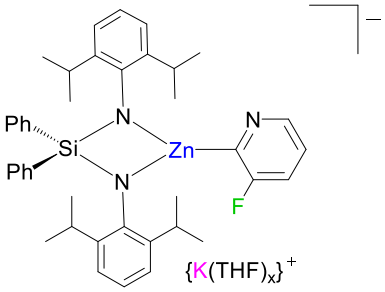

28

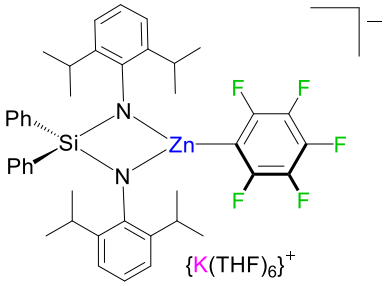

29

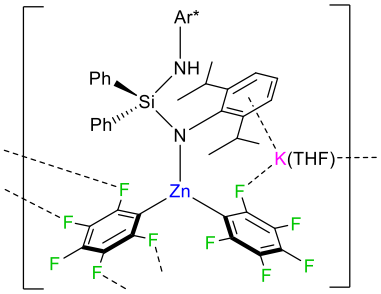

30 $[K(THF)_xZn(C_6F_5)_3]$

31

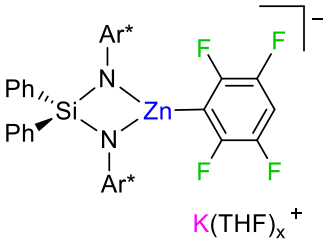

32

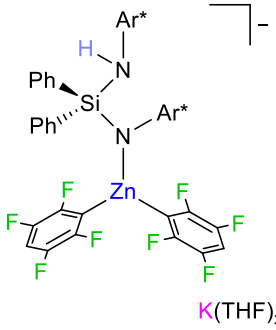

33 $[K(THF)_xZn(C_6HF_4)_3]$

34

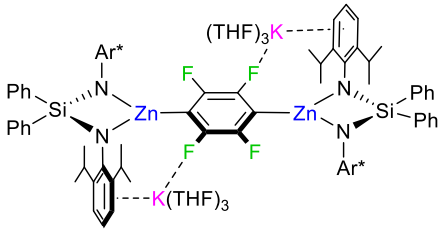

35a-e	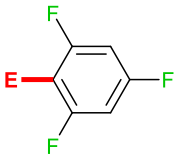	**36a-o**	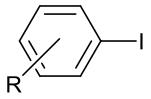
37	$[Li_2Mn(CH_2SiMe)_4]$	**38a-o**	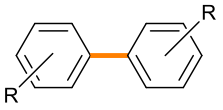
39	$[(THF)_4MgCl_2Mn(CH_2SiMe_3)_2]$	**40**	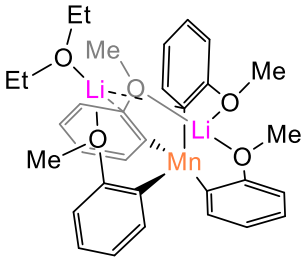
41	$[(THF)Li_4Mn_2Ar_6(\mu_6\text{-}O)]$	**42**	$[(THF)_4Li_4Mn_2Ar_4Cl_2(\mu_4\text{-}O)_2]$
43	$[Na_2Mn(CH_2SiMe)_4]$	**44**	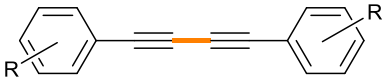
45	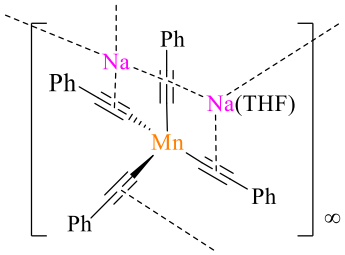	**46**	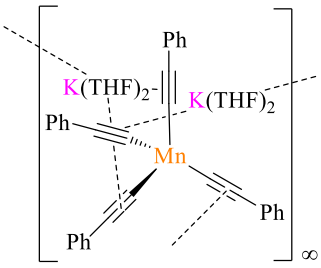

Table of Contents

Acknowledgments ..... **I**

Abstract ..... **III**

Publications ..... **V**

Conference Presentations ..... **VI**

List of Common Abbreviations ..... **VII**

Table of Numbered Compounds ..... **IX**

Chapter 1: General Introduction **1**

1.1 Organolithium chemistry 1

1.1.1 Lochmann-Schlosser Superbases (LiOR-KOR) 3

1.1.2 Direct *Ortho*-Metalatation (D*o*M) 4

1.1.3 Metal/Halogen Exchange 6

1.2 Grignard Reagents and Turbo-Grignard 7

1.3 Introduction to Cooperative Bimetallic Chemistry 8

1.4 The Chemistry of the Organo-Zincates 12

1.5 Aims and Structure of the Thesis 21

1.6 References 22

Chapter 2: Assessing Metalating Ability of Sodium Zincates Containing Sterically Demanding Bis(amide) Ligand **29**

2.1 General introduction to this chapter 29

2.2 Aims 35

2.3 Introduction from the paper 36

2.4 Results and discussion 38

2.4.1 Synthesis of Sodium Zincates Featuring a Silyl Bis(amide) Ligand 38

2.4.2 Applications of Sodium Zincates in Enolate Formation 42

2.5 Conclusions 49

2.6 Experimental Section 49

2.6.1 Synthesis and characterization of compounds **2-12** 49

2.6.2 ^{1}H NMR monitoring of the metalation of **7** by sodium zincates **3**, **4** and **6** 54

2.7 References 56

Chapter 3: Accessing Potassium Metal(ates) Supported by a Bulky Silyl(bis)amide Ligand **63**

3.1 General introduction to this chapter 63

3.2 Aims 67
3.3 Introduction from the paper 67
3.4 Results and Discussion 68
3.5 Conclusions 76
3.6 Experimental Section 77
3.7 References 80
Chapter 4: Direct Zincation of Fluoroarenes Using a Potassium-Zinc Base Supported by a Sterically Demanding Ligand 85
4.1 Introduction 85
4.2 Aim 90
4.3 Results and Discussions 91
4.3.1 Synthesis of Potassium Zincate Sustained by a Silyl bis-(Amide) 91
4.3.2 Assessing the metalating ability of **19** towards Fluoroarenes 93
4.3.3 Studies on the Functionalization of Metalated Fluoroarenes 108
4.4 Conclusions 110
4.5 Experimental Section 111
Organic Products 119
4.6 References 121
Chapter 5: Alkali-metal Manganates and their Applications in Homocoupling Processes 125
5.1 General introduction to this chapter 126
5.1.2 The Chemistry of Alkali-metal Manganates 128
5.2 Aims 132
5.3 Introduction from the paper 133
5.4 Results and Discussion 134
5.4.1 Assessing Mn-I Exchange of Iodoarenes 134
5.4.2 Manganate-Mediated Aryl-Aryl Oxidative Homocouplings 139
5.4.3 C(sp)-C(sp) homocoupling reactions mediated by [AM_2MnR_4] reagents (AM= Li, Na, K) 146
5.5 Conclusion 152
5.6 Experimental Section 153
5.7 References 157
Chapter 6: Conclusions and Outlook 161
Chapter 7: General Experimental Techniques and Procedures 163

7.1 Schlenk Techniques 163
7.2 Glovebox 164
7.3 Solvent Purification 165
7.4 Commercial Reagents 165
7.5 Standardization of the organometallic solutions 165
7.6 Analytical procedures 166
7.4 Synthesis of Common Starting Materials 167
7.5 References 170

Chapter 1: General Introduction

The chemistry of the polar organometallics could be seen as *trait du union* between inorganic chemistry, where the main interests lay on the nature of the metal-carbon bond nature, and structural features of these compounds and organic chemistry, with a special focus on the applications of these reagents for the functionalization of organic molecules, via cornerstone reactions such as metal/halogen exchange and nucleophilic addition processes. Thus, it is not surprising that it is a vast field of study. This general introduction provides a concise overview of this area of research, focusing primarily on alkali-metal zincate reagents as they constitute an important family of compounds, and this thesis has advanced the synthesis and the reactivity of these systems. This general introduction will be then further complemented by the separate introductions of every chapter that would be tailored on the specific topic of each section.

1.1 Organolithium chemistry

Amongst polar organometallic chemists the most widely used reagents are undoubtably organolithium reagents. They were first synthetized by Schlenk in 1917 through reaction of dialkylmercury with lithium metal[1,2] (nowadays the hazardous mercurial compounds are substituted by aryl- or alkyl- halides[3]). Despite their late discovers, in comparison to the organometallics such as organozinc or organomagnesium halides, organolithiums became rapidly very popular in the field of metalation, due to their high reactivity (including also the utility lithium amides LiHMDS, LiTMP and LiN(^{i}Pr)$_2$).[4] Thus these reagents can transform relatively unreactive C-H or C-X bonds in more reactive C-Li bonds. Those reactive bonds are then intermediate for further functionalization of organic molecules.[5,6] Since their wide spread use around the world, the most common organolithium compounds (^{n}BuLi, ^{t}BuLi, EtLi, MeLi, PhLi, LiHMDS) are commercially available as fundamental tools in any synthetic chemist's toolbox.

The strong reactivity of the organolithium compounds rely on the considerable electronegativity difference between lithium and carbon, where according Pauling's table those values correspond to 0.98 and 2.55, respectively.[7] As consequence, they possess a highly polarized $^{\delta+}$Li-$^{\delta-}$C bond (for examples for methyllithium the ionic character of the Li-C bond was estimated between 80 and 88%).[8]

The common notation for organolithium, RLi (R= alkyl or aryl), should not be misunderstood, since the organolithium compounds do not form monomeric structures, instead usually the molecules combine in highly aggregated structures with different dimensions depending on the steric encumbrance of the organic group and the presence (or the absence) of donors that coordinate to the lithium atoms. The reason behind the aggregation in clusters is the higher stabilization that more than one anionic ligand can provide to the highly electropositive lithium atom.[6,9]

Taking as example one of the most used and well-known organolithium compounds, ^{n}BuLi, it has been shown through single crystal X-ray diffraction and multinuclear NMR spectroscopy, that in the solid state it is arranged as hexamer (see **Figure 1. 1 a**),[10] the same arrangement is kept also when solubilised in the non-donating solvent hexane (in which it is usually sold, in a 1.6 M solution).[11] Using Lewis donors it is possible to de-aggregate the structure, in fact the formation less aggregate structures is entropically favoured by the electrons provided by donors.[9] The presence of THF promotes the formation an equilibrium between the tetrameric [(^{n}BuLi)$_4$(THF)$_4$] and dimeric forms [(^{n}BuLi)$_2$(THF)$_4$] (but with a preference for the tetrameric form) in solution, as observed using DOSY-NMR technique.[12] The tetrameric form is also retained in solid state too, with THF as donor.[13] When coordinated by polydentate donors such as TMEDA ^{n}BuLi assumes a tetrameric arrangement in solid state (**Figure 1. 1 b**)[13,14] and dimeric in solution as found by Williard using a combination of ^{6}Li, ^{15}N and ^{13}C-NMR spectroscopy.[15] Finally with the PMDETA the complex is a monomer in solution state.[16]

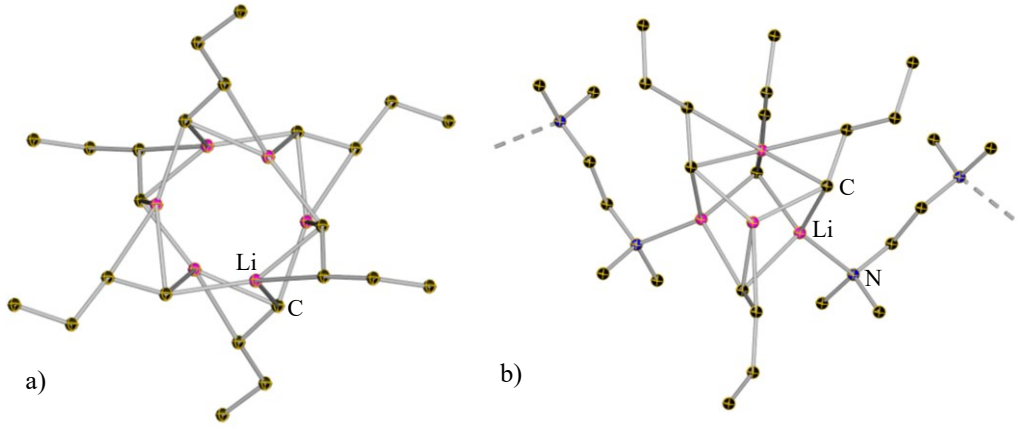

Figure 1. 1 *Crystal structure of a) hexameric ^{n}BuLi in hexane [(^{n}BuLi)$_6$] and b) tetrameric ^{n}BuLi [{(TMEDA)$_2$(^{n}BuLi)$_4$}$_\infty$] solvated by TMEDA. Ellipsoids were rendered at 50% probability. Hydrogen atoms were omitted for clarity.*

Those differences are not just speculative, in fact as often happen in organometallic chemistry, reactivity is closely related to the 3D arrangement in the structure. An example for ^{n}BuLi is the metalation of benzene. Based on a purely thermodynamic point of view (the pK_a value) there should not be any obstacles in the deprotonation of aromatic ring by the ^{n}BuLi, in fact the conjugated acid (butane) is ten orders of magnitudes less acidic than benzene. However, in practice, this reaction (in hexane) is extremely slow and useless for synthetic purpose. The reason behind this behavior is kinetic, in fact the hexameric aggregates of ^{n}BuLi (*vide supra*)[10] in hexane react very slow with benzene.[9] Providing a Lewis donor, such as TMEDA it is possible to break the hexamers in smaller aggregates and the benzene is swiftly metalated at room temperature (**Scheme 1. 1**).[17]

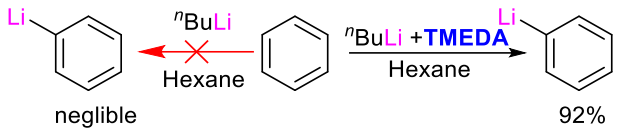

Scheme 1. 1 *Deprotonation of benzene using nBuLi, using or not the Lewis donor*

1.1.1 Lochmann-Schlosser Superbases (LiOR-KOR)

Strictly related to the organolithium, and designed to improve their performance, there are the Lochmann-Schlosser superbases (or LiC-KOR).[18] These reagents are made up by a combination of an organolithium (often the commercially available *n*BuLi) and a potassium (or sodium) alkoxide (usually KO*t*Bu is used). The synergy between those components greatly enhances their reactivity, allowing for the deprotonation of non-activated substrates like benzene (**Scheme 1. 2**) without the use of monometallic organopotassium reagents, which are thermally unstable and non-compatible with many organic substrates.

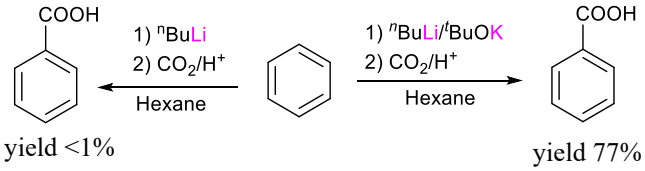

Scheme 1. 2 *nBuLi/tBuOK mediated deprotonation of benzene. It should be noted that nBuLi alone, in absence of a Lewis's donor, is uncapable to metalate benzene*

Despite their synthetic relevance, true constitution of these reagents has remained a matter of intense debate and investigation for many years.[19] In his seminal work, Schlosser excluded the possibility that a mere transmetalation occurred, suggesting the formation of a mixture of different mixed metal species.[20] Thirty years later since this report, Strohman *et al*. were able to crystalize the product of metalation of the benzene using LiC-KOR, furnishing $[K_4Li_2(C_6H_5)_5(^tBuO)(THF)_6(C_6H_6)_2]$. The crystal structure obtained exhibited a mixed-metal constitution, retaining part of the original superbase constituent and forming an hexanuclear structure with 4 lithium and 2 potassium, having as anion the metalated benzene and a tert-butoxide anion from the starting material. The *ipso*-carbon of aryl rings binds both to potassium and lithium. (**Figure 1. 2**).[21]

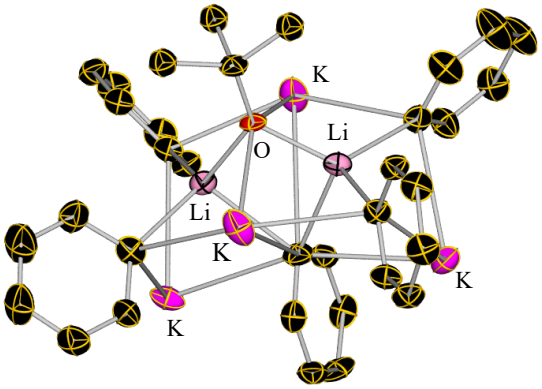

Figure 1. 2 *Crystal structure of [$K_4Li_2(C_6H_5)_5(^tBuO)(THF)_6(C_6H_6)_2$], In the structure are still present both metal of the superbase and a tert-butoxide moiety. Hydrogen atoms, THF and Benzene solvating molecule were omitted for clarity. Thermal ellipsoids were rendered with 30% probability*

Previous attempts to isolate Lochman-Schlosser reagents had failed due to the difficulty in solubilise the reagent in a non-coordinating solvent and also the tendency of the alkyl groups to undergo β-hydride elimination. Some of these problems were overcame by Klett when he introduced the co-complexation of NpLi (Np= *neo*-pentyl) with KO^{t}Bu This allowed him to isolate the mixed metal aggregate [$K_4Li_4(Np)_3(O^tBu)_5$] (**Figure 1. 3**).[22] The solution study of the mixture of NpLi, LiOtBu and KOtBu in D_{12}-cyclohexane showed the presence of multiple mixed metal species with general formula [$Li_4K_4(Np)_n(OtBu)_{8-n}$] and [$Li_4K_3Np_m(OtBu)_{7-m}$] (n= 1,2,3 m= 3,4), that are in equilibrium with each other and that confirms the Schlosser initial assumption about a mixture of different mixed-metal species.[22]

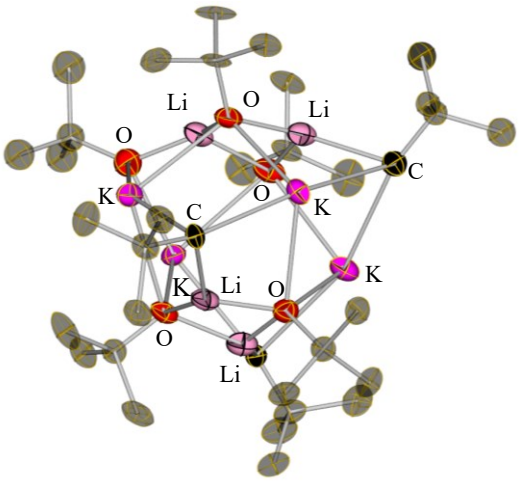

Figure 1. 3 *Molecular structure of [$K_4Li_4(Np)_3(O^tBu)_5$] thermal ellipsoids were rendered with 30% probability. Hydrogen atoms and disorder elements are omitted for clarity.*

1.1.2 Direct *Ortho*-Metalatation (D*o*M)

The *ortho*-metalation is the deprotonation of aromatic molecules selectively in the position next to a functional group.[9] The route for this reaction was independently pioneered by

Wittig[23] and Gilman,[24] who found that the anisole could be metalated by ^{n}BuLi in ethereal solvents regioselectivity at the *ortho*-position to the OCH_3 group. This reaction has arguably become one of the most widely used method to regioselectivity functionalize aromatic molecules.[9]

The presence of a substituent on the aromatic ring, not only activate the position *ortho* due to coordination effects, but also via acidifying inductive effect. This is based on the proposed mechanism for the metalation process, that is believed to occur in two steps: an initial coordination step, where the directing group coordinates the lithium and brings the organometallic species in close proximity to the hydrogen, followed by the effective deprotonation favored by the inductive effect of the directing group on the hydrogen in proximity (**Scheme 1. 3**).[9]

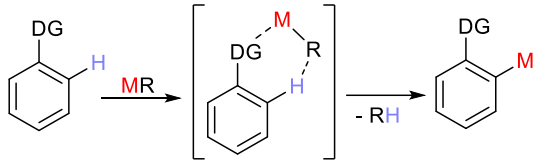

Scheme 1. 3 *General mechanism for the direct ortho-metalation*

To fulfil these tasks the directing group must exhibit both good coordinative property and negative inductive property, therefore the presence of a heteroatom is always required. Based on the characteristic of the group the inductive effect could be more predominant than the coordinative property. As example, halogens usually display very poor coordinative ability, but strong inductive property, groups such as OR or NR_2 (R= alkyl) on the contrary display a better coordinative ability, but worse inductive property.[25]

The nature of the group plays an important role to determine the regioselective of the metalation, when two different groups are present on the aryl ring. In fact, in non-donating solvent (such as hexane) the metalation will occur in *ortho*- to a more coordinative group, contrastingly with more donating additives (like THF or TMEDA) or with less aggregate bases (such as LiR-KOR) the inductive property will be the one to control the regioselectivity (**Scheme 1. 4**)

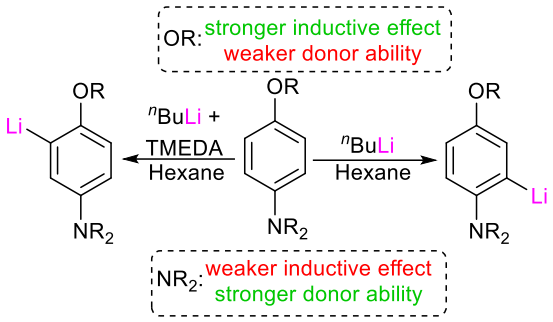

Scheme 1. 4 *Example of optional site selectivity in direct ortho-metalation. In the absence of a donor ligand the metalation occurs in ortho-position to the best donating group. In the presence of a donor, the inductive effects on the ortho-protons gains more importance*

In the context of the direct *ortho*- metalation an exception is represented by the electron poor heterocycles (such as pyridine). Despite the inductive effect from the heteroatom, which is well known by the facile nucleophilic aromatic substitution,[26] the metalation in *alpha*-position in the ring is challenging due to the repulsion with the lone pair present on the nitrogen with the emerging negative charge of the carbanion (see **Scheme 1. 5**). Therefore the preferred metalation site in this substrate is the position 4 (γ) and the α metalation is achieved only at low temperatures or with poorly kinetic active organolithium reagents.[27]

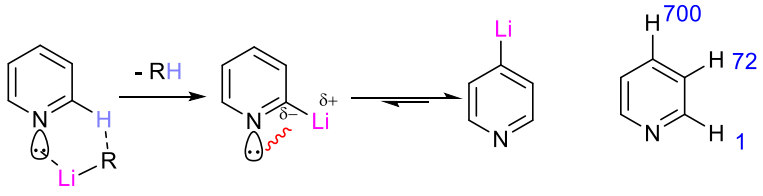

Scheme 1. 5 *Representation of instability of the α-lithiathed pyridine due to the repulsion of the nitrogen lone pair and the emerging negative charge. In blue, relative acidity of pyridine's protons*[27]

1.1.3 Metal/Halogen Exchange

Alongside the direct *ortho*-metalation, the metal/ halogen exchange is another fundamental and widely use reaction in the organolithium chemistry for the functionalization of the aromatic compounds. Independent studies by Gilman[28] and Wittig[29] showed that when treating 4,6-dibromo-1,3-dimethoxybenzene with phenyllithium, 4-bromo-1,3-dimethoxybenzene could be formed after the hydrolysis in high yields (**Scheme 1. 6**).[29]

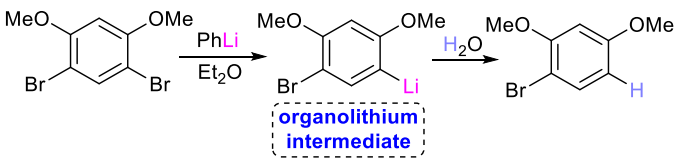

Scheme 1. 6 *Lithium/bromine exchange of the 4,6-dibromo-1,3-dimethoxybenzene*

Further studies then showed that this process is actually an equilibrium which is driven towards the formation of the most stable carbanion.[30] It is also a kinetically driven process, so it can be take place under extremely low temperatures.

The strength of the carbon-halogen bond in the starting material also plays an important role. The more electropositive iodine and bromine are easily exchanged by the organolithium reagents, and therefore chlorine are exchanged with more difficulties.[31–33] Fluoroarenes are inert towards these reactions, being more prone to undergo metalation of the *ortho*-proton instead. [34,35]

1.2 Grignard Reagents and Turbo-Grignard

Along with organolithium, Grignard reagents constitute one of the most popular family of organometallic reagents in synthesis. Pioneered by Victor Grignard by reacting the alkyl or aryl halides with magnesium metal. [36] Differently to organolithium reagents the structures of the Grignards in solution are very complicated to the existence of an equilibrium, known as Schlenk equilibrium, in which the species RMgX (the most common way to address those reagents) coexists with the correspondent diorganomagnesium species and the magnesium halides salt (**Scheme 1. 7**).[37]

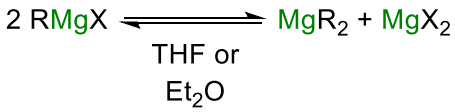

Scheme 1. 7 *Representation of the Schlenk equilibrium. In solution, the species RMgX co-exists with the respective diorganomagnesium compound (MgR_2) and the inorganic diahalides salt (R= alkyl or aryl, X= halides)*

Initially they were used in formation of new carbon-carbon bonds, taking advantage of their strong nucleophilicity through addition to carbonyl substrates.[38] Grignard reagents are also used in metal/halogen exchange reactions as an alternative of organolithium, due to their higher functional group tolerance.[39] However a limitation in their relatively slow reactivity towards arylbromides. In order to overcame this limitation Knochel and coworkes introduced the use of lithium halides to boost the reactivity of the Grignard reagents, allowing the bromine/magnesium exchange to happen significantly faster.[40,41] The mixture of lithium salts and organomagnesium reagent was being known as “turbo-Grignard reagents”. Despite the fact that the structure of those reagents remain unclear,[42] the role of the lithium salts was postulated as de-aggregator of the Grignard reagent (**Scheme 1. 8**).[43]

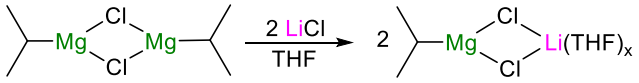

Scheme 1. 8 *Postulated structure of the turbo-Grignard reagent by complexation of ^{i}PrMgCl with LiCl*

The same rationale could be applicable to the magnesium halide amides, known as Hauser base (NR_2MgX X= halide), which is found beneficial for the complexation with LiCl to improve the reactivity in the deprotonation of heterocycles. A good example is the complete metalation of the isoquinoline using $[(THF)_2Li(Cl)_2Mg(THF)TMP]$ at room temperature in 2h.[44] Differently form the turbo-Grignard reagents the solid structure of turbo Hauser base confirmed the co-existence of the two metals in the same molecule (see **Figure 1. 4**).[45] Recent in solution studies by Stalke confirmed the prevalence of the monomeric bimetallic constitution of those reagent and the importance of LiCl in shifting the Schlenk equilibrium, in accordance with the solid state structures and the bimetallic motive proposed by Knochel, evidencing at the same time the complexity of those systems in solutions.[46]

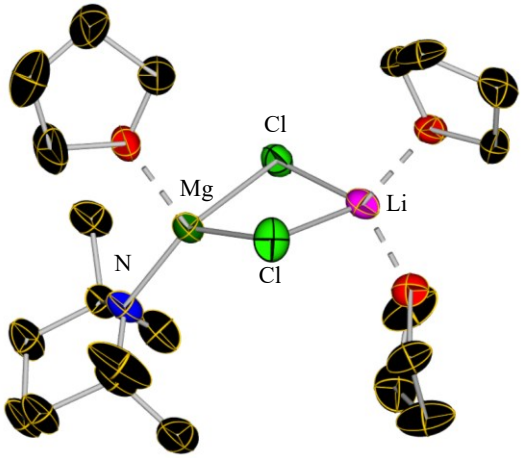

Figure 1. 4 *Crystal structure of the turbo-Hauser base $[(THF)_2Li(Cl)_2Mg(THF)TMP]$. Ellipsoids were rendered at 50% probability. Hydrogen atoms were omitted for clarity*

1.3 Introduction to Cooperative Bimetallic Chemistry

Despite the high reactivity, organolithiums suffer from several drawbacks such as the poor selectivity, limited functional group tolerance and the requirement of strictly reaction conditions (such as extremely low temperatures, -78°C) in order to control the selectivity of the process and avoid unwanted side reactions.

An alternative synthetic approach is the use of heterobimetallic reagents, combining a group 1 metal with a less electropositive metal such as magnesium, zinc or aluminium. Those compounds are also known as alkali-metal *ate* complexes.[47] The terms *ate* was introduced by Wittig to describe those bimetallic combinations with singular property, after observing the reactivity of $[LiMgPh_3]$, obtained combining LiPh and $MgPh_2$. The resulting lithium magnesiate reacted with chalcone giving as the product of 1,4 addition as main result, whereas LiPh with the same substrate has the 1,2 addition product as main outcomes (**Scheme 1. 9**).[48,49]

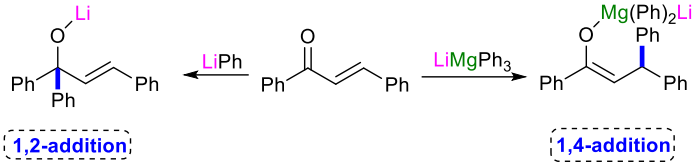

Scheme 1. 9 *Reactivity of chalcone towards LiPh and $LiMgPh_3$*

With few exceptions,[50,51] the *ates* are formed by the combination of two distinct metals, typically one is an alkali-metal (Li, Na, K and even Rb and Cs[52]), usually responsible for boosting the reactivity, the other one is a more electropositive metal that bring a better selectivity and functional group tolerance, usually those metals are from the main groups (Mg, Zn, Al and Ga)[53–58], but transition metals (Fe, Mn, Ag, Cu)[59–67] can also be used. The composition of the *ates* are also completed by anionic ligands (alkyl, amide, halides or alkoxides) and, eventually, neutral donor ligands.[47,68]

Depending on their general stoichiometry ate can be described as higher or lower order. Lower order *ate* corresponds to 1:1 ratio between the alkali metal and the divalent metal (M') affording a formally monoanionic metal species (AM)M'R_3 (R= alkyl, aryl, halides, alkoxides, amides), while a higher order *ate* will lead to a 1:2 ratio of the two metals, affording the formally dianionic species $(AM)_2M'R_4$. The difference between the higher and lower order *ates* has been observed also in reactivity. For example [$LiZnMe_3$] is unable to perform zinc/bromine exchange of bromobenzene, while the dianionic counterparts [Li_2ZnMe_4], with the same substrate gives diphenylmethanol quantitively, when the product of metalation is reacted with benzaldehyde (**Scheme 1. 10**).[69]

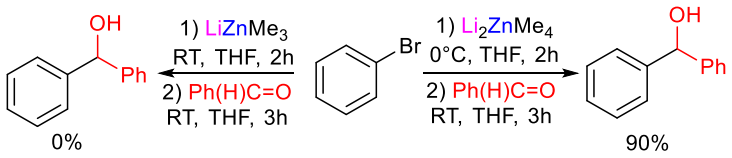

Scheme 1. 10 *Comparison of the zinc/bromine activity of [$LiZnMe_3$] and [Li_2ZnMe_4] towards bromobenzene.*

The nomenclature of the *ates* is completed by the anionic ligands. If all the anionic ligands are the same the *ate* can be described "homoleptic", whereas if different the term "heteroleptic" is exploited.

In general, the synthesis of the *ates* is achieved via co-complexation, mixing two homometallic species (AM)R and M'R_2; or via salt metathesis adding an excess of (AM)R to a salt M'X_2. Both strategies have pros and cons: the salt metathesis usually uses cheap and easy to prepare (if not commercially available) starting materials, but in most of the cases the reaction requires ethereal solvents and the purification of the final product from inorganic salts (side products of the reaction); on the other hand, the co-complexation can be achieved also in non-coordinating solvents (such as hexane) and there are not side products, however in most of the cases M'R_2 is not commercially available and its preparation can be tedious.

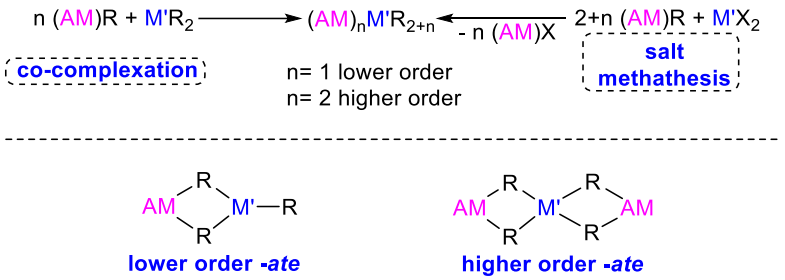

Scheme 1. 11 *General synthesis and representation of lower and higher order metal -ates (R= alkyl, aryl, alkoxide, amide; X= halides, AM= Li, Na or K, M'= divalent metal)*

Ideally, the final stoichiometry of the *ates* should be controlled by (AM)R and M'R_2 (or M'X_2) ratio employed in their preparation, in reality there are several example in the literature where higher and lower order ates can be in equilibrium with each other in solution.[70–72] A particularly intriguing example of equilibrium between higher and lower order species was untangled recently by our group.[73,74] The combination of LiOR (R= 2-ethylhexyl) and Mg(^{s}Bu)$_2$ in toluene has shown to be a powerful tool to achieve quantitively magnesium/bromine exchange at room temperature in toluene.[74] While initially the exchange reagent would have been consider the lower order magnesiate [LiMg(^{s}Bu)$_2$OR] (**A**), which after the exchange forms the diaryl magnesiate [LiMg(Ar)$_2$OR] (**II**). After the hydrolysis or reaction with an electrophile **II** provides the functionalised aryles as desired product in high yield.

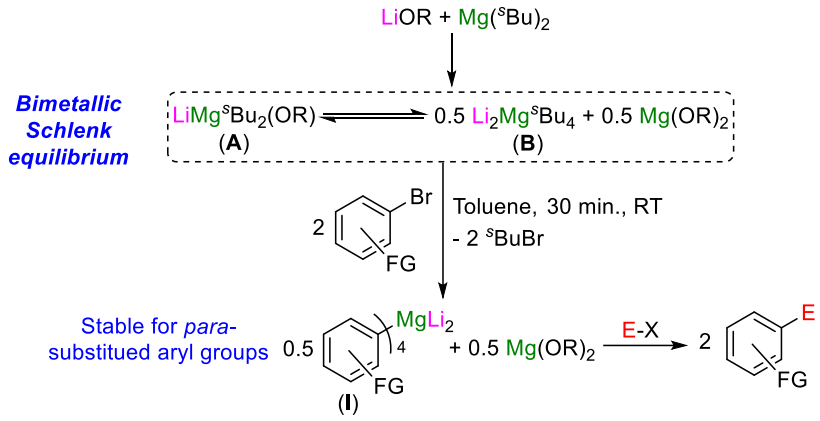

Scheme 1. 12 *Proposed mechanism for the Mg/Br exchange of arylbromides using the combination of LiOR and Mg(^{s}Bu)$_2$ (R= 2-ethylhexyl)*

Using NMR reaction monitoring studies combined by trapping and structural characterization of key reaction intermediates, it was shown that the combination of LiOR and Mg(^{s}Bu)$_2$ in solution with toluene produces a mixture of [LiMg(^{s}Bu)$_2$OR] (**A**) together with the higher order magnesiate [Li$_2$Mg(^{s}Bu)$_4$] (**B**) and [Mg(OR)$_2$], those three species are linked to each other via an equilibrium that resembles the classical Schlenk equilibrium for RMgX reagents. Moreover, it is likely that the truly active exchange reagent is **B**, and in fact when the equilibrium was pushed towards **A** the metal-halogen exchange is completely suppressed. Therefore it was proposed that the reaction proceed via of the tetra-aryl magnesiate

$[Li_2Mg(Ar)_4]$ (**I**) instead. Consistent with this interpretation $[(THF)_4Li_2MgAr_4]$ (Ar= 4-OMe-C_6H_4) could be isolated and structurally characterized from the reaction of LiOR and $Mg(^sBu)_2$ and 2 equivalents of 4-bromoanisole (see **Scheme 1. 12**).[73]

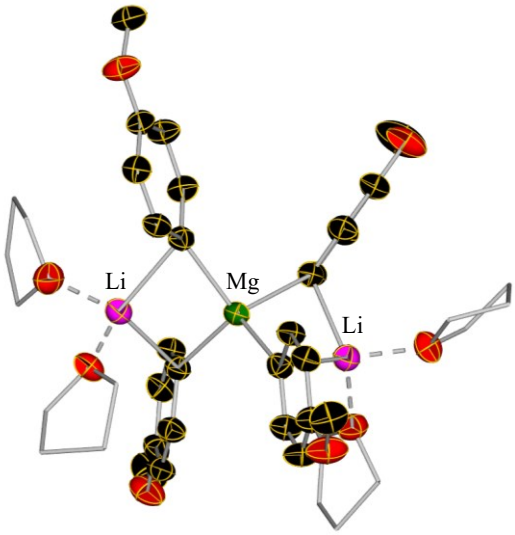

Figure 1. 5 *Crystal structure of $[(THF)_4Li_2MgAr_4]$ (Ar= 4-OMe-C_6H_4), Ellipsoids were rendered at 50% probability. Carbon atoms of THF and hydrogen atoms were omitted for clarity.*

From a structural perspective *ate* complexes can be grouped in two different categories: the Contacted Ion Pair (CIP) where the two metals are connected by one or more bridging anionic ligand (as shown in **Figure 1. 6** a with $[(PMDETA)LiZnMe_3]$) and Solvent Separated Ion Pair (SSIP) (**Figure 1. 6 b** $[\{(diglyme)_2Li\}^+\{ZnMe_3\}^-]$) where the solvents or a neutral donor ligand completely solvates the alkali metal giving rise to discrete anionic and cationic components.[75]

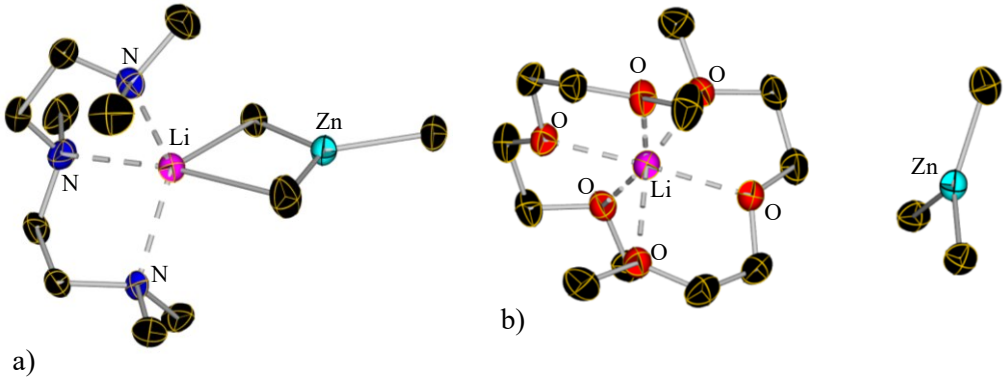

Figure 1. 6 *a) example of contacted ion pair (CIP) -ate, $[(PMDETA)LiZnMe_3]$ b) example of solvent separated ion pair (SSIP) -ate $[\{(diglyme)_2Li\}^+\{ZnMe_3\}^-]$ (PMDETA= N,N,N',N'',N''-pentamethyldiethylenetriamine). Ellipsoids was rendered at 50% probability. Hydrogen atoms were omitted for clarity*

The differences between those two arrangements can be observed, also in the reactivity. When the alkali metal is completely separated from the less electropositive metal, in some cases, the reactivity is different from what is shown by the CIP analogue. This is attributed to the lack of

communication between the two metal centers and inhibition of cooperativity between them. An example is the metalation of anisole operated by potassium magnesiates. When the CIP structure $[(PMDETA)_2K_2MgR_4]$ is used the metalation of anisole proceed quantitatively in hexane at room temperature. The addition of the sequestrating Lewis donor 18-crown-6 induce the formation of a SSIP and the suppression of reactivity (**Scheme 1. 13**).[76] The most known Lewis donor for the sequestering of the alkali metals and the formation of SSIP are the crown ethers and the cryptands.[77,78]

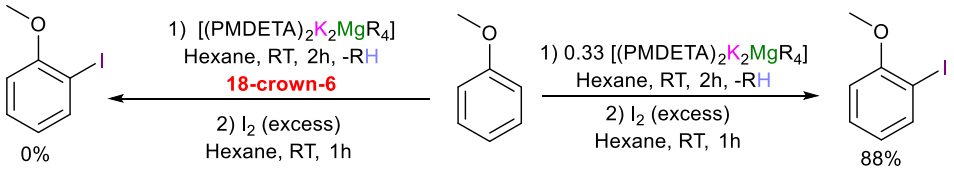

Scheme 1. 13 *Metalation of anisole using [(PMDETA)$_2$K$_2$MgR$_4$] with or without the sequestering Lewis donor 18-crown-6*

1.4 The Chemistry of the Organo-Zincates

Organozinc reagents are amongst the oldest of organometallic reagents known. Their history dates back to 1849 when Frankland prepared for the first time $ZnMe_2$ and $ZnEt_2$.[79,80] Less than 10 years after, Wanklyn prepared the first example of zincate $[NaZnMe_3]$.[81]

Neutral organozinc demonstrated useful tool in organic chemistry, for instance they are the intermediate in Reformatsky reaction.[82,83] Moreover they are important in combination with transition metal[84–88] in particular as nucleophile species in Negishi cross coupling reaction[89,90], in fact the organozinc reagents not only are more stable than other organometallic species (such as organocopper) to disproportionation,[89] but also the empty low-lying *p* orbitals thermodynamically favors the transmetalation to other transition metal salts.[85] However the application of those compounds in deprotonative metalation or zinc-halogen exchange have been limited due to their poor kinetic reactivity. Neutral organozinc compounds, having 14 electrons in their outer shell, tend to behave as Lewis acids and rarely transfer their anionic ligands. This condition could be reverse adding anionic ligand to the zinc center, in fact forming zincates the outer shell of the zinc has 16 or 18 electrons (for the lower and higher order *ate* respectively) (**Figure 1. 7**). Therefore a more thermodynamically stable species while reducing at the same time the Lewis acidity of zinc. In addition having a more filled outer shell should lead to an enhancement of their electronegativity of the molecule facilitating the transfer of the anionic ligands.[91]

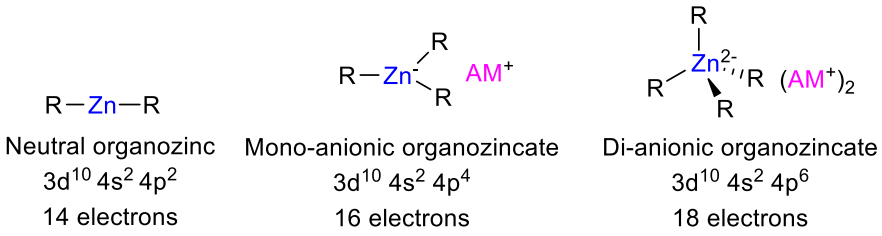

Figure 1. 7 *Molecular formulation for the general diorganozinc, triorganozincate and tetraorganozincate (R= alkyl or aryl-)*

Despite the poor kinetic basicity of ZnR_2 reagents, to be able to promote Zn-H exchange reactions have several advantages in comparison with Li-H and Mg-H exchanges. Thus provide a better functional group tolerance and higher stability of the metalated intermediate. This greater stability can be rationalized considering the almost covalent character of the zinc-carbon bond, with electronegativity value according to Pauling scale for zinc closer to carbon (Zn= 1.65, C= 2.55) than lithium or magnesium (Li= 0.98, Mg=1.31).[7]

A striking example of the superior stability of zincated species due to the strong Zn-C bond is displayed by the metalation of THF. THF is common solvent in Organometallic Chemistry, especially related to the chemistry of Grignard reagents. Organolithiums have an ambivalent relationship with this ethereal solvent, one hand it partially de-aggregate the structure of organolithium reagents in solution,[12] enhancing their reactivity. On the other hand hard organolithium bases can metalate THF at its α-position which triggers a [3+2] cycloreversion forming ethene and lithium enolate as products.[92] Sodium magnesiates can also interact in a destructive way with THF, in fact [(TMEDA)Na(TMP)(CH_2SiMe_3)Mg(TMP)] catastrophically cleaves the ethereal solvent sequestering the oxygen in the inverse crown complex [$Na_2Mg_2(TMP)_4O$] and capturing the remaining butadiene in the complex [{(TMEDA)Na(TMP)}$_2${1,4-[Mg-(TMP)]$_2$-C_4H_4}].[93] Contrastingly sodium zincate [(TMEDA)Na(TMP)(CH_2SiMe_3)Zn(CH_2SiMe_3)] metalates THF at room temperature and affords the complex [[(TMEDA)Na(TMP)(C_4H_7O)Zn(CH_2SiMe_3)] where the structure of the ethereal ring is perfectly preserved (**Scheme 1. 14**).[94]

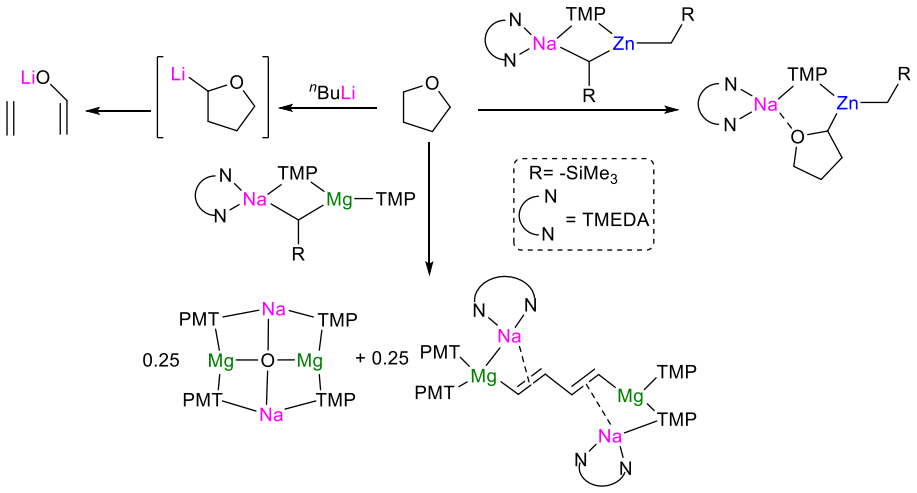

Scheme 1. 14 *Reaction of THF with various organometallic reagents. Notably using [(TMEDA)Na(TMP)Zn(CH_2SiMe_3)$_2$] the THF was not cleaved after the metalation*

In the field of the direct *ortho*-metalation, Kondo has shown the application of the zincates to promote the deprotonative metalation of aromatic molecules. Using the heteroleptic lithium zincate [LiZn(TMP)^{t}Bu$_2$] has proven to be efficient base operating under mild reaction conditions and being compatible with sensitive groups such as ester and cyano. The base is also tolerant to N-hetero aromatic substrates.[95] This zincate was prepared by mixing together the lithium amide LiTMP[4] and the bulky diorganozinc Zn^{t}Bu$_2$. Subsequent structural studies confirmed the formation of a lithium zincate, with the two metals are part of the same molecular entity with a TMP and ^{t}Bu ligands in bridging position (**Figure 1. 8**).[96]

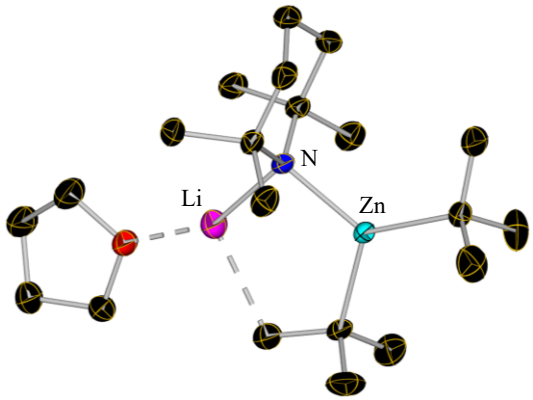

Figure 1. 8 *Crystal structure of [(THF)LiZn(TMP)^{t}Bu$_2$]. Ellipsoids were rendered at 50% probability. Hydrogen atoms were omitted for clarity*

The presence of the two bulky-alkyl ligands is important to stabilize the product of metalation. Thus when a less sterically hindered zincate [LiZn(TMP)Me$_2$] was used for the metalation of substituted bromoarenes, after the metalation (in the presence of halogens in *ortho*-position) there was the elimination of halides salts and the generation of a benzyne intermediate. The benzynes intermediate was trapped via Diels-alder reaction with dienes (**Scheme 1. 15**).[97,98]

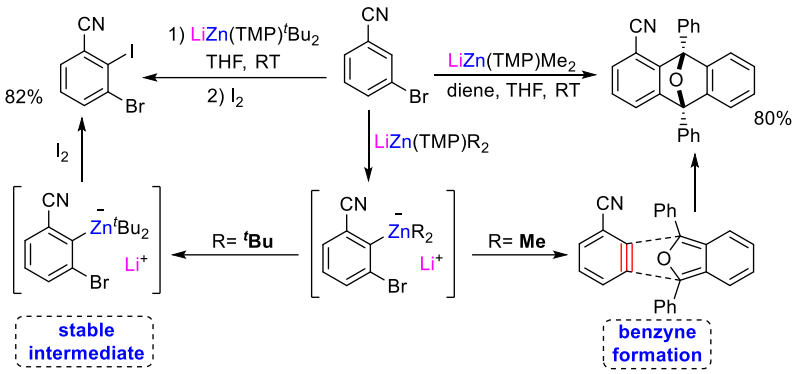

Scheme 1. 15 *Direct metalation of 3-bromobenzonitrile using [LiZn(TMP)^{t}Bu$_2$] or [LiZn(TMP)Me$_2$], the nature of the alkyl anion determines the final product of the reaction*

Mulvey and coworkers intensively developed the sodium analogue of Uchiyama's zincate [(TMEDA)NaZn(^{t}Bu)$_2$TMP], This compound demonstrated an impressive reactivity in deprotonation achieving the metalation of various aromatic substrates. For example, benzene, despite its pK_a value of 41, was metalated under mild conditions using hexane as solvent. In the same conditions NaTMP and Zn^{t}Bu$_2$ are both unreactive towards the same substrate.[99] The methodology could be also expanded to other non-activated substrate such as naphthalene or N-methylpyrrole (**Scheme 1. 16**).[100–102]

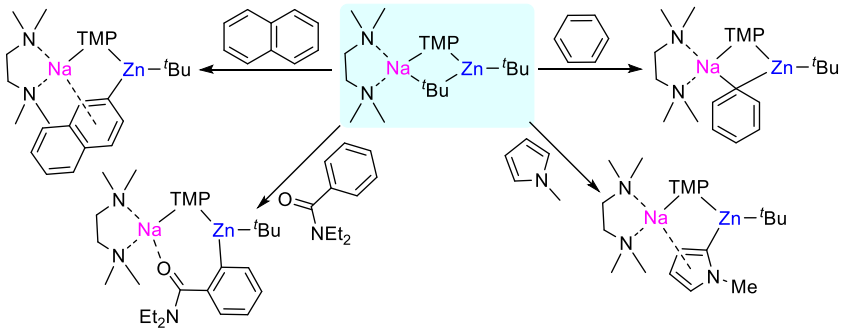

Scheme 1. 16 *Examples of reactivity of [(TMEDA)NaZn(^{t}Bu)$_2$TMP] with various non-activated aromatic substrates*

The heteroleptic character of [(TMEDA)NaZn(^{t}Bu)$_2$TMP] means that it can act as an alkyl or an amido base. The products shown in **Scheme 1. 16** ,characterized unambiguously thanks to single crystal X-ray diffraction, shown an overall alkyl basicity, that is also the thermodynamically favored reactivity. For instance, the metalation of the benzene it was calculated that the free energy associated with the liberation of isobutane is -21.9 Kcal/mol, while the metalation of the benzene via amido basicity (and liberation of TMP(H) as side product) has a value of free energy of -1.5 Kcal/mol (**Scheme 1. 17**).[99]

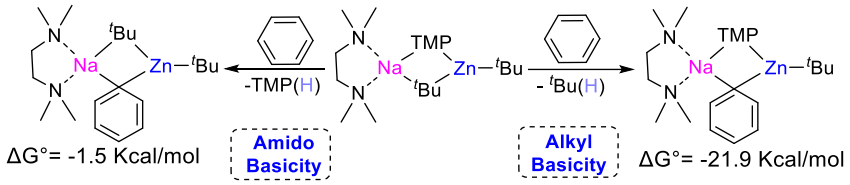

Scheme 1. 17 *Calculated Gibb's free energy for the metalation of benzene having [(TMEDA)NaZn(ᵗBu)₂TMP] as alkyl or amido base*

However, Uchiyama and coworkers through theoretical calculations suggested that the zincation of aromatic substrates proceed as a kinetic-driven process. In their model reagent [$Me_2Zn(NMe_2)Li$], a simplification of lithium zincate [$LiZn(TMP)^tBu_2$], has an activation energy associated with the cleavage of zinc-carbon bond higher than the energy needed for the cleavage of zinc-nitrogen bond.[103–105] The same behavior is found in the neutral zinc species, while $ZnTMP_2$ is an efficient base for the deprotonation of enolates, affording the corresponding zinc-enolate. The dialkyl $ZnEt_2$ is unable to perform the metalation, since the barrier now corresponds to the nearly covalent zinc-carbon bond and therefore much higher. Despite from an thermodynamic point of view there is an higher gain in free energy generating ethane than TMP(H).[106]

To conjugate the results of the experimental work and theoretical calculations a two steps pathway was proposed to explain the mechanism of the direct *ortho*-zincation. In the first step the zincate acted as amido base affording the kinetic product [(TMEDA)NaZn(^{t}Bu)$_2$Ar] and generating TMP(H) as side product. The second step is the further metalation of the TMP(H) that was reinserted in the zincate with the liberation of isobutane, affording the thermodynamically-favored product (**Scheme 1. 18**).[107]

This two steps mechanism was demonstrated by our group in 2009. The putative first step product of the mechanism [(THF)$_3$Li(C_6H_4-OMe)(^{t}Bu)Zn(^{t}Bu)] was prepared indirectly by co-complexation of the *ortho*-lithiated anisole with the neutral zinc species Zn(^{t}Bu)$_2$. This zincate is stable in solution and in solid state, but after addition of TMP(H) one of the tert-butyl arm is consumed to give [(THF)Li(C_6H_4-OMe)(TMP)Zn(^{t}Bu)], the final product that derived from the zincation of the anisole using [$LiZn(TMP)^tBu_2$] as base (**Scheme 1. 18**).[107]

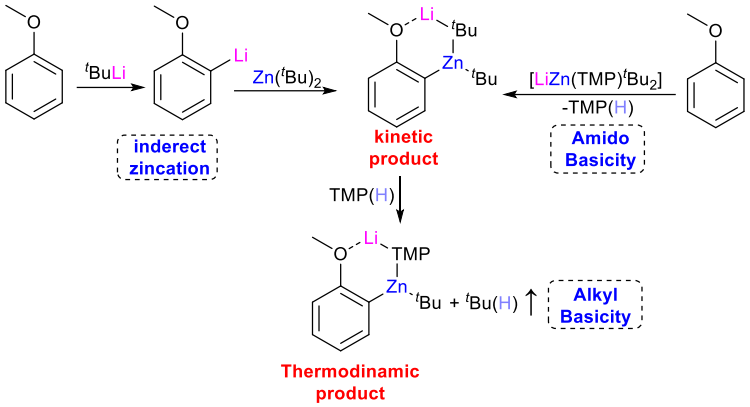

Scheme 1. 18 *Two steps mechanism for the direct ortho metalation of anisole. After a first kinetically-driven metalation the putative kinetic product ([(THF)$_3$Li(C_6H_4-OMe)(^{t}Bu)Zn(^{t}Bu)]) reacts with TMP(H) affording the thermodynamic product. The kinetic product can be prepared indirectly via co-complexation and it reacts with provided TMP(H) affording [(THF)Li(C_6H_4-OMe)(TMP)Zn(^{t}Bu)]*

In a successive report the kinetic product of zincation was then isolated conducting the deprotonation of trifluoromethylbenzene with [(TMEDA)NaZn(^{t}Bu)$_2$TMP]. When the temperature of the reaction was kept below 0°C, the product of amide basicity [{Na(TMEDA)$_2$}{Zn(^{t}Bu)$_2$(*o*-C_6H_4-CF_3)}], was obtained and isolated as single product. The addition of TMP(H) to isolated crystals of the kinetic product lead to the formation of a mixture of products made by [{Na(TMEDA)$_2$}{Zn(^{t}Bu)$_2$(*o*-C_6H_4-CF_3)}], [Na(TMP)(*o*-C_6H_4-CF_3)Zn(^{t}Bu)] (together with the isomer *meta* and *para* in the ratio 20:11:1 respectively) and trifluoromethylbenzene (product of the competing protonation of the aryl anion). The same mixture of products was obtained when the zincation was carried out at room temperature (**Scheme 1. 19**).[108]

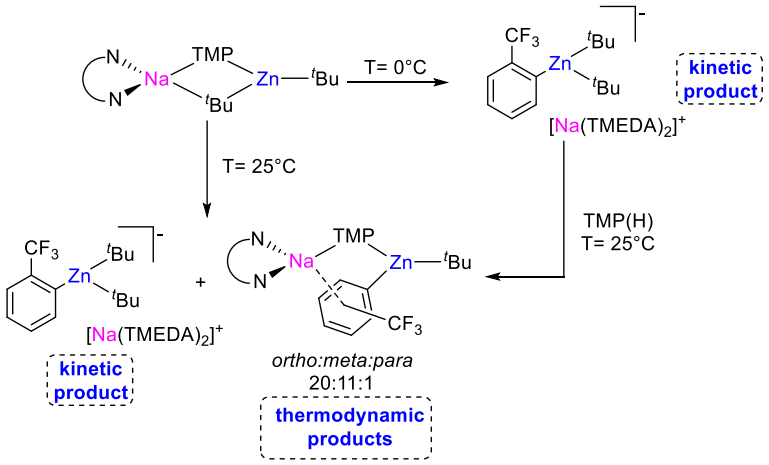

Scheme 1. 19 *Reactivity of [(TMEDA)NaZn(^{t}Bu)$_2$TMP] with trifluoromethylbenzene.*

While substituted aromatics such as anisole, benzamide or carbamates tend to metalated by these bases at their *ortho* position, in some cases with zincates unique regioselectivity, that cannot be replicated by single metal bases, can also be observed. One example is represented by the reaction of N,N-dimethylaniline, where [(TMEDA)NaZn(^{t}Bu)$_2$TMP] selectively

metalates the substrate in meta-position (with the product unambiguously characterized by single X-ray diffraction **Figure 1. 9**) in sharp contrast with the preferred *ortho* regioselectivity obtained when using conventional bases such as ^{n}BuLi·TMEDA.[109] This regioselectivity was attributed to the cooperative effect between the metals, with sodium first π-bonding to the substrate favoring the *meta* deprotonation. Theoretical calculations showed how the zincated species [(TMEDA)·Na(μ-Ar*)(μ-TMP)Zn(^{t}Bu)] (Ar*= 3-$C_6H_4NMe_2$), that is the isolated product of the zincation, is more energetically favored over the correspondent *ortho*-isomer.[110]

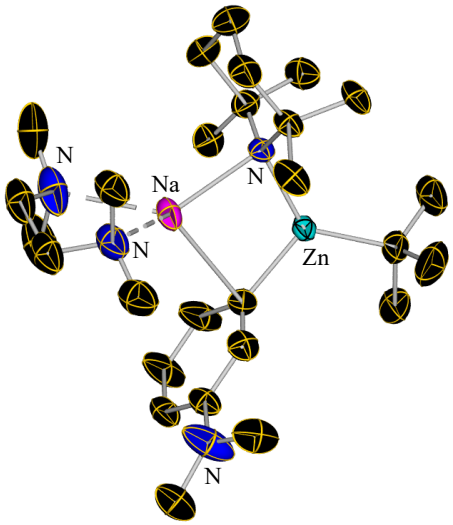

Figure 1. 9 *Crystal structure of [(TMEDA)·Na(μ-Ar*)(μ-TMP)Zn(^{t}Bu)] (Ar*= 3-$C_6H_4NMe_2$). Ellipsoids were rendered at 50% probability. Hydrogen atoms were omitted for clarity*

In the context of the regioselectivity of deprotonation using alkali-metal zincates an interesting case is represented by the metalation of toluene. Toluene usually reacts with very activated organometallics, such as organopotassium or organolithium reagents activated by the presence of a donor ligand, and the deprotonation site is the reactive benzylic position, due to the superior stabilization offered to the emerging negative charge. However [(TMEDA)NaZn(^{t}Bu)$_2$TMP] deprotonates toluene at the aromatic ring, affording a mixture of *meta* and *para* zincated products, with statically distribution of the ratio between the two species.[111] Nevertheless wisely choosing the reagents, is possible to achieve the benzylic metalation of the toluene also with the zincates, in fact [KZn(HMDS)$_3$][112] (**Figure 1. 10**) reacts at room temperature with a large excess of toluene (19 times the amount of zincate) affording [{KZn(HMDS)$_2$(CH_2Ph)}$_\infty$] (**Scheme 1. 20**).[113]

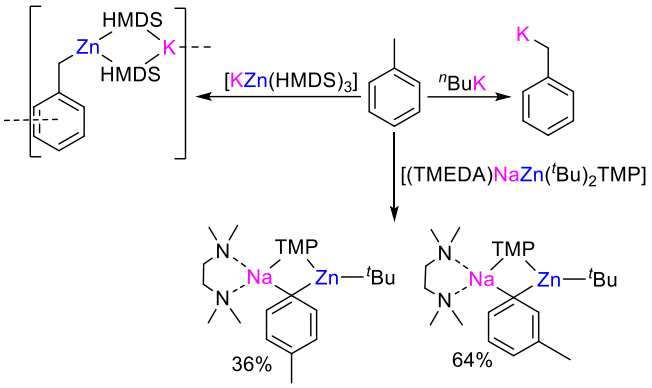

Scheme 1. 20 *Metalation of toluene using different metalating reagent*

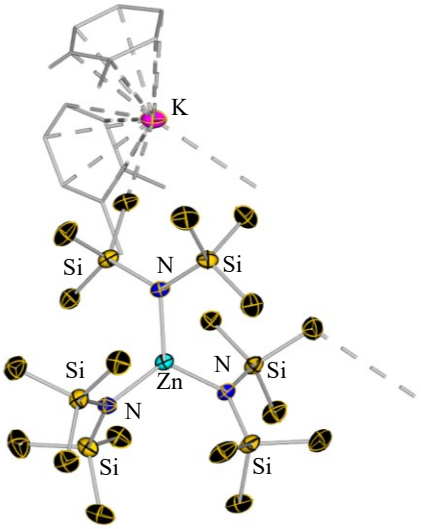

Figure 1. 10 *Crystal structure of [{K(o-xylene)$_2$}$^+${Zn(HMDS)$_3$}$^-$], ellipsoids were rendered at 50% probability. Hydrogen atoms and carbon atoms of o-xylene were omitted for clarity.*

Alkali-metal zincates have also found applications in metal/halogen exchange.[114] Neutral organozinc reacts very sluggish in metal/halogen exchange and often a large excess of the organozinc reagent is required.[115,116] As in the case of Grignard reagents[40,41] the reactivity can be enhanced adding salts as additive such as $MgBr_2$,[117] Li(acac)[118,119] (acac= acetylacetonate). The enhanced reactivity has been attributed to the formation of zincate species.[114]

The first approach to the zinc/halogen exchange using zincates with organic anions was made by Oku and Harada that presented [LiZn^{n}Bu$_3$] (prepared via salt methathesis between ^{n}BuLi and $ZnCl_2$) as an efficient reagent for zinc/bromine exchange in dibromoalkenes affording monobromoalkenes as final product after hydrolysis.[120] The same reagent can be used for the metal-halogen exchange in dibromoalkanes, but in this case after the exchange the second bromine was eliminated as well via rearrangement (**Scheme 1. 21**).[121]

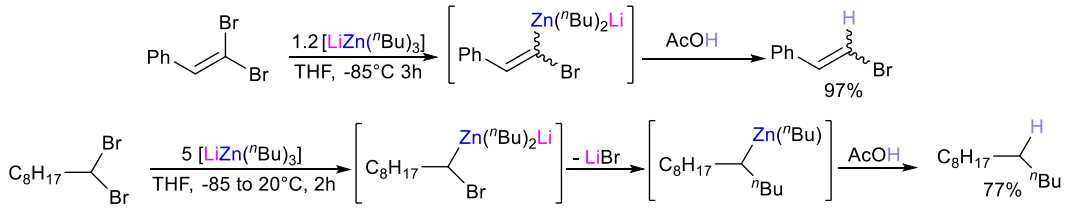

Scheme 1. 21 *Zinc/bromine exchange using [LiZn(^{n}Bu)$_3$] on dibromoalkenes and dibromoalkanes.*

Kondo and Sakamoro extended the zinc/halogen exchange concept using lithium zincate to the arylhalides introducing [LiZn(Me)$_3$][122] and [LiZn(^{t}Bu)$_3$],[123] which demonstrated to be good reagents for the zinc iodine exchange while being compatible with a wide range of functional groups, such as cyano and ether, and heterocylces such as indole. One of the limitations of these lower order zincates was the lack of reactivity towards arylbromides. Therefore Kondo, introduced more reactive higher order zincates, in particular [Li$_2$ZnMe$_4$][124] and [Li$_2$Zn^{t}Bu$_4$].[97] Despite the higher reactivity those zincates retain a wide group tolerance, in particular [Li$_2$Zn^{t}Bu$_4$], due to the bulkier anion ^{t}Bu, generates metalated intermediates resistent to side reactions with the electrophiles and decomposition, avoiding the formation of benzynes. Remarkably even the hydroxy group are tolerated without any form of protective group (**Scheme 1. 22**).[125] Mongin and coworwerks also reported how higher order zincates are very efficient in the exchange, in fact one equivalent of [Li$_2$Zn(^{n}Bu)$_4$] is able to perform the exchange with 3 equivalent of bromoarenes.[126]

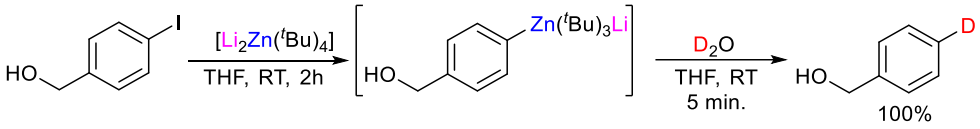

Scheme 1. 22 *Reaction of [Li$_2$Zn(^{t}Bu)$_4$] with (4-iodophenyl)methanol. Remarkably the OH group was left completely untouched*

Despite the numerous examples of the use of those zincates for the metal halogen exchange, a clear view on the mechanism of the metalations is usually obscure. Our group was able to shade some lights on the process by studying the mixed magnesium tris(alkyl) zincate [{Mg$_2$Cl$_3$(THF)$_6$}$^+${Zn(^{t}Bu)$_3$}$^-$], obtained via salt-metathesis using 3 equivalents of ^{t}BuMgCl and ZnCl$_2$. The structure has been determined unambiguously thanks to a combination of single crystal X-ray analysis and in solution state studies. The tris(alkyl) zincate was then reacted with 3 equivalents of 4-iodotoluene in THF at room temperature in 30 minutes, affording the tris (aryl)zincate [{Mg$_2$Cl$_3$(THF)$_6$}$^+${Zn(*p*-Tol)$_3$}$^-$] (*p*-Tol= 4-methylphenyl) and revealing that all the three ^{t}Bu groups are active towards the exchange. Furthermore, the zincate can be used as precursor in palladium catalysed Negishi cross coupling to form byaryls (**Scheme 1. 23**).[50,127]

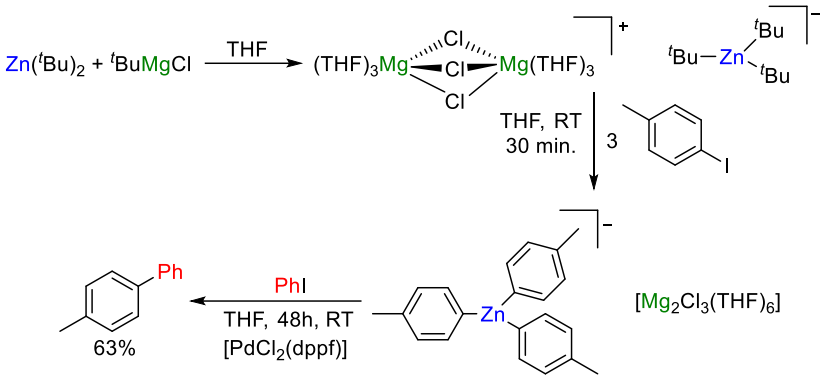

Scheme 1. 23 *Proposed mechanism for the zinc/halogen exchange using the magnesium/zinc species [{$Mg_2Cl_3(THF)_6$}$^+${$Zn(^tBu)_3$}$^-$] (dppf =1,1'-Bis(diphenylphosphino)ferrocene)*

1.5 Aims and Structure of the Thesis

This thesis explores the synthesis and reactivity of a new family of heterobimetallic reagents supported by a bulky silyl(bis)amide ligand. By systematically modifying the nature of the alkali-metal and the divalent metal as well as the remaining ligand, the ability of these compounds to act as metalating reagents is assessed. By isolation and characterization of key reaction intermediates as well as using NMR monitoring each chapter of the thesis investigates a different aspect on the chemistry of these systems. **Chapter 2** focusses on the ability of a variety of sodium zincates to form metal enolates via ketone deprotonation. The synthetic approaches to access potassium metal(*ates*) containing Mg, Zn or Mn. are the main focus of **Chapter 3**. Exploiting the steric protection provided by the bulky silyl(bis)amide ligand, **Chapter 4** studies the zincation of hypersensitive substrates using a potassium zincate base. The applications of tetra(alkyl) alkali-metal manganates to promote direct Mn-I and Mn-H exchange in tandem with oxidative homocoupling reactions is also investigated in **Chapter 5**. **Chapter 6** provides a general overview of the main conclusions of the work presented in the thesis while **Chapter 7** details general experimental techniques and the preparation of starting materials.

1.6 References

[1] W. Schlenk, J. Holtz, *Berichte der Dtsch. Chem. Gesellschaft* **1917**, *50*, 262–274.

[2] T. T. Tidwell, *Angew. Chem. Int. Ed.* **2001**, *40*, 331–337.

[3] T. Rathman, J. A. Schwindeman, *Org. Process Res. Dev.* **2014**, *18*, 1192–1210.

[4] R. E. Mulvey, S. D. Robertson, *Angew. Chem. Int. Ed.* **2013**, *52*, 11470–11487.

[5] Z. Rappoport, I. Marek, Eds. , *The Chemistry of Organolithium Compounds*, Wiley-VCH, Chichester, UK, **2004**.

[6] M. Schlosser, *Organometallics in Synthesis: A Manual*, Wiley-VCH, Chichester, UK, **2002**.

[7] L. Pauling, *J. Am. Chem. Soc.* **1932**, *54*, 3570–3582.

[8] E. Weiss, *Angew. Chem., Int. Ed. Engl.* **1993**, *32*, 1501–1523.

[9] J. Clayden, *Organolithium: Selectivity for Synthesis*, Pergamon, **2002**.

[10] T. Kottke, D. Stalke, *Angew. Chem., Int. Ed. Engl.* **1993**, *32*, 580–582.

[11] H. L. Lewis, T. L. Brown, *J. Am. Chem. Soc.* **1970**, *92*, 4664–4670.

[12] O. Tai, R. Hopson, P. G. Williard, *Org. Lett.* **2017**, *19*, 3966–3969.

[13] M. A. Nichols, P. G. Williard, *J. Am. Chem. Soc.* **1993**, *115*, 1568–1572.

[14] N. D. R. Barnett, R. E. Mulvey, W. Clegg, P. A. O'Neil, *J. Am. Chem. Soc.* **1993**, *115*, 1573–1574.

[15] D. Waldmuller, B. J. Kotsatos, M. A. Nichols, P. G. Williard, *J. Am. Chem. Soc.* **1997**, *I*, 5479–5480.

[16] A. C. Pöppler, H. Keil, D. Stalke, M. John, *Angew. Chem. Int. Ed.* **2012**, *51*, 7843–7846.

[17] M. D. Rausch, D. J. Ciappenelli, *J. Organomet. Chem.* **1967**, *10*, 127–136.

[18] M. Schlosser, *J. Organomet. Chem.* **1967**, *8*, 9–16.

[19] M. Schlosser, *Angew. Chem. Int. Ed.* **2005**, *44*, 376–393.

[20] M. Schlosser, S. Strunk, *Tetrahedron Lett.* **1984**, *25*, 741–744.

[21] C. Unkelbach, D. F. O'Shea, C. Strohmann, *Angew. Chem. Int. Ed.* **2014**, *53*, 553–556.

[22] P. Benrath, M. Kaiser, T. Limbach, M. Mondeshki, J. Klett, *Angew. Chem. Int. Ed.* **2016**, *55*, 10886–10889.

[23] G. Wittig, G. Pieper, G. Fuhrmann, *Berichte der Dtsch. Chem. Gesellschaft (A B Ser.* **1940**, *73*, 1193–1197.

[24] R. L. Bebb, H. Gilman, *J. Am. Chem. Soc.* **1939**, *61*, 109–112.

[25] V. Snieckus, *Chem. Rev.* **1990**, *90*, 879–933.

[26] F. Mongin, G. Quéguiner, *Tetrahedron* **2001**, *57*, 4059–4090.

[27] F. Marsais, G. Queguiner, *Tetrahedron* **1983**, *39*, 2009–2021.

[28] H. Gilman, W. Langham, L. Jacoby, *J. Am. Chem. Soc.* **1939**, *61*, 106–109.

[29] G. Wittig, U. Pockels, H. Dröge, *Berichte der Dtsch. Chem. Gesellschaft (A B Ser.* **1938**, *71*, 1903–1912.

[30] A. Music, D. Didier, *Synlett* **2019**, *30*, 1843–1849.

[31] R. G. Jones, H. Gilman, in *Org. React.*, **2011**, pp. 339–356.

[32] H. Gilman, A. H. Haubein, *J. Am. Chem. Soc.* **1945**, *67*, 1420–1421.

[33] H. Gilman, D. S. Melstrom, *J. Am. Chem. Soc.* **1946**, *68*, 103–104.

[34] F. Mongin, M. Schlosser, *Tetrahedron Lett.* **1996**, *37*, 6551–6554.

[35] C. Heiss, F. Leroux, M. Schlosser, *European J. Org. Chem.* **2005**, 5242–5247.

[36] C. Elschenbroich, *Organometallics. 3rd Ed.*, Wiley-VCH, Weinheim, **2006**.

[37] W. Schlenk, W. Schlenk jun., *Berichte der Dtsch. Chem. Gesellschaft (A B Ser.* **1929**, *62*, 920–924.

[38] R. M. Peltzer, J. Gauss, O. Eisenstein, M. Cascella, *J. Am. Chem. Soc.* **2020**, *142*, 2984–2994.

[39] P. Knochel, W. Dohle, N. Gommermann, F. F. Kneisel, F. Kopp, T. Korn, I. Sapountzis, V. A. Vu, *Angew. Chem. Int. Ed.* **2003**, *42*, 4302–4320.

[40] A. Krasovskiy, P. Knochel, *Angew. Chem. Int. Ed.* **2004**, *43*, 3333–3336.

[41] D. S. Ziegler, B. Wei, P. Knochel, *Chem. Eur. J.* **2019**, *25*, 2695–2703.

[42] R. Li-Yuan Bao, R. Zhao, L. Shi, *Chem. Commun.* **2015**, *51*, 6884–6900.

[43] A. Krasovskiy, P. Knochel, *Angew. Chem. Int. Ed.* **2004**, *43*, 3333–3336.

[44] A. Krasovskiy, V. Krasovskaya, P. Knochel, *Angew. Chem. Int. Ed.* **2006**, *45*, 2958–2961.

[45] P. García-Álvarez, D. V. Graham, E. Hevia, A. R. Kennedy, J. Klett, R. E. Mulvey, C. T. O'Hara, S. Weatherstone, *Angew. Chem. Int. Ed.* **2008**, *47*, 8079–8081.

[46] R. Neufeld, T. L. Teuteberg, R. Herbst-Irmer, R. A. Mata, D. Stalke, *J. Am. Chem. Soc.* **2016**, *138*, 4796–4806.

[47] R. E. Mulvey, *Acc. Chem. Res.* **2009**, *42*, 743–755.

[48] G. Wittig, *Angew. Chemie* **1958**, *70*, 65–71.

[49] G. Wittig, F. J. Meyer, G. Lange, *Justus Liebigs Ann. Chem.* **1951**, *571*, 167–201.

[50] E. Hevia, J. Z. Chua, P. García-Álvarez, A. R. Kennedy, M. D. McCall, *Proc. Natl. Acad. Sci. U. S. A.* **2010**, *107*, 5294–5299.

[51] D. R. Armstrong, W. Clegg, P. García-Úlvarez, A. R. Kennedy, M. D. McCall, L. Russo, E. Hevia, *Chem. Eur. J.* **2011**, *17*, 8333–8341.

[52] T. X. Gentner, M. J. Evans, A. R. Kennedy, S. E. Neale, C. L. McMullin, M. P. Coles, R. E. Mulvey, *Chem. Commun.* **2022**, DOI 10.1039/d1cc05379e.

[53] S. D. Robertson, M. Uzelac, R. E. Mulvey, *Chem. Rev.* **2019**, *119*, 8332–8405.

[54] A. Harrison-Marchand, F. Mongin, *Chem. Rev.* **2013**, *113*, 7470–7562.

[55] J. M. Gil-Negrete, E. Hevia, *Chem. Sci.* **2021**, *12*, 1982–1992.

[56] D. Tilly, F. Chevallier, F. Mongin, P. C. Gros, *Chem. Rev.* **2014**, *114*, 1207–1257.

[57] M. Uzelac, A. Hernán-Gómez, D. R. Armstrong, A. R. Kennedy, E. Hevia, *Chem. Sci.* **2015**, *6*, 5719–5728.

[58] M. Uzelac, A. R. Kennedy, A. Hernán-Gómez, M. Á. Fuentes, E. Hevia, *Zeitschrift fur Anorg. und Allg. Chemie* **2016**, *642*, 1241–1244.

[59] L. C. H. Maddock, A. Kennedy, E. Hevia, *Chimia (Aarau).* **2020**, *74*, 866–870.

[60] L. C. H. Maddock, M. Mu, A. R. Kennedy, M. García-Melchor, E. Hevia, *Angew. Chem. Int. Ed.* **2021**, *60*, 15296–15301.

[61] L. C. H. Maddock, T. Nixon, A. R. Kennedy, M. R. Probert, W. Clegg, E. Hevia, *Angew. Chem. Int. Ed.* **2018**, *57*, 187–191.

[62] L. M. Carrella, W. Clegg, D. V. Graham, L. M. Hogg, A. R. Kennedy, J. Klett, R. E. Mulvey, E. Rentschler, L. Russo, *Angew. Chem. Int. Ed.* **2007**, *46*, 4662–4666.

[63] V. L. Blair, W. Clegg, B. Conway, E. Hevia, A. Kennedy, J. Klett, R. E. Mulvey, L. Russo, *Chem. Eur. J.* **2008**, *14*, 65–72.

[64] M. Uzelac, I. Borilovic, M. Amores, T. Cadenbach, A. R. Kennedy, G. Aromí, E. Hevia, *Chem. Eur. J.* **2016**, *22*, 4843–4854.

[65] N. Tezuka, K. Hirano, A. J. Peel, A. E. H. Wheatley, K. Miyamoto, M. Uchiyama, *Chem. Sci.* **2020**, *11*, 1855–1861.

[66] S. Usui, Y. Hashimoto, J. V. Morey, A. E. H. Wheatley, M. Uchiyama, *J. Am. Chem.*

Soc. **2007**, *129*, 15102–15103.

[67] R. P. Davies, S. Hornauer, P. B. Hitchcock, *Angew. Chem. Int. Ed.* **2007**, *46*, 5191–5194.

[68] R. E. Mulvey, *Organometallics* **2006**, *25*, 1060–1075.

[69] M. Uchiyama, Y. Kondo, *J. Synth. Org. Chem.* **2006**, *64*, 1180–1190.

[70] L. M. Seitz, T. L. Brown, *J. Am. Chem. Soc.* **1966**, *88*, 4140–4147.

[71] S. E. Baillie, W. Clegg, P. García-Álvarez, E. Hevia, A. R. Kennedy, J. Klett, L. Russo, *Organometallics* **2012**, *31*, 5131–5142.

[72] S. E. Baillie, W. Clegg, P. García-Álvarez, E. Hevia, A. R. Kennedy, J. Klett, L. Russo, *Chem. Commun.* **2011**, *47*, 388–390.

[73] L. J. Bole, N. R. Judge, E. Hevia, *Angew. Chem. Int. Ed.* **2021**, *60*, 7626–7631.

[74] A. Desaintjean, T. Haupt, L. J. Bole, N. R. Judge, E. Hevia, P. Knochel, *Angew. Chem. Int. Ed.* **2021**, *60*, 1513–1518.

[75] S. Merkel, D. Stern, J. Henn, D. Stalke, *Angew. Chem. Int. Ed.* **2009**, *48*, 6350–6353.

[76] S. E. Baillie, T. D. Bluemke, W. Clegg, A. R. Kennedy, J. Klett, L. Russo, M. de Tullio, E. Hevia, *Chem. Commun.* **2014**, *50*, 12859–12862.

[77] J. W. Steed, J. L. Atwood, *Supramolecular Chemistry: Second Edition*, John Wiley & Sons, Ltd, **2009**.

[78] J. Hicks, P. Vasko, J. M. Goicoechea, S. Aldridge, *J. Am. Chem. Soc.* **2019**, *141*, 11000–11003.

[79] E. von Frankland, *Justus Liebigs Ann. Chem.* **1849**, *71*, 171–213.

[80] D. Seyferth, *Organometallics* **2001**, *20*, 2940–2955.

[81] J. A. Wanklyn, *Justus Liebigs Ann. Chem.* **1858**, *108*, 67–79.

[82] S. Reformatsky, *Berichte der Dtsch. Chem. Gesellschaft* **1887**, *20*, 1210–1211.

[83] M. W. Rathke, *Org. React.* **2011**, 423–460.

[84] E. Erdik, *Tetrahedron* **1992**, *48*, 9577–9648.

[85] P. Knochel, R. D. Singer, *Chem. Rev.* **1993**, *93*, 2117–2188.

[86] P. Knochel, J. J. Almena Perea, P. Jones, *Tetrahedron* **1998**, *54*, 8275–8319.

[87] P. Knochel, *Synlett* **1995**, *1995*, 393–403.

[88] P. Knochel, N. Millot, A. L. Rodriguez, C. E. Tucker, *Org. React.* **2004**, 417–759.

[89] A. O. King, N. Okukado, E. I. Negishi, *J. Chem. Soc. Chem. Commun.* **1977**, 683–684.

[90] J. A. Casares, P. Espinet, B. Fuentes, G. Salas, *J. Am. Chem. Soc.* **2007**, *129*, 3508–3509.

[91] A. E. H. Wheatley, M. Uchiyama, *Polar Organometallic Reagents*, Wiley & Sons Ltd, **2022**.

[92] A. Maercker, *Angew. Chem., Int. Ed. Engl.* **1987**, *26*, 972–989.

[93] R. E. Mulvey, V. L. Blair, W. Clegg, A. R. Kennedy, J. Klett, L. Russo, *Nat. Chem.* **2010**, *2*, 588–591.

[94] A. R. Kennedy, J. Klett, R. E. Mulvey, D. S. Wright, *Science* **2010**, *706*, 706–709.

[95] Y. Kondo, M. Shilai, M. Uchiyama, T. Sakamoto, *J. Am. Chem. Soc.* **1999**, *121*, 3539–3540.

[96] W. Clegg, S. H. Dale, E. Hevia, G. W. Honeyman, R. E. Mulvey, *Angew. Chem. Int. Ed.* **2006**, *45*, 2370–2374.

[97] M. Uchiyama, T. Miyoshi, Y. Kajihara, T. Sakamoto, Y. Otani, T. Ohwada, Y. Kondo, *J. Am. Chem. Soc.* **2002**, *124*, 8514–8515.

[98] M. Uchiyama, Y. Kobayashi, T. Furuyama, S. Nakamura, Y. Kajihara, T. Miyoshi, T. Sakamoto, Y. Kondo, K. Morokuma, *J. Am. Chem. Soc.* **2008**, *130*, 472–480.

[99] P. C. Andrikopoulos, D. R. Armstrong, H. R. L. Barley, W. Clegg, S. H. Dale, E. Hevia, G. W. Honeyman, A. R. Kennedy, R. E. Mulvey, *J. Am. Chem. Soc.* **2005**, *127*, 6184–6185.

[100] B. Conway, E. Hevia, A. R. Kennedy, R. E. Mulvey, *Chem. Commun.* **2007**, 2864–2866.

[101] W. Clegg, S. H. Dale, E. Hevia, L. M. Hogg, G. W. Honeyman, R. E. Mulvey, C. T. O'Hara, *Angew. Chem. Int. Ed.* **2006**, *45*, 6548–6550.

[102] L. Balloch, A. R. Kennedy, R. E. Mulvey, T. Rantanen, S. D. Robertson, V. Snieckus, *Organometallics* **2011**, *30*, 145–152.

[103] M. Uchiyama, Y. Matsumoto, D. Nobuto, T. Furuyama, K. Yamaguchi, K. Morokuma, *J. Am. Chem. Soc.* **2006**, *128*, 8748–8750.

[104] M. Uchiyama, Y. Matsumoto, S. Usui, Y. Hashimoto, K. Morokuma, *Angew. Chem. Int. Ed.* **2007**, *46*, 926–929.

[105] Y. Kondo, J. V. Morey, J. C. Morgan, H. Naka, D. Nobuto, P. R. Raithby, M. Uchiyama, A. E. H. Wheatley, *J. Am. Chem. Soc.* **2007**, *129*, 12734–12738.

[106] D. R. Armstrong, A. M. Drummond, L. Balloch, D. V. Graham, E. Hevia, A. R. Kennedy, *Organometallics* **2008**, *27*, 5860–5866.

[107] W. Clegg, B. Conway, E. Hevia, M. D. McCall, L. Russo, R. E. Mulvey, *J. Am. Chem. Soc.* **2009**, *131*, 2375–2384.

[108] D. R. Armstrong, V. L. Blair, W. Clegg, S. H. Dale, J. Garcia-Alvarez, G. W. Honeyman, E. Hevia, R. E. Mulvey, L. Russo, *J. Am. Chem. Soc.* **2010**, *132*, 9480–9487.

[109] A. R. Lepley, W. A. Khan, A. B. Giumanini, A. G. Giumanini, *J. Org. Chem.* **1966**, *31*, 2047–2051.

[110] D. R. Armstrong, W. Clegg, S. H. Dale, E. Hevia, L. M. Hogg, G. W. Honeyman, R. E. Mulvey, *Angew. Chem. Int. Ed.* **2006**, *45*, 3775–3778.

[111] D. R. Armstrong, J. García-Álvarez, D. V. Graham, G. W. Honeyman, E. Hevia, A. R. Kennedy, R. E. Mulvey, *Chem. Eur. J.* **2009**, *15*, 3800–3807.

[112] G. C. Forbes, A. R. Kennedy, R. E. Mulvey, B. A. Roberts, R. B. Rowlings, *Organometallics* **2002**, *21*, 5115–5121.

[113] W. Clegg, G. C. Forbes, A. R. Kennedy, R. E. Mulvey, S. T. Liddle, *Chem. Commun.* **2003**, *3*, 406–407.

[114] M. Balkenhohl, P. Knochel, *Chem. Eur. J.* **2020**, *26*, 3688–3697.

[115] J. Furukawa, N. Kawabata, J. Nishimura, *Tetrahedron Lett.* **1966**, *7*, 3353–3354.

[116] M. J. Rozema, A. Sidduri, P. Knochel, *J. Org. Chem.* **1992**, 1956–1958.

[117] L. Micouin, P. Knochel, *Synlett* **1997**, *1997*, 327–328.

[118] F. F. Kneisel, M. Dochnahl, P. Knochel, *Angew. Chem. Int. Ed.* **2004**, *43*, 1017–1021.

[119] F. F. Kneisel, H. Leuser, P. Knochel, *Synthesis* **2005**, *2*, 2625–2629.

[120] T. Harada, D. Hara, K. Hattori, A. Oku, *Tetrahedron Lett.* **1988**, *29*, 3821–3824.

[121] T. Harada, Y. Kotani, T. Katsuhira, A. Oku, *Tetrahedron Lett.* **1991**, *32*, 1573–1576.

[122] Y. Kondo, N. Takazawa, C. Yamazaki, T. Sakamoto, *J. Org. Chem.* **1994**, *59*, 4717–4718.

[123] Y. Kondo, M. Fujinami, M. Uchiyama, T. Sakamoto, *J. Chem. Soc. Perkin Trans. 1* **1997**, 799–800.

[124] M. Uchiyama, M. Kameda, O. Mishima, N. Yokoyama, M. Koike, Y. Kondo, T. Sakamoto, *J. Am. Chem. Soc.* **1998**, *120*, 4934–4946.

[125] M. Uchiyama, T. Furuyama, M. Kobayashi, Y. Matsumoto, K. Tanaka, *J. Am. Chem. Soc.* **2006**, *128*, 8404–8405.

[126] N. T. T. Chau, M. Meyer, S. Komagawa, F. Chevallier, Y. Fort, M. Uchiyama, F. Mongin, P. C. Gros, *Chem. Eur. J.* **2010**, *16*, 12425–12433.

[127] T. D. Bluemke, W. Clegg, P. García-Alvarez, A. R. Kennedy, K. Koszinowski, M. D. McCall, L. Russo, E. Hevia, *Chem. Sci.* **2014**, *5*, 3552–3562.

Chapter 2: Assessing Metalating Ability of Sodium Zincates Containing Sterically Demanding Bis(amide) Ligand

This Chapter is adapted with permission from: P. Mastropierro, Z. Livingstone, S. D. Robertson, A. R. Kennedy, E. Hevia Structurally Mapping Alkyl and Amide Basicity in Zincate Chemistry: Diversity in the Synthesis of Mixed Sodium-Zinc Complexes and Their Applications in Enolate Formation *Organometallics* **2020**, *39*, 4273-4281. DOI: 10.1021/acs.organomet.0c00339 Copyright 2020 American Chemical Society.

Contributing authors to their manuscript and their role:

Pasquale Mastropierro: Conceived the project, performed most of the experimental work, analysed the data, wrote the first draft of the manuscript and the supporting information, measured and solved structure of compounds **3**.

Zoe Livingstone: Synthetized compounds **5**, **11**, **12**; measured and solved structure of compounds **5**, **11**.

Stuart D. Robertson: Measured and solved structure of compound **12**.

Alan R. Kennedy: Checked the accuracy of X-Ray diffraction data processing.

Eva Hevia: Principal Investigator, conceived the project, secured the funding, directed the work, and wrote the final version of the manuscript with contributions from all authors.

2.1 General introduction to this chapter

The highly sterically demanding ligands such as β-diketiminate or silyl bis(amide) have found many applications in main group metal chemistry for metalation,[1,2] catalysis,[3,4] stabilization of low valent oxidation state[5,6] and small molecule activation[7] just to name few. In this chapter the structure of new sodium zincates supported by a bulky bidentate ligand and their reactivity will be discussed. Therefore, some highlights of the chemistry of the bidentate ligands bis silyl(amide) and the related β-diketiminate will be presented in this introduction, focusing on the alkali-earth metal and zinc.

The sterically encumbered bidentate β-diketiminate ligands incorporate the metal centre in a planar six-member ring with a delocalized imine/amide motif, and furnish a kinetic shelter thanks to a variety of encumbered substituent (such as 2,6-$^{i}Pr_2$-C_6H_3 or Dipp and 2,4,6-Me_3-C_6H_2).[8] Those characteristics allowed the isolation of the first compound with a formal Mg(I) centre, [(^{Dipp}Nacnac)MgMg(^{Dipp}Nacnac)] (^{Dipp}Nacnac= {(Ar*)NC(Me)}$_2$CH Ar*= 2,6-diisopropylphenyl) characterized by the unusual Mg-Mg contact. This compound broke the dogma of magnesium having only one possible oxidation state: +2 (**Figure 2. 1**).[5] It was obtained via reduction of correspondent Mg(II) species [MgI(Et_2O)(^{Dipp}Nacnac)] using sodium

or potassium mirror, or alkali metal supported by alkali-metal halides.[5,9,10] Since its discovery in 2007, several groups across the world have studied its reactivity, finding many interesting applications as a reducing agent[11,12] or in small molecule activation.[7,13–15]

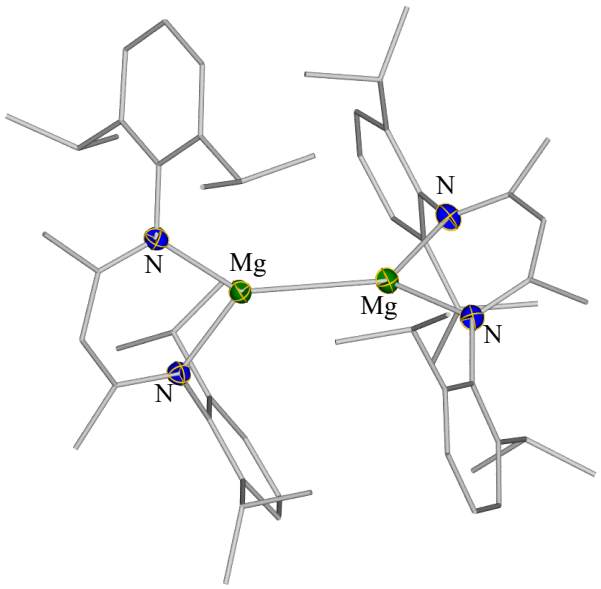

Figure 2. 1 *Molecular structure of [(Dipp Nacnac)MgMg(Dipp Nacnac)]. Hydrogen atoms are omitted, and carbon atoms are drowned as wireframe for clarity. Thermal ellipsoids are rendered with 50% probability*

Following the same synthetic rationale and using the same kind of ligand, Harder *et al.*, were recently able to reach a step forward, achieving $[\{(BDI^*)Mg\}^-\{Na^+\}]_2$ (BDI*= HC{C(tBu)N[2,6-(3-pentyl)-phenyl]}$_2$), the first isolated compound with a formal Mg(0) atom (see **Scheme 2. 1**).[6]

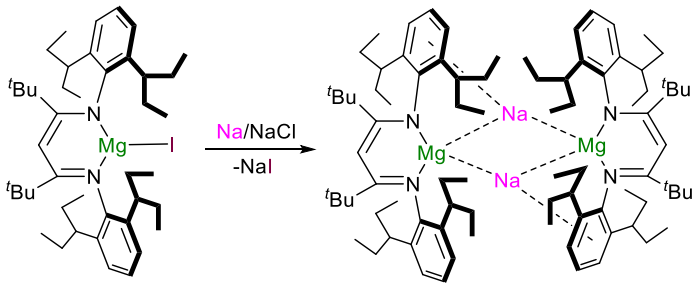

Scheme 2. 1 *Synthesis of $[\{(BDI^*)Mg\}^-\{Na^+\}]_2$ reducing the correspondent magnesium iodide [(BDI*)MgI] with excess of metal sodium supported on NaCl*

β-diketiminate ligands have also been applied in the chemistry of alkali-earth metal hydrides which, owing to their steric bulk, can break the insoluble clusters of $[MgH_2]_\infty$ into discrete molecular units, in the form of the dimeric $[\{(^{Dipp}Nacnac)MgH\}_2]$.[16,17] This compound can be prepared via metathesis between [(Dipp Nacnac)Mg^{n}Bu] and phenylsilane heating at reflux for 2 days in hexane.[18]

The magnesium (II) alkyl species coordinated by β-diketiminate was used also as a catalyst in hydroamination reactions of alkenes[3]. Calcium hydrides supported by β-diketiminate ligand have also shown promise in catalysis. [19,20] Thus [(^{Dipp}Nacnac)CaH(THF)]$_2$ catalysed the hydrogenation of alkenes succeeding in completely reduction of styrene in 15h at room temperature in benzene,[21] and also in the hydrosilylation of ketones and pyridines, in 3h at 50°C or in 24h at 60°C respectively (**Scheme 2. 2**). [4,22] In all of those three reactions a good selectivity was found. In case of the reduction of the styrene, the major product was ethane-1,2-diyldibenzene achieved in 81% yield, with the rest represented by a mixture of oligomers including dimers (identified as the cyclodimerization product 1-methyl-3-phenylindane), trimers and tetramers.[21] The hydrosilylation of the ketones was very selective towards the formation of the correspondent dialkoxide-silane (see **Scheme 2. 2**); in particular the reaction of 2 equivalents of cyclohexanone affords the major product in 86% yield with very small amount of side product identified in the trialkoxide silane and the correspondent product of enolization.[4] Similarly when pyridine and phenylsilane reacted under this calcium hydride catalysis the only product isolated was the silane substituted with a double 1,2-dihydropyridine (**Scheme 2. 2**).[22]

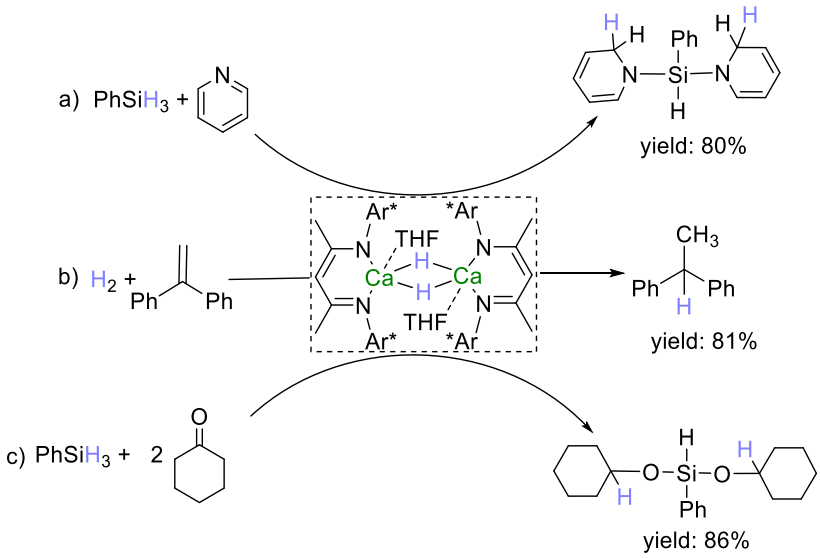

Scheme 2. 2 *Reactions catalysed by the [(^{Dipp}Nacnac)CaH(THF)]$_2$ a) hydrosilylation of pyrimidine, 5% catalyst loading, C_6D_6, 24h at 60°C b) hydrogenation of alkenes, 5% catalyst loading 20 atm of H_2, 15h at RT c) hydrosilylation of ketones. 1.25% catalyst loading, C_6D_6 3h at 50°C Ar*= 2,6-diisopropylphenyl. For clarity only the major product is shown (Ar*= 2,6-diisopropylphenyl)*

Our group has also contributed to the chemistry of magnesium supported by β-diketiminate ligands.[1,2,23–25] The sterically encumbered base [(^{Dipp}Nacnac)Mg(TMP)] (TMP= 2,2,6,6-tetramethylpiperidide) has demonstrated to be a valuable base for the deprotonation of heterocycles.[1,2,23,24] Taking advantages of the β-diketiminate ligand to isolate the metalated species and stopping side-reactions. For example of benzothiazole and N-methyl benzimidazole were metalated and isolated at room temperature without undergoing to ring-opening reaction.[23] The protection from side reactions of the metalated product was beneficial also for the isolation of metalated fluoroarenes at room temperature,[1,24] because the presence

of the ligand prevented the formation of benzyne intermediate via elimination of inorganic fluorine salt, which affects those substrates when they are metalated with more conventional metallating agent such as ^{t}BuLi.[26] Moreover the presence of the bulky ligand played a role in dictating the regioselective of the metalation, in fact pyrazine was selectively metalated to the α position of the heteroatom, at room temperature, avoiding multiple metalation or homocoupling side reactions,[1] that occurred when this substrates was metalated by a base without this steric shelter, such as LiTMP[27] or $Mg(TMP)_2{\cdot}2LiCl$.[28] The regioselectivity metalation at 2-position for N-heterocycle using [(^{Dipp}Nacnac)Mg(TMP)] was observed also in the metalation of 4-picoline (in THF at 69°C) and it was crucial to obtain the product of homocoupling 4,4'-Me_2-2,2'-bipyridine after oxidation by O_2, that derived from the rapid 1,2 addition by a second equivalent of 4-picoline. Bases without chelating ligand such as $Mg(TMP)_2$ preferred the metalation of the same substrate at the methyl group in position 4(**Scheme 2. 3**).[2]

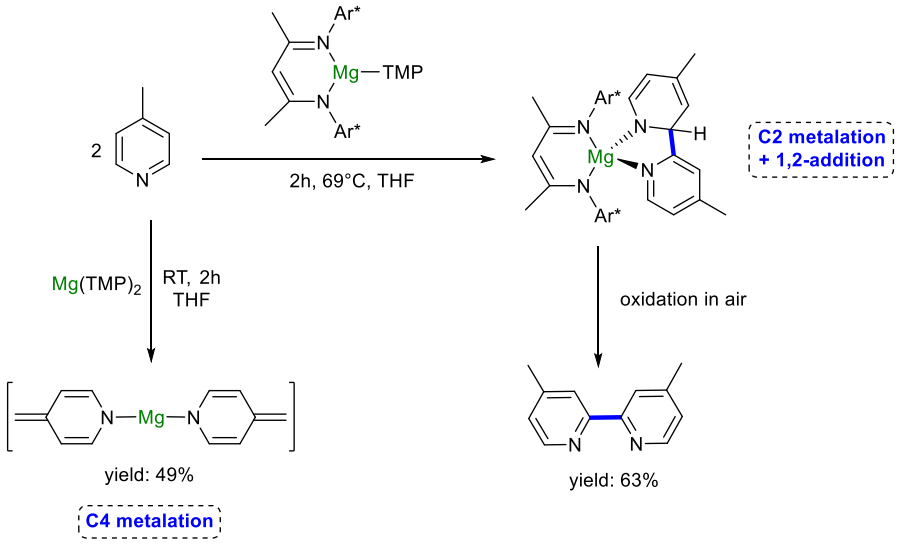

Scheme 2. 3 *Divergent metalation of 4-picoline using $Mg(TMP)_2$ or [(^{Dipp}Nacnac)Mg(TMP)]. The farmer afforded the C4 metalation product, the latter promoted a C2 metalation that led to 4,4'-Me_2-2,2'-bipyridine (Ar*= 2,6-diisopropylphenyl, TMP= 2,2,6,6-tetramethylpiperidide)*

The alkyl analogue, [(^{Dipp}Nacnac)Mg(^{n}Bu)(THF)] was a less reactive reagent in Mg/H exchange due to the less kinetical basicity of the ^{n}Bu anion compared to TMP^-, in fact when [(^{Dipp}Nacnac)Mg(^{n}Bu)(THF)] reacted with pyridine only the formation of a Lewis acid-base adduct was observed, where pyridine displaced the THF as donor. Contrastingly [(^{Dipp}Nacnac)Mg(TMP)] promoted the metalation of pyridine and the subsequent homocoupling.[2] However taking advantage of the superior nucleophilicity of ^{n}Bu moiety and the unique environment around the metal centre furnished by the β-diketiminate ligand, [(^{Dipp}Nacnac)Mg(^{n}Bu)(THF)] showed the ability of activating the robust C-F bond[29] of 2-(2,4-difluorophenyl)pyridine affording the product of nucleophilic substitution (2-(2-butyl-4-fluorophenyl)pyridine) and the inorganic salt [{(^{Dipp}Nacnac)MgF(THF)}$_2$] in mild condition (24 hours at room temperature) without using any transition metal catalyst.[24] In sharp contrast [(^{Dipp}Nacnac)Mg(TMP)], on the same substrate, simply abstracted the most acidic proton (the

one flanked by the two fluorines), forming [(^{Dipp}Nacnac)Mg($C_{11}H_6F_2N$)(THF)].[1] This reactivity was expanded to β-diketiminate magnesium amide complexes (if more nucleophilic amide than TMP were used, such as piperidinide, dibuthylamide and morpholinide) (**Scheme 2. 4**). The fluorine-nitrogen aromatic substitution proceeded at room temperature and in short time (1 hour) when assisted by the presence of a pyridyl directing group or perfluorinated octafluorotoluene. With hexafluorobenzene the assistance of microwave irradiation was required (125°C for 20 minutes).[25]

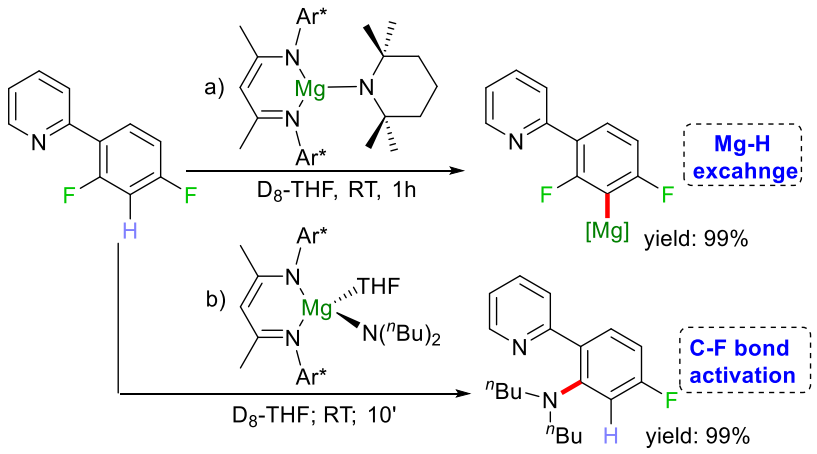

Scheme 2. 4 *Contrasting reactivity of magnesium amides supported by β-diketiminate towards 2-(2,4-Difluorophenyl)pyridine, a) Mg-H exchange and b) C-F bond activation (Ar*= 2,6-diisopropylphenyl)*

Other relevant bidentate ligand that are used in bimetallic chemistry are the dianionic silyl bis(amide)s[30,31]: $\{CH_2SiMe_2(NAr^*)\}_2^{2-}$ and $\{Ph_2Si(NAr^*)_2\}^{2-}$ the former was recently introduced from Hill and coworkers to prepare Mg(I) and Al(I) species.[32,33] The latter[34] was used in our group to investigate the chemistry of the sodium magnesiates.[35–37]

Taking advantages of the unique coordination environment offered by the sterically encumbered dianion $\{Ph_2Si(NAr^*)_2\}^{2-}$ our group [37] was able to isolate a sodium magnesiate containing an unusual quinoxaline radical anion – the product of a single electron transfer (SET) process between $[\{Ph_2Si(NAr^*)_2Mg(THF)(^nBu)\}^-\{Na(THF)_6\}^+]$ and quinoxaline. Contrastingly, homoleptic $NaMg(CH_2SiMe_3)_3$, which does not contain a sterically demanding bis(amide) support, promotes the C2 nucleophilic addition of its monosilyl group (see **Scheme 2. 5**).

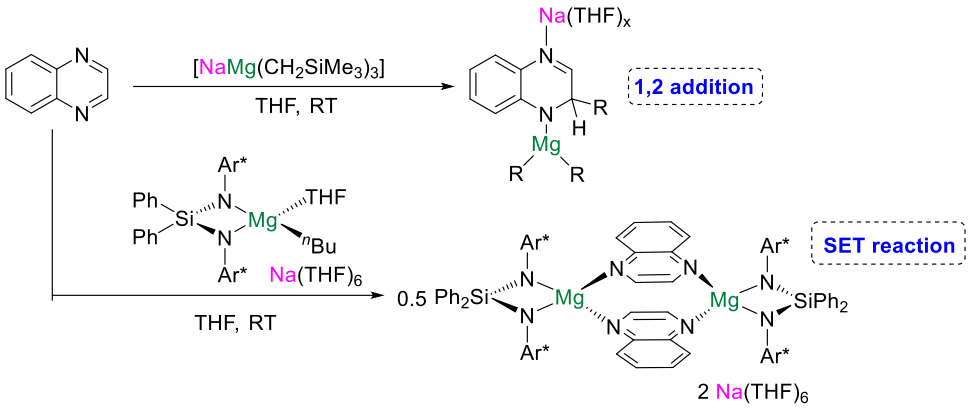

Scheme 2. 5 *Reactivity of quinoxaline with sodium magnesiates. With trialkyl magnesiate $NaMgR_3$ it undergoes to 1,2 addition, with $[\{Ph_2Si(NAr^*)_2Mg(^nBu)\}^-\{Na(THF)_6\}^+]$ there is a SET reaction ($R= CH_2SiMe_3$, Ar^*= 2,6-diisopropylphenyl)*

Sodium magnesiate $[\{Ph_2Si(NAr^*)_2Mg(THF)(^nBu)\}^-\{Na(THF)_6\}^+]$ has also demonstrated to be reactive as base, being able to deprotonate activated substrates (in terms of pKa values) like pyrrole, N-methyl benzimidazole and disopropylaniline and isolate their product of metalation[36]. Interestingly the bis(amide) $\{Ph_2Si(NAr^*)_2\}^{2-}$ did not act only as a mere spectator, but took actively part in the reactivity acting as base itself.[36]

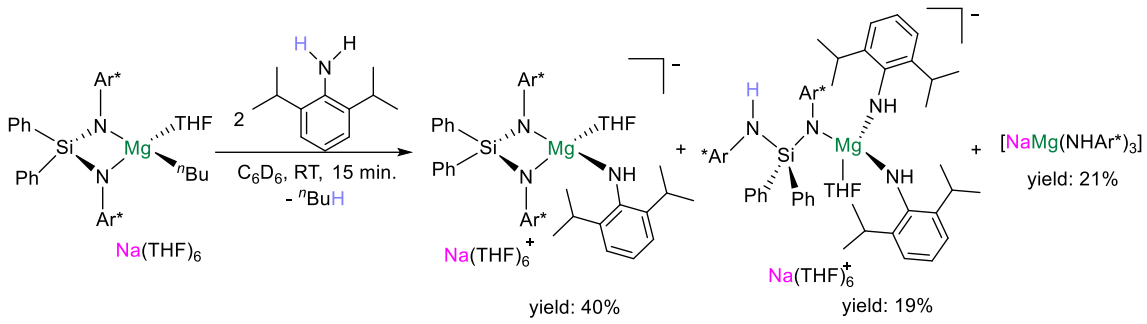

Scheme 2. 6 *Metalation of 2,6 diisopropylaniline using $[\{Ph_2Si(NAr^*)_2Mg(THF)(^nBu)\}^-\{Na(THF)_6\}^+]$. ($Ar^*$= 2,6-diisopropylphenyl)*

The active participation in the reaction is even more dramatic when a substrate like benzothiazole was used.[35] The presence of the bulky substituent is fundamental in activating the substrate in a cascade process that includes ring-opening and nucleophilic addition (see **Scheme 2. 7**). This contrasted with the straightforward C2 metalation observed when using another magnesium base such as a Turbo Hasuer base.[38]

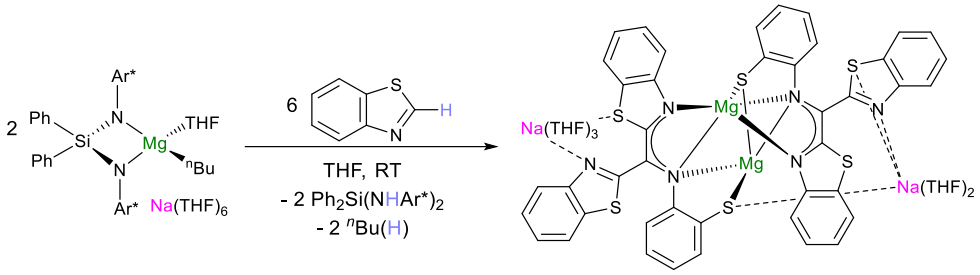

Scheme 2. 7 *Activation of Benzothiazole by [{Ph$_2$Si(NAr*)$_2$Mg(THF)(^{n}Bu)}$^-$ {Na(THF)$_6$}$^+$]* (Ar*= 2,6-diisopropylphenyl)

Those dianionic ligands have also be explored in zinc chemistry. Tsai and co-workers isolated and characterized a rare Zn(I) complex,[39] reducing with potassium graphite (KC_8) the correspondent Zn(II) [Me$_2$Si(NAr*)$_2$Zn]$_2$ furnishing [K$_2${(η^2-Me$_2$Si(NAr*)$_2$)ZnZn(η^2-Me$_2$Si(NAr*)$_2$)}], which structure was elucidated by x-ray crystallography (**Scheme 2. 8**).

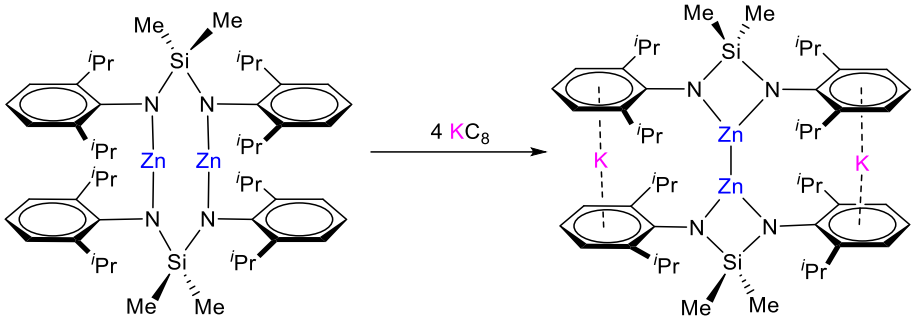

Scheme 2. 8 *Reduction of [Me$_2$Si(NAr*)$_2$Zn]$_2$ in [KMe$_2$Si(NAr*)$_2$Zn]$_2$ using KC_8* (Ar*= 2,6-diisopropylphenyl)

2.2 Aims

Building on previous study on zincate chemistry, here we focus on the synthesis of a new family of sodium zincate containing the sterically demanding bis(amide) ligand {Ph$_2$Si(NAr*)$_2$}$^{2-}$ and an assessing their reactivity towards ketones to form enolate compounds.

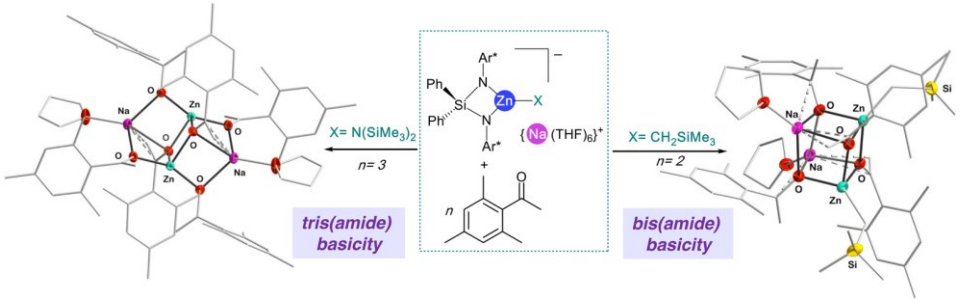

Scheme 2. 9 *Different behaviours in metalation of the 2',4',6'-trimethylacetophone of zincates supported by silyl bis(amide) ligands. The resulting enolate changes based on the anions that surrounded the metal centre.*

2.3 Introduction from the paper

Alkali-metal zincates were pioneered by Wanklyn more than 160 years ago, with the discovery of $NaZnEt_3$, obtained by reacting sodium metal with $ZnEt_2$[40,41]. For many years they lay in obscurity as mere curiosities but over the past two decades they have emerged as highly versatile reagents in organic synthesis enabling direct zincation of a wide range of aromatic substrates via deprotonative metalation or metal-halogen exchange,[42–47] reactions that traditionally have been considered the domain of more polar organometallic reagents such as organolithium or Grignard reagents.[48] Some key landmarks in this area include Uchiyama's $Li_2Zn^tBu_4$, which effectively promotes direct Zn-I and Zn-Br exchange reactions of an assortment of aromatic substrates with remarkable functional group tolerance (**Scheme 2. 10**)

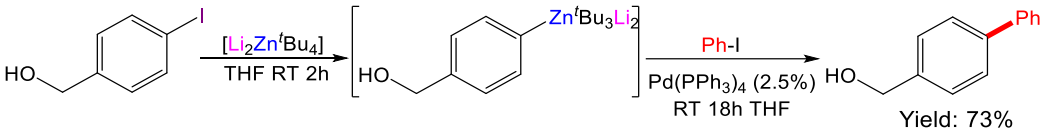

Scheme 2. 10 *Metal Halogen Exchange reaction mediated by [$Li_2Zn^tBu_4$], followed by a Negishi cross coupling type reaction.*

As well the development of strong, regioselective deprotonating reagents powered by TMP (2,2,6,6-tetramethylpiperidide) ligands such as Knochel's turbo reagents TMPZnCl·LiCl and $(TMP)_2Zn·2MgCl_2·2LiCl$ which allow access to highly functionalised aryl and heteroaryl zinc organometallics.[49–54] More often than not, these bimetallic reagents are prepared in situ by either co-complexation of the single-metal reagents or salt metathesis reactions, and limited attention has been given to their isolation or characterization. Shedding some light in this intriguing field, through the structural authentication of a family of heteroleptic alkyl/amide zincates $[(L)M^I(TMP)Zn^tBu_2]$ (M^I= Li, L=THF; M^I= Na, L=TMEDA),[55,56] Mulvey has developed the concept of alkali-metal-mediation-zincation (AMMZn) where both metals, M^I and Zn, work cooperatively to facilitate the direct zincation of a wide range of aromatic molecules as well as metallocenes.[42,43,47] The reach of these bimetallic partnerships has been recently exemplified in the unprecedented regioselective 1,1',3,3'-tetrazincation of ferrocene achieved by using a fourfold excess of $[Na(TMP)Zn^tBu_2]$ (**Figure 2. 2**).[57]

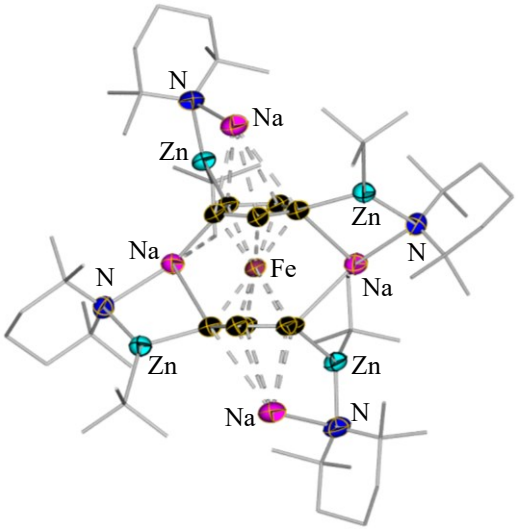

Figure 2. 2 *Molecular structures of [Na$_4$(TMP)$_4$Zn$_4$^{t}Bu$_4${(C$_5$H$_3$)$_2$Fe}, obtained via metalation of ferrocene using the zincate [Na(TMP)Zn^{t}Bu$_2$]. in 4-fold excess. Hydrogen atoms and minor disordered component are omitted for clarity. Carbon atoms are drawn as wire frame, except the ferrocene moiety*

The ability of these heteroleptic zincates to act as amido and/or alkyl bases has stimulated activity and debate, suggesting that kinetic amido basicity seems to be preferred. Despite the thermodynamic product of alkyl basicity was usually obtained as final product (**Scheme 2. 11**).[58–61]

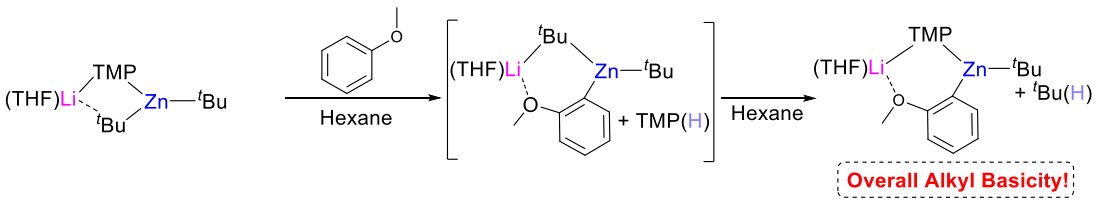

Scheme 2. 11 *Proposed two-step mechanism for the zincation of anisole by lithium zincate [(THF)Li(TMP)Zn^{t}Bu$_2$]in hexane*

A common strategy in all these studies is to use sterically demanding ligands such as ^{t}Bu and TMP groups which are not only basic and reactive but that can also contribute to the overall stability of metalation products, by providing steric shelter to the sensitive anions generated in the zincation process.[62] In this regard, within magnesiate chemistry we have recently investigated the synthesis and reactivity of sodium magnesiates containing the bulky silyl(bis)amide ligand {Ph$_2$Si(NAr*)$_2$}$^{2-}$.[35–37] Interestingly, while in some cases this sterically demanding ligand acts as a steric stabilizer enabling the isolation of radical anions[37] or the magnesiation of N-heterocyclic molecules such as N-methyl benzimidazole,[36] on other occasions {Ph$_2$Si(NAr*)$_2$}$^{2-}$ can also act as a base, facilitating metalation of amines[36] or activation of small organic molecules such as benzothiazole.[35]

Within zinc chemistry Tsai has exploited the steric protection of bulky silyl(bis)amide ligands for stabilizing Zn(I) complexes possessing Zn-Zn bonds,[39] but to date these ligands have not been exploited in a systematic way to access alkali-metal zincates. To expand their knowledge

base, here we report the synthesis and characterization of a new family of sodium zincates derived from $Ph_2Si(NHAr^*)_2$ (**1**) and investigate their ability to access zinc enolates via direct zincation of ketones, using 2,4,6-trimethylacetophenone (**7**) as a model substrate. By structurally mapping these reactions, we shed light on the different strategies available to access this new family of bimetallic complexes, depending on the base employed for the deprotonation of **1**, advancing the understanding of cooperative effects in zincate chemistry and the preferred kinetic reactivity of Zn-N bonds in comparison with Zn-C bonds. Furthermore, the application of these new zincates for enolate formation, reveals not only the unexpected amplification of the metallating power of the silyl(bis)amide ligand $\{Ph_2Si(NAr^*)_2\}^{2-}$, but also its key role in determining the composition of the developing enolate.

2.4 Results and discussion

2.4.1 Synthesis of Sodium Zincates Featuring a Silyl Bis(amide) Ligand

To prepare new zincates derived from the bis(amino)silane **1**, it needs to be doubly deprotonated to generate into the dianionic silylbis(amide) ligand.[31,63,64] We focussed on this N-aryl derivative, containing bulky and readily available 2,6-diisopropylphenyl groups (Ar*) since related ligand sets have found applications as dianionic ancillary ligands to support main group elements[65,66] and transition metals.[67–71] We began by investigating the deprotonation of **1** using sodium zincate $[NaZn(HMDS)_2R]$ (**2**) [$R = CH_2SiMe_3$; $HMDS = N(SiMe_3)_2$], which can be prepared straightforwardly in situ by co-complexation of the homometallic components $NaCH_2SiMe_3$ and $Zn(HMDS)_2$[72–76]. This co-complexation was carried out at room temperature over 12 h affording the heteroleptic sodium zincate $[\{Ph_2Si(NAr^*)_2Zn(R)\}^-\{Na(THF)_6\}^+]$ (**3**) in a 71 % crystalline yield (**Scheme 2. 12**)

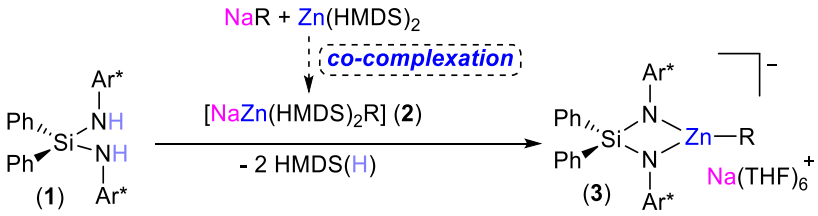

Scheme 2. 12 *Metalation of **1** with sodium zincate **2**, all reactions were carried out at room temperature, using hexane/Et_2O mixture as solvent. THF was also added to aid crystallization. R= CH_2SiMe_3, HMDS= $N(SiMe_3)_2$, Ar*=2,6-diisopropylphenyl*

^{1}H-NMR spectrum in deuterated benzene provided confirmation of the double-deprotonation of **1** as well as of the presence of the alkyl CH_2SiMe_3 group on zinc (**Figure 2. 3**). Thus, along with the disappearance of a distinctive broad resonance at 3.51 ppm attributed to the NHAr* groups of **1** in ^{1}H NMR spectrum, a new set of signals is observed for the newly formed dianionic bis(amide). The most informative resonance for the alkyl group is that of the Zn-CH_2 unit which appears significantly downfield at -0.70 ppm compared to that observed for the more polarised sodium precursor NaR (at -2.06 ppm), and closer to that found for ZnR_2 (-0.63 ppm), following the same trend previously reported in zincate chemistry.[77,78]

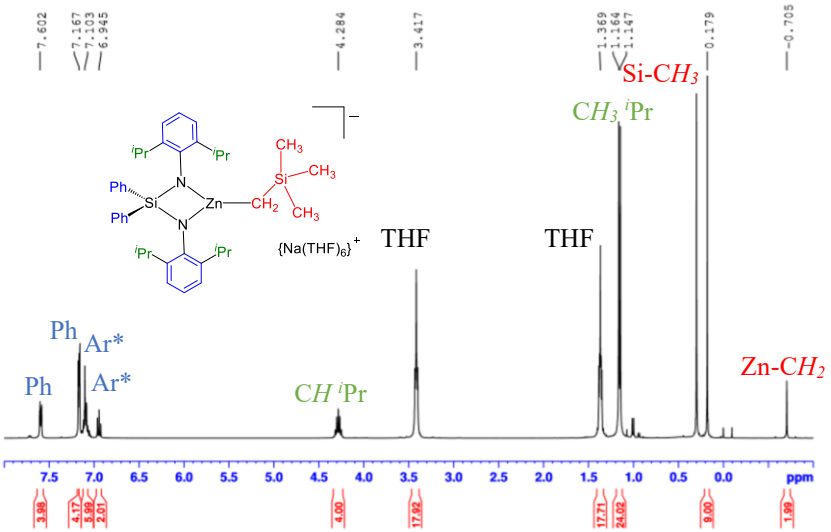

Figure 2. 3 *^{1}H-NMR (C_6D_6, 400 MHz, 298 K) spectrum of **3**. Ar*= 2,6-diisopropylphenyl*

Confirming the bimetallic structure of **3**, X-ray crystallographic studies revealed a solvent-separated ion pair (SSIP) motif, comprising a sodium cation solvated by six THF molecules in a distorted octahedral geometry. Its anionic moiety is made up of a trigonal planar Zn centre (sum of angles around Zn, 359.7 (6)°) which binds to the bidentate silyl-bis(amido) ligand [Zn-N, 1.991(4) and 1.984(4) Å] resulting from the di-deprotonation of **1**, and the terminal monosilyl group [Zn-C, 1.964(5) Å]. Interestingly while the Zn-N distances in **3** compare well with those found in other zincates which contain a terminal amido group,[79–83] the Zn-C in **3** is relatively short in comparison to those witnessed in other zincate complexes containing the same terminally attached alkyl group [ranging from 2.005 to 2.086 Å],[84–88] which is rather surprising considering the large steric bulk of the bis(amide) co-ligand present in **3** (see **Figure 2. 4**)

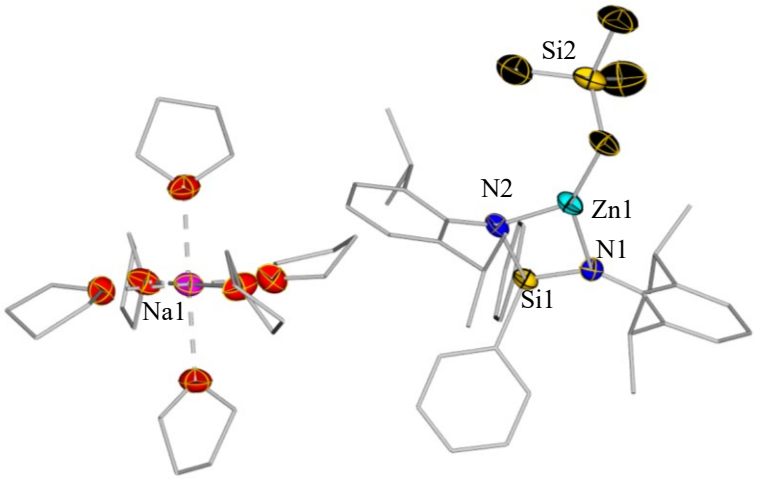

Figure 2. 4 *Ion-pair structure of **3**. Thermal ellipsoids are rendered at 30% probability. Hydrogen atoms and disordered components in THF and CH_2SiMe_3 are omitted, carbon atoms of $\{Ph_2Si(NAr^*)_2\}^{2-}$ and THF are drawn as wire frame for clarity. Selected distances (Å) and angles (°)*

N2-Zn1 1.978(4), N1-Zn1 1.999(4), Zn1-C37 1.956(5), N2-Zn1-N1 8056(17), N2-Zn1-C37 138.0(2), N1-Zn1-C37 141.4(2), N2-Si1-N1 97.28(19)

The selective formation of **3** indicates a clear preference for heteroleptic zincate **2** to act as a bis(amide) base upon metallating **1** with the concomitant formation of two equivalents of HMDS(H). Related to these findings, computational and structural studies on the reactivity of the heteroleptic alkyl/amide sodium zincate [(TMEDA)NaZn(TMP)^{t}Bu$_2$] for the direct zincation of arenes have established its dual amide/alkyl basicity.[58–61] Thus while initial deprotonation is carried out by the TMP amide group, forming a [(TMEDA)NaZn(aryl)^{t}Bu$_2$] intermediate and releasing TMP(H), both species can react together subsequently, via one alkyl group of this intermediate to give [(TMEDA)NaZn(TMP)(aryl)^{t}Bu] as the final isolated product of the reaction.[61] This duality of behaviour does not seem to be in operation for the synthesis of **3**, since even when prolonged reaction times are employed (up to 48h), no further reactivity of the remaining CH_2SiMe_3 group in **3** with the concomitant HMDS(H) (produced during the metalation of **1**) is observed. This lack of secondary alkyl basicity correlates well with the strong carbophilicity of zinc, the relatively short Zn-C bond present in **3** and the reduced kinetic basicity previously noted for Zn-C bonds in single metal organozinc reagents. This has been noticed on using dialkylzinc reagents for the deprotonation of amines or alcohols. While potentially they could be used as two-fold bases, generally only one alkyl group is labile.[89–91]

Interestingly, **1** can be di-deprotonated by tris(alkyl) sodium zincate $NaZnR_3$ (**4**) (prepared in situ by reaction of NaR and ZnR_2, **Scheme 2. 13**) furnishing **3** in a 63% yield, indicating that when part of the zincate, two out of the three alkyl groups are active towards metalation.[91,92] Demonstrating the power of the cooperative partnership of sodium and zinc, while for forming **3**, silyl bis(amine) **1** has formally undergone di-zincation, **1** is completely inert towards metalation when confronted with ZnR_2 even under forcing refluxing conditions (**Scheme 2. 13**).

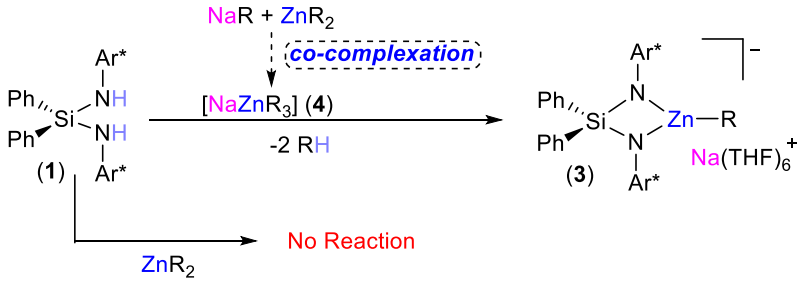

Scheme 2. 13 *Contrasting metalation towards **1** with sodium zincate **4**, all reactions were carried out at room temperature, using hexane/Et_2O mixture as solvent. THF was also added to aid crystallization. R= CH_2SiMe_3, Ar*=2,6-diisopropylphenyl*

With the aim of preparing an amide derivative of **3**, we next probed an alternative strategy, using a stepwise metalation approach, employing two single-metal reagents in sequence (**Scheme 2. 14**). Previous work by Coles has shown that selective monometalation of bis(silyl) amines can be accomplished using common group 1 reagents such as NaH or BuLi.[69] Using

a stepwise approach, **1** was first reacted with one molar equivalent of NaR to furnish [{$Ph_2Si(NHAr^*)(NAr^*)Na\}_2$] (**5**) which in turn was reacted with one equivalent of the $Zn(HMDS)_2$ to afford sodium zincate [{$Ph_2Si(NAr^*)_2Zn(HMDS)\}^-\{Na(THF)_6\}^+$] (**6**) in a 80% yield (**Scheme 2. 14**). Taking into account that the weak base $Zn(HMDS)_2$ fails to metalate **1** on its own, we envisage the formation of **6** takes place via an intermediate bimetallic species (see **Scheme 2. 14**) resulting from co-complexation of **5** with the zinc amide. The anionic activation on zinc by formation of the putative zincate species along with the close proximity of the NHAr* group should facilitate intramolecular deprotonation of the remaining N-H bond, to yield **6**

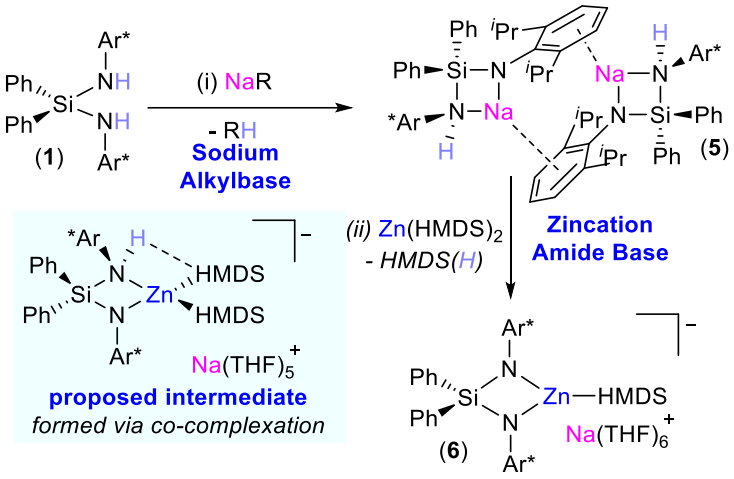

Scheme 2. 14 *Stepwise dideprotonation of **1** using single metal reagents NaR and $Zn(HMDS)_2$ in sequence to afford amide sodium zincate 6. (i) RT, hexane, 1h; (ii) THF, 60°C, 10h. 5 and 6 were isolated as crystalline solids in 66 and 80% respectively, see Experimental Section for details*

The molecular structures of **5** and **6** (**Figure 2. 5** and **Figure 2. 6** respectively) were established by X-ray crystallographic studies. Homometallic **5** exhibits a centrosymmetric dimeric arrangement (**Figure 2. 5**), with sodium bidentately bound by the monoanionic chelate {$Ph_2Si(NHAr^*)(NAr^*)\}^-$ that results from monodeprotonation of **1**. Unsurprisingly, the Na-N(amide) bond [Na1-N1, 2.380(2) Å] is noticeably shorter than the Na-N(amine) bond [Na1-N2, 2.486(3) Å]. Sodium completes its coordination sphere by engaging in a η^6-fashion with the aryl ring of the amido group of the neighbouring unit, thus effecting dimerization [Na…C distances ranging from 2.752(3)-2.960(3) Å].[92,93] The structure of **5** contrasts markedly with that reported by Coles for the methyl analogue [$(THF)_3Na\{Me_2Si(NHAr^*)(NAr^*)\}$] which is monomeric with the silyl(amide)(amine) ligand coordinated in terminally through its amide group.[70]

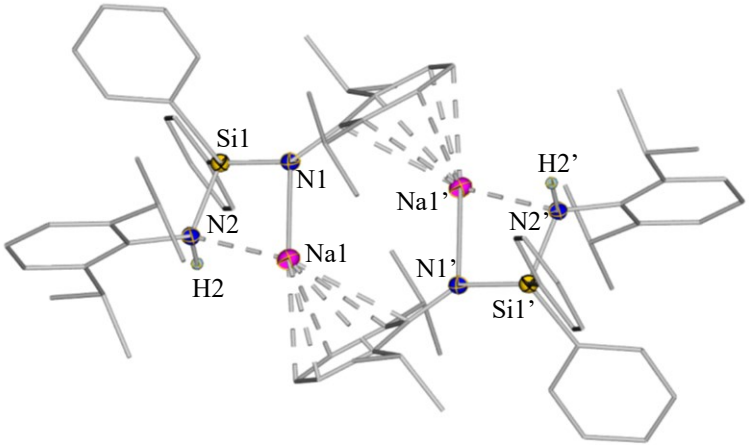

Figure 2. 5 *Molecular structure of **5**. Thermal ellipsoids are rendered at 50% probability. Hydrogen atoms (except the N-H pair) and disordered component (present in i-Pr groups) are omitted, with carbon atoms drawn wire frame for clarity. Symmetry transformations used to generate symmetrical atoms: 2-x, -y, 2-z. Selected bond distances (Å) and angles (°) N1-Na1 2.383(3), N2-Na1 2.488(4), N1-Na1-N2 68.20(11), N1-Si1-N2 104.47(16)*

The zincate moiety of **6** (**Figure 2. 6**) exhibits a similar structural motif to that of **3**, with a trigonal planar Zn centre (sum of angles around Zn, 360.0 (2)°) bonded to three N atoms, N1 and N2 from the chelating silylbis(amide) ligand [average Zn-N distance, 1.978(2) Å] and N3 from the HMDS group [Zn-N3, 1.902(2) Å]. These distances compare well with those reported in other SSIP species containing the $[Zn(HMDS)_3]^-$ anion (mean Zn-N distance, 1.964 Å).[75]

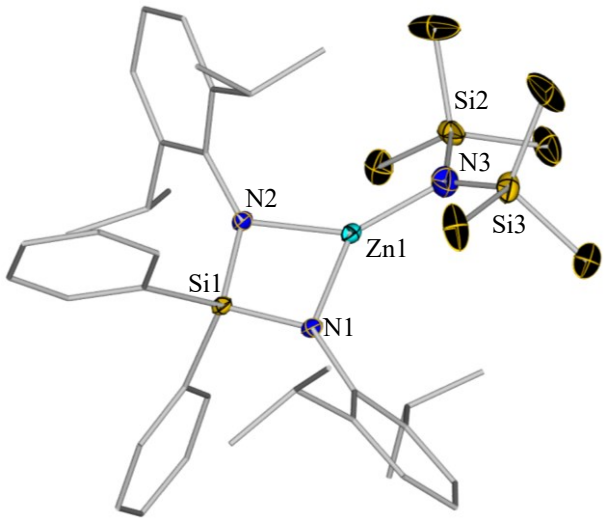

Figure 2. 6 *Anionic moiety of **6**. Thermal ellipsoids are rendered at 30% probability. Hydrogen atoms (except the N-H pair) and disordered component (present on $SiMe_3$) are omitted, with carbon atoms of $Ph_2SiN(Ar^*)_2^{2-}$ drawn wire frame for clarity. Selected distances (Å) and angles (°) N2-Zn1 1.982(2), N1-Zn1 1.973(2), N3-Zn1 1.902(2), N2-Zn1-N1 80.69(7), N2-Zn1-N3 139.65(8), N1-Zn1-N3 139.66(8), N2-Si1-N1 97.19(8)*

2.4.2 Applications of Sodium Zincates in Enolate Formation

Next we explored the metallating reactivity of new zincates **3** and **6** on their ability to deprotonate ketones to access zinc enolates, which are important intermediates in many

organic transformations including C-C couplings and addition reactions.[94–100] In most such transformations, the zinc enolates are prepared in situ and subsequently treated with the relevant electrophile. Several methods to access these enolates have been reported including deprotonation of a ketone with a group 1 base followed by salt metathesis with ZnX_2,[95] direct insertion of zinc in halogen-substituted ketones,[94,97] as well as direct deprotonation of a ketone using a zinc base.[96,98,100,101] For this third approach the zinc bis(amide) $Zn(TMP)_2$, comprising the basic 2,2,6,6-tetramethylpiperidide groups has shown good promise as a metallating reagent,[102–104] whereas dialkyl zinc reagents such as $ZnEt_2$ display more sluggish reactivities.[105] As previously mentioned, TMP-containing alkali-metal zincates have found applications in direct Zn-H exchange reactions[3,7,8,14–19,22-27] including ketone metalation.[106] Thus, we contemplated whether heteroleptic sodium zincates **3** and **6** could act as bases to access zinc enolate complexes, using as a model substrate the sterically demanding ketone, 2',4',6'-trimethylacetophenone (**7**).

^{1}H NMR monitoring of the reaction of equimolar amounts of **7** and alkyl sodium zincate **3** led to the formation of mixed-metal enolate [{(THF)NaZnR(OC(=CH_2)Mes)$_2$}$_2$] (**8**) with concomitant formation of silylbis(amine) (**1**) (**Scheme 2. 15**(i)).

The presence in the spectrum of unreacted **3** (in the same ratio of **1**) that eventually disappear after the addition of a second equivalent of **7** confirms the stochiometric ratio between **3** and **7** as 1:2 respectively.

The preferred bis(amide) reactivity of **3** is somewhat surprising considering that in many reported applications of complexes containing related bulky silyl(bis)amides, these ligands act primarily as steric stabilizers for main group elements.[35,36,39,65,66] Some of our previous magnesiate work has shown that this ligand can be activated towards deprotonation reactions when part of a bimetallic scaffold, although in these cases the relevant sodium magnesiate always reacts first by the alkyl group while the one or two amide groups only become active in a second metalation step, whereas here, the alkyl group remains intact on the zinc. It should also be noted that in previous reports on alkali-metal zincates, where preferred amide basicity is observed over the reaction involving one of their alkyl groups, these feature significantly more basic amides such HMDS or TMP than the anilide groups present in **3**. By using 2 equivalents of **7**, mixed Na/Zn enolate **8** could be isolated as a crystalline solid in a 60% yield. Attempts to extract further reactivity of the remaining alkyl group in **8** using an excess of **7** were unsuccessful even under forcing reaction conditions (4h, 69 °C), illustrating the kinetic resilience of the CH_2SiMe_3 anion.

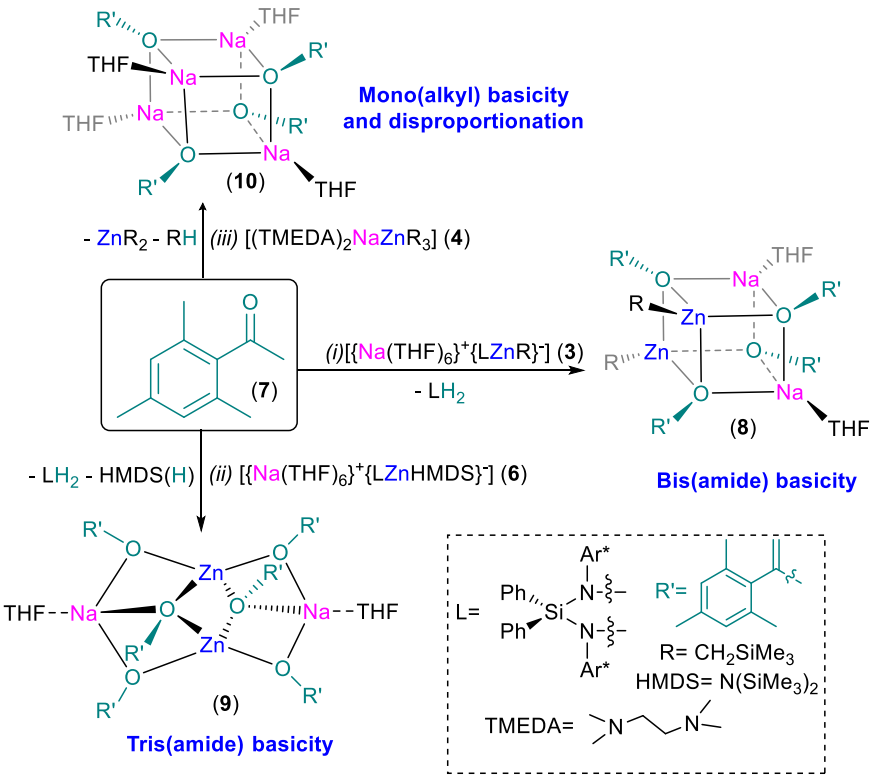

Scheme 2. 15 *Contrasting reactivities of sodium zincates **3**, **4** and **6** towards ketone **7**. All reactions were carried out in D_8-THF. (i) RT, 10 min; (ii) 69°C, 1h or RT, 12h; (iii) RT, 10 min. Enolates **8**, **9** and **10** were formed in quantitative yields according to ^{1}H NMR monitoring studies and were isolated as crystalline solids in 60, 39 and 15% yields respectively*

Interestingly, tris(enolate) $[\{(THF)_2NaZn(OC(=CH_2)Mes)_3\}_2]$ (**9**) was obtained from the reaction of HMDS-sodium zincate **6** with **7**, even when only one equivalent of the ketone was employed (**Scheme 2. 15**(ii)) showing that by being part of a zincate scaffold, the basic amide HMDS and bis(amide) $\{Ph_2Si(NAr^*)_2\}^{2-}$ have comparable reactivities towards the deprotonation of **7**. When the reaction was repeated with 3 equivalents of **7**, sodium-zinc enolate **9** was isolated with a crystalline yield of 39%.

For comparison, the reaction of tris(alkyl) zincate **4** with **7** was performed. Despite its lack of amido groups, **4** can also deprotonate this ketone, although now only one of its three potential sites reacts affording the homometallic sodium enolate $[\{(THF)Na(OC(=CH_2)Mes)\}_4]$ (**10**) (isolated in 15% crystalline yield) along with the elimination of the homometallic zinc component ZnR_2.

The distinct constitutions of enolate complexes **8**, **9** and **10** illustrates the versatile reactivity that zinc bases can have towards ketones, which can be particularly relevant when zinc enolates are prepared in situ for further organic functionalisation. This is particularly important for the reaction of $NaZnR_3$ (**4**) as the resulting enolate species is actually a sodium enolate which because of its more polar character is expected to display significant different reactivity and functional group tolerance to those of a zinc enolate. The mono(alkyl) basicity preferred basicity of **4** is also in sharp contrast to that previously reported by us for the related sodium

magnesiate $NaMgBu_3$ which reacts quantitatively with 3 equivalents of **7** to give a tris(enolate) sodium magnesiate.[107]

It should also be noted that compounds **8** and **10** where the only species formed when ketone **7** was treated with zincates **3** and **4** respectively, even when 3 equivalents of **7** was employed under forcing reaction conditions, which is consistent with the strong carbophilic character of zinc, which translates into a reduced basicity of the alkyl group attached to this metal.

To illustrate the higher covalent and carbophilic character of Zn versus Mg, **7** was reacted with the magnesium analogue of **3**, sodium magnesiate $[\{Ph_2Si(NAr^*)_2Mg(THF)(R)\}^-\{Na(THF)_6\}^+]$ (**11**), the bis(silyl)amido ligand remains as a spectator, coordinated to Mg, while the ketone is deprotonated by the alkyl group, affording $[\{Ph_2Si(NAr^*)_2Mg(THF)(OC(=CH_2)Mes)\}^-\{Na(THF)_6\}^+]$ (**12**) in a 40% isolated yield (**Scheme 2. 16**).

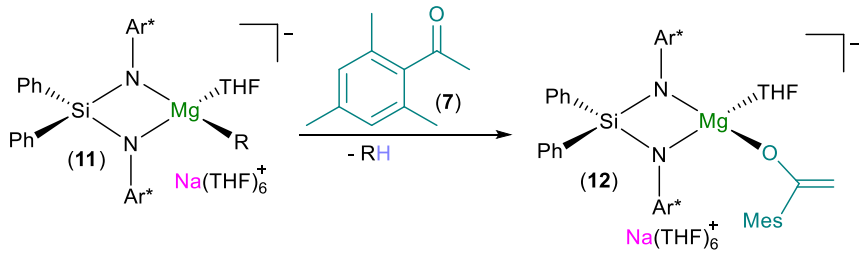

Scheme 2. 16 *Metalation of ketone 7 by sodium magnesiate **11**. Reaction carried out in THF, 2h, -40°C, 40% isolated crystalline yield. Mes=2,4,6 trimethylphenyl*

Considering the similar size of Mg and Zn, formation of **12** also suggests that the enhanced basicity observed for silyl(bis)amide in zincates **3** and **6** is not a consequence of its steric congestion when chelated to the metal in these *-ate* systems. Heteroleptic magnesiate **12** was fully characterized by ^1H and ^{13}C NMR spectroscopy as well as X-ray crystallographic studies (**Figure 2. 10**). We have previously reported alkyl basicity for this type of sodium magnesiate in magnesiation of N-heterocyclic molecules such as N-methyl benzimidazole and it is only when more acidic molecules such as pyrrole when one amido arm of the bis(amide) ligand in **11** is found to react with a second equivalent of substrate, thus showing overall dual alkyl/amido basicity.[36] Highlighting the more pronounced amide reactivity preference in zincates versus magnesiate, previous work on assessing the deprotonation of unsaturated N-heterocyclic carbenes with mixed alkyl-TMP bimetallic bases has shown that while sodium magnesiates react using their alkyl groups[108] amide basicity is the preferred *modus operandi* for the related sodium zincates[109]

The molecular structures of enolates **8-10** and **12** were determined using X-ray crystallographic studies. Early seminal work by Willard[110–115] and Seebach[116–120] has shown the relevance of structural elucidation of synthetically useful s-block metal enolates in order to understand and rationalise many fundamental organic transformations including aldol condensations. Sodium enolate **10** forms a tetramer with a distorted cubane structure, similar

to that found in other sodium enolates (**Figure 2. 7**).[111,121–123] Substantial disorder in **10** precludes a meaningful discussion of its geometric parameters though connectivity is definitive.

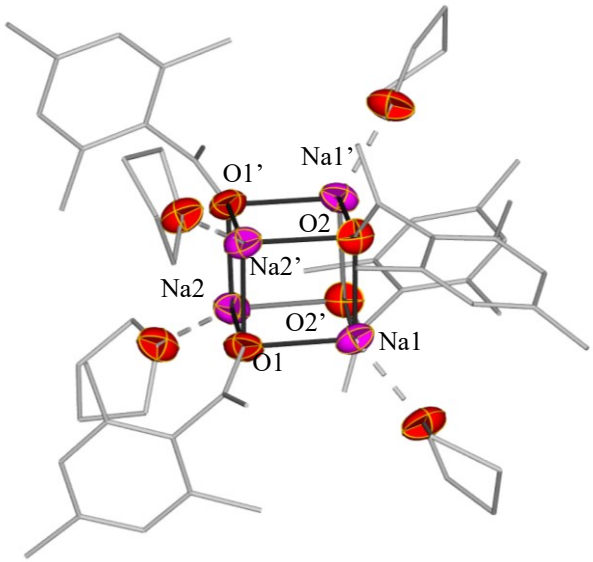

Figure 2. 7 *Molecular structures of enolate complexes **10**. Thermal ellipsoids are rendered at 30% probability. Hydrogen atoms and minor disordered component are omitted, carbon atoms drawn as wire frame for clarity. Symmetry transformations used to generate symmetrical atoms: 1-x, 1-y, 1-z*

Despite having similar compositions, sodium zincate enolates **8** and **9** adopt different dimeric arrangements (**Figure 2. 8** and **Figure 2. 9**). Complex **8** can be interpreted as a heterobimetallic variant of **10**, where two Na(THF) corners have been replaced by ZnR corners, forming a distorted mixed-metal cubane with alternating enolate O and metal (2 Na, 2 Zn) corners (**Figure 2. 8**). While this motif is unknown in zinc enolate chemistry, it is reminiscent of that previously reported for mixed lithium/zinc alkyl-alkoxide clusters.[124,125]

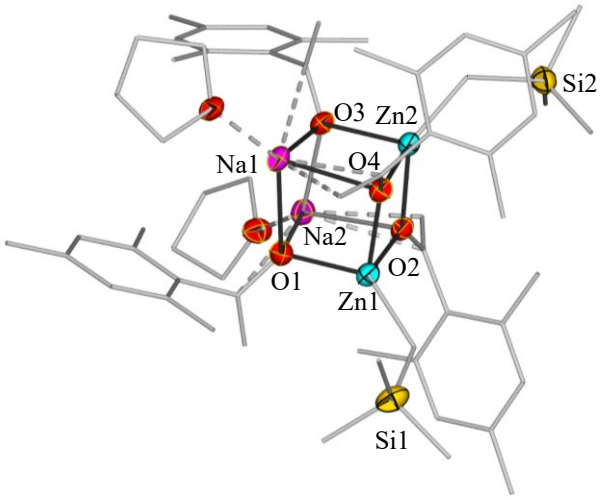

Figure 2. 8 *Molecular structures of enolate complex 8. Thermal ellipsoids are rendered at 30% probability. Hydrogen atoms and minor disordered component are omitted, carbon atoms drawn as wire frame for clarity. Selected distances (Å) and angles (°) 01-Zn1 2.079(3), O2-Zn1 2.054(3), O2-Na2 2.470(3), O1-Na1 2.458(3), Zn1-O4 2.075(3), O2-Zn2 2.088(3), Na2-O3 2.349(3), O4-Na2 2.274(3), O4-Zn2 2.088(3), Zn2-O3 2.059(3), O3-Na2 2.349(3), Na1-O4 2.470(3), Na2-O2-Zn2 99.53(11), O4-Zn1-O1 94.65(11), Zn1-O1-Na1 90.48(11), Na1-O4-Zn1 94.08(11), Zn1-O2-Na2 94.07(10)*

In contrast, **9** comprises two metal-enolate-connected [(THF)NaZn(OR)$_3$] units, where each Na-Zn pair and both Zn atoms are connected by two bridging enolates, giving rise to a face-fused double heterocubane structure with two missing corners (**Figure 2. 9**). Alternatively, by using the Mulvey inverse-crown nomenclature for bimetallic ring structures,[126–129] **9** can be described as [(NaOZnO)$_2$] cationic eight-membered ring hosting two enolate anion guests. It should be noted that a variant of **9** where each sodium is solvated by a molecule of unreacted ketone **7** instead of THF has been previously reported by us as the result of the reaction of NaZn(HMDS)$_3$ with a four molar excess of **7**.[106] This motif has also been described by Henderson for mixed K/Ca enolates.[130] The Zn-O bond distances in **8** and **9** compare well with those of other zinc enolate complexes,[105,106,131] whereas their Na-O distances [mean values, 2.356 (3) Å and 2.379 (2) Å for **8** and **9** respectively) are slightly elongated compared to those found in related enolate sodium magnesiate complexes such as [(TMEDA)$_2$Na$_2$Mg(OC(=CH$_2$)Mes)$_4$] [mean value = 2.256 Å].[107] In order to compensate for the comparative weakness of these Na-O bonds, in both bimetallic complexes each sodium atom π-engages with olefinic carbons of one enolate ligand (shown as dashed bonds in **Figure 2. 8** and **Figure 2. 9**) as indicated by the relatively short Na-C distances (mean values 2.960 and 2.928 Å for **8** and **9**, respectively)

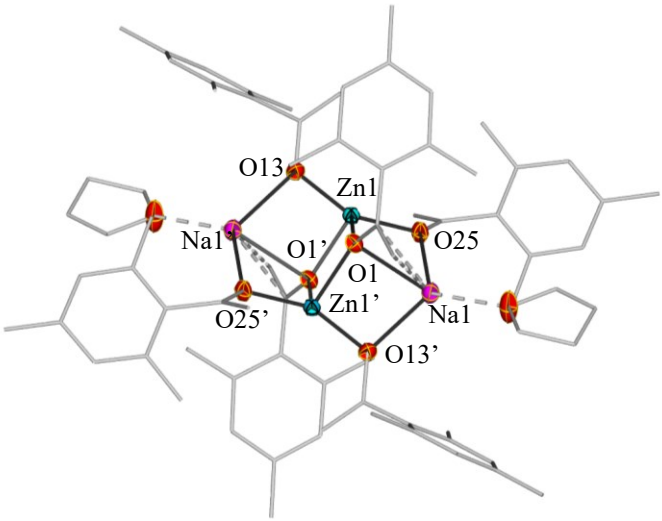

Figure 2. 9 *Molecular structures of enolate complexes **9**. Thermal ellipsoids are rendered at 30% probability. Hydrogen atoms and minor disordered component are omitted, carbon atoms drawn as wire frame for clarity. Symmetry transformations used to generate symmetrical atoms: 0.5-x, y, 1.5-z Selected distances (Å) and angles (°): Zn1-O25 1.898(1), Zn1-O1 2.017(1), O25-Na1 2.342(2), Zn1-O13 1.892(1), O1-Na1 2.469(2), Zn1-O25-Na1 97.16(6), O1-Zn1-O25 94.09(6),*

In contrast, the structure of sodium magnesiate **12** is a solvent separated ion pair (**Figure 2. 10**), with the same cationic $\{Na(THF)_6\}^+$ moiety as in zincates **3** and **5**, and an anionic moiety comprising a distorted tetrahedral Mg bonded to the chelating silylbis(amide) ligand, an enolate O and a THF O atom.

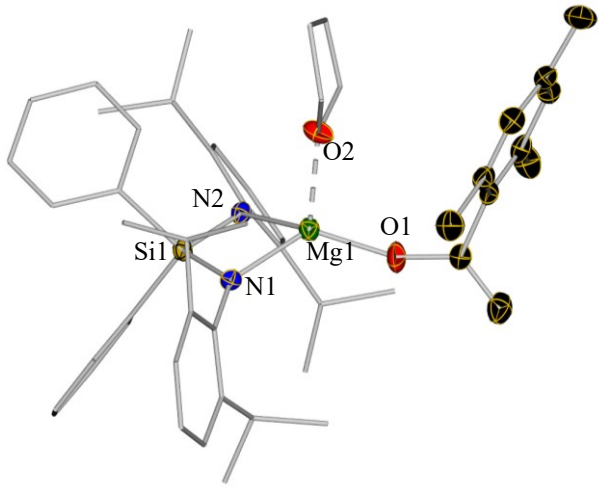

Figure 2. 10 *Molecular structures of enolate anionic moiety of **12**. Thermal ellipsoids are rendered at 30% probability. Hydrogen atoms and minor disordered component are omitted, carbon atoms (except those of enolate ligand) drawn as wire frame for clarity. Selected distances (Å) and angles (°) N2-Mg1 2.076(2), N1-Mg1 2.013(2), Mg1-O2 2.067(4), Mg1-O1 1.858(2), N2-Mg1-N1 78.87(7), N2-Si1-N1 99.68(9), N2-Mg1-O2 96.79(7), N1-Mg1-O2 117.03(7) N2-Mg1-O1 137.22(8), N1-Mg1-O1 124.79(8)*

2.5 Conclusions

Exploiting the preferred kinetic basicity of amides over alkyl groups in zinc chemistry, a new family of sodium zincates supported by a bulky chelating bis(silyl)amide ligand using $Ph_2Si(NHAr^*)_2$ (**1**) as a precursor has been made. Illustrating the importance on the order of addition of the single-metal components of the sodium zincate, if **1** was reacted with the bimetallic base $[NaZn(HMDS)_2R]$ (**2**), alkyl complex $[\{Ph_2Si(NAr^*)_2Zn(R)\}^-\{Na(THF)_6\}^+]$ (**3**) was obtained; whereas using a sequential approach, the mono-deprotonation of **1** by NaR, followed by addition of zinc amide $Zn(HMDS)_2$ furnished amido zincate $[\{Ph_2Si(NAr^*)_2Zn(HMDS)\}^-\{Na(THF)_6\}^+]$ (**6**). Reactivity studies of these new heteroleptic sodium zincates and for comparative purposes the all alkyl sodium zincate $[NaZnR_3]$ (**4**) towards ketone 2',4',6'-trimethylacetophenone (**7**) revealed the diverse behaviour of these mixed metal species. This diversity ranges from tris(amide) basicity of **6**, with its three amido arms deprotonating **7** (to give **10**), to bis(amide) basicity of **3**, furnishing **8** which retains the alkyl group intact, and to mono(alkyl) basicity of **4** which occurs with a subsequent disproportionation step affording sodium enolate **10** and ZnR_2. Structural and spectroscopic studies revealed an unexpected enhancement of the basicity of the bis(silyl)amide ligand which far from acting as a mere steric stabilizer, when part of a sodium zincate framework, it is capable of deprotonating two equivalents of the ketone. Emphasising the greater electropositive character of Mg and the greater polarity of its bonds, this reactivity is in sharp contrast with that found for related sodium magnesiate $[\{Ph_2Si(NAr^*)_2Mg(THF)(R)\}^-\{Na(THF)_6\}^+]$ (**11**) towards **7**, where the silyl(bis)amide remains as an spectator in the metalation process which is achieved selectively using the alkyl group on the magnesiate.

Collectively these studies not only reveal the complicated and unique reactivity of heteroleptic alkali-metal zincates, they also spotlight the structural diversity of s-block (and pseudo s-block) metal enolates, which in many synthetic studies remain concealed since species of this type are usually prepared in situ for onward functionalization in organic transformations.

2.6 Experimental Section

2.6.1 Synthesis and characterization of compounds **2-12**

Synthesis of $[NaZn(HMDS)_2(CH_2SiMe_3)]$ (**2**)

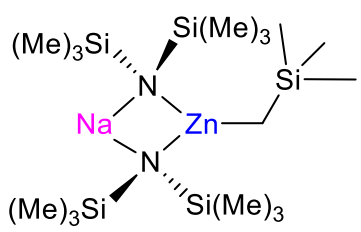

In the reactivity studies compound **2** was prepared in situ. For its characterization, 11mg of $NaCH_2SiMe_3$ (0.1 mmol) were solubilized in 0.5 mL of D_8-THF. 39 mg of freshly prepared $Zn(HMDS)_2$ (0.1 mmol) were added affording a colorless solution. ^{1}H DOSY NMR analysis reveals the co-diffusion of all resonances suggesting that both of the metallic species are part of the same molecular entity in THF solution (diffusion coefficient: $6.256e^{-10}$ m^2/s)

^{1}H-NMR (D_8-THF; 298K; 300 MHz) δ(ppm): -0.11 [s, 36H, CH_3 HMDS], -0.2 [s, 9H, CH_3 CH_2SiMe_3], -1.09 [s, 2H, CH_2 CH_2SiMe_3] **^{13}C{^{1}H}-NMR** (D_8-THF; 298K; 75 MHz) δ (ppm): 6.8 [CH_3 HMDS], 4.5 [CH_3 CH_2SiMe_3], 2.8 [CH_2 CH_2SiMe_3]

Synthesis of [{($Ph_2Si(NAr^*)_2$)Zn(CH_2SiMe_3)}$^-${$Na(THF)_6$}$^+$] (**3**)

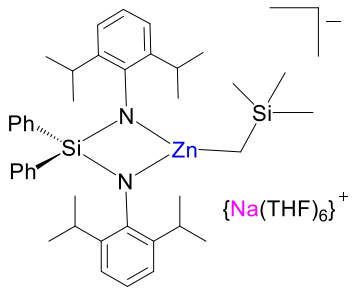

Procedure A: 386 mg of freshly prepared $Zn(HMDS)_2$ (1 mmol) was solubilized in 3mL of hexane. The solution was added via canula to a suspension of 110 mg of $NaCH_2SiMe_3$ (1 mmol) and 3 mL of hexane and the mixture was allowed to stir at room temperature for 30 min. 530 mg of **1** (1 mmol) was added to the mixture and the suspension was allowed to stir at room temperature overnight. Volatiles were removed under vacuum and to the white residue was dissolved in 3 mL of hexane and 1 mL of THF, affording a pale-yellow solution. Overnight storage in a fridge (4°C) furnished colorless crystal of **3** (880 mg; 71%)

Procedure B: 100.7 mg of LiR (1.06 mmol) and 72 mg of $ZnCl_2$ (0.53 mmol) were suspended in 5 mL of Et_2O at -40°C. The cold bath was removed, and the mixture was allowed to stir at room temperature for 1h. The mixture was filtered from LiCl affording a colorless solution. Volatiles were removed under vacuum. The white solid was suspended in 4 mL of hexane, 58.3 mg of NaR were added (0.53 mmol) and the resulting suspension was allowed to stir at room temperature for 1h. Volatiles were removed under vacuum and 5 mL of fresh THF were added affording a pale-yellow solution. 283 mg of **1** (0.53 mmol) were added and the solution was allowed to stir at reflux (69 °C) overnight. Volatiles were removed under vacuum and to the white residue was dissolved in 3 mL of hexane and 1 mL of THF, affording a pale-yellow solution. Overnight storage in a fridge (4°C) furnished colorless crystal of **3** (289 mg; 63%)

^{1}H-NMR (C_6D_6; 298K; 400 MHz) δ(ppm): 7.6 [m, 4H, Ph], 7.16 [m, 4H, Ar*], 7.1 [m, 6H, Ph], 6.95 [t, 2H, Ar*], 4.28 [sept, 4H, CH ^{i}Pr], 3.42 [m, 18H, O-CH_2 THF], 1.37 [m, 18H, CH_2 THF], 1.16[d, 24H, CH_3 ^{i}Pr], 0.18 [s, 9H, CH_3 CH_2SiMe_3], -0.7 [s, 2H, CH_2 CH_2SiMe_3] It should be noted that around 2 molecules of the solvating THF present in **3** were removed under vacuum when drying the crystals **^{13}C{^{1}H}-NMR** (C_6D_6; 298K, 100 MHz) δ(ppm): 151.3, 145.0, 144.7 [$C_{quaternary}$ Ar* and Ph], 135.7, 127.3, 123.9, 119.4 [CH, Ar* and Ph], 68.4 [O-CH_2 of THF], 28.6 [CH ^{i}Pr], 26.0 [CH_2 THF], 25.2 [CH_3 ^{i}Pr], 3.4 [CH_3 CH_2SiMe_3], -5.2 [CH_2 CH_2SiMe_3]

Elemental analysis: analytical calculated: $C_{54}H_{82}N_2NaO_4Si_2Zn$ C 67.02, H 8.54, N 2.89. Found: C 66.35, H 8.49, N 3.07. When drying crystals under vacuum some of solvating THF was removed. The ^{1}H-NMR spectrum of the batch used for the elemental analysis, shows in the solid there are an average of 3.5 molecules of THF instead of 6

Synthesis of [{$Ph_2Si(NHAr^*)(NAr^*)Na\}_2$] (**5**)

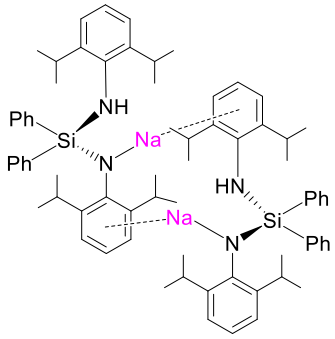

5 was prepared following a procedure reported by Livingstone[133]. $NaCH_2SiMe_3$ (110 mg, 1 mmol) was suspended in a Schlenk tube in 5 mL of hexane. An equivalent of already prepared $Ph_2Si(NHAr^*)_2$ (**1**) (530 mg, 1 mmol) was added and the suspension was allowed to stir for one hour. Toluene (5 mL) was introduced affording a clear solution. A batch of colourless crystals was isolated after storage of this solution in the freezer for 2 days (364 mg, 66%). Despite several attempts due to the extremely air sensitive nature of this compound, no satisfactory elemental analysis could be obtained.

^{1}H-NMR (C_6D_6, 298K, 400 MHz) δ(ppm): 7.58 [m, 8H, Ph], 7.16 [m, 13H, Ph and toluene], 7.02 [m, 13H, toluene and Ar*], 6.51 [t, 2H, Ar*], 3.99 [s, 2H, NH], 3.78 [sept, 4H, CH ^{i}Pr], 3.24 [sept, 4H, CH ^{i}Pr], 2.15 [s, 3H, CH_3, toluene], 1.07 [d, 24H, CH_3, ^{i}Pr], 0.97 [d, 24H, CH_3 ^{i}Pr]. **^{13}C{^{1}H}-NMR** (C_6D_6, 298K, 100 MHz) δ(ppm): 154.7, 142.5, 142.0, 141.6, 139.6 [$C_{quaternary}$ Ph, toluene and Ar*], 135.0, 129.2, 128.6, 127.4, 125.5, 123.4, 123.1, 121.9, 113.1 [CH Ph, toluene and Ar*], 28.8, 27.1 [CH ^{i}Pr], 23.5 23.2 [CH_3, ^{i}Pr], 21.1 [CH_3, toluene] Toluene signals due to co-crystalization of this solvent with.

Synthesis of [{$(Ph_2Si(NAr^*)_2)Zn(HMDS)\}^-\{Na(THF)_6\}^+$] (**6**)

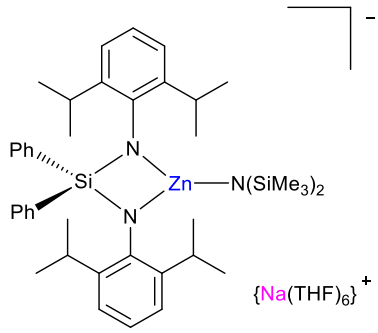

643.3 mg of freshly prepared $Zn(HMDS)_2$ (1.67 mmol) was solubilized in 5mL of THF . The solution was added via cannula to 920 mg of **5** (1.67 mmol). The mixture was allowed to stir at reflux overnight. Volatiles were removed under vacuum and the white residue was dissolved in 5 mL of hexane and 1.6 mL of THF, affording a pale-yellow solution. Overnight storage in a freezer (-33°C) furnished colourless crystals of **6** (1250 mg; 80%).

^{1}H-NMR (D_8-THF; 298K; 300 MHz) δ(ppm): 7.4 [m, 4H, Ph], 6.96 [m, 6H, Ph], 6.71 [d, 4H, Ar*], 6.45 [t, 2H, Ar*], 4.06 [sept, 4H, CH ^{i}Pr], 3.62 [m, 6H, O-CH_2 THF], 1.77 [m, 6H, CH_2 THF], 0.8 [d, 24H, CH_3 ^{i}Pr], -0.16 [s, 18H, CH_3 HMDS]. It should be noted that around 5 molecules of the solvating THF present in **6** were removed under vacuum when drying the crystals. **^{13}C{^{1}H}-NMR** (D_8-THF; 298K; 75 MHz) δ (ppm): 152.1, 146.5, 144.6 [$C_{quaternary}$ Ar* and Ph], 136.2, 122.2, 117.4 [CH Ar* and Ph], 68.0 [O-CH_2 of THF], 27.9 [CH ^{i}Pr], 26.2 [CH_2 THF], 24.9 [CH_3 ^{i}Pr], 5.8 [CH_3 HMDS]

Elemental analysis: analytical calculated: $C_{104}H_{164}N_6Na_2O_5Si_6Zn_2$ C 64.93, H 8.53, N 4.50. Found: C 64.93, H 8.59, N 4.37. When drying crystals under vacuum some of solvating THF was removed. The ^{1}H-NMR, of the batch used for the elemental analysis, shows in the solid there are an average of 2.5 molecules of THF instead of 6.

Synthesis of [{(THF)NaZn(CH_2SiMe_3)(OC(=CH_2)Mes)$_2$}$_2$] (**8**)

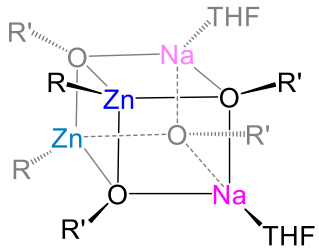

0.33 mL (2mmol) of **7** were added to a solution of 2100 mg of **3** (2 mmol) and 5 mL of THF, in that instant colour change of the solution is observed, from colourless to light yellow. After stirring the reaction mixture at room temperature for 1h volatiles were removed under vacuum, and the solid residue was dissolved in warm Toluene (2 mL). Colourless crystals of **8** were obtained after slowing cooling down the solution. (697mg yield: 60%) When the reaction was monitored by ^{1}H-NMR quantitative conversion of **3** into **8** was observed.

^{1}H-NMR (D_8-THF; 298K; 300 MHz) δ (ppm): 6.69 [s, 8H, Mes], 4.09 [s, 4H, =C*H*H'], 3.34 [s, 4H, =CH*H'*], 3.61 [m, 8H, OCH_2 THF], 2.32 [s, 24H, CH_3 Mes] 2.16 [s, 12H, CH_3 Mes], 1.78 [m, 8H, CH_2 THF] 0.03 [s, 18H, CH_3 CH_2SiMe_3], -0.87 [s, 4H, CH_2 CH_2SiMe_3] **^{13}C{^{1}H}-NMR** (D_8-THF; 298K; 75 MHz) δ (ppm): 165.9 [C-O], 143.8, 135.5, 135.3 [$C_{quaternary}$ Mes], 128.4 [CH Mes], 83.2 [CO=*C*HH'], 21.2, 20.6 [CH_3 Mes], 3.9 [CH_3 CH_2SiMe_3] -7.8 [CH_2 CH_2SiMe_3]

Elemental analysis: analytical calculated: $C_{60}H_{90}Na_2O_6Si_2Zn_2$ C 63.20 H 7.96. Found: C 66.32, H 8.01.

Synthesis of [{(THF)NaZn(OC(=CH_2)Mes)$_3$}$_2$] (**9**)

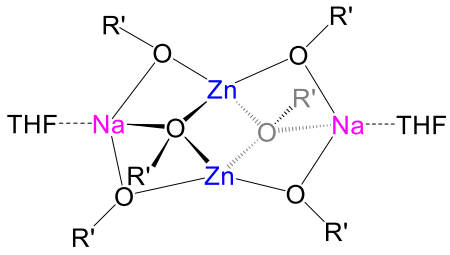

938 mg of **6** (1 mmol) were solubilised in 5 mL of THF, then 0.5 mL of **7** (3 mmol) were added to the solution. The mixture was allowed to stir for 1h at 69°C. The solution was cooled down to room temperature. All the volatiles were removed under vacuum and to the white residue 2 mL of toluene were added, affording an orange suspension. In order to facilitate the crystallization one additional equivalent of **7** (0.17 mL) were added. The mixture was heated under reflux in an oil bath and let slowly cool down at room temperature for a night furnished colourless crystal of **9** (228 mg yield: 39%). When the reaction was monitored by ^{1}H-NMR quantitative conversion of **6** into **9** was observed. Despite several attempts due to the extremely air sensitive nature of this compound, no satisfactory elemental analysis could be obtained.

^{1}H-NMR (D_8-THF; 298K; 300 MHz) δ(ppm): 6.69 [s, 12H, Mes], 4.38 [s, 6H, =C*H*H'], 3.62 [m, 16H, OCH_2 THF), 3.38 [s, 6H, =CH*H'*], 2.17 [s, 36H, CH_3, Mes] 2.17 [s, 18H, CH_3, Mes], 1.77 [m, 16H, CH_2 THF]. **^{13}C{^{1}H}-NMR** (D_8-THF; 298K; 75 MHz) δ (ppm): 165.1 [C-O], 144.3, 136.1, 134.9 [$C_{quaternary}$ Mes], 128.1 [CH Mes], 83.3 [CO=*C*HH'], 20.9 [CH_3 Mes].

Synthesis of [{(THF)Na(OC(=CH_2)Mes)}$_4$] (**10**)

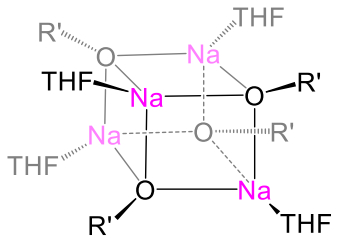

0.17 mL (1 mmol) of **7** were added to a solution of 580 mg (1mmol) of freshly prepared **4**[77] and 5 mL of THF. The colourless solution obtained was allowed to stir for 1h at room temperature, then volatiles were removed under vacuum. 2 mL of fresh hexane were added to the white solid residue, the resulting suspension was gently heated, affording a colourless solution. Overnight storage in a fridge (4°C) furnished colourless crystal of **10** (40 mg, 15%) When the reaction was monitored by ^{1}H-NMR quantitative conversion of **6** into **9** was observed.

^{1}H-NMR (C_6D_6; 298K; 300 MHz) δ (ppm): 6.85 [s, 8H, Mes], 4.06 [s, 4H, CH =C*H*H'], 3.71 [s, 4H, CH =CH*H'*] 3.46 [s, 16H, OCH_2 THF] 2.54 [s, 24H, CH_3 Mes], 2.20 [s, 12H, CH_3 Mes], 1.36 [s, 16H, CH_2 THF] **^{13}C{^{1}H}-NMR** (C_6D_6; 298K; 75 MHz) δ (ppm): 170.2 [C-O] 144.8, 134.5, 134.1 [$C_{quaternary}$ Mes] 128.2 [CH Mes], 78.1 [=*C*HH'], 68.0 [OCH_2 THF], 21.0 [CH_3 Mes], 20.5 [CH_3 Mes]

Synthesis of [{(Ph_2Si(NAr*)$_2$)Mg(THF)(CH_2SiMe_3)}$^-${Na(THF)$_6$}$^+$] (**11**)

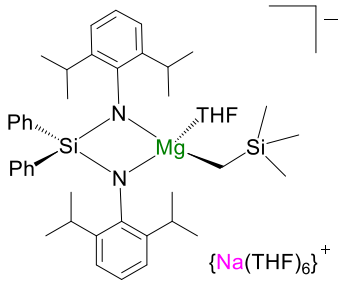

11 was prepared following a procedure reported by Livingstone.[133]220 mg of $NaCH_2SiMe_3$ (2 mmol) and 400 mg of $Mg(CH_2SiMe_3)_2$ (2 mmol) were suspended in 10 mL of hexane and allowed to stir for 10' at room temperature. Then 1060 mg of **1** (2 mmol) were added and the white suspension was allowed to stir for 1h. 4 mL of THF were dripped in the suspension and the mixture was gently heated in order to obtain a pale-yellow solution. Overnight storage in a freezer (-33°C) furnished colorless crystal of **11** (1612 mg; 78%)

^{1}H-NMR (C_6D_6; 298K; 400 MHz) δ (ppm): 7.89 [d, 4H, Ph], 7.11 [dd, 4H, Ph], 7.02 [d, 2H, Ph], 6.98 [d, 4H, Ar*], 6.64 [t, 2H, Ar*], 4.22 [s, 4H, CH, ^{i}Pr], 3.47 [t, 28H, O-CH_2, THF], 1.36 [m, 28H, CH_2, THF], 1.15 [d, 24H, CH_3, ^{i}Pr], 0.34 [s, 9H, CH_3 CH_2SiMe_3], -1.28 [s, 2H, CH_2, CH_2SiMe_3]. **^{13}C{^{1}H}-NMR** (C_6D_6; 298 K; 100 MHz) δ (ppm):153.91, 146.13, 143.21 [$C_{quaternary}$, Ph or Ar*], 135.11 [CH, Ph], 126.21 [CH, Ph], 126.14 [CH, Ph], 122.94 [CH, Ar*], 115.25 [CH, Ar*], 68.20 [O-CH_2, THF], 28.94 [CH, ^{i}Pr, Ar*], 25.41 [CH_2, THF], 25.26 [CH_3, ^{i}Pr, Ar*], 4.73 [CH_3 CH_2SiMe_3], -0.82 [CH_2 CH_2SiMe_3].

Synthesis of [{($Ph_2Si(NAr^*)_2$)Mg(THF)(OC(=CH_2)Mes)}$^-${$Na(THF)_5$}$^+$] (**12**)

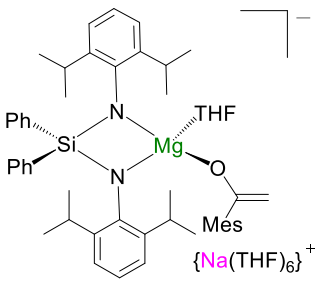

516 mg of **11** (0.5 mmol) were solubilized in 3 mL of THF. The solution was placed in a cold bath at -40°C and 0.08 mL of **7** (0.5 mmol) was added. The solution was stirred for 30' and then the mixture was allowed to warm up to room temperature and then it was stirred for an additional hour. Volatiles were removed under vacuum. The white residue was solubilized with 3 mL of hexane, 0.5 mL of THF and a gently heating. Overnight storage in a fridge (4°C) furnished colourless crystal of **12** (212 mg; 40%)

^{1}H-NMR (D_8-THF; 298K; 300 MHz) δ (ppm):7.26 [m, 4H, Ph], 6.91 [m, 6H, Ph], 6.69 [d, 4H, Ar*, J=7.37 Hz], 6.57 [s, 2H, Mes], 6.39 [t, 2H, Ar*], 4.1 [sept, 4H, CH ^{i}Pr], 3.75 [d, 1H, =C*H*H'], 3.66 [m, 18H, OCH_2 THF], 3.10 [d, 1H, =CH*H'*], 2.15 [s, 9H, CH_3, Mes], 1.81 [m, 18H, CH_2 THF], 0.78 [d, 24H, CH_3 ^{i}Pr] **^{13}C{^{1}H}-NMR** (D_8-THF; 298K; 75 MHz) δ (ppm): 165.5 [C-O],154.6, 145.5, 144.3, 135.7, 133.7 [$C_{quaternary}$ Ph, Ar*,Mes],136.5 [CH Ph], 127.7 [CH Mes], 122.3, 115.6 [CH Ar*] 81.4 [CO=*C*HH'], 68.4 [OCH_2 THF], 28.3 [CH ^{i}Pr], 26.5 [CH_2 THF], 25.4[CH_3 ^{i}Pr], 21.2, 20.6 [CH_3 Mes]

2.6.2 ^{1}H NMR monitoring of the metalation of **7** by sodium zincates **3**, **4** and **6**

^{1}H-NMR monitoring of reaction of **3** with variable amounts of (**7**)

100 mg of **3** (0.1 mmol) were solubilized in 0.5 mL of D_8-THF in a flushed and dried J. Young's NMR tube. Subsequentially addition of 16.6 µL **7** (0.1 mmol, 1 eq.) were made, until 49.8 µL of **7** (0.3 mmol, 3 eq.) were added. After every addition, the mixture was observed by ^{1}H NMR

When **3** was reacted with three equivalents of **7**, compound **8** was detected in the same yield as seen in the reaction with 2 equivalents, but the additional equivalent of **7** was detected in the reaction mixture. Alternative if the reaction is carried out using just one equivalent of ketone, the yield for **8** diminished to 50% and the unreacted zincate **3** is observed in solution.

^{1}H-NMR monitoring of reaction of **6** with variable amounts of (**7**)

41,5 mg of **6** (0.05 mmol) were solubilized in 0.5 mL of D_8-THF in a flushed and dried J. Young's NMR tube. Subsequentially addition of 8.3 µL of **7** (0.05 mmol, 1 eq.) were made, until 24.9 µL of **7** (0.15 mmol, 3 eq.) were added. After every addition, the mixture was heated for 1h at 69°C and then was observed by ^{1}H NMR

When **6** is reacted with one molar equivalent of **7** only compound **9** is detected along with **1** and HMDS(H) in almost 33% conversion along with unreacted **6**. When the reaction was carried out with 3 equivalents of **7** only **9**, **1** and HMDS(H) were observed.

^{1}H-NMR monitoring of reaction of **4** with variable amounts of (**7**)

58 mg of **4** (0.1 mmol) were solubilized in 0.5 mL of D_8-THF in a flushed and dried J. Young's NMR tube. Subsequentially addition of 1 equivalent of **7** (16.6 µL, 0.1 mmol) were made, until 33 µL of **7** (0.2 mmol, 2 eq.) were added. After every addition, the mixture was observed by ^{1}H NMR

When **4** was reacted with **2** equivalents of **7**, afforded **10** in the same yields as when only one equivalent of **7** was employed. $Zn(CH_2SiMe_3)_2$ was also detected together with **10.**

2.7 References

[1] L. Davin, R. McLellan, A. Hernán-Gómez, W. Clegg, A. R. Kennedy, M. Mertens, I. A. Stepek, E. Hevia, *Chem. Commun.* **2017**, *53*, 3653–3656.

[2] L. Davin, W. Clegg, A. R. Kennedy, M. R. Probert, R. McLellan, E. Hevia, *Chem. Eur. J.* **2018**, *24*, 14830–14835.

[3] M. R. Crimmin, M. Arrowsmith, A. G. M. Barrett, I. J. Casely, M. S. Hill, P. A. Procopiou, *J. Am. Chem. Soc.* **2009**, *131*, 9670–9685.

[4] J. Spielmann, S. Harder, *Eur. J. Inorg. Chem.* **2008**, 1480–1486.

[5] S. P. Green, C. Jones, A. Stasch, *Science* **2007**, *318*, 1754–1758.

[6] B. Rösch, T. X. Gentner, J. Eyselein, J. Langer, H. Elsen, S. Harder, *Nature* **2021**, *592*, 717–721.

[7] K. Yuvaraj, I. Douair, A. Paparo, L. Maron, C. Jones, *J. Am. Chem. Soc.* **2019**, *141*, 8764–8768.

[8] L. Bourget-merle, M. F. Lappert, J. R. Severn, *Chem. Rev.* **2002**, 3031–3065.

[9] J. Hicks, M. Juckel, A. Paparo, D. Dange, C. Jones, *Organometallics* **2018**, *37*, 4810–4813.

[10] S. J. Bonyhady, C. Jones, S. Nembenna, A. Stasch, A. J. Edwards, G. J. McIntyre, *Chem. Eur. J.* **2010**, *16*, 938–955.

[11] C. Jones, *Nat. Rev. Chem.* **2017**, *1*, 59.

[12] A. Stasch, C. Jones, *Dalton Trans.* **2011**, *40*, 5659–5672.

[13] R. Lalrempuia, C. E. Kefalidis, S. J. Bonyhady, B. Schwarze, L. Maron, A. Stasch, C. Jones, *J. Am. Chem. Soc.* **2015**, *137*, 8944–8947.

[14] K. Yuvaraj, I. Douair, D. D. L. Jones, L. Maron, C. Jones, *Chem. Sci.* **2020**, *11*, 3516–3522.

[15] A. Paparo, K. Yuvaraj, A. J. R. Matthews, I. Douair, L. Maron, C. Jones, *Angew. Chem. Int. Ed.* **2021**, *60*, 630–634.

[16] D. Mukherjee, J. Okuda, *Angew. Chem. Int. Ed.* **2018**, *57*, 1458–1473.

[17] S. Harder, J. Spielmann, J. Intemann, H. Bandmann, *Angew. Chem. Int. Ed.* **2011**, *50*, 4156–4160.

[18] S. P. Green, C. Jones, A. Stasch, *Angew. Chem. Int. Ed.* **2008**, *47*, 9079–9083.

[19] S. Harder, J. Brettar, *Angew. Chem. Int. Ed.* **2006**, *45*, 3474–3478.

[20] A. G. M. Barrett, M. R. Crimmin, M. S. Hill, P. B. Hitchcock, P. A. Procopiou, *J.*

Chem. Soc. Dalt. Trans. **2008**, 4372–4386.

[21] J. Spielmann, F. Buch, S. Harder, *Angew. Chem. Int. Ed.* **2008**, *47*, 9434–9438.

[22] J. Intemann, H. Bauer, J. Pahl, L. Maron, S. Harder, *Chem. Eur. J.* **2015**, *21*, 11452–11461.

[23] S. E. Baillie, V. L. Blair, T. D. Bradley, W. Clegg, J. Cowan, R. W. Harrington, A. Hernán-Gómez, A. R. Kennedy, Z. Livingstone, E. Hevia, *Chem. Sci.* **2013**, *4*, 1895–1905.

[24] L. Davin, R. McLellan, A. R. Kennedy, E. Hevia, *Chem. Commun.* **2017**, *53*, 11650–11653.

[25] L. J. Bole, L. Davin, A. R. Kennedy, R. McLellan, E. Hevia, *Chem. Commun.* **2019**, *55*, 4339–4342.

[26] M. Schlosser, L. Guio, F. Leroux, *J. Am. Chem. Soc.* **2001**, *123*, 3822–3823.

[27] N. Pié, A. Turck, K. Couture, G. Quéguiner, *J. Org. Chem.* **1995**, *60*, 3781–3786.

[28] Z. Dong, G. C. Clososki, S. H. Wunderlich, A. Unsinn, J. Li, P. Knochel, *Chem. Eur. J.* **2009**, *15*, 457–468.

[29] D. O'Hagan, *Chem. Soc. Rev.* **2008**, 308–319.

[30] M. Veith, *Angew. Chem., Int. Ed. Engl.* **1987**, *26*, 1–14.

[31] M. Veith, *Chem. Rev.* **1990**, 3–16.

[32] R. J. Schwamm, M. P. Coles, M. S. Hill, M. F. Mahon, C. L. McMullin, N. A. Rajabi, A. S. S. Wilson, *Angew. Chem. Int. Ed.* **2020**, *59*, 3928–3932.

[33] H. Liu, R. J. Schwamm, S. E. Neale, M. S. Hill, C. L. Mcmullin, M. F. Mahon, *J. Am. Chem. Soc.* **2021**, DOI 10.1021/jacs.1c09467.

[34] R. Murugavel, N. Palanisami, R. J. Butcher, *J. Organomet. Chem.* **2003**, *675*, 65–71.

[35] V. L. Blair, W. Clegg, A. R. Kennedy, Z. Livingstone, L. Russo, E. Hevia, *Angew. Chemie* **2011**, *123*, 10031–10034.

[36] D. R. Armstrong, W. Clegg, A. Hernán-Gómez, A. R. Kennedy, Z. Livingstone, S. D. Robertson, L. Russo, E. Hevia, *Dalton Trans.* **2014**, *43*, 4361–4369.

[37] Z. Livingstone, A. Hernán-Gómez, S. E. Baillie, D. R. Armstrong, L. M. Carrella, W. Clegg, R. W. Harrington, A. R. Kennedy, E. Rentschler, E. Hevia, *Dalton Trans.* **2016**, *45*, 6175–6182.

[38] A. Krasovskiy, V. Krasovskaya, P. Knochel, *Angew. Chem. Int. Ed.* **2006**, *45*, 2958–2961.

[39] Y. C. Tsai, D. Y. Lu, Y. M. Lin, J. K. Hwang, J. S. K. Yu, *Chem. Commun.* **2007**, 4125–4127.

[40] D. Seyferth, *Organometallics* **2001**, *20*, 2940–2955.

[41] J. A. Wanklyn, *Justus Liebigs Ann. Chem.* **1858**, *108*, 67–79.

[42] S. D. Robertson, M. Uzelac, R. E. Mulvey, *Chem. Rev.* **2019**, *119*, 8332–8405.

[43] D. Tilly, F. Chevallier, F. Mongin, P. C. Gros, *Chem. Rev.* **2014**, *114*, 1207–1257.

[44] M. Balkenhohl, P. Knochel, *Chem. Eur. J.* **2020**, *26*, 3688–3697.

[45] M. Balkenhohl, D. S. Ziegler, A. Desaintjean, L. J. Bole, A. R. Kennedy, E. Hevia, P. Knochel, *Angew. Chem. Int. Ed.* **2019**, *58*, 12898–12902.

[46] M. Uchiyama, C. Wang, in (Ed.: Z. Xi), Springer International Publishing, Cham, **2014**, pp. 159–202.

[47] R. E. Mulvey, *Acc. Chem. Res.* **2009**, *42*, 743–755.

[48] M. Schlosser, *Organometallics in Synthesis: Third Manual*, Wiley-VCH, **2013**.

[49] M. Mosrin, P. Knochel, *Org. Lett.* **2009**, *11*, 1837–1840.

[50] D. Haas, M. Mosrin, P. Knochel, *Org. Lett.* **2013**, *15*, 6162–6165.

[51] D. S. Ziegler, R. Greiner, H. Lumpe, L. Kqiku, K. Karaghiosoff, P. Knochel, *Org. Lett.* **2017**, *19*, 5760–5763.

[52] S. H. Wunderlich, P. Knochel, *Angew. Chem. Int. Ed.* **2007**, *46*, 7685–7688.

[53] T. Bresser, P. Knochel, *Angew. Chem. Int. Ed.* **2011**, *50*, 1914–1917.

[54] J. M. Hammann, D. Haas, P. Knochel, *Angew. Chem. Int. Ed.* **2015**, *54*, 4478–4481.

[55] P. C. Andrikopoulos, D. R. Armstrong, H. R. L. Barley, W. Clegg, S. H. Dale, E. Hevia, G. W. Honeyman, A. R. Kennedy, R. E. Mulvey, *J. Am. Chem. Soc.* **2005**, *127*, 6184–6185.

[56] W. Clegg, S. H. Dale, E. Hevia, G. W. Honeyman, R. E. Mulvey, *Angew. Chem. Int. Ed.* **2006**, *45*, 2370–2374.

[57] G. W. Honeyman, D. R. Armstrong, W. Clegg, E. Hevia, A. R. Kennedy, R. McLellan, S. A. Orr, J. A. Parkinson, D. L. Ramsay, S. D. Robertson, S. Towie, R. E. Mulvey, *Chem. Sci.* **2020**, *11*, 6510–6520.

[58] W. Clegg, B. Conway, E. Hevia, M. D. McCall, L. Russo, R. E. Mulvey, *J. Am. Chem. Soc.* **2009**, *131*, 2375–2384.

[59] D. R. Armstrong, V. L. Blair, W. Clegg, S. H. Dale, J. Garcia-Alvarez, G. W. Honeyman, E. Hevia, R. E. Mulvey, L. Russo, *J. Am. Chem. Soc.* **2010**, *132*, 9480–9487.

[60] Y. Kondo, J. V. Morey, J. C. Morgan, H. Naka, D. Nobuto, P. R. Raithby, M. Uchiyama, A. E. H. Wheatley, *J. Am. Chem. Soc.* **2007**, *129*, 12734–12738.

[61] D. Nobuto, M. Uchiyama, *J. Org. Chem.* **2008**, *73*, 1117–1120.

[62] S. E. Baillie, V. L. Blair, D. C. Blakemore, D. Hay, A. R. Kennedy, D. C. Pryde, E. Hevia, *Chem. Commun.* **2012**, *48*, 1985–1987.

[63] M. F. Lappert, P. P. Power, A. R. Sanger, R. C. Srivastava, *Metal and Metalloid Amides: Synthesis, Structures, and Physical and Chemical Properties*, Ellis Horwood Ltd., Chichester, UK, **1980**.

[64] M. F. Lappert, P. P. Power, A. V. Protchenko, A. Seeber, *Metal Amide Chemistry*, John Wiley & Sons, Ltd, Chichester, UK, **2009**.

[65] M. S. Hill, P. B. Hitchcock, *Organometallics* **2002**, *21*, 3258–3262.

[66] Y. C. Tsai, Y. M. Lin, J. S. K. Yu, J. K. Hwang, *J. Am. Chem. Soc.* **2006**, *128*, 13980–13981.

[67] D. Yang, J. Guo, H. Wu, Y. Ding, W. Zheng, *Dalton Trans.* **2012**, *41*, 2187–2194.

[68] B. M. Day, P. W. Dyer, M. P. Coles, *Dalton Trans.* **2012**, *41*, 7457–7460.

[69] B. M. Day, M. P. Coles, *Organometallics* **2013**, *32*, 4270–4278.

[70] R. J. Schwamm, B. M. Day, M. P. Coles, C. M. Fitchett, *Inorg. Chem.* **2014**, *53*, 3778–3787.

[71] R. J. Schwamm, M. P. Coles, C. M. Fitchett, *Organometallics* **2015**, *34*, 2500–2507.

[72] W. Clegg, G. C. Forbes, A. R. Kennedy, R. E. Mulvey, S. T. Liddle, *Chem. Commun.* **2003**, *3*, 406–407.

[73] D. R. Armstrong, W. Clegg, S. H. Dale, J. García-Álvarez, R. W. Harrington, E. Hevia, G. W. Honeyman, A. R. Kennedy, R. E. Mulvey, C. T. O'Hara, *Chem. Commun.* **2008**, 187–189.

[74] D. V. Graham, E. Hevia, A. R. Kennedy, R. E. Mulvey, *Organometallics* **2006**, *25*, 3297–3300.

[75] D. R. Armstrong, E. Herd, D. V. Graham, E. Hevia, A. R. Kennedy, W. Clegg, L. Russo, *J. Chem. Soc. Dalt. Trans.* **2008**, 1323–1330.

[76] W. Clegg, S. H. Dale, D. V. Graham, R. W. Harrington, E. Hevia, L. M. Hogg, A. R. Kennedy, R. E. Mulvey, *Chem. Commun.* **2007**, 1641–1643.

[77] D. R. Armstrong, H. S. Emerson, A. Hernán-Gómez, A. R. Kennedy, E. Hevia, *Dalton Trans.* **2014**, *43*, 14229–14238.

[78] M. Dell'Aera, F. M. Perna, P. Vitale, A. Altomare, A. Palmieri, L. C. H. Maddock, L. J. Bole, A. R. Kennedy, E. Hevia, V. Capriati, *Chem. Eur. J.* **2020**, *26*, 8742–8748.

[79] A. J. Roberts, A. R. Kennedy, R. McLellan, S. D. Robertson, E. Hevia, *Eur. J. Inorg. Chem.* **2016**, *2016*, 4752–4760.

[80] A. R. Kennedy, J. Klett, R. E. Mulvey, D. S. Wright, *Science* **2010**, *706*, 706–709.

[81] J. Francos, A. R. Kennedy, C. T. O'Hara, *Dalton Trans.* **2016**, *45*, 6222–6233.

[82] A. P. Purdy, C. F. George, *Organometallics* **1992**, *11*, 1955–1959.

[83] M. Westerhausen, B. Rademacher, W. Schwarz, S. Henkel, *Z. Naturforsch., B: J. Chem. Sci.* **1994**, *49*, 199–210.

[84] V. P. Colquhoun, C. Unkelbach, C. Strohmann, *Chem. Commun.* **2012**, *48*, 5034–5036.

[85] M. Westerhausen, T. Bollwein, A. Pfitzner, T. Nilges, H. J. Deiseroth, *Inorg. Chim. Acta* **2001**, *312*, 239–244.

[86] M. M. Olmstead, W. J. Grigsby, D. R. Chacon, T. Hascall, P. P. Power, *Inorg. Chim. Acta* **1996**, *251*, 273–284.

[87] S. Jana, Y. Aksu, M. Driess, *J. Chem. Soc. Dalt. Trans.* **2009**, 1516–1521.

[88] M. M. Olmstead, P. P. Power, S. C. Shoner, *J. Am. Chem. Soc.* **1991**, *113*, 3379–3385.

[89] M. Palenzuela, M. T. Muñoz, J. F. Vega, Á. Gutiérrez-Rodríguez, T. Cuenca, M. E. G. Mosquera, *Dalton Trans.* **2019**, *48*, 6435–6444.

[90] Y. Zhao, Y. Lei, Q. Dong, B. Wu, X. J. Yang, *Chem. Eur. J.* **2013**, *19*, 12059–12066.

[91] M. A. Putzer, A. Pilz, U. Müller, B. Neumüller, K. Dehnicke, *Zeitschrift für Anorg. und Allg. Chemie* **1998**, *624*, 1336–1340.

[92] G. C. Forbes, A. R. Kennedy, R. E. Mulvey, P. J. A. Rodger, *Chem. Commun.* **2001**, *1*, 1400–1401.

[93] M. A. Putzer, B. Neumüller, K. Dehnicke, *Zeitschrift für Anorg. und Allg. Chemie* **1997**, *623*, 539–544.

[94] T. Hama, S. Ge, J. F. Hartwig, *J. Org. Chem.* **2013**, *78*, 8250–8266.

[95] A. Pérez-Luna, C. Botuha, F. Ferreira, F. Chemla, *New J. Chem.* **2008**, *32*, 594–606.

[96] O. Knopff, A. Alexakis, *Org. Lett.* **2002**, *4*, 3835–3837.

[97] T. Hama, D. A. Culkin, J. F. Hartwig, *J. Am. Chem. Soc.* **2006**, *128*, 4976–4985.

[98] G. K. Jarugumilli, S. P. Cook, *Org. Lett.* **2011**, *13*, 1904–1907.

[99] M. Yasuda, S. Tsuji, Y. Shigeyoshi, A. Baba, *J. Am. Chem. Soc.* **2002**, *124*, 7440–7447.

[100] D. Vargová, I. Némethová, K. Plevová, R. Šebesta, *ACS Catal.* **2019**, *9*, 3104–3143.

[101] X. Rathgeb, S. March, A. Alexakis, *J. Org. Chem.* **2006**, *71*, 5737–5742.

[102] M. L. Hlavinka, J. R. Hagadorn, *Organometallics* **2007**, *26*, 4105–4108.

[103] D. Huang, Y. Zhao, T. R. Newhouse, *Org. Lett.* **2018**, *20*, 684–687.

[104] Y. Chen, D. Huang, Y. Zhao, T. R. Newhouse, *Angew. Chem. Int. Ed.* **2017**, *56*, 8258–8262.

[105] D. R. Armstrong, A. M. Drummond, L. Balloch, D. V. Graham, E. Hevia, A. R. Kennedy, *Organometallics* **2008**, *27*, 5860–5866.

[106] S. E. Baillie, E. Hevia, A. R. Kennedy, R. E. Mulvey, *Organometallics* **2007**, *26*, 204–209.

[107] E. Hevia, K. W. Henderson, A. R. Kennedy, R. E. Mulvey, *Organometallics* **2006**, *25*, 1778–1785.

[108] A. J. Martínez-Martínez, M. Á. Fuentes, A. Hernán-Gõmez, E. Hevia, A. R. Kennedy, R. E. Mulvey, C. T. O'Hara, *Angew. Chem. Int. Ed.* **2015**, *54*, 14075–14079.

[109] D. R. Armstrong, S. E. Baillie, V. L. Blair, N. G. Chabloz, J. Diez, J. Garcia-Alvarez, A. R. Kennedy, S. D. Robertson, E. Hevia, *Chem. Sci.* **2013**, *4*, 4259–4266.

[110] P. G. Williard, G. B. Carpenter, *J. Am. Chem. Soc.* **1985**, *107*, 3345–3346.

[111] P. G. Williard, G. B. Carpenter, *J. Am. Chem. Soc.* **1986**, *108*, 462–468.

[112] C. Sun, P. G. Williard, *Organometallics* **2000**, *122*, 7829–7830.

[113] P. J. Pospisil, S. R. Wilson, E. N. Jacobsen, *J. Am. Chem. Soc.* **1992**, *114*, 7585–7587.

[114] K. W. Henderson, A. E. Dorigo, Q. Y. Liu, P. G. Williard, P. V. R. Schleyer, P. R. Bernstein, *J. Am. Chem. Soc.* **1996**, *118*, 1339–1347.

[115] P. G. Williard, Q. Y. Liu, *J. Am. Chem. Soc.* **1993**, *115*, 3380–3381.

[116] M. Braun, *Helv. Chim. Acta* **2015**, *98*, 1–31.

[117] R. Amstutz, W. Bernd Schweizer, D. Seebach, J. D. Dunitz, *Helv. Chim. Acta* **1981**, *64*, 2617–2621.

[118] D. Seebach, *Angew. Chem., Int. Ed. Engl.* **1988**, *27*, 1624–1654.

[119] D. Seebach, R. Amstutz, T. Laube, W. B. Schweizer, J. D. Dunitz, *J. Am. Chem. Soc.* **1985**, *107*, 5403–5409.

[120] W. Bauer, T. Laube, D. Seebach, *Chem. Ber.* **1985**, *118*, 764–773.

[121] Y. Chi, S. Ranjan, P. W. Chung, C. S. Liu, S. M. Peng, G. H. Lee, *J. Chem. Soc. Dalt. Trans.* **2000**, 343–347.

[122] S. Debnath, N. Arulsamy, M. P. Mehn, *Inorg. Chim. Acta* **2019**, *486*, 441–448.

[123] K. W. Henderson, P. G. Williard, P. R. Bernstein, *Angew. Chem., Int. Ed. Engl.* **1995**, *34*, 1117–1119.

[124] R. P. Davies, D. J. Linton, P. Schooler, R. Snaith, A. E. H. Wheatley, *Chem. Eur. J.* **2001**, *7*, 3696–3704.

[125] W. Marciniak, K. Merz, M. Moreno, M. Driess, *Organometallics* **2006**, *25*, 2003–2005.

[126] R. E. Mulvey, *Chem. Commun.* **2001**, 1049–1056.

[127] E. Hevia, A. R. Kennedy, R. E. Mulvey, S. Weatherstone, *Angew. Chem. Int. Ed.* **2004**, *43*, 1709–1712.

[128] N. D. R. Barnett, W. Clegg, A. R. Kennedy, R. E. Mulvey, S. Weatherstone, *Chem. Commun.* **2005**, *190*, 375–377.

[129] A. J. Martínez-Martínez, D. R. Armstrong, B. Conway, B. J. Fleming, J. Klett, A. R. Kennedy, R. E. Mulvey, S. D. Robertson, C. T. O'Hara, *Chem. Sci.* **2014**, *5*, 771–781.

[130] X. He, B. C. Noll, A. Beatty, R. E. Mulvey, K. W. Henderson, *J. Am. Chem. Soc.* **2004**, *126*, 7444–7445.

[131] M. L. Hlavinka, J. R. Hagadorn, *Organometallics* **2006**, *25*, 3501–3507.

[132] D. Y. Lee, J. F. Hartwig, *Org. Lett.* **2005**, *7*, 1169–1172.

[133] Z. Livingstone, *Novel N-Heterocyclic Activations Mediated by Magnesium Reagents Having Sterically Hindered Ligands*, University Of Strathclyde, PhD Thesis, Glasgow, **2012**.

Chapter 3: Accessing Potassium Metal(ates) Supported by a Bulky Silyl(bis)amide Ligand

This Chapter is adapted with permission from: P. Mastropierro, A. R. Kennedy, E. Hevia Exploiting deprotonative co-complexation to access potassium metal(ates) supported by a bulky silyl(bis)amide ligand *Eur. J. Inorg. Chem.* **2021**, *11*, 1016-1022. DOI: 10.1002/ejic.202001051. Copyright 2020 Wiley-VCH GmbH.

Contributing authors to their manuscript and their role:

Pasquale Mastropierro: Conceived the project, performed all the experimental work, analyzed the data, wrote the first draft of the manuscript and the supporting information, measured and solved structures of compound **13** and **14**

Alan R. Kennedy: Checked the accuracy of X-Ray diffraction data processing

Eva Hevia: Principal Investigator, conceived the project, secured the funding, directed the work, and wrote the final version of the manuscript with contributions from all authors.

3.1 General introduction to this chapter

Main group bimetallic compounds combining an alkali metal with a more electronegative metal (such as magnesium, zinc or aluminum) are nowadays a well-established family of reagents in Organometallic Chemistry.[1–8] Also known as -*ate* compounds, these systems have found numerous applications in cornerstone organic transformation such as deprotonative metalation,[7,9–15] metal-halogen exchange[5,16–18] or nucleophilic additions[19–23] to name just a few. A significant amount of effort has been devoted to the isolation and characterization of these mixed metal species in the solid state and in solution.[24–29] Most of the these studies have focused on lithium and sodium compounds, whereas potassium -*ates* have received significant less attention. [30–34] This chapter focuses on the synthesis of a new family of potassium metal(ates) supported by the sterically demanding bis(amide) ligand $\{Ph_2Si(NAr^*)_2\}^{2-}$ (introduced in **Chapter 2**), thus some key results from the recent literature on potassium metal(ates) complexes are summarized in this introduction.

Several synthetic studies have shown that combining potassium with magnesium in the same molecule leads to an enhancement of the reactivity of the resulted bimetallic compounds.[29,35–41] For example $[(PMDETA)_2K_2MgR_4]$ (PMDETA= N,N,N',N'',N''-pentamethyldiethylenetriamine, R= CH_2SiMe_3), is capable of quantitatively *ortho*-metalate anisole (**Scheme 3. 1**), while the neutral organomagnesium $Mg(CH_2SiMe_3)_2$ is totally inert towards this substrate. In this work a remarkable alkali-metal effect is also observed, with the potassium magnesiate being more reactive than the sodium and lithium analogues.[29]

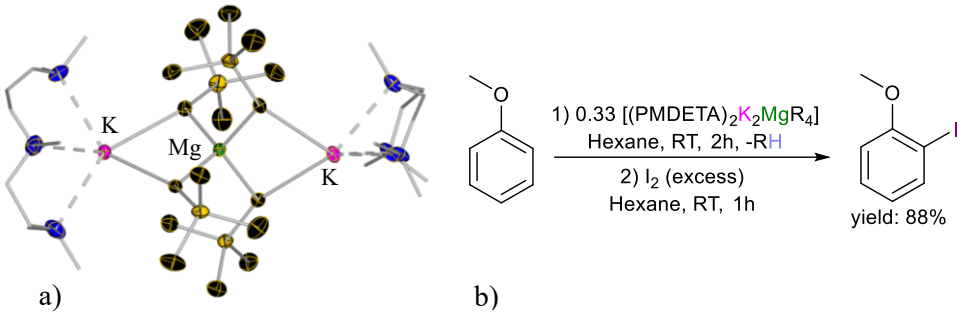

Scheme 3. 1 *a) Molecular structure of [(PMDETA)$_2$K$_2$MgR$_4$]. Thermal ellipsoids are rendered with 30% probability. Hydrogen atoms and disorder components are omitted for clarity. b) Metalation of anisole using the high order magnesiate [(PMDETA)$_2$K$_2$MgR$_4$].*

Another example of alkali-metal effect in deprotonative metalation reactions, using alkali-metal magnesiates, was observed for the deprotonation of naphthalene using [NaMg(TMP)$_2$^{n}Bu] and its potassium analogue [KMg(TMP)$_2$^{n}Bu]. The sodium magnesiate promoted a twofold deprotonation at position 1 and 4, while the potassium magnesiate base induced the selective C2 mono-metalation (**Scheme 3. 2**).[41]

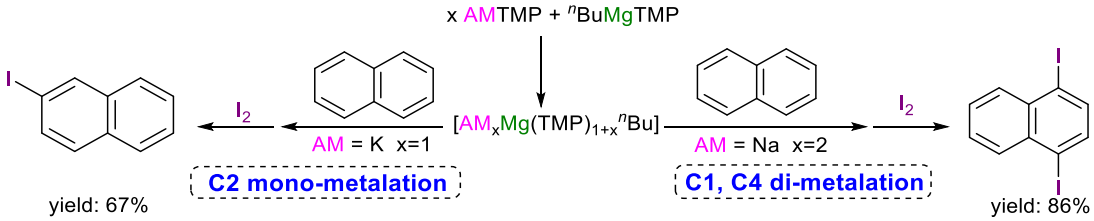

Scheme 3. 2 *Divergent regioselective in metalation using [KMg(TMP)$_2$^{n}Bu] or [NaMg(TMP)$_2$^{n}Bu] in deprotonation of naphthalene*

Isolation of the organometallic intermediates prior to electrophilic interception also revealed significant differences. The mixed sodium/magnesium system afforded a supramolecular arrangement exhibiting an "inverse crown" motif,[11,42] containing a demethylated TMP variant in the structure [{Na$_4$Mg$_2$(TMP)$_4$(TMP*)$_2$}(1,4-C$_{10}$H$_6$)] (TMP*= 2,2,6-trimethyl-1,2,3,4-tetrahydropyridide, can be described as a demethylated variant of TMP and TMP= 2,2,6,6-tetramethylpiperidide), characterized by a dicataionic12-member {(NaNNaNMgN)$_2$} ring which hosting in its core a 1,4 di-magnesiated naphthalene. Contrastingly, the potassium magnesiate induced the formation of a 24-membered ring {KNMgN}$_6$ hosting six C2-metallated naphthalene anions. Thanks to this conformation the potassium cations can maximize the π interactions with the aromatic anions, affording [{KMg(TMP)$_2$(C$_{10}$H$_7$)}$_6$] (**Figure 3. 1**).

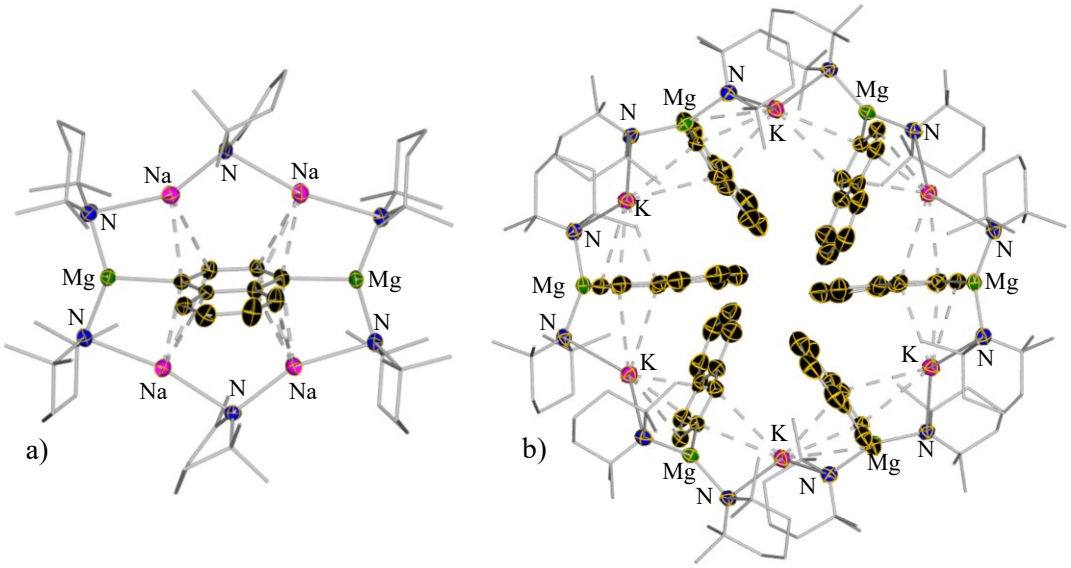

Figure 3. 1 *a) Molecular structure of [{$Na_4Mg_2(TMP)_4(TMP^*)_2$}($C_{10}H_8$)] b) Molecular structure of [{$KMg(TMP)_2(C_{10}H_9)$}$_6$] Notably the size of the two inverse crown rings are very different. Hydrogen atoms are omitted and carbon atom of TMP anions shown as wireframe for clarity. The thermal ellipsoids are rendered with 30% probability. Symmetry transformations used to generate symmetrical atoms in b): -y, x-y, z; -x, -y, 1-z; -x+y, -x, z; y, -x+y, 1-z; x-y, x, 1-z.*

Potassium magnesiates have also shown excellent potential in catalysis.[3,43,44] Thus $[(PMDETA)_2K_2MgR_4]$ has been successfully applied as pre-catalyst for the cyclization of alkynols[43] (**Scheme 3. 3**) and intermolecular hydroamination of alkynes and alkenes.[44] In those reactions the potassium magnesiate performed better than neutral organomagnesium, MgR_2. This has been rationalised in terms of chemical cooperativity, with potassium acting as built-in Lewis acid, coordinating the unsaturated fragment bringing it closer to the magnesiate anion, that is more kinetically activated than a neutral organomagnesium species.[45]

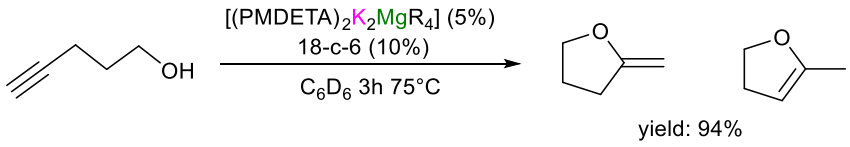

Scheme 3. 3 *Cyclization of 4-pentynol catalysed by $[(PMDETA)_2K_2MgR_4]$ and 18-crown-6 (18-c-6) to afford 2-methylenetetrahydrofuran and 5-methyl-2,3-dihydrofuran (ratio of the two isomers 90:10 respectively)*

In parallel to these studies, there have also been examples reported on the exceptional reactivity of potassium zincates. Within metalation chemistry, heteroleptic potassium zincates containing alkyl and the amido TMP groups, [46–51] have been found to be able to promote direct zincation of non-activated substrates like pyridines[46,47], metallocenes[49] and other unsaturated organic molecules such as ethene.[50] An interesting example of the role played by potassium in these bimetallic systems is represented by the metallation of ethene achieved by the heteroleptic potassium zincate $[(PMDETA)KZn(TMP)R_2]$.[50] Whereas the sodium analog $[(TMEDA)NaZn(TMP)R_2]$ which fails to promote this reaction. Using a potassium zincate was also possible, for the first time, the isolation and characterization of the metalated

intermediate [(PMDETA)K(μ-TMP)(μ-CH=CH$_2$)ZnR] where the potassium contribute in stabilizing the vinyl anion π-engaging the double bond, while zinc had a σ-bond with the metalated carbon.

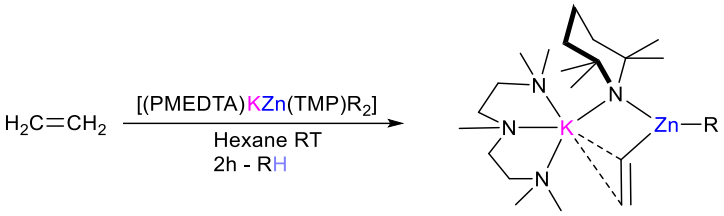

Scheme 3. 4 *Metalation of ethene operating by [(PMDETA)KZn(TMP)R$_2$] (R= CH$_2$SiMe$_3$)*

Potassium zincates can also be used as catalysts, [KZn(HMDS$_2$)Bnz][51] (Bnz= benzyl) was used as a precatalyst in the addition of diphenyl to styrene (**Scheme 3. 5**), either as an isolated compound or prepared *in-situ* from the combination of KBnz and Zn(HMDS)$_2$.[52] Potassium, probably, played a role in the coordination and activation of the organic substrate in a similarly on what happened in the chemistry of the magnesiate. Interestingly in this reaction it is visible an alkali-metal effect since the mixture of NaBnz or LiBnz, in combination with Zn(HMDS)$_2$ were unable to catalyse the transformation.

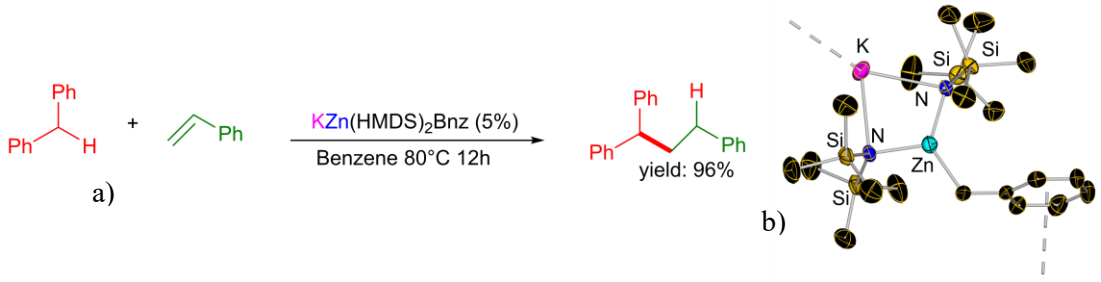

Scheme 3. 5 *a) Zinc-catalysed addition of diphenyl to styrene and b) molecular structure of [KZn(HMDS)$_2$Bnz], the thermal ellipsoids are rendered at 50% probability (Bnz= Benzyl, HMDS= N(SiMe$_3$)$_2$)*

Extending some of the reactivity to earth-abundant transition metals, potassium manganate, with manganese in the oxidation state of +2, have also shown some promise in synthesis. Thus [KMn(CH$_2$SiMe$_3$)$_3$], a manganate obtained by the combination of KCH$_2$SiMe$_3$ and Mn(CH$_2$SiMe)$_2$, has shown notably reactivity deprotonating 1,4 dioxane and inducing its ring opening (**Scheme 3. 6**).[53] The metalation of the dioxane should be facilitated by the close proximity of the cyclic ether (after the coordination) to activated alkyl group of the manganate. Remarkably both sodium and lithium manganates analog are unreactive towards this type of dioxane activation, which in these systems, it acts as a simple Lewis donor.

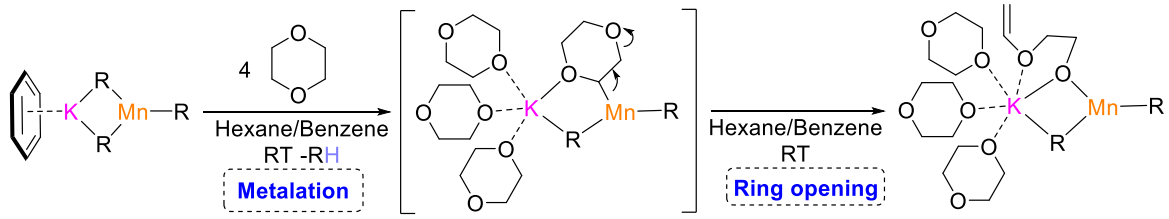

Scheme 3. 6 *Reaction of $KMn(CH_2SiMe_3)_3$ with 1,4 dioxane, in the brackets it is reported the assumed intermediate step between the metalation and the ring opening of the dioxane.*

3.2 Aims

The aim of the chapter is to advance the synthetic and structural understanding on potassium metal-*ates* using the sterically demanding ligand $\{Ph_2Si(NAr^*)_2\}^{2-}$ introduced in **Chapter 2**. A stepwise deprotonative metalation/co-complexation approach **(Scheme 3. 7)** has been explored and tested for magnesium, zinc and manganese.

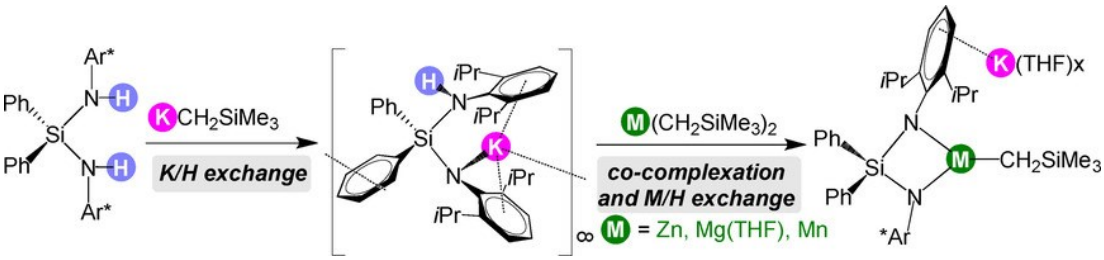

Scheme 3. 7 *Sequential deprotonative metalation to access new potassium metalates supported by a bulky silyl(bis)amide*

3.3 Introduction from the paper

Alkali-metal magnesiates and zincates have found widespread use in organic synthesis with key applications in deprotonative metalation[1,3,8] and metal-halogen exchange,[4–6] as well as nucleophilic arylation/alkylation of unsaturated organic molecules[19,21,23,54], Their unique reactivities, offering in some cases greater control of the regioselectivity and exceptional functional group tolerance have been attributed to the cooperativity inherent in these metal partnership.[1] Furthermore advances in this field have shown that the reactivities of these bimetallic systems can be finely tuned by modifying the anionic ligands, the presence (or absence) of a Lewis donors as well as the choice of alkali-metal. In this regard most of the studies mentioned above have focussed on heterobimetallic systems where the alkali-metal is either Li or Na whereas the number of potassium metal(ates) structurally defined is noticeably smaller and their applications in synthesis have been less explored.[1] Nevertheless they have already shown enormous promise as illustrated by the deprotonation of naphthalene using potassium magnesiate $[KMg(TMP)_2Bu]$ (TMP=2,2,6,6-tetramethylpiperidide) furnishing an eye-catching inverse crown structure containing 24-membered $\{KNMgN\}_6$ ring with six naphthalene molecules hosted in its core which have been selectively magnesiated at their C2 position, hosted in its core.[11] Partnering K and Zn within a zincate framework can also give results, as for example leading to synergic sedation of sensitive anions such as vinyl arising

from deprotonation of ethene[50] Such potassium-zinc cooperativity has also been recently extended to the catalytic regime.[51,52] Among our contributions to this area, recently we investigated the synthesis of sodium magnesiates and zincates which contain the bulky silyl(bis)amide ligand $\{Ph_2Si(NAr^*)_2\}^{2-}$ (Ar* = 2,6-diisopropylphenyl) (see **Chapter 2**).[55] Interestingly, while sometimes this sterically demanding ligand acts as steric stabilizer enabling the isolation of radical anions[50–52,56] or the deprotonation of N-heterocyclic molecules such as N-methyl benzimidazole,[57] on other occasions $\{Ph_2Si(NAr^*)_2\}^{2-}$ can also act as a base, facilitating the metalation of amines[57] and ketones (see **Chapter 2**) as well as the activation of small organic molecules such as benzothiazole.[55] Building on these precedents, here we report a general protocol to access a new family of structurally-defined mixed-metal complexes supported by this bulky silyl(bis)amide ligand, combining potassium with an earth abundant divalent less electropositive metal M where M= Zn, Mg and Mn.

3.4 Results and Discussion

Previous studies on alkali-metal ate chemistry have established co-complexation approaches of the relevant monometallic components in the desired stoichiometry as a versatile strategy to access heterobimetallic complexes.[1] Furthermore DFT calculations on this type of reactions have revealed that in many cases the formation of the relevant heterobimetallic complexes is thermodynamically driven.[58] For this study, to prepare new potassium metal(ates) derived from the bis(amino)silane $Ph_2Si(NHAr^*)_2$ (**1**), double deprotonation of **1** is required to generate into a dianionic silylbis(amide) ligand.[59] This was probed using a stepwise approach, employing two single-metal reagents in sequence (**Scheme 3. 8** and **Scheme 3. 9**). To start, we investigated the deprotonation of $Ph_2Si(NHAr^*)_2$ (**1**) by the alkyl base KCH_2SiMe_3 (**Scheme 3. 8**). Interestingly, the reaction of **1** with one molar equivalent of more reactive KCH_2SiMe_3 proved to be temperature dependent, thus while a complex mixture of products was obtained when the reaction was carried out in hexane at room temperature, performing the deprotonation at 0°C afforded monopotassiated $[\{Ph_2Si(NHAr^*)(NAr^*)K\}_\infty]$ (**13**) in a 77% yield which was characterized by multinuclear NMR spectroscopy and its structure was determined by X-ray crystallographic studies.

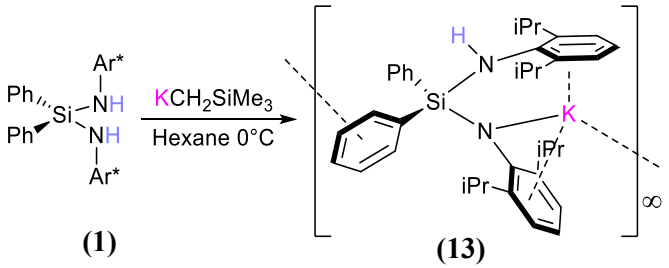

(1) **(13)**

Scheme 3. 8 *Selective mono-metalation of **1** performed by KCH_2SiMe_3, Ar*= 2,6-diisopropylphenyl*

^{1}H NMR spectra of **13** in deuterated THF solutions confirm the mono-deprotonation of **1** displaying a broad signal of N-H at 3.65 ppm, along with the presence of two inequivalent Ar* groups, consistent with the presence of NAr* and NHAr* groups (see Experimental Section). This was confirmed by X-ray crystallographic studies of **13** which revealed the formation of a

one dimensional polymeric chain made up by {$Ph_2Si(NHAr^*)(NAr^*)K$} units in which potassium forms a single K-N bond with the amide arm of the ligand (K-N2, 2.711 (3) Å) while π-engaging with both Ar* groups, in η^6- and η^2-fashions on the amine and amide fragments respectively of the silyl(amide)amine ligand (**Figure 3. 2a**). Reflecting the softer character of K, this coordination mode differs significantly to that reported earlier by us for the sodium congener of **13** where its silyl(amide)amine ligand coordinates as a chelate to sodium via both N atoms (see **Chapter 2**, compound **5**). Potassium completes its coordination by forming additional π-contacts with one of Ph groups attached to Si from a neighbouring unit giving rise to the polymeric structure shown in **Figure 3. 2b**.

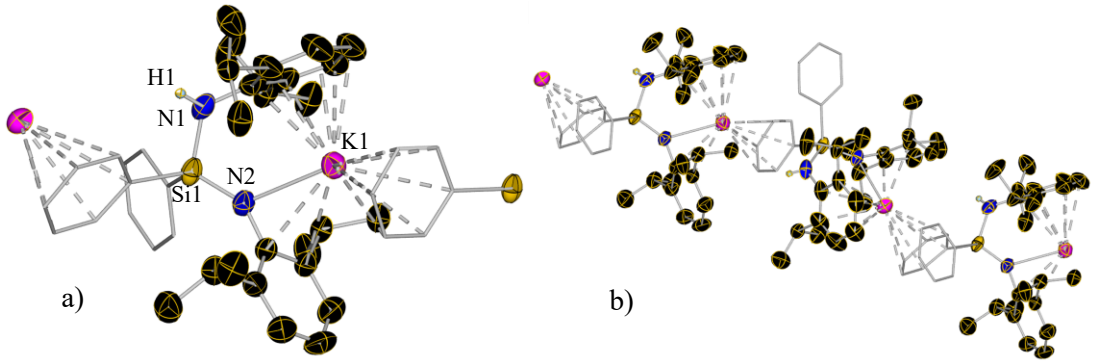

Figure 3. 2 ***a)*** *Molecular fragment and* ***b)*** *polymeric structure of* ***13*** *[{$Ph_2Si(NHAr^*)(NAr^*)K$}$_\infty$] Thermal ellipsoids are rendered at 50% probability. Hydrogen atoms (except NH group) and disordered component (in the methyl groups of Dipp) are omitted, carbon atoms phenyl ring of {$Ph_2Si(NAr^*)_2$}$^{2-}$ are drawn as wire frames for clarity. Selected bond distances (Å) and angles (°) N2-K1 2.711(3), K1-C_{aryl} ranging from 2.944(3) to 3.548(7), N1-Si1-N2 107.87(15), Si-N2-K1 128.44(15) Symmetry transformations used to generate symmetrical atoms: x, 3/2-y, -1/2+z; x, 3/2-y,1/2+z for* ***a)*** *and x, 3/2-y, -1/2+z; x, 3/2-y,1/2+z; x, y, 1+z for* ***b)***

This polymeric arrangement contrasts with the molecular hexameric motif reported by Coles for related potassium (amino-amido)silane complex [{$Me_2Si(NHAr^*)(NAr^*)K$}$_6$],[59] which can be attributed to the lack of aromatic substituents on silicon. Thus, in these case potassium forms π-interactions with the aromatic ring of the NHAr* group and with the NAr* ring of a neighbouring unit, giving rise to cyclic hexameric structure. While the number of unsolvated potassium amides structurally defined is scarce,[30–34] probably due to the low solubility of these species in non-donor solvents, the structure of **13** can be compared with that reported for [K{$N(SiMe_3)(Ar^*)$}]$_\infty$ which also exhibits a polymeric arrangement which propagates via η^6-C−K engagement.[60] Potassium π-arene interactions not only have been found to be a common structural feature in many heavy alkali metal organometallic complexes,[45] it has also been noted that they can play a major role in their reactivity. Thus, seminal work by Schlosser has proposed that K-C π-interactions can modulate the reactivity of LIC-KOR reagents.[61] Similarly, Mulvey has found that potassium magnesiate and zincate systems that can promote unique regioselectivities for the metalation of arenes which seem to be directed by initial π-coordination of the substrate to potassium.[1,3,8,11,50–52] More recently studies assessing the catalytic ability of alkali magnesiates for hydroamination and hydroalkoxylation of C-C triple bonds have revealed significantly enhanced performances for mixed potassium/magnesium

catalysts which has been attributed to the activation of the unsaturated organic substrate by K via the formation of electrostatic π-arene interactions.[43,44]

Next, we pondered whether **13** could act as a precursor to access potassium zincate and magnesiate complexes. In this regard, previous work from our group has shown that the sodium congener of **13** (see **Chapter 2** compound **5**) can react with zinc amide $Zn(HMDS)_2$ to furnish the charge-separated sodium zincate $[\{Ph_2Si(NAr^*)_2Zn(HMDS)\}^-\{Na(THF)_6\}^+]$ resulting from the deprotonation of the remaining NH group of the (amino)-amidosilane by one of the HMDS groups on Zn (see **Chapter 2**, compound **6**). Building on these results we first tried the reaction of **13** with dialkylzinc $Zn(CH_2SiMe_3)_2$ although it should be noted that unlike Zn amides which have shown some promise as deprotonating reagents,[62] dialkylzinc reagents are significantly more kinetically retarded bases.[63] Pleasingly, this reaction produced potassium alkyl zincate $[\{Ph_2Si(NAr^*)_2Zn(CH_2SiMe_3)\}^-\{K(THF)_4\}^+]$ (**14**) as a crystalline solid in a 76% yield. This approach could also be extended to Mg via $Mg(CH_2SiMe_3)$ as a precursor, affording $[\{Ph_2Si(NAr^*)_2Mg(THF)(CH_2SiMe_3)\}^-\{K(THF)_3\}^+]$ (**15**) in a 55% isolated yield (**Scheme 3. 9**). Formation of **14** and **15** can be reasoned to occur sequentially via co-complexation of **13** and $M(CH_2SiMe_3)_2$ followed by deprotonation of the remaining amine NHAr group of the silyl(amide)amine ligand initially coordinated to K in **13**. This second metalation is probably favoured by the close proximity of the NHAr* and the basic alkyl groups on the metal (see proposed intermediate **I** in **Scheme 3. 9**), whose basicity is enhanced by the formation of a zincate (or magnesiate) species. This is special in the case of zinc since $Zn(CH_2SiMe_3)_2$ fails to react with silyl(bis)amine **1** even under forcing reaction conditions (16 hours, 65°C). On the other hand, previous DFT calculations assessing the co-complexation of alkali-metal alkyls with alkyl complexes of lower polarity metals such as Ga or Zn have revealed that the formation of the heterobimetallic complexes is, on many occasions, thermodynamically driven.[64,65] This supports the initial formation of a bimetallic intermediate such as **I** which in turn could rapidly evolve by intramolecular deprotonation of the silyl(amide)amine ligand to potassium magnesiate and zincate **14** and **15** respectively (**Scheme 3. 9**).

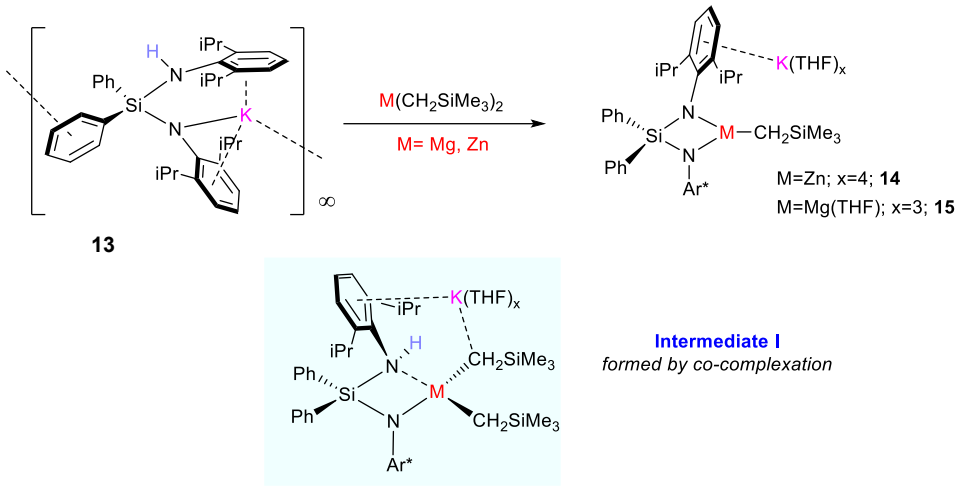

Scheme 3. 9 *Stepwise two-fold deprotonation of $Ph_2Si(NHAr^*)_2$ (**1**) using single metal reagents KCH_2SiMe_3 and $M(CH_2SiMe_3)_2$ (M=Zn, Mg) in sequence to access potassium metal(ates) $[\{Ph_2Si(NAr^*)_2Zn(CH_2SiMe_3)\}^-\{K(THF)_4\}^+]$ (**14**) and $[\{Ph_2Si(NAr^*)_2Mg(CH_2SiMe_3)(THF)\}^-\{K(THF)_3\}^+]$ (**15**)* ^{1}H and ^{13}C NMR characterization of **14** and **15** in D_8-THF solution confirmed the di(deprotonation) of **1** to form a symmetrical bis(amide) ligand, showing a single set of signals for the Ar* groups (see Experimental Section). In addition, a distinctive shielded singlet at -0.9 ppm for **14** and -1.61 ppm for **15** is observed which can be assigned to the M-CH_2 group of the monosilyl ligand and that are slightly more deshielded than those observed for the same group in the M^{II} alkyl precursors (-0.88 and -1.77 ppm for M= Zn and Mg respectively). Considering that $Mn(CH_2SiMe_3)_2$ has also been used as a precursor to prepare other alkali-metal manganates via co-complexation,[53,66–68] we also studied its reaction with **13** which afforded the potassium manganate $[\{Ph_2Si(NAr^*)_2Mn(CH_2SiMe_3)\}^-\{K(THF)_3\}^+]$ (**16**) in a 24% crystalline yield (**Scheme 3. 10**).

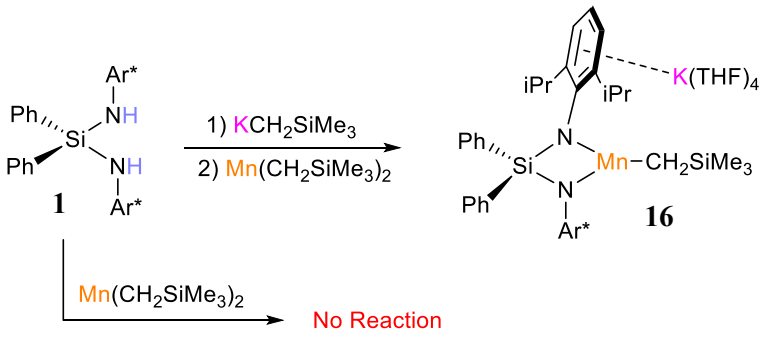

Scheme 3. 10 *Synthesis of potassium manganate **16** via stepwise metalation and co-compleaxation*

Formation of **16** with concomitant metalation of the NHAr* fragment in **13** contrasts with the lack of reactivity of $Mn(CH_2SiMe_3)_2$ which fails to deprotonate **1** on its own. Interestingly the remaining alkyl group in **16** can still react as a base as evidenced when assessing its reactivity against phenylacetylene and the amine HMDS(H), which yielded the potassium manganates $[\{Ph_2Si(NAr^*)_2Mn(THF)(C{\equiv}CPh)\}^-\{K(THF)_3\}^+]$ (**17**) and

[{$Ph_2Si(NAr^*)_2Mn(HMDS)$}$^-${$K(THF)_2$}$^+$] (**18**) in 61 and 76% yield respectively (**Scheme 3. 11**).

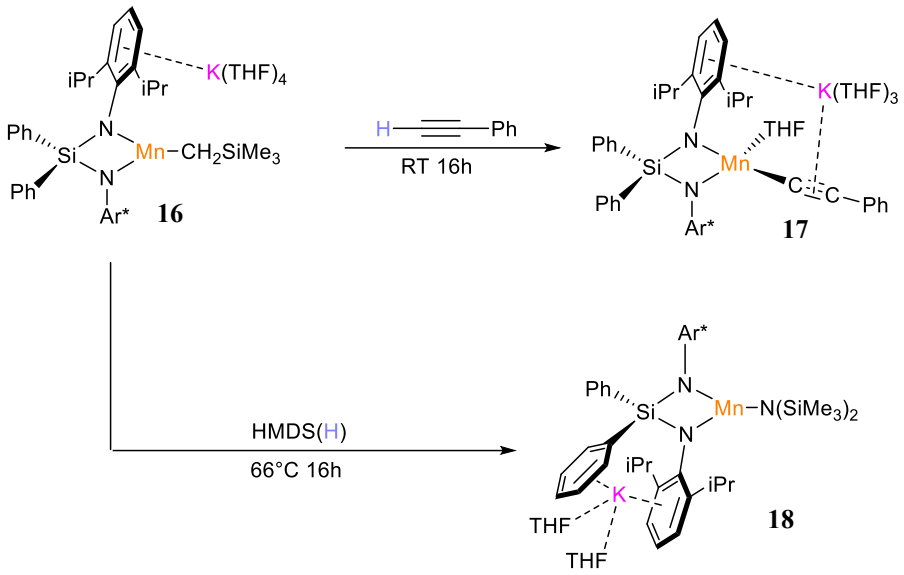

Scheme 3. 11 *Metalation of phenylacetylene and HMDS(H) using **16** as alkyl base*

This reactivity can be compared to those reported by us for related sodium magnesiates and zincates containing the same silyl(bis)amide ligand.[55] (see **Chapter 2**) Thus the alkyl group in the manganate present in **16** seems to offer an intermediate basicity to that found for butyl magnesiate [{$Ph_2Si(NAr^*)_2Mg(THF)(Bu)$}$^-${$Na(THF)_6$}$^+$] which reacts at room temperature with amines[55] and zincate [{$Ph_2Si(NAr^*)_2Zn(CH_2SiMe_3)$}$^-${$Na(THF)_6$}$^+$] which is inert towards HMDS(H) under refluxing conditions (see **Chapter 2**). On the other hand, hinting at an stabilising effect of the sterically demanding bis(amide) ligand in **16**, it is noticeable that this potassium manganate can tolerate THF under refluxing conditions for a long period of time, considering previous studies on the synthesis of related all-alkyl potassium manganate [$KMn(CH_2SiMe_3)_3$] which induces metalation and ring opening of ethereal solvent dioxane at room temperature (see **Scheme 3. 6**).[53] The molecular structures of potassium metal(ates) **14-18** were determined by X-ray crystallography (see **Figure 3. 3**, **Figure 3. 4 Figure 3. 5**, and **Figure 3. 6**). Despite containing a different divalent metal, the general structural features of **14**, **15** and **16** are almost identical. The three ates display pseudo-contacted ion pair structures, with K solvated by three (in **15**) or four (in **14** and **16**) molecules of the donor solvent THF and completing its coordination sphere by π-engaging with the aromatic carbons of one of the di(isopropyl)phenyl groups of one amido group. For zincate **14** and manganate **16** the aryl Ar* interacts with the potassium cation in a η^3-fashion; whereas in magnesiate **15** η^5- coordination is preferred at the expense of K bonding to one molecule less of THF than in **14** or **16** (see **Table 3. 1** for K···C_{aryl} bond distances). In addition, a long-distance electrostatic interaction between K and the one methyl unit of the $SiMe_3$ group is also observed for **15** [K···C41, 3.358(3) Å] (**Figure 3. 3**b). Evidencing the softer character of potassium, its coordination preference of these metal(ates) contrasts to those reported for sodium in related sodium zincates and magnesiates, which formed solvent-separated ion pair species with sodium being

fully solvated by THF molecules (see **Chapter 2**).[55–57] The anion present in **14**, **15** and **16** contain silyl(bis)amide $\{Ph_2Si(NAr^*)_2\}^{2-}$ which coordinates in a chelating fashion to the relevant divalent metal. Each M coordinates to a terminal monosilyl group, generating in the case of **14** and **16** a distorted trigonal geometry around Zn and Mn respectively; whereas **15** displays a distorted tetrahedral Mg which also includes a molecule of THF. The geometrical parameters of the zincate anion in **14** are almost identical to those previously reported for its solvent-separated sodium zincate analogue (see **Chapter 2** compound **3**).

The structure found for potassium magnesiate **15** contrasts with those previously found by Zheng for the higher order potassium magnesiates $[\{(Me_2Si(NAr^*)_2\}_2MgK_2(THF)_x]$ (x = 0, 3), which also contain silyl(bis)amide ligands.[69] Synthesized by reduction of the magnesium bis(amide) $[\{(Me_2Si(NAr^*)_2\}Mg]_2$ with potassium graphite, these complexes exhibit contacted ion pair structures with each potassium sandwiched between two η^6-coordinated Ar* groups.[69] The Mg-C bond in **15** [2.153(2) Å] is relatively short compared to those in other magnesiate complexes containing the same terminally attached alkyl group.[70–73] Consistent with its ate constitution, **15** has Mg-N distances [mean value, 2.067 Å] slightly elongated compared to those reported for neutral Mg silyl(bis)amide $[\{(Ph_2Si(NAr^*)_2\}Mg\ (THF)_2]$ [mean value, 2.009 Å], where Mg also displays a distorted tetrahedral geometry (**Figure 3. 3** b).[55]

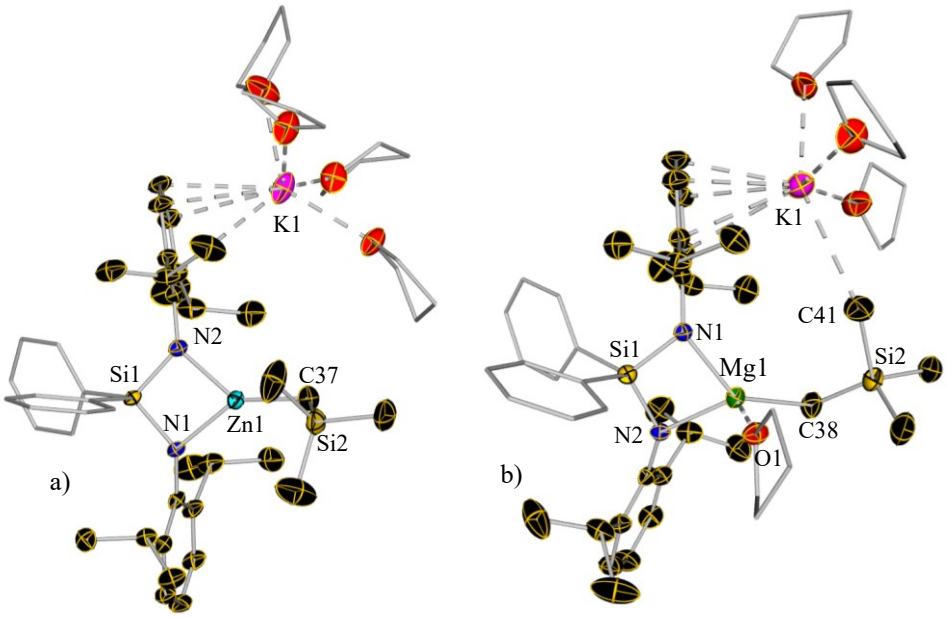

Figure 3. 3 *Molecular structure of **14** (a) and **15** (b). Thermal ellipsoids are rendered at 50% probability. Hydrogen atoms and disorder components in THF and CH_2SiMe_3 groups are omitted, and carbons atoms of phenyl and THF fragments are drawn as wise frames for clarity*

While alkali-metal manganates have already shown good promise in synthesis,[74–76] (see **Chapter 5**) the number of structurally defined examples still remains scant.[53,66–68] While, to the best of our knowledge, **16** represents the first example of an alkali-metal manganate supported by a sterically demanding silyl(bis)amide ligand its structure can be compared to those reported by Mulvey for heteroleptic systems that combine alkyl (or aryl) groups with the

amide TMP.[66–68,77] Sodium manganates [(TMEDA)Na(TMP)(Ar)Mn(CH_2SiMe_3)](Ar=2-C(O)N(^{i}Pr)$_2$C$_6$H$_4$, 2-MeOC$_{10}$H$_6$)[66,77] exhibit contacted ion pair motifs with Na and Mn connected by an aryl and TMP group with the alkyl group also residing terminal at Mn. Interestingly, in these complexes the Mn-C distances [2.158(5), 2.141(2) Å] are slightly more elongated to that found in **16** [2.109(4) Å], which is rather surprising considering the large steric bulk of the bis(amide) coligand present in **16** (**Figure 3. 4**). Within single-metal Mn(II) complexes, related silyl(bis)amide complex [{($Me_2Si(NAr*)_2$}$_2$Mn$_2$] has been prepared by salt metathesis of the relevant dilithiated bis(amide) with $MnCl_2$.[78]

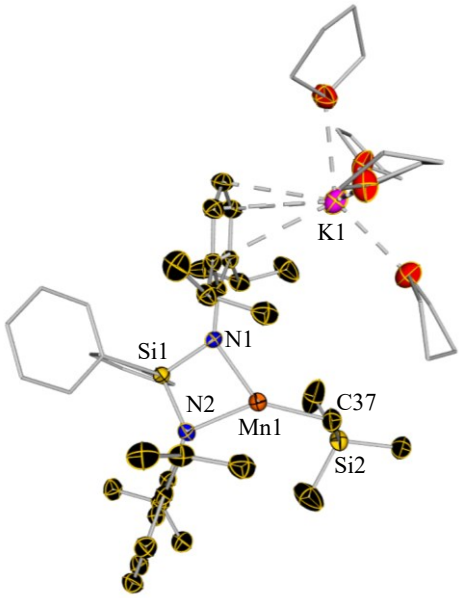

Figure 3. 4 *Molecular structure of **16**. Thermal ellipsoids are rendered at 50% probability. Hydrogen atoms and disordered components in THF and CH_2SiMe_3 groups are omitted, carbon atoms of phenyl, and THF fragments are drawn as wire frames for clarity*

	14 (M=Zn)	**15** (M=Mg)	**16** (M=Mn)
N1-M	1.995(3)	2.051(2)	2.055(3)
N2-M	1.983(3)	2.083(2)	2.068(3)
M-CH_2	1.964(4)	2.153(2)	2.109(4)
M-O1		2.132(2)	
K-C_{aryl}	3.185(4)-3.366(4)	3.105(3)-3.492(2)	3.102(4)-3.393(4)
N1-M-N2	80.14(11)	77.92(7)	77.52(11)
N2-M-C	136.38(15)	131.98(9)	142.17(15)
N1-M-C	142.5(15)	132.94(9)	137.80(15)
Si1-N1-M	90.81(12)	91.07(8)	91.54(13)
Si1-N2-M	90.61(12)	90.45(8)	91.58(13)
N1-Si1-N2	97.20(14)	99.23(8)	98.08(14)

Table 3. 1 *Comparison of selected bond distances (Å) and bond angles (°) for compounds **14**, **15** and **16***

In similar manner to **16**, **17** exhibits a pseudo separated ion pair structure (**Figure 3. 5**). Potassium π- engages with one Ar* group in a η^6-fashion (K-C_{aryl} bond distances ranging from

3.244(2) to 3.371(2) Å), as well as the triple bond of phenylacetylide anion (K···C37 3.279(2) Å; K···C38 3.448(2) Å), those values are the among the longest found in the literature for related K-πC interactions with a C≡C fragment.[79–84] Finally, potassium completes its coordination sphere with 3 molecules of THF. Manganese centre, differently from **16** and **18,** has a very distorted tetrahedral geometry (angles around Mn1 ranging between 77.16(5)° and 144.32(6)°, mean 108.46°). The manganese centre coordinates: the chelating silylbis(amide) ligand through N1 and N2 [average Mn-N distance 2.07 Å], the phenylacetylide anion [Mn-C37, 2.087(2) Å] and a molecule of THF. The distance between the manganese metal centre and the carbon of the alkynyl anion is shorter than Mn-phenylacetylide distances of related manganese supported by bulky ligands previously reported,[85–87] such as the lithium manganates Ar'Mn(C≡CPh)$_3$Li$_3$(THF)(Et$_2$O)$_2$(μ$_3$-I) (Ar'= C$_6$H$_3$-2,6-(C$_6$H$_2$-2,6-^{i}Pr$_3$)$_2$)[85] and [Li$_2$(THF)$_2$Mn(2,6-(Me$_3$Si)$_2$PhC≡C)$_4$][86] or the alkynil manganate supported by β-diketamide ligand [{HC(CMeNAr)$_2$}Mn(μ-C≡CPh)]$_2$ (Ar= 2,6-^{i}Pr$_2$C$_6$H$_3$).[87]However the Mn-C37 distance is still longer than distances reported for the neutral bis-alkynyl manganese [(dmpe)$_2$Mn(C≡CPh)$_2$] (dmpe = bis(dimethylphosphino)ethane).[88] All of the compounds just mentioned, differently from **17**, are made by salt metathesis between MnCl$_2$ and the correspondent lithiated anions.

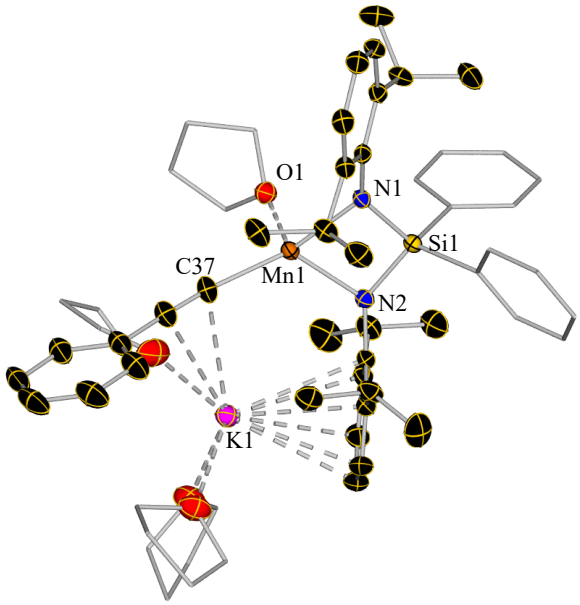

Figure 3. 5 *Molecular structure of **17**. Thermal ellipsoids are rendered at 50% probability. Hydrogen atoms and disordered components in THF groups are omitted. Carbon atoms of phenyl, and THF fragments are drawn as wire frames for clarity. Selected bond distances (Å) and angles (°): Si1-N1 1.705(1), Si1-N2 1.703(1), Mn1-O1 2.210(1), Mn1-C37 2.087(2), Mn1-N1 2.079(1), Mn1-N2 2.061(1), K1-C$_{aryl}$ ranging from 3.244(2) to 3.371(2), K1-C37 3.279(2), K1-C38 3.448(2), Si1-N1-Mn1 91.42(5), N1-Mn1-N2 77.16(5), N2-Si1-N1 98.50(6), Si1-N2-Mn1 92.07(5), N1-Mn1-O1 97.51(4), N1-Mn1-C37 144.32(6), N2-Mn1-O1 104.86(4), N2-Mn1-C37 124.36(8), C37-Mn1-O1 102.52(5)*

Differing for **14**-**17**, in **18** potassium π-engages with one Ar* group as well as with one of the Ph groups on the silicon in a η^6- and η^3-fashion respectively, exhibiting the K-C$_{aryl}$ bond distances ranging from 3.105(5) to 3.468(5) Å. Potassium completes its coordination sphere by bridging the two molecules of solvent THF. The manganate anion in **18** (**Figure 3. 6**)

exhibits a similar structural motif to that of **16**, with a trigonal planar Mn centre (sum of angles around Mn, 359.3°), coordinating to three N atoms, N1 and N2 from the chelating silylbis(amide) ligand [average Mn-N distance, 2.069 Å] and N3 from the HMDS group [Mn-N3, 2.002(4) Å]. These distances compare well with those reported in other alkali-metal species containing the $[Mn(HMDS)_3]^-$ anion.[89,90] This distance is very close to the one reported for $Mn(HMDS)_2$ for the terminal HMDS groups.[91]

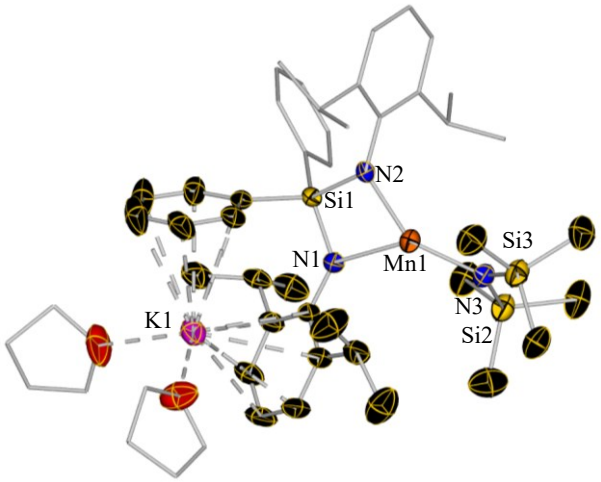

Figure 3. 6 *Molecular structure of **18**. Thermal ellipsoids are rendered at 50% probability. Hydrogen atoms and disordered components in THF groups are omitted, carbon atoms of aryl, and THF fragments are drawn as wire frames for clarity. Selected bond distances (Å) and angles (°): Si-N2 1.712(4), Si-N3 1.707(4), Mn-N1 2.002(4), Mn1-N2 2.038(4), Mn1-N3 2.101(4), K-C_{aryl} ranging from 3.105(5)-3.458(5) Si1-N2-Mn1 92.32(15), N2-Mn1-N3 77.59(13), N2-Mn1-N1 146.58(14), N3-Mn-N1 135.10(14), Si-N3-Mn1 90.31(16), N2-Si1-N3 98.69(17)*

3.5 Conclusions

Sequential di(deprotonation) of bis(amide) silane $Ph_2Si(NHAr^*)_2$ (**1**) with potassium alkyl KCH_2SiMe_3 followed by reaction with a lower polarity divalent metal alkyl $M(CH_2SiMe_3)_2$ (M= Zn, Mg, Mn) provides access to a new family of structurally authenticated potassium metal(ates) $[\{Ph_2Si(NAr^*)_2M(THF)_x(CH_2SiMe_3)\}^-\{K(THF)_y\}^+]$ (x = 0-1, y = 3-4) . Contrasting with the poor reactivity of homoleptic $M(CH_2SiMe_3)_2$ (M= Zn, Mn) towards **1**, the second deprotonation step seems to be facilitated by initial co-complexation of the relevant M di(alkyl) reagent with the potassium silyl(amide)amine generated in the first metalation step. The proposed bimetallic co-complex should provide kinetic activation of one the alkyl groups on the less electropositive metal, enabling the second metalation to yield a bis(amide) ligand that coordinates to M in a chelating fashion. Reactivity studies on potassium manganate **16** demonstrates the kinetic activation of its alkyl group towards alkyne and amine deprotonation affording manganates **17** and **18**, in particular the last example contrasts with lack of reactivity observed for bis(alkyl) precursor $Mn(CH_2SiMe_3)_2$ towards **1**.

3.6 Experimental Section

Synthesis of [{($Ph_2Si(NAr^*)(NHAr^*)_2$)K}$_\infty$] (**13**)

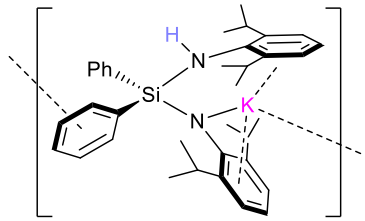

530 mg of **1** (1mmol) and 126 mg of KCH_2SiMe_3 (1mmol) were placed in an argon flushed and flame dried Schenk tube. The tube was placed in a cold bath at 0°C and 5mL of hexane were added. The suspension was stirred for 1h and then the mixture was allowed to warm up at room temperature and stirred for another hour. Solvent and all volatiles were removed under vacuum. 20 mL of toluene were added, furnishing a yellow suspension, that was gently heated until a yellow solution was obtained. Colourless crystals of **13** were obtained after slow cooling of this solution (437 mg, yield: 77%).

^{1}H-NMR (D_8-THF; 298K, 400 MHz) δ (ppm): 7.65 [m, 4H, Ph], 7.11 [m, 6H, Ph], 6.78 [d, 2H, Ar*], 6.71 [d, 2H, Ar*], 6.58 [t, 1H, Ar*], 6.19 [t, 1H, Ar*], 3.93 [sept, 2H, CH ^{i}Pr], 3.65 [s broad, 1H, NH], 3.36 [sept, 2H, CH ^{i}Pr], 0,9 [d, 12H, CH_3 ^{i}Pr], 0.79 [d, 12H, CH_3 ^{i}Pr]. **^{13}C{^{1}H}-NMR** (D_8-THF; 298K, 100 MHz) δ (ppm): 155.0, 146.3, 144.5, 140.6, 139.8 [$C_{quaternary}$ Ph and Ar*], 135.7, 127.3, 127.0, 122.9, 122.5, 119.6, 111.6 [CH Ph and Ar*], 28.9,27.7 [CH ^{i}Pr], 24.5, 23.6 [CH_3 ^{i}Pr]

Elemental analysis: analytical calculated $C_{36}H_{45}KN_2Si$ C 75.47, H 7.92, N 4.89. Found: C 75.42, H 7.83, N 4.80.

Synthesis of [{$Ph_2Si(NAr^*)_2$)Zn(CH_2SiMe_3}$^-${$K(THF)_4$}$^+$] (**14**)

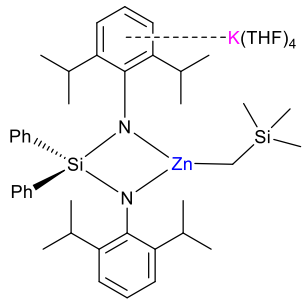

$Zn(CH_2SiMe_3)_2$ (1 mmol) was prepared *in-situ* by mixing 136 mg of $ZnCl_2$ (1 mmol) with 2 mL of a 1 M solution of $LiCH_2SiMe_3$ in pentane (2 mmol) in 15 mL of Et_2O at -40°C. After 1h of stirring at RT, LiCl was removing by filtration affording a clear solution to which 1 mmol of **13** (568 mg) was added. The mixture was allowed to stir at room temperature overnight. Volatiles were removed under vacuum and to the white residue 7 mL of hexane and 0.7 mL of THF was added, affording a pale-yellow suspension. The mixture was heated under reflux and let slowly cool down at room temperature depositing a crop of colourless crystals of **14** after 24h at room temperature. (550 mg, yield 76%).

^{1}H-NMR (D_8-THF; 298K; 600 MHz) δ (ppm): 7.27 [m, 4H,Ph], 6.94 [m, 6H, Ph], 6.7 [d, 4H Ar*], 6.42 [t, 2H, Ar*], 4.15 [sept, 4H, CH ^{i}Pr], 0.8 [d, 24H, CH_3 ^{i}Pr], -0.14 [s, 9H, CH_3 CH_2SiMe_3], -0.9 [s, 2H, CH_2 CH_2SiMe_3]. It should be noted that almost all the solvating THF present in **14** were removed under vacuum when drying the crystals (only one molecule was left according to NMR and CHN data). **^{13}C{^{1}H}-NMR** (D8-THF; 298K; 150 MHz) δ (ppm):

153.3, 148.2, 144.8 [$C_{quaternary}$ Ar* and Ph], 136.1, 126.66, 126.5 [CH Ph], 122.2, 117.0 [CH of Ar*], 28.3 [CH ^{i}Pr], 25.0 [CH_3 ^{i}Pr], 3.4 [CH_3, CH_2SiMe_3], -6.1 [CH_2 CH_2SiMe_3].

Elemental analysis: analytical calculated: $C_{44}H_{63}KN_2OSi_2Zn$ C 66.34, H 7.97, N 3.52. Found: C 65.27, H 7.4, N 3.64.

Synthesis of [{($Ph_2Si(NAr^*)_2$)Mg(THF)(CH_2SiMe_3)}$^-${$K(THF)_3$}$^+$] (**15**)

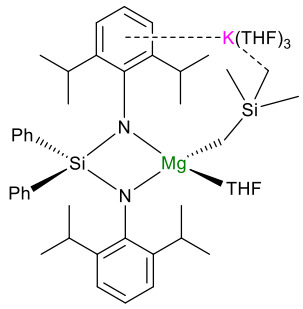

100 mg of $Mg(CH_2SiMe_3)_2$ (0.5 mmol) and 284 mg of **13** (0.5 mmol) were solubilized in 5mL of THF. The mixture was allowed to stir at RT for 1 hour. Volatiles were removed under vacuum and the orange residue were solubilized in 3 mL of Hexane and 2.5 mL of THF affording a yellow solution. The solution was stored in the freezer (-33°C) furnished colourless crystals of **15** (246 mg, yield 55%).

^{1}H-NMR (D_8-THF; 298K; 300 MHz) δ (ppm): 7.20 [m, 4H,Ph], 6.85 [m, 6H, Ph], 6.65 [d, 4H Ar*], 6.33 [t, 2H, Ar* J=7.30 Hz], 4.16 [sept, 4H, CH ^{i}Pr,], 3.62 [m, 12H, OCH_2 THF], 1.77 [m, 12H, CH_2 THF], 0.72 [d, 24H, CH_3 ^{i}Pr], -0.31 [s, 9H, CH_3 CH_2SiMe_3], -1.61 [s, 2H, CH_2 CH_2SiMe_3] It should be noted that some of the solvating THF present in **15** was removed under vacuum when drying the crystals **^{13}C{^{1}H}-NMR** (D_8-THF; 298K; 75 MHz) δ (ppm): 154.3, 148.9, 143.5 [$C_{quaternary}$ Ar* and Ph], 135.6, 126.66, 125.1 [CH Ph], 121.4, 114.5 [CH Ar*], 27.1 [CH ^{i}Pr], 25.6 [CH_3 ^{i}Pr], 4.3 [CH_3 CH_2SiMe_3], 0.5 [CH_2 CH_2SiMe_3].

Elemental analysis: analytical calculated: $C_{51}H_{79}KMgN_2O_3Si_2$ C 69.41, H 8.85, N 3.11. Found: C 69.28, H 9.09, N 2.91.

Synthesis of [{($Ph_2Si(NAr^*)_2$)Mn(CH_2SiMe_3)}$^-${$K(THF)_4$}$^+$] (**16**)

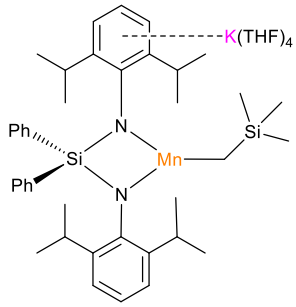

115 mg of $Mn(CH_2SiMe_3)_2$ (0.5 mmol) was solubilized in 3mL of THF, then 284 mg of **13** (0.5 mmol) was added to the solution. The mixture was allowed to stir at RT for 3 hours. Volatiles were removed under vacuum and the orange residue were solubilized in 1.5 mL of hexane and 0.9 mL of THF affording an orange suspension. The suspension was stored in the freezer (-33°C) furnishing orange crystals of **16** (118 mg, yield 24%).

Elemental analysis: analytical calculated: $C_{40}H_{55}KMnN_2Si_2$ C 67.28, H 7.76, N 3.92. Found: C 66.68, H 7.75, N 3.80 (all THF molecules solvating K were removed when drying the crystals under vacuum).

Synthesis of [{$Ph_2Si(NAr^*)_2Mn(THF)(C{\equiv}CPh)\}^-\{K(THF)_3\}^+$] (**17**)

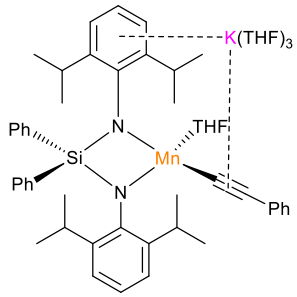

115 mg of $Mn(CH_2SiMe_3)_2$ (0.5 mmol) and 284 mg of **13** (0,5 mmol) were dissolved in 5 ml of THF and allowed to stir at room temperature for 3 h to generate compound **16** *in-situ*. 0.05 mL of phenylacetylene (0.5 mmol) was added to the yellow solution. The solution was allowed to stir at room temperature overnight. Volatiles were removed and the resulting yellow powder was solubilized in 1 mL of hexane and 0.5 mL of THF affording an orange solution. This solution was then stored in the freezer (-33°C) for 24 hours, furnishing a crop of orange crystals of **17** (244 mg; yield: 61%)

Elemental analysis: analytical calculated $C_{50}H_{78}KMnN_3O_2Si_3$ C 72.06, H 7.18, N 3.5. Found: C 70.43, H 6.87, N 2.87. (3 THF molecules solvating K were removed when drying the crystals under vacuum)

Synthesis of [{$Ph_2Si(NAr^*)_2Mn(HMDS)\}$ $\{K(THF)_2\}^+$] (**18**)

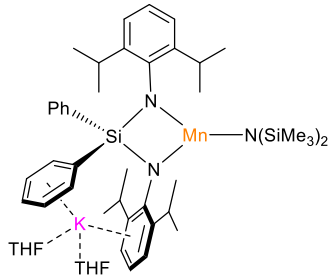

115 mg of $Mn(CH_2SiMe_3)_2$ (0.5 mmol) and 284 mg of **13** (0,5 mmol) were dissolved in 5 ml of THF and allowed to stir at room temperature for 3 h to generate compound **16** *in-situ*. 0.1 mL of hexamethyldisilazane (HMDS(H)) (0.5 mmol) were added to the yellow solution. The solution was allowed to stir at 65°C overnight. Volatiles were removed and the resulting yellow powder was solubilized in 2 mL of hexane and 0.5 mL of THF affording an orange solution. This solution was then stored in the freezer (-33°C) for 24 hours, furnishing a crop of orange crystals of **18** (354 mg; yield: 76%)

Elemental analysis: analytical calculated: $C_{50}H_{78}KMnN_3O_2Si_3$ C 64.47, H 8.44, N 4.51. Found: C 63.99, H 8.42, N 4.00.

3.7 References

[1] S. D. Robertson, M. Uzelac, R. E. Mulvey, *Chem. Rev.* **2019**, *119*, 8332–8405.

[2] F. Mongin, A. Harrison-Marchand, *Chem. Rev.* **2013**, *113*, 7563–7727.

[3] J. M. Gil-Negrete, E. Hevia, *Chem. Sci.* **2021**, *12*, 1982–1992.

[4] D. Tilly, F. Chevallier, F. Mongin, P. C. Gros, *Chem. Rev.* **2014**, *114*, 1207–1257.

[5] M. Balkenhohl, P. Knochel, *Chem. Eur. J.* **2020**, *26*, 3688–3697.

[6] D. S. Ziegler, B. Wei, P. Knochel, *Chem. Eur. J.* **2019**, *25*, 2695–2703.

[7] R. E. Mulvey, F. Mongin, M. Uchiyama, Y. Kondo, *Angew. Chem. Int. Ed.* **2007**, *46*, 3802–3824.

[8] A. Harrison-Marchand, F. Mongin, *Chem. Rev.* **2013**, *113*, 7470–7562.

[9] H. Awad, F. Mongin, F. Trécourt, G. Quéguiner, F. Marsais, F. Blanco, B. Abarca, R. Ballesteros, *Tetrahedron Lett.* **2004**, *45*, 6697–6701.

[10] A. Krasovskiy, V. Krasovskaya, P. Knochel, *Angew. Chem. Int. Ed.* **2006**, *45*, 2958–2961.

[11] A. J. Martínez-Martínez, A. R. Kennedy, R. E. Mulvey, C. T. O'Hara, *Science* **2014**, *346*, 834–837.

[12] Y. Kondo, M. Shilai, M. Uchiyama, T. Sakamoto, *J. Am. Chem. Soc.* **1999**, *121*, 3539–3540.

[13] M. Uchiyama, Y. Matsumoto, D. Nobuto, T. Furuyama, K. Yamaguchi, K. Morokuma, *J. Am. Chem. Soc.* **2006**, *128*, 8748–8750.

[14] W. Clegg, S. H. Dale, E. Hevia, G. W. Honeyman, R. E. Mulvey, *Angew. Chem. Int. Ed.* **2006**, *45*, 2370–2374.

[15] M. Uchiyama, H. Naka, Y. Matsumoto, T. Ohwada, *J. Am. Chem. Soc.* **2004**, *126*, 10526–10527.

[16] M. Uchiyama, T. Furuyama, M. Kobayashi, Y. Matsumoto, K. Tanaka, *J. Am. Chem. Soc.* **2006**, *128*, 8404–8405.

[17] A. Krasovskiy, P. Knochel, *Angew. Chem. Int. Ed.* **2004**, *43*, 3333–3336.

[18] T. Klatt, K. Groll, P. Knochel, *Chem. Commun.* **2013**, *49*, 6953–6955.

[19] M. Dell'Aera, F. M. Perna, P. Vitale, A. Altomare, A. Palmieri, L. C. H. Maddock, L. J. Bole, A. R. Kennedy, E. Hevia, V. Capriati, *Chem. Eur. J.* **2020**, *26*, 8742–8748.

[20] S. E. Baillie, V. L. Blair, D. C. Blakemore, D. Hay, A. R. Kennedy, D. C. Pryde, E. Hevia, *Chem. Commun.* **2012**, *48*, 1985–1987.

[21] M. Hatano, T. Matsumura, K. Ishihara, *Org. Lett.* **2005**, *7*, 573–576.

[22] S. E. Baillie, V. L. Blair, T. D. Bradley, W. Clegg, J. Cowan, R. W. Harrington, A. Hernán-Gómez, A. R. Kennedy, Z. Livingstone, E. Hevia, *Chem. Sci.* **2013**, *4*, 1895–1905.

[23] M. De Tullio, A. Hernán-Gómez, Z. Livingstone, W. Clegg, A. R. Kennedy, R. W. Harrington, A. Antiñolo, A. Martínez, F. Carrillo-Hermosilla, E. Hevia, *Chem. Eur. J.* **2016**, *22*, 17646–17656.

[24] A. Desaintjean, T. Haupt, L. J. Bole, N. R. Judge, E. Hevia, P. Knochel, *Angew. Chem. Int. Ed.* **2021**, *60*, 1513–1518.

[25] L. J. Bole, N. R. Judge, E. Hevia, *Angew. Chem. Int. Ed.* **2021**, *60*, 7626–7631.

[26] P. García-Álvarez, D. V. Graham, E. Hevia, A. R. Kennedy, J. Klett, R. E. Mulvey, C. T. O'Hara, S. Weatherstone, *Angew. Chem. Int. Ed.* **2008**, *47*, 8079–8081.

[27] P. García-Álvarez, R. E. Mulvey, J. A. Parkinson, *Angew. Chem. Int. Ed.* **2011**, *50*, 9668–9671.

[28] P. C. Andrikopoulos, D. R. Armstrong, H. R. L. Barley, W. Clegg, S. H. Dale, E. Hevia, G. W. Honeyman, A. R. Kennedy, R. E. Mulvey, *J. Am. Chem. Soc.* **2005**, *127*, 6184–6185.

[29] S. E. Baillie, T. D. Bluemke, W. Clegg, A. R. Kennedy, J. Klett, L. Russo, M. de Tullio, E. Hevia, *Chem. Commun.* **2014**, *50*, 12859–12862.

[30] A. I. Ojeda-Amador, A. J. Martínez-Martínez, G. M. Robertson, S. D. Robertson, A. R. Kennedy, C. T. O'Hara, *Dalton Trans.* **2017**, *46*, 6392–6403.

[31] M. Gärtner, H. Görls, M. Westerhausen, *Acta Crystallogr. Sect. E Struct. Reports Online* **2007**, *63*, 3921–3931.

[32] C. Glock, H. Görls, M. Westerhausen, *Eur. J. Inorg. Chem.* **2011**, 5288–5298.

[33] A. Hinz, *Chem. Eur. J.* **2019**, *25*, 3267–3271.

[34] M. Arrowsmith, M. S. Hill, G. Kociok-Köhn, *Organometallics* **2011**, *30*, 1291–1294.

[35] N. D. R. Barnett, W. Clegg, A. R. Kennedy, R. E. Mulvey, S. Weatherstone, *Chem. Commun.* **2005**, *190*, 375–377.

[36] D. J. Liptrot, M. S. Hill, M. F. Mahon, *Chem. Eur. J.* **2014**, *20*, 9871–9874.

[37] C. Lichtenberg, T. P. Spaniol, I. Peckermann, T. P. Hanusa, J. Okuda, *J. Am. Chem. Soc.* **2013**, *135*, 811–821.

[38] M. A. Anions, P. C. Andrews, A. R. Kennedy, R. E. Mulvey, C. L. Raston, B. A. Roberts, *Angew. Chem. Int. Ed.* **2000**, *39*, 1960–1962.

[39] W. Clegg, B. Conway, P. García-Álvarez, A. R. Kennedy, R. E. Mulvey, L. Russo, J. Sassmannshausen, T. Tuttle, *Chem. Eur. J.* **2009**, *15*, 10702–10706.

[40] E. Hevia, F. R. Kenley, A. R. Kennedy, R. E. Mulvey, R. B. Rowlings, *Eur. J. Inorg. Chem.* **2003**, 3347–3353.

[41] A. J. Martínez-Martínez, D. R. Armstrong, B. Conway, B. J. Fleming, J. Klett, A. R. Kennedy, R. E. Mulvey, S. D. Robertson, C. T. O'Hara, *Chem. Sci.* **2014**, *5*, 771–781.

[42] D. R. Armstrong, A. R. Kennedy, R. E. Mulvey, R. B. Rowlings, *Angew. Chem. Int. Ed.* **1999**, *38*, 131–133.

[43] M. Fairley, L. Davin, A. Hernán-Gómez, J. García-Álvarez, C. T. O'Hara, E. Hevia, *Chem. Sci.* **2019**, *10*, 5821–5831.

[44] L. Davin, A. Hernán-Gómez, C. McLaughlin, A. R. Kennedy, R. McLellan, E. Hevia, *Dalton Trans.* **2019**, *48*, 8122–8130.

[45] T. X. Gentner, R. E. Mulvey, *Angew. Chem. Int. Ed.* **2020**, *60*, 9247–9262.

[46] W. Clegg, B. Conway, D. V. Graham, E. Hevia, A. R. Kennedy, R. E. Mulvey, L. Russo, D. S. Wright, *Chem. Eur. J.* **2009**, *15*, 7074–7082.

[47] B. Conway, D. V. Graham, E. Hevia, A. R. Kennedy, J. Klett, R. E. Mulvey, *Chem. Commun.* **2008**, 2638–2640.

[48] G. C. Forbes, A. R. Kennedy, R. E. Mulvey, B. A. Roberts, R. B. Rowlings, *Organometallics* **2002**, *21*, 5115–5121.

[49] W. Clegg, B. Conway, P. García-Álvarez, A. R. Kennedy, J. Klett, R. E. Mulvey, L. Russo, *Dalton Trans.* **2010**, *39*, 62–65.

[50] A. R. Kennedy, J. Klett, R. E. Mulvey, D. S. Wright, *Science* **2010**, *706*, 706–709.

[51] W. Clegg, G. C. Forbes, A. R. Kennedy, R. E. Mulvey, S. T. Liddle, *Chem. Commun.* **2003**, *3*, 406–407.

[52] Y. F. Liu, D. D. Zhai, X. Y. Zhang, B. T. Guan, *Angew. Chem. Int. Ed.* **2018**, *57*, 8245–8249.

[53] M. Uzelac, I. Borilovic, M. Amores, T. Cadenbach, A. R. Kennedy, G. Aromí, E. Hevia, *Chem. Eur. J.* **2016**, *22*, 4843–4854.

[54] A. Hernán-Gómez, T. D. Bradley, A. R. Kennedy, Z. Livingstone, S. D. Robertson, E. Hevia, *Chem. Commun.* **2013**, *49*, 8659–8661.

[55] V. L. Blair, W. Clegg, A. R. Kennedy, Z. Livingstone, L. Russo, E. Hevia, *Angew. Chemie* **2011**, *123*, 10031–10034.

[56] Z. Livingstone, A. Hernán-Gómez, S. E. Baillie, D. R. Armstrong, L. M. Carrella, W. Clegg, R. W. Harrington, A. R. Kennedy, E. Rentschler, E. Hevia, *Dalton Trans.* **2016**, *45*, 6175–6182.

[57] D. R. Armstrong, W. Clegg, A. Hernán-Gómez, A. R. Kennedy, Z. Livingstone, S. D. Robertson, L. Russo, E. Hevia, *Dalton Trans.* **2014**, *43*, 4361–4369.

[58] M. F. Lappert, P. P. Power, A. V. Protchenko, A. Seeber, *Metal Amide Chemistry*, John Wiley & Sons, Ltd, Chichester, UK, **2009**.

[59] R. J. Schwamm, M. P. Coles, C. M. Fitchett, *Organometallics* **2015**, *34*, 2500–2507.

[60] M. Á. Fuentes, A. Zabala, A. R. Kennedy, R. E. Mulvey, *Chem. Eur. J.* **2016**, *22*, 14968–14978.

[61] E. Masson, M. Schlosser, *Org. Lett.* **2005**, *7*, 1923–1925.

[62] M. L. Hlavinka, J. R. Hagadorn, *Organometallics* **2007**, *26*, 4105–4108.

[63] D. R. Armstrong, A. M. Drummond, L. Balloch, D. V. Graham, E. Hevia, A. R. Kennedy, *Organometallics* **2008**, *27*, 5860–5866.

[64] D. R. Armstrong, E. Brammer, T. Cadenbach, E. Hevia, A. R. Kennedy, *Organometallics* **2013**, *32*, 480–489.

[65] D. R. Armstrong, H. S. Emerson, A. Hernán-Gómez, A. R. Kennedy, E. Hevia, *Dalton Trans.* **2014**, *43*, 14229–14238.

[66] V. L. Blair, W. Clegg, R. E. Mulvey, L. Russo, *Inorg. Chem.* **2009**, *48*, 8863–8870.

[67] L. M. Carrella, W. Clegg, D. V. Graham, L. M. Hogg, A. R. Kennedy, J. Klett, R. E. Mulvey, E. Rentschler, L. Russo, *Angew. Chem. Int. Ed.* **2007**, *46*, 4662–4666.

[68] V. L. Blair, L. M. Carrella, W. Clegg, B. Conway, R. W. Harrington, L. M. Hogg, J. Klett, R. E. Mulvey, E. Rentschler, L. Russo, *Angew. Chem. Int. Ed.* **2008**, *47*, 6208–6211.

[69] C. Pi, L. Wan, Y. Gu, H. Wu, C. Wang, W. Zheng, L. Weng, Z. Chen, X. Yang, L. Wu, *Organometallics* **2009**, *28*, 5281–5284.

[70] S. E. Baillie, W. Clegg, P. García-Álvarez, E. Hevia, A. R. Kennedy, J. Klett, L. Russo, *Organometallics* **2012**, *31*, 5131–5142.

[71] S. E. Baillie, W. Clegg, P. García-Álvarez, E. Hevia, A. R. Kennedy, J. Klett, L. Russo, *Chem. Commun.* **2011**, *47*, 388–390.

[72] X. H. Wei, M. P. Coles, P. B. Hitchcock, M. F. Lappert, *Zeitschrift fur Anorg. und Allg. Chemie* **2011**, *637*, 1807–1813.

[73] A. R. Kennedy, J. Klett, R. E. Mulvey, S. D. Robertson, *Eur. J. Inorg. Chem.* **2011**, 4675–4679.

[74] R. A. Layfield, *Chem. Soc. Rev.* **2008**, *37*, 1098–1107.

[75] G. Cahiez, C. Duplais, J. Buendia, *Chem. Rev.* **2009**, *109*, 1434–1476.

[76] D. A. Valyaev, G. Lavigne, N. Lugan, *Coord. Chem. Rev.* **2016**, *308*, 191–235.

[77] V. L. Blair, W. Clegg, B. Conway, E. Hevia, A. Kennedy, J. Klett, R. E. Mulvey, L. Russo, *Chem. Eur. J.* **2008**, *14*, 65–72.

[78] D. Y. Lu, J. S. K. Yu, T. S. Kuo, G. H. Lee, Y. Wang, Y. C. Tsai, *Angew. Chem. Int. Ed.* **2011**, *50*, 7611–7615.

[79] T. Chlupatý, J. Turek, F. De Proft, Z. Růžičková, A. Růžička, *Dalton Trans.* **2015**, *44*, 17462–17466.

[80] U. Cremer, I. Pantenburg, U. Ruschewitz, *Inorg. Chem.* **2003**, *42*, 7716–7718.

[81] J. Heppekausen, R. Stade, A. Kondoh, G. Seidel, R. Goddard, A. Fürstner, *Chem. Eur. J.* **2012**, *18*, 10281–10299.

[82] L. A. Berben, J. R. Long, *J. Am. Chem. Soc.* **2002**, *124*, 11588–11589.

[83] M. Schiefer, H. Hatop, H. W. Roesky, H. Schmidt, **2002**, 1300–1303.

[84] W. J. Evans, R. A. Keyer, J. W. Ziller, *Organometallics* **1993**, *12*, 2618–2633.

[85] C. Ni, J. C. Fettinger, G. J. Long, P. P. Power, *Dalton Trans.* **2010**, *39*, 10664–10670.

[86] G. M. Yee, K. Kowolik, S. Manabe, J. C. Fettinger, L. A. Berben, *Chem. Commun.* **2011**, *47*, 11680–11682.

[87] J. Chai, H. Zhu, H. W. Roesky, Z. Yang, V. Jancik, R. Herbst-Irmer, H. G. Schmidt, M. Noltemeyer, *Organometallics* **2004**, *23*, 5003–5006.

[88] V. V Krivykh, I. L. Eremenko, D. Veghini, I. A. Petrunenko, D. L. Pountney, D. Unseld, H. Berke, *J. Organomet. Chem.* **1996**, *511*, 111–114.

[89] H. Chen, R. A. Bartlett, V. R. Dias, M. M. Olmstead, P. P. Power, *Inorg. Chem.* **1991**, *30*, 2487–2494.

[90] M. A. Putzer, B. Neumüller, K. Dehnicke, J. Magull, *Chem. Ber.* **1996**, *129*, 715–719.

[91] B. D. Murray, P. P. Power, *Inorg. Chem.* **1984**, *23*, 4584–4588.

[92] C. Yeardley, A. R. Kennedy, P. C. Gros, S. Touchet, M. Fairley, R. McLellan, A. J. Martínez-Martínez, C. T. O'Hara, *Dalton Trans.* **2020**, *49*, 5257–5263.

[93] A. Alberola, V. L. Blair, L. M. Carrella, W. Clegg, A. R. Kennedy, J. Klett, R. E. Mulvey, S. Newton, E. Rentschler, L. Russo, *Organometallics* **2009**, *28*, 2112–2118.

Chapter 4: Direct Zincation of Fluoroarenes Using a Potassium-Zinc Base Supported by a Sterically Demanding Ligand

4.1 Introduction

Fluorinated compounds are useful building blocks present in a variety pharmaceuticals and agrochemicals (see some relevant examples of drugs containing fluorine in **Figure 4. 1**).[1–4] Fluorine is usually added to biologically active molecules to modify their electronic and pharmacokinetic properties: (*i*) pK_a, (*ii*) lipophilicity, (*iii*) conformation, and (*iv*) resistance to metabolic enzymes[5] without altering significantly the steric encumbrance, since the comparable size of fluorine and hydrogen. In fact, the van der wall radius of Fluorine is 1.47 Å, while the hydrogen is reported to be 1.20 Å.[6] Since the virtually inexistence of fluorine in compounds extracted from natural sources, fluorine atoms (or building block containing fluorine atoms) have to be inserted via chemical synthesis, consequently the development of methods which can allow for the regioselective functionalization of fluoroarenes is an area of great relevance and intense research activity.[6–10] The direct metalation of aromatic substrates, replacing a C-H bond with a more reactive carbon/metal bond, is a valuable strategy in synthesis, especially if it is achieved avoiding the use of toxic and expensive transition metals.[11] Therefore the importance of the fluorinated building block, in this introduction the chemistry of the direct metalation of fluoroarenes using main group metals (and pseudo-main group, such as zinc) will be discussed in this chapter.

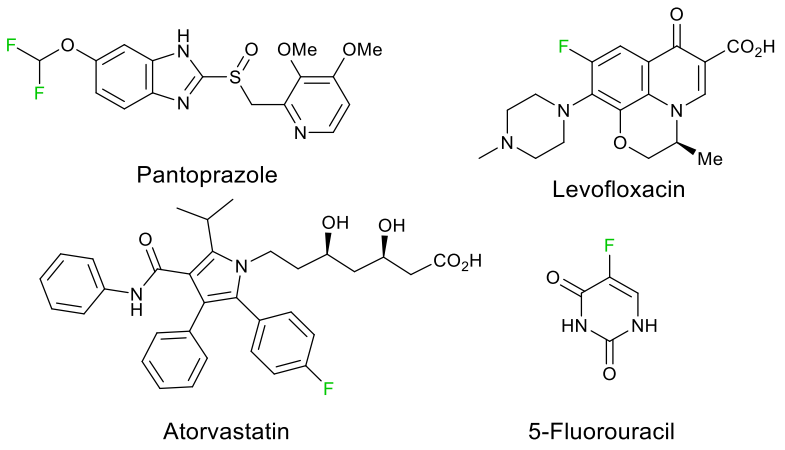

Figure 4. 1 *Examples of commercially available drugs containing fluorine atoms: Pantoprazole (proton pump inhibitor, antiulcer agent), Levofloxacin (antibiotic), Atorvastatin (HMG-CoA reductase inhibitor, hypercholesterolemia treatment), 5-Fluorouracil (antimetabolite of pyrimidine nucleobase, anticancer)*

Being most electronegative element in Pauling's table,[12] fluorine has a very strong inductive effect, greatly enhancing the acidity of the nearby hydrogens.[13,14] Fluorine is an effective *ortho*-directing group, via inductive effect, being more powerful than other halogens or trifluoromethyl groups.[14,15] However its coordination ability makes fluorine a weaker *ortho*-directing group than other common substituent such as -OR (R= alkyl). Thus, in the absence

of a donor solvent, OR groups tend to direct metalation in *ortho* outperforming the inductive effect of the fluorine. [15,16] For example ^{n}BuLi in THF is present in form of dimers and tetramers[17], when reacted with 4-fluoroanisole the metalation occurs next to the methoxy group, affording 4-fluoro-2-metoxy-benzoic acid after treatment with CO_2.[16] Contrastingly using a Lewis donor like PMDETA (N,N,N',N'',N'-pentamethyldiethylenetriamine), which dictates the formation of monomers of ^{n}BuLi in solution,[18] the pK_a became again the driving force for the metalation and the regioselectivity in ortho to fluorine can be restored (**Scheme 4. 1**).[15,16] The same regioselectivity was achieved without donor, using bases like LiTMP (TMP= 2,2,6,6-tetramethylpiperidide) or Lochmann-Schlosser Superbase (LiC-KOR).[15,16]

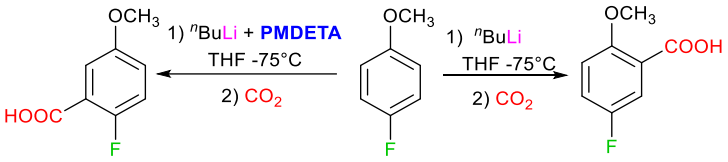

Scheme 4. 1 *Optional site selectivity in the metalation of 4-fluoroanisole. Using ^{n}BuLi the metalation occurred in ortho to -OCH$_3$, adding the chelating donor PMDETA the metalation in ortho position to the fluorine is preferred (PMDETA= N,N,N',N'',N''-pentamethyldiethylenetriamine)*

Despite the *ortho*-directing effect of fluorine, metalation of fluoroarenes with group 1 bases is challenging due to the fragility of the relevant intermediate product which can subsequently undergo elimination of MF (M= Li, Na or K) forming benzyne species.[19] This lack of stability was already noticed by Wittig, when assessing the metalation of fluorobenzene by PhLi which furnished biphenyl. This has been rationalised in terms of the addition of PhLi to an *in-situ* generated benzyne after the elimination of LiF (**Scheme 4. 2**).[20,21] To avoid this problem the metalation of fluoroarenes must be conducted in cryogenic condition (-78°C) and electrophilic interception should be carried out *in-situ* at very low temperature. This has made particularly challenging the isolation and characterization of metalated intermediates. [14–16,22,23] Moreover if the fluoroarene is more reactive, due the presence of more fluorine for example, then the use of cryogenic condition does not necessarily preclude the decomposition of the organometallic intermediates.[19] In such cases, the result could be so exergonic that could represent a threat of explosion.[24]

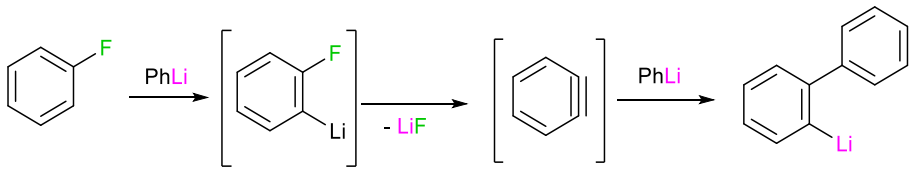

Scheme 4. 2 *Mechanism of coupling of PhLi with fluorobenzene via benzyne formation*

In order to improve the stability of these intermediates, a significant amount of research efforts have focused on replacing lithium with a less electropositive metal, in order to instil some stability in those systems, disfavouring the elimination of fluorine salts, while retaining a reactive carbon-metal bond for further functionalization. In this context Mongin has shown that, $ZnCl_2$ can be used to trap the metalated the metalated product of reactivity of 2-

Fluoropyridine with LiTMP (in cryogenic condition, -78°C).[25] The resulting zincated species is stable at room temperature and it was functionalised via palladium catalysed cross-coupling.[25]Moreover using other trapping organometallic agents such as $^{i}Bu_2Al(TMP)$ and GaR_3, the isolation and structural elucidation of the metalated intermediate has been possible.[26] This bimetallic approach, coined by Mulvey as trans-metal trapping (TMT) has been successfully applied for the selective gallation of 1,3,5-trifluorobenzene (see **Scheme 4. 4**). Previous work by Schlosser has shown that when this substrate was reacted with ^{t}BuLi even at -78°C, a complex mixture of products, resulting from multimetalation and LiF elimination, was obtained (**Scheme 4. 3**).[19]

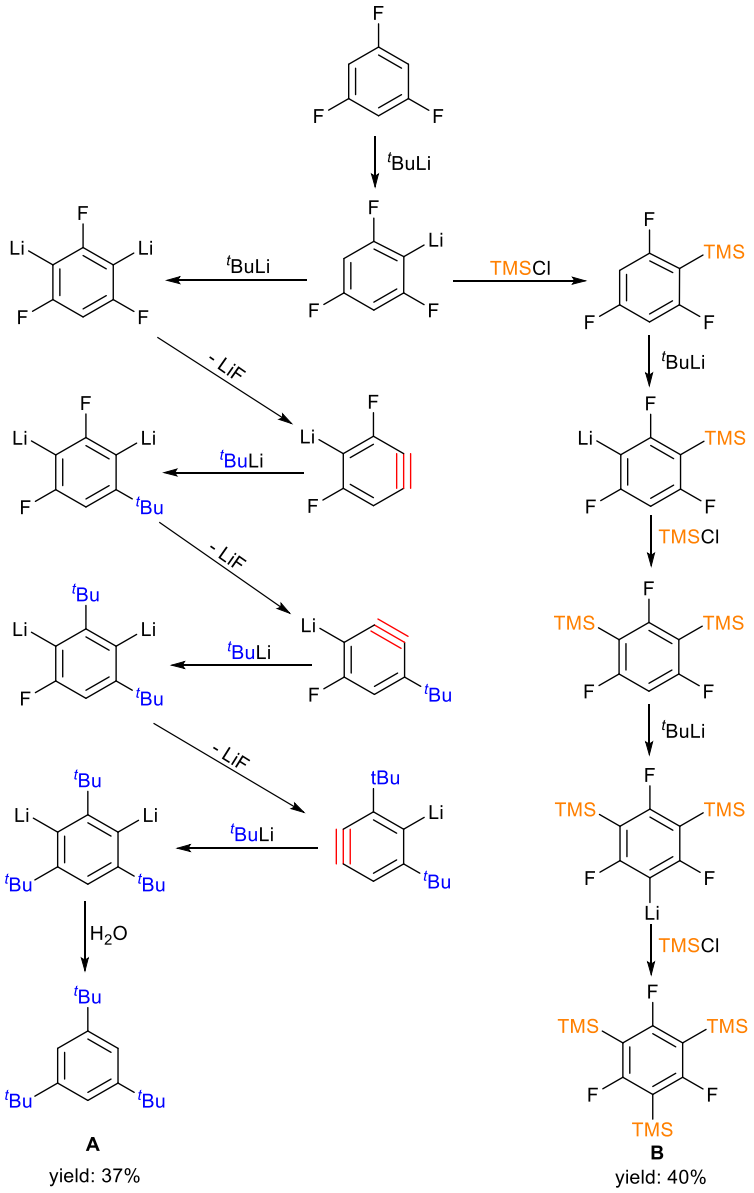

Scheme 4. 3 *Reactions cascade following the metalation of trifluorobenzene with ^{t}BuLi. A and B (37% and 40% yield respectively) are the major product, having the reaction at -75°C with 3 equivalents of ^{t}BuLi and TMSCl (TMS= Me_3Si-)*

However when 1,3,5-trifluorobenzene is treated with LiTMP at -75°C in the presence of GaR_3 and PMDETA, lithium gallate [2-Ga(CH_2SiMe_3)$_3$-1,3,5-F_3-C_6H_2·Li(PMDETA)] was isolated. This compound is the result of stepwise metalation, with LiTMP first deprotonating the substrate followed by a transmetalation to gallium, affording this bimetallic product which can be further functionalised with palladium catalysed C-C bond forming process.[26]

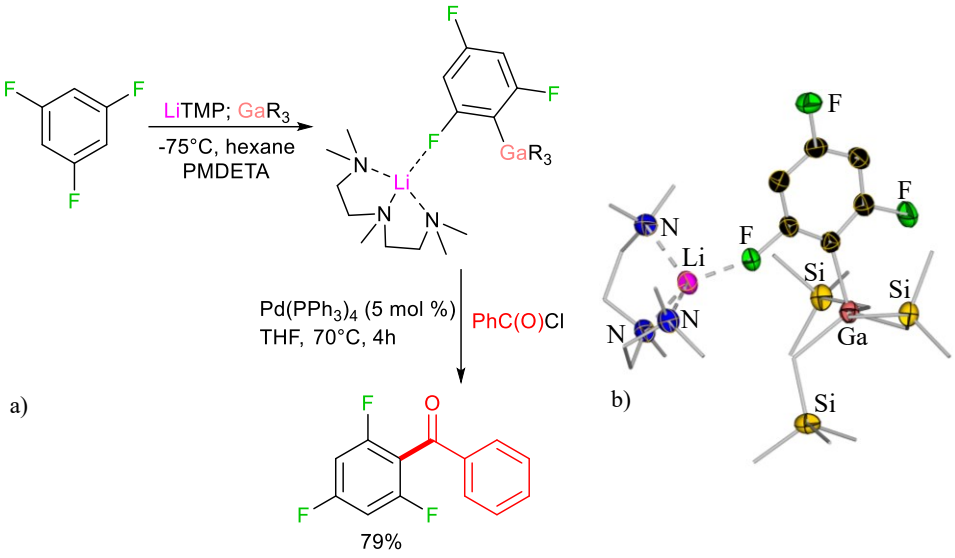

Scheme 4. 4 *a) Synthesis of [2-Ga(CH_2SiMe_3)$_3$-1,3,5-F_3-C_6H_2·Li(PMDETA)] via metalation of 1,3,5 trifluorobenzene by LiTMP and subsequent trap with GaR_3 and palladium catalysed acylation b) crystal structure of [2-Ga(CH_2SiMe_3)$_3$-1,3,5-F_3-C_6H_2·Li(PMDETA)], hydrogens are omitted, carbon atoms (with the exception of the ones of the aryl ring) are drawn as wire frame for clarity. Thermal ellipsoids are rendered with 50% probability. (R= CH_2SiMe_3, TMP= 2,2,6,6-tetramethylpiperidide, PMDETA= N,N,N',N'',N''-pentamethyldiethylenetriamine)*

While encouraging, it should be noted that in these trans-metal trapping approaches low temperatures are still required. Consequently Turbo-Hauser base TMPMgCl·LiCl pioneered by Knochel[27,28] and lithium magnesiate $LiMgBu_3$ or $Li_2Mg(TMP)Bu_3$[29] have also demonstrated their ability to promote the metalation of fluoroarenes, however, despite the higher stability compared to organolithium derivatives, the relevant magnesiated fluoroaryls still needed to be handled at low temperatures to avoid their decomposition(-20°C or 0°C). Interestingly using a sterically encumbered base such as [{^{Dipp}Nacnac}MgTMP] (^{Dipp}Nacnac= Ar*NC(Me)CHC(Me)NAr*; Ar* = Dipp = 2,6-^{i}Pr$_2$-C_6H_3) our group has shown that it is possible to magnesiate fluoroarenes at room temperature. The steric protection provided by the sterically demanding β-diketaminate ligand seems to offer additional stability to the C-Mg bond, avoiding decomposition via benzyne and enabling the isolation of the metalated intemediate, [{^{Dipp}Nacnac}Mg(THF)(C_6F_4H)].[30]

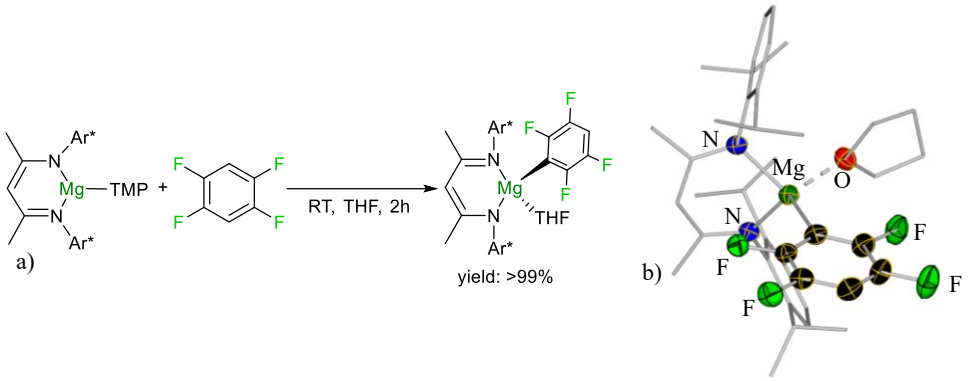

Scheme 4. 5 *a) Synthesis of [{^{Dipp}Nacnac}Mg(THF)(C_6F_4H)]. b) Crystal structure of [{^{Dipp}Nacnac}Mg(THF)(C_6F_4H)], hydrogens are omitted, carbon atoms (with the exception from those from the fluoroaryl ring) are drawn as wireframe for clarity. Thermal ellipsoids are rendered with 50% probability.*

Along with magnesium, zinc was used in the metalation of the fluoroarenes, considering that Zn-C bonds have a more covalent character than Mg-C bonds, which should make zincated fluoroalkyl species should be expected to be less prone to undergo into elimination of ZnF_2.[31] Successful lithium zincate which have managed to accomplish the regioselective deprotonation of fluoroaryls are: [LiZn(^{t}Bu)$_2$TMP] by Kondo and Uchiyama[32–34], [(TMP)$_2$Zn·2MgCl$_2$·2LiCl] and [(TMP)ZnCl·LiCl] by Knochel.[35–37] In particular, the metalated fluoroaryls derived from those bases are so robust that they were compatible even when high temperatures were, for example in reactions performed using in the microwave.[36] It should be noted that no information about the constitution of these intermediates is known.

More recently Crimmin and co-workers have been able to isolate and fully characterize an extensive number of metalated fluoroaryls taking advantages of the stabilization offered by ^{Dipp}Nacnac. In this particular case, however, fluoroarenes were not directly metalated by the zinc, but there was a C-H activation operated by bimetallic complex of palladium and zinc. In fact, the zinc species used (^{Dipp}NacnacZnH) was unreactive towards fluoroarenes, but in combination with catalytic amount of palladium (in the form of [Pd(PCy$_3$)$_2$] Cy = cyclohexyl) the selective metalation of fluoroarenes was achieved, together with heterocycles and unactivated substrates such as benzene.[38] The mechanism proposed for the reaction presented the formation of a bimetallic complex between the zinc species and palladium as first step. The emerging complex underwent oxidative addition via C-H activation of the fluoroarene. Reaction with a second equivalent of ^{Dipp}NacnacZnH facilitates a ligand exchange on palladium, followed by elimination of the ^{Dipp}NacnacZn(ArF) (ArF= fluoroarene) species and H_2, regenerating the active Pd-Zn complex (see **Figure 4. 2**). A monometallic mechanism was considered unlikely since the facile formation of the complex between ^{Dipp}NacnacZnH and [Pd(PCy$_3$)$_2$] and the catalytically incompetence of *trans*-[Pd(PCy$_3$)$_2$(H)(4-C_5F_4N)], while the bimetallic system is able to metalate 2,3,5,6-tetrafluoropyridine under catalytic regime.[38]

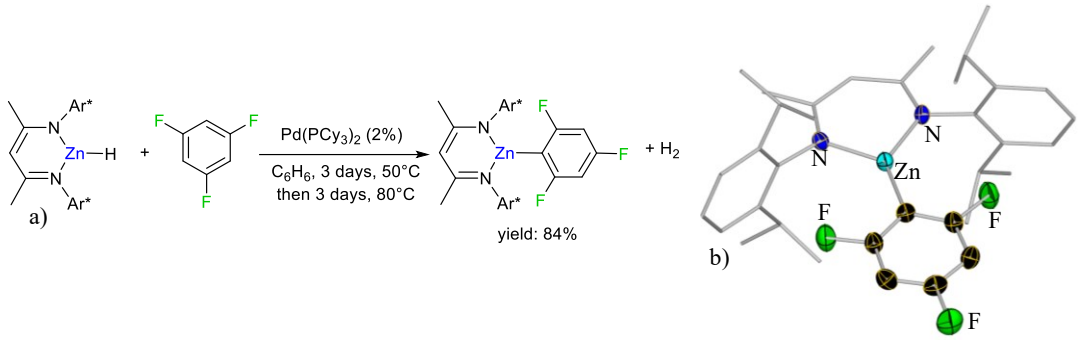

Scheme 4. 6 *a) Zincation of 1,3,5 trifluorobenzene catalysed by palladium (Cy= cyclohexane), b) crystal structure of [(*^{Dipp}*Nacnac)Zn(*$C_6F_3H_2$*)], hydrogens are omitted, carbon atoms (except for the ones of the fluoroaryl ring) are drawn as wire frame for clarity. Thermal ellipsoids are rendered with 50% probability. Symmetry transformations used to generate symmetrical atoms: x, 3/2-y, z*

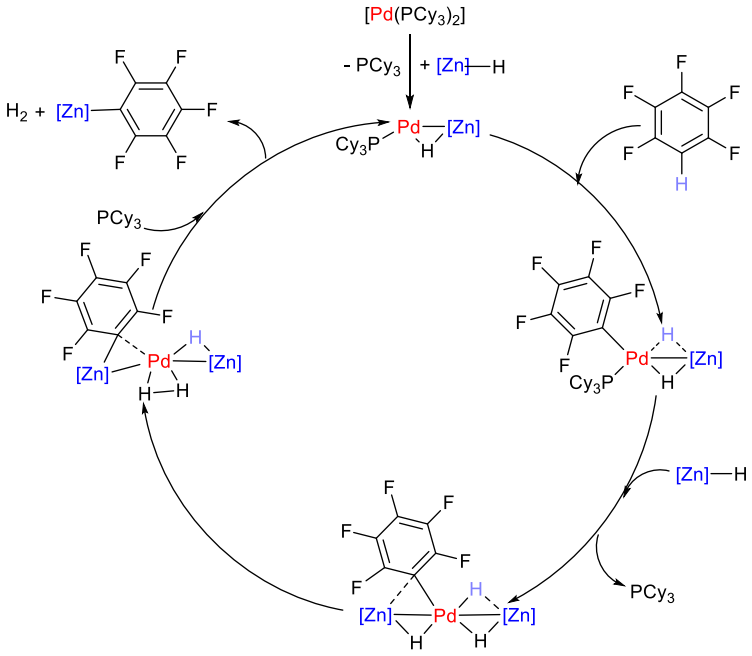

Figure 4. 2 *Catalytic cycle proposed by Crimmin and coworkers for the palladium catalysed zincation of fluoroarenese, using pentafluorobenzene as example (Cy= cyclohexane, [Zn]=* ^{Dipp}*NacnacZn)*

Building on those precedents we ponder if we could use potassium zincates containing the bulky $\{Ph_2Si(NAr^*)_2\}^{2-}$ for regioselective zincation of fluoroarenes. This ligand was successfully applied as scaffold in the chemistry of magnesiates, manganates and zincates accessing new structurally defined *ates* which were reactive towards deprotonation reactions (see **Chapter 2** and **3**).[39–42]

4.2 Aim

Building on the work presented in **Chapter 2** and **3** in this thesis, here we present our findings on the rational design of a mixed potassium/zinc base for the direct zincation of highly sensitive fluoroarenes substrates. Special emphasis is placed on the isolation and characterization of the key reaction intermediates involved in these reactions. Efforts on further organic functionalization of those heterobimetallics are also presented.

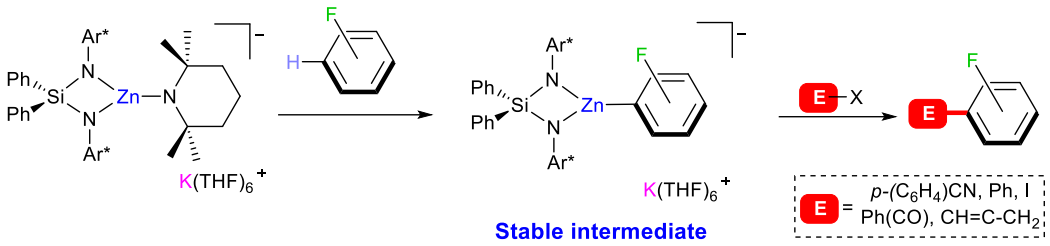

Scheme 4. 7 *Metalation of fluoroarenes using an encumbered potassium zincate and subsequent functionalization of the metalated intermediate.*

4.3 Results and Discussions

4.3.1 Synthesis of Potassium Zincate Sustained by a Silyl bis-(Amide)

We started this study assessing the metalation ability of compound **6** towards 1,3,5 trifluorobenzene. At room temperature no reaction was observed, and after 5h at 69°C only 16% conversion was observed. Since **6** did not seem reactive enough to metalate this substrate we next decided to prepare a potassium TMP variant of this zincate. This builds on previous studies that have shown the enhanced reactivity of TMP-based zincates. [43]

For the preparation of $[\{Ph_2Si(NAr^*)_2Zn(TMP)\}^-\{K(THF)_6\}^+]$ **(19),** the same synthetic strategy successfully applied to access $[\{Ph_2Si(NAr^*)_2)Zn(CH_2SiMe_3\}^-\{K(THF)_4\}^+]$ (**14** in **Chapter 3**) was used. The parent amine $Ph_2Si(NHAr^*)_2$ (**1**) was first metalated with KCH_2SiMe_3 to give $[Ph_2Si(NHAr^*)(NAr^*)K]$ (**13**), which is then reacted with $Zn(TMP)_2$ at 69°C for 16h in THF, furnishing zincate **19** (**Scheme 4. 8**) which could be isolated in 67% crystalline yield. Interestingly, if KR (R= CH_2SiMe_3) and $Zn(TMP)_2$ are reacted together with **1** in hexane then, the alkyl analogue **14** is obtained instead of **19**. On the other hand, the zinc-bis-amide alone fails in metalating **1,** even in forcing condition (69°C, 16h in THF).

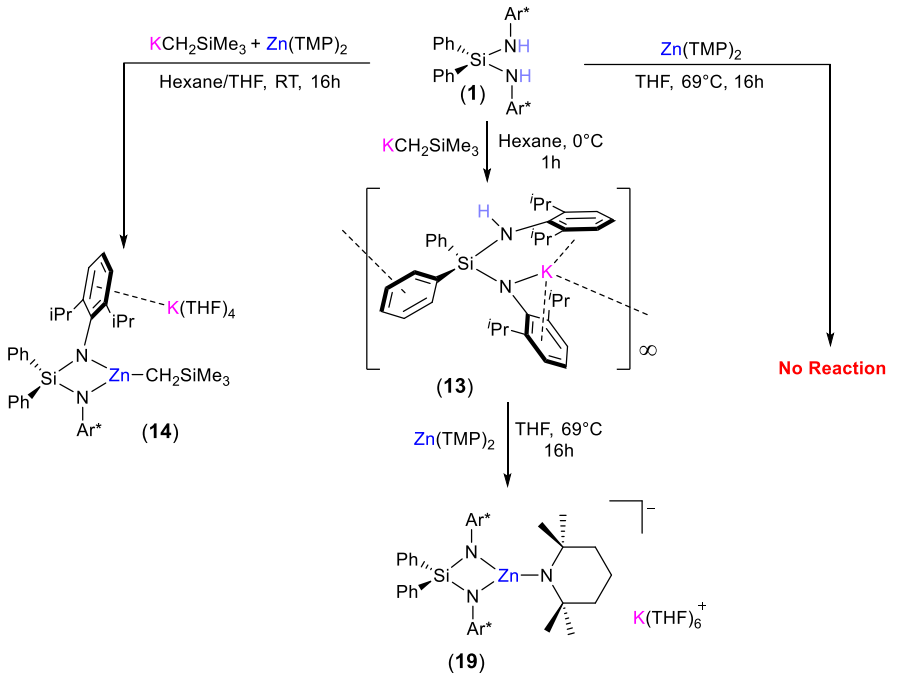

Scheme 4. 8 *Synthesis of **19** via stepwise metalation/co-complexation of **1** using KCH_2SiMe_3 and $Zn(TMP)_2$ (TMP=2,2,6,6-tetramethylpiperidide)*

Compound **19** was characterised in D_8-THF solution by ^1H and $^{13}C\{^1H\}$-NMR spectroscopy. The bimetallic constitution of **19** was established by X-ray crystallographic studies. Exhibiting a similar solvent-separated ion pair motif as those previously described for the sodium magnesiate analogue $[\{Ph_2Si(NAr^*)_2Mg(TMP)\}^-\{Na(THF)_6\}^+]$,[40] and **19** comprises a potassium cation solvated by six molecules of THF and a zincate anion where zinc is chelated by $\{Ph_2Si(NAr^*)_2\}^{2-}$ and binds to a terminal TMP group. Zn exhibits a distorted trigonal geometry (sum of angles 359.06°) and the Zn-N_{TMP} bond (N3 in **Figure 4. 3**) is 1.8925(16) Å, which as expected it is elongated when compared to the Zn-N bonds distances is $Zn(TMP)_2$.[44]

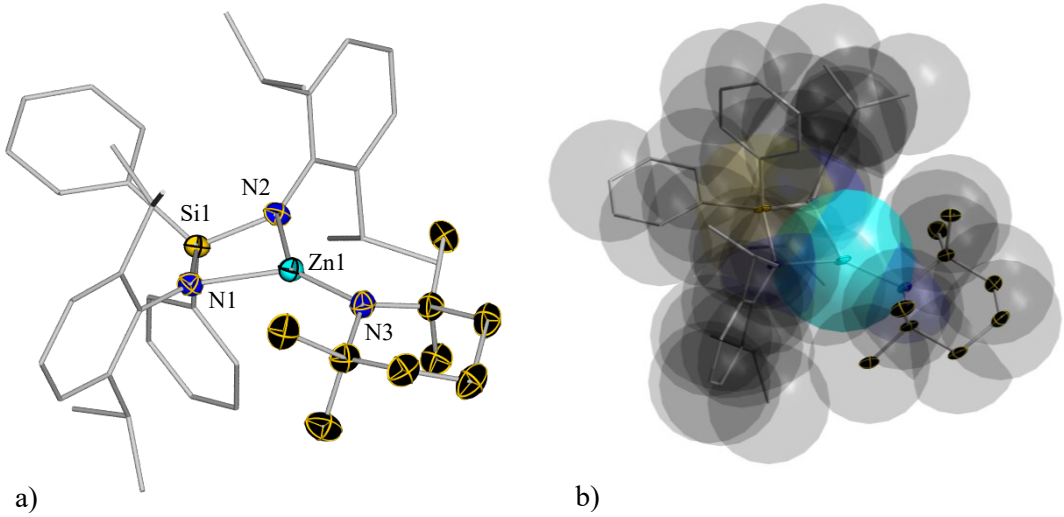

Figure 4. 3 *a) Crystal structure of anionic moiety of **19** and b) superimpose space filling model of the same structure. Thermal ellipsoids are rendered at 50% probability. Hydrogen atoms and disordered components in THF are omitted, carbon atoms of Aryl and THF fragments are drawn as wire frames for clarity. Selected bond distance (Å) and angles (°): N10-Zn4 1.9814(19), N11-Zn4 2.0080(18), Zn4-N12 1.887(19), N10-Zn4-N11 80.26(8), N10-Zn4-N12 138.43(8), N11-Zn4-N12 139.96(8), N10-Si4-N11 97.94(9), Si4-N10-Zn4 90.68(9), Si4-N11-Zn4 89.61(8)*

The sodium analogue of **19** could be prepared using sodium complex [{$Ph_2Si(NHAr^*)(NAr^*)Na\}_2$] (**5**) (see **Chapter 2**) and $Zn(TMP)_2$ at 69°C for 16h in THF, affording [{$Ph_2Si(NAr^*)_2Zn(TMP)\}\{Na(THF)_6\}$] (**19b**) in 63% crystalline yield. **19b** displays some anion as the one described for **19**. Due to the structural similarities between these two species, the discussion of **19b** has been omitted for the sake of brevity.

4.3.2 Assessing the metalating ability of **19** towards Fluoroarenes

We next studied the reactivity of **19** towards a selection of fluoroarenes. We started our investigation using 1,3,5-trifluorobenzene as benchmark substrate. Using **19** the substrate is completely deprotonated in 48h at RT in THF. Following the reaction by ^{19}F-NMR spectroscopy we can observe the disappearance of the signal for the starting material at -106.7 ppm and at the same time the rise of two new resonances at -83.5 and -116.0 ppm, compatible with deprotonation in its C2 position. This was accompanied by the detection of TMP(H) in the ^{1}H-NMR spectrum. It was possible to crystalize the product of the metalation of the fluoroarene, [{$Ph_2Si(NAr^*)_2Zn(C_6H_2F_3)\}^-\{K(THF)_6\}^+$] (**20**) in 85% yield. Since **20** proved to be thermally stable, the reaction time can be reduced to three hours heating the solution at reflux (69°C). The same results can be obtained with the sodium analogue of **19**, in fact the reaction of **19b** with 1,3,5-trifluorobenzene led to the isolation of [{$Ph_2Si(NAr^*)_2Zn(C_6H_2F_3)\}^-\{Na(THF)_5\}^+$] (**20b**).

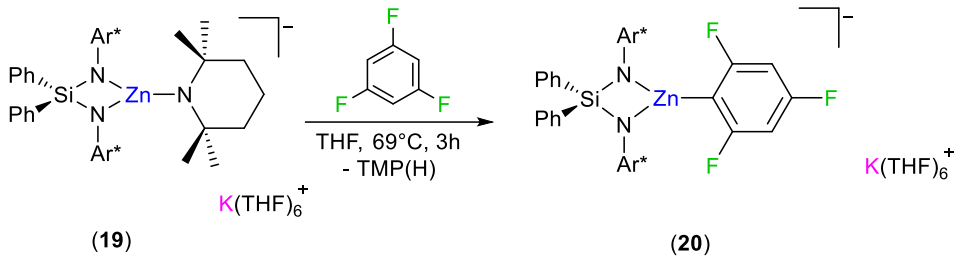

Scheme 4. 9 *Metalation of 1,3,5-trifluorobenzene using **19** as base. Alternatively, the metalation occurs in 48h at room temperature.*

The addition of a second equivalent to **19** to isolated crystals of **20** in THF do not lead to a second metalation of the $[C_6H_2F_3]$ fragment. This contrast with our previous studies using $[(dioxane)_{0.5}NaFe(HMDS)_3]$ which can di-ferrate this substrate at room temperature when using a two folder excess of the base.[45]

In order to understand the role of potassium in the zincation of trifluorobenzene we repeated the reaction using the sodium congener **19b** and using **19** in presence of [2.2.2]-cryptand (a macrocyclic Lewis donor and sequestering agent for potassium).[46] In both of the cases 20, or its sodium congener **20b**, was prepared in the same condition of temperature and time obtaining the same yields. This suggests a not direct involvement of the potassium in the process, with the metalation of 1,3,5 trifluorobenzene happening only in the coordination sphere of the zinc with potassium acting only as counter cation. Therefore since $Zn(TMP)_2$ alone is unreactive towards 1,3,5-trifluorobenzene, even in forcing condition (16h at 69°C), we can postulate that the higher reactivity of **19** over the neutral zinc amide is due to the kinetic activation of the zincate anion.

The somehow "passive" role of the potassium in the metalation is surprising considering the well-known alkali-metal effect observed in the reactivity of many heterobimetallic complexes.[47] Moreover, mechanistic studies on the ferration of fluoroarenes by $[NaFe(HMDS)_3]$ suggest the great importance of the sodium for the metalation. For instance the ferration of fluoroarenes was seen as a two step process with an initial Na-H exchange, followed by a fast intramolecular transmetalation.[48]

The solid state structure of **20** was established by single crystal X-ray diffraction (**Figure 4. 4**). Exhibiting the same solvent separated ion pair motif as **19**, its anion is made up by a distorted trigonal Zn centre chelated by $\{Ph_2Si(NAr^*)_2\}^{2-}$ and bonded to the aryl fragment.

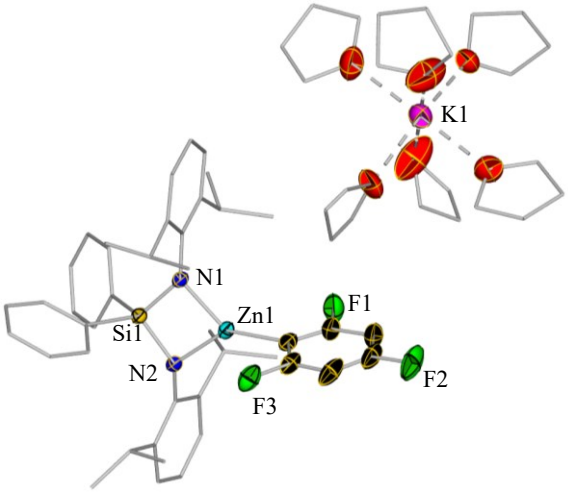

Figure 4. 4 *Crystal structure of **20**. Thermal ellipsoids are rendered at 50% probability. Hydrogen atoms and disordered components in THF are omitted, and carbon atoms of Ar*, phenyl ring and THF fragments are drawn as wire frames for clarity. Selected bond distances (Å) and angles (°) N2-Zn1 1.969(3), N1-Zn1 1.952(2), Zn1-C37 1.970(3), N2-Si1-N1 96.74(13), N2-Zn1-N1 81.01(11), Si1-N1-Zn1 91.32(11), Si1-N2-Zn1 90.71(12), N2-Zn1-C37 140.66(13), N1-Zn1-C37 137.56(13)*

The Zn-C distances between N and Zn had an average value of 1.96 Å, that is shorter than the ones reported for other zincates with the same chelating ligand (see **Chapter 2** and **3**). The distance between zinc and the carbon is 1.970(3) Å that is very close to what reported by Crimmin for his [^{Dipp}NacnacZn($C_6H_2F_3$)][38] (1.98 Å), which is very similar to **20**, since there is a sterically encumbered ligand that chelate a zinc bonded to a trifluoroaryl anion. Since **20b** is isostructural to **20**, the feature of its crystal structure will be not discussed.

Encouraged by these findings we next assessed the substrate scope of the fluoroarenes substrates.

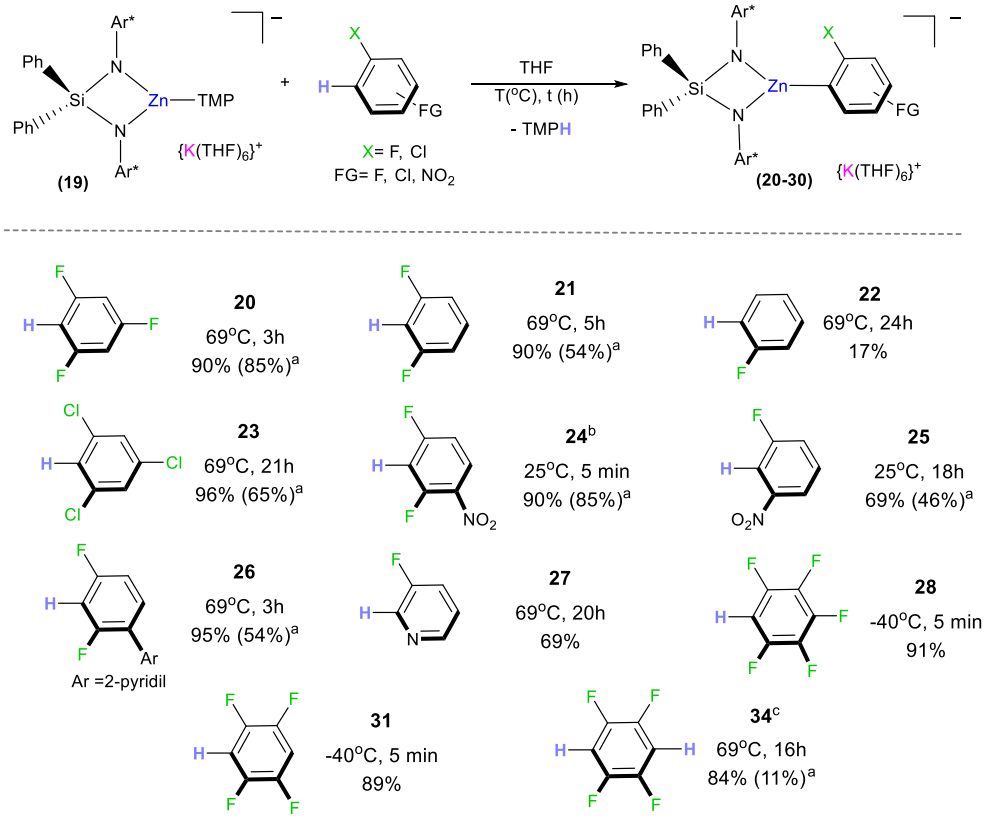

Scheme 4. 10 *Scope of the C-H zincation of fluoroarenes using potassium zincate **19**. NMR yields determined by ^{1}H-NMR spectroscopic data using hexamethylbenzene as internal standard. [a] Isolated yields. [b] Compound **24** is light sensitive. [c] Reaction carried out using 0.5 equivalents of 1,2,4,5-tetrafluorobenzene*

1,3-difluorobenzene (**Scheme 4. 10**) was less reactive than trifluorobenzene, achieving a full conversion after 5 hours at 69°C in THF, affording [{$Ph_2Si(NAr^*)_2Zn(C_6H_3F_2)$}$^-${$K(THF)_6$}$^+$] (**21**). With 1,3-difluorobenzene the metalation occurred selectively on C2 position as demonstrate by solid single crystal X-ray diffraction and multinuclear NMR spectroscopy. Following the same trend fluorobenzene is sluggishly reactive towards **19**, in fact even after forcing reaction condition (69°C for 24h), [{$Ph_2Si(NAr^*)_2Zn(C_6H_4F)$}$^-${$K(THF)_x$}$^+$] (**22**) was formed only in 17% yield (calculated in 1H-NMR spectrum using hexamethylbenzene as internal standard).

Replacing the fluorine atoms by the less electronegative chlorine in the same substrates, result in significant longer reaction time. Thus 1,3,5-trichlorobenzene can be metalated within 21h at 69°C in THF, giving [{$Ph_2Si(NAr^*)_2Zn(C_6H_2Cl_3)$}$^-${$K(THF)_6$}$^+$] (**23**) quantitively (monitoring the reaction by ^{1}H-NMR spectroscopy) and a crystalline yield of 65%. The stability of the metalated trichlorobenzene underlines the importance of this sterically encumbered ligand to avoid the decomposition of the zincate, in fact *ortho*-zincated chloroarenes can rapidly decompose at room temperature via benzyne formation. For instance, Mulvey has shown that sodium zincate [(TMEDA)·Na(μ-TMP)(μ-^{t}Bu)Zn(^{t}Bu)] is able to metalate chlorobenzene, but instead of isolating the product of ortho-zincation to the chlorine, the isolated product was the unexpected [{1-Zn(^{t}Bu)}$^-$-{2-N(Me)(CH_2)CH_2-CH_2NMe_2}$^+$-

C_6H_4] (**Scheme 4. 11**).[49] According to the mechanism proposed after the *ortho*-zincation of the substrate, the bonds between the aryl and the zinc and the chlorine could be cleaved affording benzyne and "(^{t}Bu)$_2$Zn·NaCl·TMEDA", which eventually eliminated NaCl. Subsequentially TMEDA and Zn(^{t}Bu)$_2$ were added across the benzyne triple bond. Finally the methyl group of TMEDA was deprotonated (due to the close proximity with the to the ^{t}Bu group attached to the zinc) affording the final product and isobutane. [49]

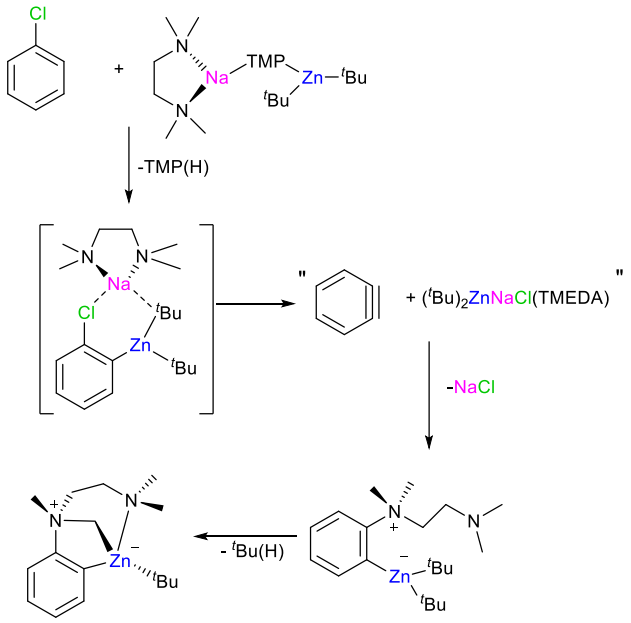

Scheme 4. 11 *Proposed mechanism for the formation of [{1-Zn(^{t}Bu)}$^-$-{2-N(Me)(CH$_2$)CH$_2$-CH$_2$NMe$_2$}$^+$-C$_6$H$_4$] via formation of benzyne and elimination of NaCl. The two zwitterionic species were isolated, suggesting the implication of a benzyne intermediate*

Isolation of sensitive fluoroarenes containing nitro groups was also possible. Typically this functional group is not compatible with polar organometallics such as organolithium or Grignard reagents.[50–52] The electrophilic nature of NO_2 group makes these substrates susceptible of side reactions such as alkylation/arylation process. Previous work by Knochel *et al.* has shown that organozinc reagents has a great potential in the field. [37,53] For example [(TMP)ZnCl·LiCl] reacts with 2,4 difluoro-nitrobenzene in 45 minutes at room temperature achieving the 92% yield of biaryl products after Negishi-type cross coupling.[37] Illustrating its activating effect, the reaction of **19** with 2,4 difluoro-nitrobenzene afforded [{Ph$_2$Si(NAr*)$_2$Zn(C$_6$H$_2$F$_2$NO$_2$)}$^-${K(THF)$_3$}$^+$] (**24**) in quantitively yield in just 5 minutes at room temperature. Zincation of 3-fluorobenzene could also be achieved at room temperature although longer reaction times were needed (18h) furnishing [{Ph$_2$Si(NAr*)$_2$Zn(C$_6$H$_3$FNO$_2$)}$^-${K(THF)$_3$}$^+$] (**25**) (see **Scheme 4. 10**)

Despite the boosting of the reactivity induced by the nitro group, the regioselectivity of the metalation is dictated by the fluorine atom. In fact, as demonstrate by the solid-state studies and in-solution state studies, the metalation occurs selectively in *ortho*-position to the fluorine for the major product. This is visible in **24** were the inductive effect of two fluorine atoms outperform the inductive and mesomeric effect of the nitro group, this in accordance with the

pK_a calculated for 2,4 difluoro-nitrobenzene by Knochel and coworker, the proton flanked by the two fluorines has a pK_a value of 22.6, while the proton next to nitro group has "only" 29.1 as calculated value.[54]

It should be noted that **24** is sensitive to the heating and also to light. **25** also has a certain grade of instability, monitoring the reaction by ^{1}H-NMR spectroscopy, the yield for **25** was 69%, despite a complete consumption of **19** and 3-fluoro-nitrobenzene. The exact nature of the of the side-products or products of decomposition of **25** could not be attributed.

When the related potassium zincate [(PMDETA)K(TMP)ZnEt$_2$][55] was used to access the zincation of 2,4-difluoronitrobenzene, an insoluble precipitate was formed and small amounts of metalated product were observed (calculate about 10% by ^{19}F-NMR against hexafluorobenzene as internal standard). These findings evidence the stabilising effect of the silyl bis-(amide) ligand on the metalated intermediate.

To the best of our knowledge, up to this date, compounds **24** and **25** are the first examples of structurally defined intermediates for direct metalation of a nitroarene containing s or p block metals. Although some nitroarenes containing transitions metals are known, they are prepared via indirect routes oxidative addition to palladium (0) using fluoro-[56] or bromoarenes[57], by C-H activation promoted by platinum (II) species,[58] metallation using organic amines and inorganic salt in the presence of Iridium or Ruthenium,[59,60] or transmetalation from the correspondent organoboron to gold (I).[61]

The use of **19** for deprotonative zincation is compatible also with pyridine rings, in fact 2-(2,4-difluorophenil)pyridine was metalated in position 6 in 3h at 69°C in THF, showing how the pyridine ring boost the reactivity of a difluorinated ring, giving [{Ph$_2$Si(NAr*)$_2$Zn(C$_{11}$H$_6$F$_2$N)}$^-${K(THF)$_x$}$^+$] **26** as product(**Scheme 4. 10**). In this case the crystallization was not possible, but the NMR studies of isolated solid indicated the selective metalation at the carbon in *ortho* to both of the fluorines, as demonstrate by ^{1}H-COSY spectrum, in fact every proton in the C$_{11}$H$_6$F$_2$N anion was found coupled with another one (see **Figure 4. 5**). The metalation resulted quantitative following the reaction by ^{1}H-NMR spectroscopy and the isolated yield of **26** is 54%. A similar metalation was achieved in our group using [{^{Dipp}Nacnac}MgTMP] as base, in this case 2-(2,4-difluorophenil)pyridine was metalated in 5h at room temperature in the same position, exhibiting similar spectra in multinuclear NMR studies.[62]

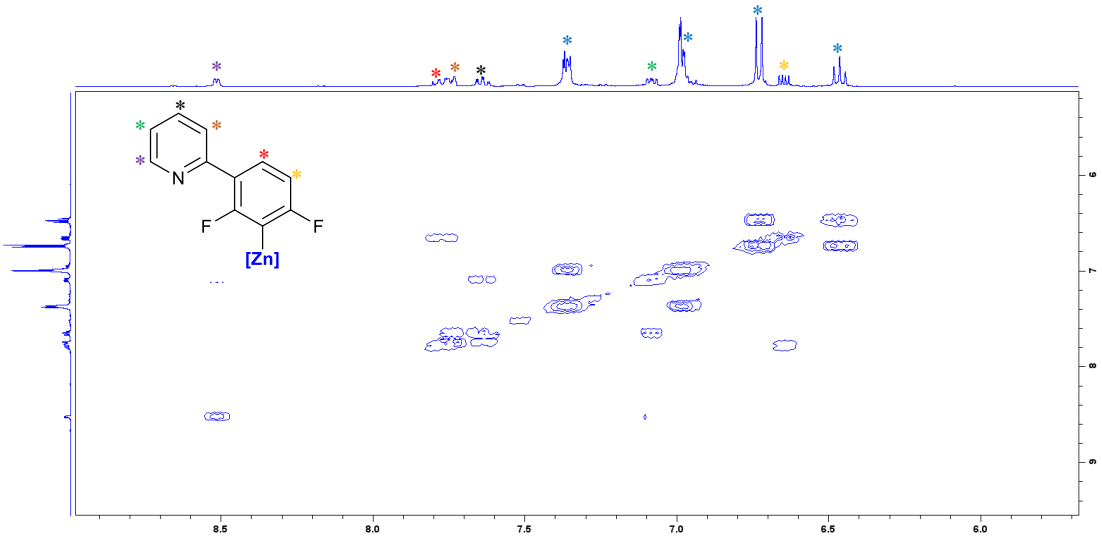

Figure 4. 5 *^{1}H-COSY (D_8-THF, 300.1 MHz, 298 K) spectrum of **26**, showing the proton assigned to the corresponding resonances ([Zn] = [{$Ph_2Si(NAr^*)_2Zn$}$^-$])*

Metallation of 3-fluoropyridine was observed after 18h at 69°C in D_8-THF. Despite several attempt it was impossible to isolate the product of the reaction, so the reaction was studied using ^{1}H and ^{19}F-NMR spectroscopy affording [{$Ph_2Si(NAr^*)_2Zn(C_5H_3FN)$}$^-${$K(THF)_x$}$^+$] (**27**) resulting from the deprotonation at the C2-position of the pyridine ring. For the 3-fluoropyridine the selective metalation in position 2 is not so trivial, in fact this represent the product of kinetic metalation, opposed to the metalation in position 4 that is the thermodynamic product[63] (as demonstrated by the value of the calculated pK_a for the H2 and H4, 37 and 31.5 respectively[63]). This feature is due to the destabilization of the nitrogen lone pair, by charge repulsion, of the emerging anion in C2 position.[64] Following this rationale it is not surprising that alkyllithium (complexed by TMEDA) had the metalation in C2 position as major product only if the reaction was conducted at very low temperature (-60°C), in very short time or using a less-donating solvent such as Et_2O (**Table 4. 1**).[65] In those conditions, the metalation is directed by the coordinative ability of the nitrogen lone pair. Using an higher temperature or a more coordinating solvent such as THF, the metalation has the value of pK_a as driving force, and therefore the metalation with the same reagents occurred preferentially in C4 position, affording the thermodynamic product.[65] The C4 position was also the preferential site for the metalation using the Lochmann-Schlosser superbase[66] or lithium magnesiates ($LiMgBu_3$) (**Table 4. 1**).[29] Using the combination of LiTMP and $Zn(TMP)_2$ Mongin and coworkers achieved the metalation in C2 position of 3-Fluoropyridine (in THF at RT), but the reaction was not very selective and the product of kinetic metalation was found in 57% yield (metalation in C2 position), together with the product of metalation in C4 position in 37% and traces of the product of dimetalation.[63] A more selective base for 3-fluoropyridine was [(TMP)MgCl·LiCl] which metalated the substrate selectively in C2 position in high yield.[28] Interestingly the selectivity change completely adding $BF_3{\cdot}Et_2O$, using the same base and the same condition the metallation occurred selectively in C4 position (see **Table 4. 1**).[28]

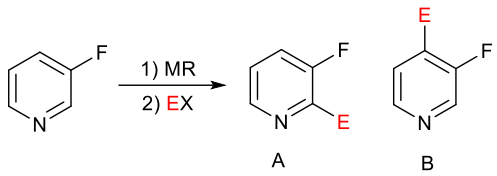

MR	A[a]	B[a]	Metalation condition
^{n}BuLi·TMEDA	68%	3%	Et_2O -60°C 30 min.
^{n}BuLi·TMEDA	0%	75%	THF -40°C 30 min.
^{n}BuLi/KO^{t}Bu	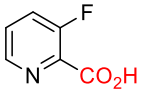 0%	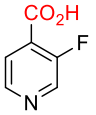 51%	THF -75°C 3 h
0.33 $LiMgBu_3$	0%	64%	THF -10°C 2h
0.5 $ZnCl_2$ + 1.5 LiTMP	57%	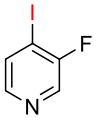 37%	THF RT 2h
TMPMgCl·LiCl	72%	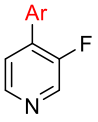 0%	THF -78°C 30min.
$BF_3·Et_2O$ + TMPMgCl·LiCl	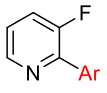 0%	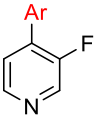 74%	THF -78°C 30 min.

Table 4. 1 *Direct metalation of 3-fluoropyridine using different organometallic species. (Ar= -$(C_6H_4)CO_2Et$) [a] isolated yield*

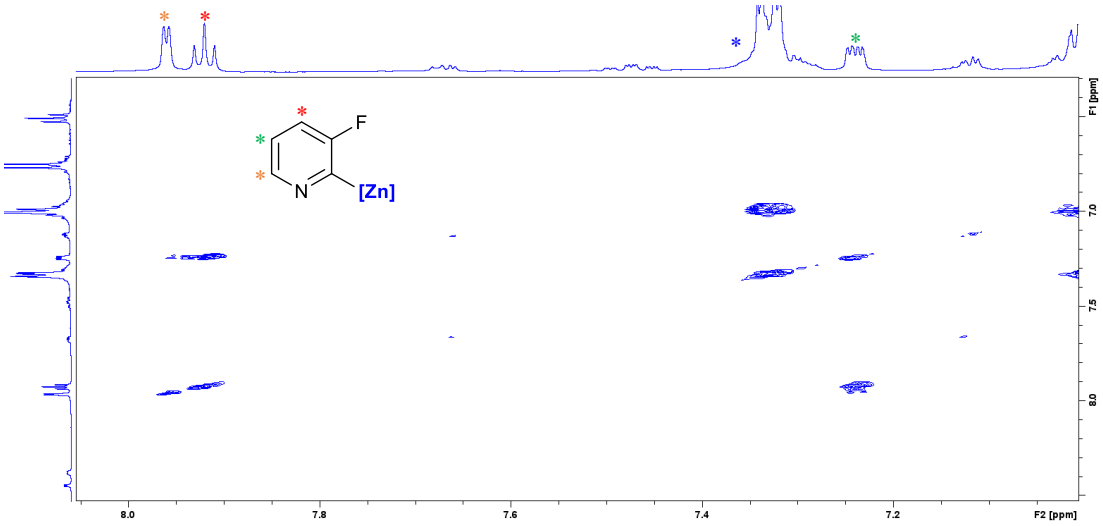

Figure 4. 6 *^{1}H-COSY (D_8-THF, 300.1 MHz, 298 K) spectrum of **27**, in the spectrum it is possible notice the correlation between the proton in C5 position (*) and both the protons in C4 position (*) and in C6 position (*). The resonance of the proton in C4 appears as a triplet due to the coupling with the fluorine atom. ([Zn] = [{$Ph_2Si(NAr^*)_2Zn$}$^-$], *)*

Pentafluorobenzene, being a more activated substrate, reacted readily with **19** in 5 minutes affording [{$Ph_2Si(NAr^*)_2Zn(C_6F_5)$}$^-${$K(THF)_6$}$^+$] (**28**) in 91% yield, measured against internal standard (hexamethylbenzene) in ^{1}H-NMR spectrum. Despite the cryogenic condition adopted (the reaction was carried at -40°C) traces of **1** together with TMP(H) were detected by ^{1}H-NMR spectroscopy suggesting that pentafluorobenzene is able to be deprotonated by the silyl bis-(amide) ligand. This was demonstrated by reacting **19** with 3 equivalents of C_6F_5H which yielded a mixture of [{$Ph_2Si(NHAr^*)$ $(NAr^*)Zn(C_6F_5)_2$}$^-${$K(THF)_1$}$^+$] (**29**) and [$K(THF)_xZn(C_6F_5)_3$] (**30**), result of protonation of one nitrogen or both nitrogens of the silyl bis-(amide) ligand respectively (**Scheme 4. 12**). This is in sharp contrast with the reactivity observed for 1,3,5 trifluorobenzene, in this case **20** is inert towards further reactivity with the same fluoroarene. Interestingly the zincation of the first equivalent of pentafluorobenzene is very selective and only very small amount of **29** and **30** were detected. However, adding a second equivalent of pentafluorobenzene led to a mixture of the three products (24% yield of **28**, 43% yield of **29**, 27% yield of **1**). Notably the protonation of {$Ph_2Si(NAr^*)_2$}$^{2-}$ proceeds slower than the deprotonation mediated by TMP(H), in fact after the addition of the third equivalent of pentafluorobenzene all the different compounds of the mixture collapse in **30** and **1** only after 16h at room temperature. From the mixture of products, it was possible to crystallographic characterize **28** and **29.**

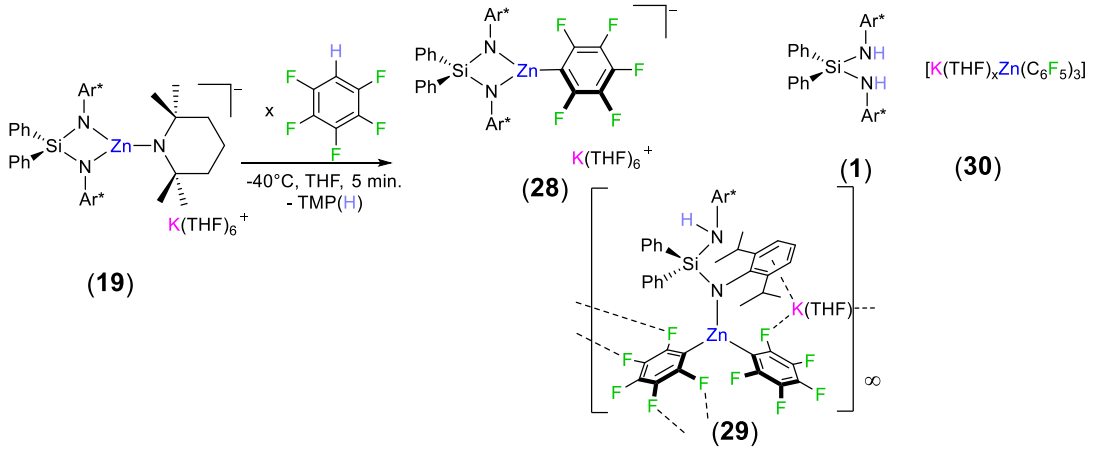

	28	29	30
x= 1	91%	traces	7%
x= 2	24%	43%	27%
x= 3	0%	46%	54%
x= 3, 16h RT	0%	0%	100%

Scheme 4. 12 *Metallation of the pentafluorobenzene using **19** as base. All the yields reported are calculated using ^{1}H-NMR against hexamethylbenzene.*

A similar behaviour could be observed for 1,2,4,5 tetrafluorobenzene. The reaction with 19 goes to completion in less than 5 minutes at -40°C affording the product [{$Ph_2Si(NAr^*)_2Zn(C_6HF_4H)$}$^-${$K(THF)_x$}$^+$] (**31**) in 89% yield. Also, in this case the reaction was not completely selective, even with cryogenic temperature, since **1** was detected, together with the triaryl zincate [$K(THF)_xZn(C_6HF_4)_3$] (**33**). Adding another two equivalents of tetrafluorobenzene it is possible to convert all the **31** in **33** after 16h at room temperature. As observed for pentafluorobenzene, increasing the amount of 1,2,4,5 tetrafluorobenzene is possible to observe in multinuclear NMR studies the presence of the bis-amide partially protonated [{$Ph_2Si(NHAr^*)$ $(NAr^*)Zn(C_6HF_4)_2$}$^-${$K(THF)_x$}$^+$] (**32**).

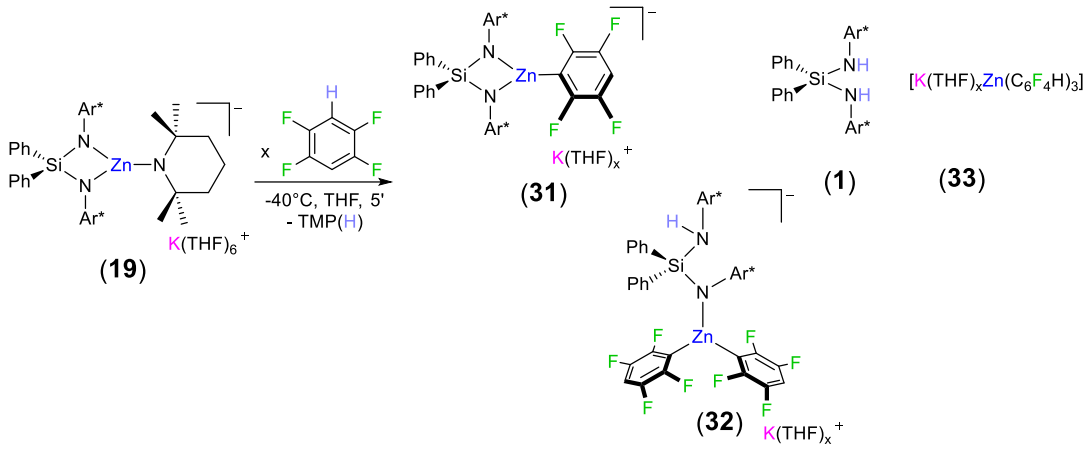

	31	**32**	**33**
x= 1	89%	0%	11%
x= 2	77%	traces%	21%
x= 3	40%	17%	42%
x= 3, 16h RT	0%	0%	100%

Scheme 4. 13 *Metallation of the 1,2,4,5 tetrafluorobenzene using **19** as base. All the yields reported are calculated using ^{1}H-NMR against hexamethylbenzene.*

Differently from the example of the trifluorobenzene mentioned above **19** is still reactive enough to deprotonate the last proton left on **31**. Reacting 1,2,4,5 tetrafluorobenzene and two equivalents of **19** in THF, for 16h at reflux, the product of dimetalation $[(THF)_6K_2Zn_2\{Ph_2Si(NAr^*)_2\}_2(C_6F_4)]$ (**34**) was observed and isolated as crystalline solid in 10% yield. The spectroscopic studies of the reaction suggest a two steps mechanism, the first step is the rapid deprotonation of the tetrafluorobenzene, by the first equivalent of **19**, affording **31**. The second step is the slowly deprotonation of **31** by the second equivalent of **19**. The ^{19}F-NMR spectrum of **34** show the presence of one singlet for the four fluorines of **34** at -119 ppm, opposed to the two multiplets at -116.5 and -142 ppm which are characteristic for **31**, showing the grade degree of symmetry of **34**. At the same time in the ^{1}H-NMR spectrum the quantitative formation of TMP(H) was observed. The spectroscopy studies demonstrated that despite the long reaction time the double metalation is quantitative. The crystal structure of **34** was then isolated confirming the proposed geometry. Crystal structures of dimetaleted tetrafluorobenzene was already known, but only one examples is derived from a double deprotonation and it was achieved in the past from our group using the sodium ferrate $[(dioxane)_{0.5}NaFe(HMDS)_3]$.[45]

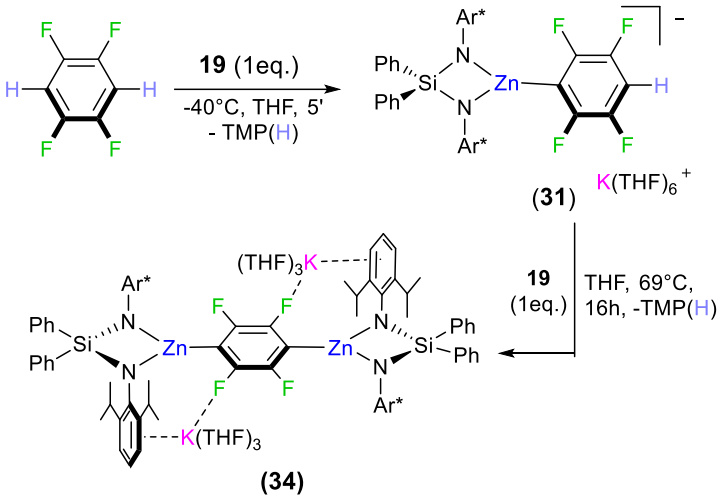

Scheme 4. 14 *Stepwise metallation of 1,2,4,5 tetrafluorobenzene having **31** as intermediate step, using **19** as base.*

The structures of the metalate fluoroarenes **21**, **23**, **25**, **26**, **28, 29** and **34** are analysed by single crystal X-ray diffraction.

Compounds **21** and **23** presented very similar structures (**Figure 4. 7**) to that of compound **20.** In fact, in both cases the bidentate anion $\{Ph_2Si(NAr^*)_2\}^{2-}$ coordinates a trigonal zinc atom, bonded also to an aryl anion (2,6-difluorophenyl and 2,4,6-trichlorophenyl respectively) which was metalated in the most acidic position, that is, in between the two halogens. Unfortunately, the high degrees of disorder in both structures precluded a significative discussion of the geometrical parameters. Notwithstanding the connectivity in these studies is unequivocal.

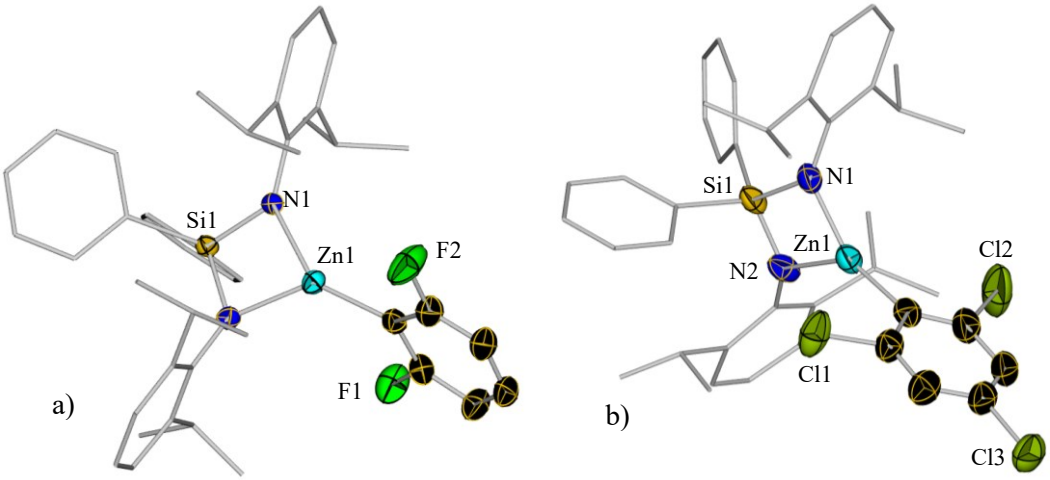

Figure 4. 7 *Anionic moiety of **21** a) and **23** b). Thermal ellispsoids are rendered with 30% probability. Hydrogen atoms are omitted and carbon atoms of $Ph_2Si(NAr^*)_2\}^{2-}$ are drawn as wireframe for clarity.* in a) *The asymmetric unit has 2 different molecular structures very similar, so only one was represented in b) The asymmetric unit is neutral by the presence of two half $K(THF)_6$ units, where both half occupied K atoms are sitting on a special position (inversion centre) not shown here.*

Exhibiting a different structural motif, **25** displays a pseudo-separated ion pair structure. Where potassium cation interacts with one aryl group of the ligand via π-interactions and with the lone pairs of a fluorine and of one oxygen in the nitro group. (**Figure 4. 8**)

The zinc is tricoordinate in a distorted trigonal planar geometry (sum of the angles around Zn 357.69°). The ligand coordinated the zinc in a chelated fashion way with both the amide nitrogens; the average N-Zn distance is 1.958 Å, which is slightly shorter than those observed in other zincates reported before in the previous chapters of this thesis. The coordination sphere of the zinc is completed by the aryl moiety, the Zn1-C1 bond is 1.9648(16) Å; this value is close to other reported fluoroarenes coordinated by bulky zinc moiety; such as the ones observed by Crimmin *et al.*, in particular it is almost identical for the compound [DippNacnacZn(2, 3, 6-$C_6H_2F_3$)], in which the Zn-C distance is 1.963(8) Å.[38]

In **25** potassium was coordinated not only by 3 molecules of THF, but also to the π-system of the Ar* group of the ligand in a η^4 fashion (K-C_{aryl} distances ranging from 3.1875(17) to 3.5912(16) Å). Potassium completes its coordinating sphere by bonding to one fluorine atom and one of the oxygens of the NO_2 group (K-F1 2.7149(10) Å and K-O1 2.8946(13) Å, see **Figure 4. 8**).

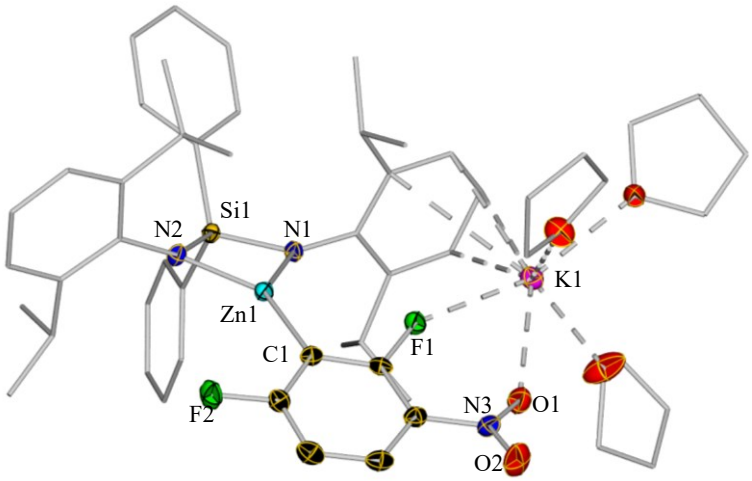

Figure 4. 8 *Crystal structure of **25**, ellipsoids are rendered with 50% probability. Hydrogen atoms and disordered components in THF are omitted, carbon atoms of Aryl and THF fragments are drawn as wireframe for clarity. Selected bond distances (Å) and angles (°): Zn1-C1 1.9648(16), N1-Zn1 1.9633(13), N2-Zn1 1.9536(14), K1-F1 2.7149(10), K1-O1 2.8946(13), K1-C_{aryl} ranging from 3.1875(17) to 3.5912(16), Si1-N2-Zn1 90.52(6), N2-Zn1-N1 81.58(6), N1-Zn1-C1 129.41(6), N2-Zn1-C1 146.70(6), Si1-N1-Zn1 90.05(6)*

Contrastingly **26** exhibit a solvent separated ion pair structure as those described for **21** and **23**, despite the presence of a nitro group in this ring no K-O_{nitro} contacts are observed (see **Figure 4. 9** for the anion). The structure of **26** also did not provide meaningful data to discuss the geometry, since the excessive disorder and needs to be considered only for proving the connectivity, which confirms the spectroscopic evidence for the metalation occurring in between the fluorine and the nitro group.

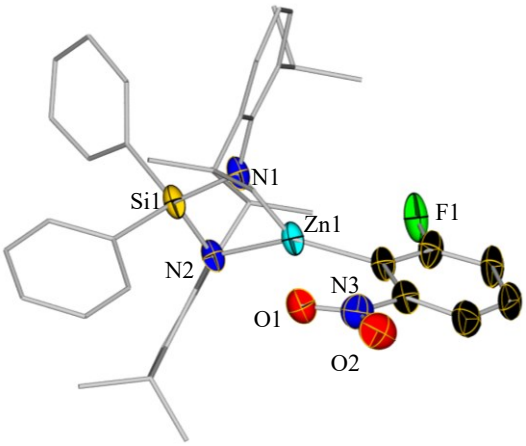

Figure 4. 9 *Anionic Moiety of **26**. Hydrogen atoms and disorder in the ^{i}Pr group are omitted for clarity. Carbon atoms of $Ph_2Si(NAr^*)_2\}^{2-}$ are drawn as wireframe. Thermal ellipsoids are rendered at 20% probability. The asymmetric unit is neutral by the presence of two half $K(THF)_6$ units, where both half-occupied K atoms are sitting on a special position (inversion centre) not shown here.*

The structure of **28** resulted in a solvent separated ion pair, similar to the those already described for **20**, **23** and **26**, with the potassium cation solvated by THF and the anionic part represented by $\{Ph_2Si(NAr^*)_2Zn(C_6F_5)\}^-$ (**Figure 4. 10**). Once again the zinc resulted coordinated in a distorted trigonal planar geometry from the silyl (bis)amide ligand and the aryl moiety (sum of angles, 358°). The distances nitrogen-zinc are in the average of the other compounds presented before (average value 1.955 Å). The distance between zinc and the C1 of the aryl moiety is 1.984(5) Å. This value is longer than the one found for other zincated pentafluorobenzene supports by chelating bulky ligand, such as [(^{Dipp}Nacnac)Zn(C_6F_5)][38,67]

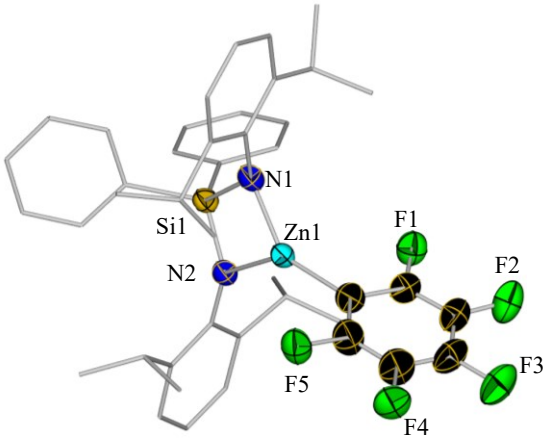

Figure 4. 10 *Crystal structure of anionic moiety of **28**. Hydrogens are omitted and carbon atoms (except for the pentafluoroaryl anion) are drawn as wireframe for clarity. The asymmetric unit is neutral by the presence of two half $K(THF)_6$ units, where both half occupied K atoms are sitting on a special position (inversion centre and a two fold axis) not shown here. Selected bond distances (Å) and angles (°): N1-Zn1 1.921(4), N2-Zn1 1.988(4), Zn1-C1 1.984(5), Si1-N1-Zn1 40.97(10), Si1-N2-Zn1 40.80(9), N1-Zn1-N2 81.75(16), N1-Zn1-C1 141.5(2), N2-Zn1-C1 135.1(2)*

Displaying a different structural motif, **29** contains silyl (amine) amide ligand resulting from the partial protonation of $\{Ph_2Si(NAr^*)_2\}^{2-}$, since the highly reactivity of pentafluorobenzene,

the ligand acted as a base too and it is partially protonated. As consequence protonated N2 did not coordinate anymore the metal centre, leaving only the amidic N1 as donor to the zinc. This behaviour is very similar to [{(Ph_2Si(NAr*)(NHAr*))Mg(NC_4H_4)$_2$(THF)Na(THF)$_2$}], product of deprotonation of pyrrole using [{Ph_2Si(NAr*)$_2$Mg(THF)(^{n}Bu)}$^-$ {Na(THF)$_6$}$^+$] as base.[41] Contrastingly when the metal centre is small the aminic nitrogen is still able to use its lone pair in coordination, how it was observed in **5** (**Chapter 2**, having Na as metal centre) or in [{Me_2Si(NHAr*)(NAr*)}$BiCl_2$].[68]

The zinc atom binds to two pentafluorophenyl groups and the amide nitrogen of the {(Ph_2Si(NAr*)(NHAr*)} ligand in a distorted trigonal planar geometry (sum of angles around the zinc atom 360°, ranging from 116.67(12)° to 123.17(10)°). Contrastingly the potassium centre binds to five fluorine atoms of the C_6F_5 rings and π-engaging with the diisopropylphenyl substituent of the amido group in a η^4 fashion. Its coordination is completed by a molecule of THF. The interactions between the potassium cation and fluorine atoms from different molecules creates a 3D polymer.

The coordination sphere of the zinc is then completed by two pentafluorophneyl anions, resulting in a trigonal plane geometry. This coordination around the zinc reminds the neutral Zn(C_6F_5)$_2$ coordinated by carbenes,[69] in fact the Zn1-C45 and Zn1-C39 distances (2.037(3) and 2.023(2)Å respectively) in **29** are close to the distances reported by Dragorne et al. for those carbenic complexes.[69] Another structure with a similar trigonal planar coordination sphere for a zinc atom (that shares similar value of Zn-C distances) is [{Zn(C_6F_5)$_3$}$^-${CPh_3}$^+$] that was obtained as product of disproportionation after the reaction of Ph_3CCl with Zn(C_6F_5)$_2$.[70]

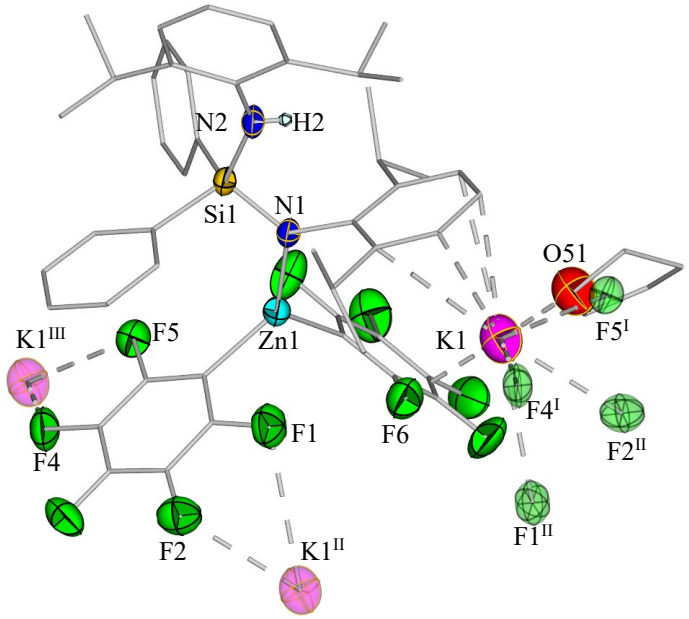

Figure 4. 11 *Crystal structure of **29**, ellipsoids are rendered with 50% probability. Hydrogen atoms and disordered components in THF are omitted, and carbon atoms of Aryl and THF fragments are drawn as wire frames for clarity. Symmetry transformations used to generate symmetrical atoms I: 1+x, y, z; II: 1-x,1- y, 1-z; III: -1+x, y, z. Selected bond distances (Å) and angles (°):N1-Zn1 1.940(2), Zn1-*

C39 2.022(3), Zn1-C45 2.033(3), K1-F ranging from 2.681(3) to 3.436(3), K1-C_{Ar*} 3.061(3) to 3.536(3), N1-Zn1-C39 123.11(11), N1-Zn1-C45 120.01(11), C39-Zn1-C45 116.69(12)

The crystal structure of **34** results in pseudo-separeted ion pair, with the dianion $[C_6F_4]^{2-}$ bridging between two $[Ph_2Si(NAr^*)_2Zn]$ moieties, with two potassium cations to balance the charges. Potassium cation is coordinated by three molecules of THF, and its coordination sphere is satisfied by the coordination with a fluorine atom and engaging π-interactions with the aryl moiety of Ar* group and without any connection with the carbon C1 metalated by the zinc. The zinc has a distorted trigonal planar geometry (sum of angles 359.39°) and other than C1 is coordinated by the dianion $[Ph_2Si(NAr^*)_2]^{2-}$ in a chelating fashion way. The distances between zinc and carbon and nitrogens (1.9689(17) and 1.9474(14), 1.9872(14) Å respectively) are very similar to the ones reported before in this chapter and to the one reported by Crimmin and coworkers for the mono-metalated tetratfluorobenzene [{^{Dipp}Nacnac}Zn(C_6F_4H)].[38]

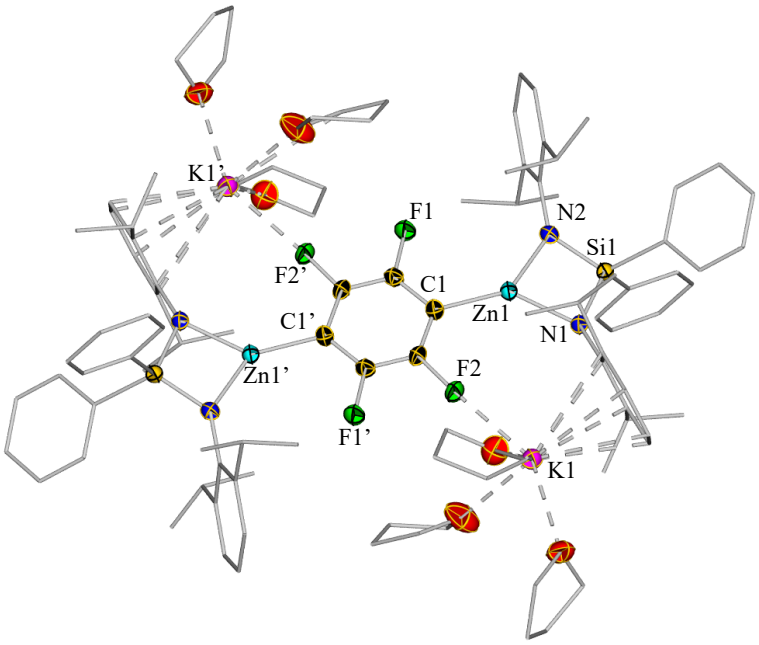

Figure 4. 12 *Crystal structure of **34**, ellipsoids are rendered with 50% probability. Hydrogen atoms and disordered components in THF, ^{i}Pr group and phenyl are omitted, carbon atoms of Aryl (except for the tetrafluoro dianion) and THF fragments are drawn as wire frames for clarity. Symmetry transformations used to generate symmetrical atoms: 1-x, 1- y, 1-z. Selected bond distances (Å) and angles (°):N1-Zn1 1.9872(14),N2-Zn1 1.9474(14) Zn1-C1 1.9689(17), K1-F2 2.6792(13), K1-C_{Ar*} ranging from 3.080(2) to 3.2702(19),), Si1-N1-Zn1 90.03(6), Si1-N2-Zn1 91.66(6), N1-Zn1-N2 81.12(6), N1-Zn1-C1 139.39(6), N2-Zn1-C1 138.88(7)*

4.3.3 Studies on the Functionalization of Metalated Fluoroarenes

With this library of compound in our hands, we next investigated the possibility of functionalising the newly formed Zn-carbon bond. We used compound **20** as model system. The reaction outcomes are summarized in **Table 4. 2**.

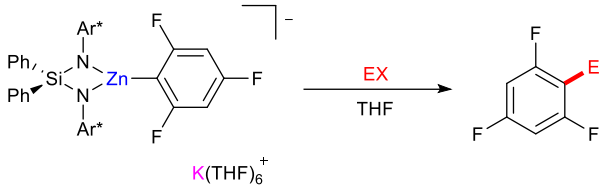

20 **34a-e**

entry	EX	Product (34a-e)	condition	yield
a	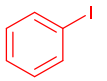	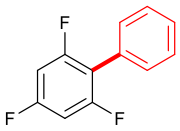	$Pd(PPh_3)_4$ (5%) T= 66°C t=16h	45%
b	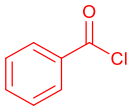	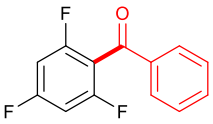	CuI (3eq.) T=25°C t=16h	70%[a]
c	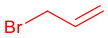	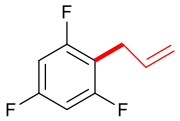	CuI(60%) T=50°C t=6h	52%[a]
d	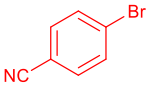	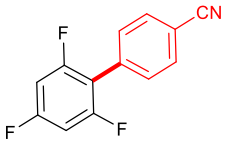	$Pd(Cl_2)(Dppf)$ (5%) PPh_3 (10%) T=66°C t=20h	63% (49%)[b]
e	I_2	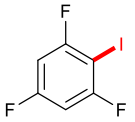	T=25°C t=16h	32%

Table 4. 2 *Functionalization of the zincate **20** with different electrophiles. [a] 3 equivalents of EX were used [b] isolated yield*

As shown in the **Table 4. 2**, entry **a** and **d**, **20** is capable to undergo Negishi cross-coupling reactions affording (**35a** and **35d** respectively) although relatively harsh reaction conditions need to be used. It is noted that compound **35d** was obtained in higher yield of **35a**, however to maximise the yield using [$Pd(Cl_2)(Dppf)$] (Dppf= 1,1′-Bis-(diphenylphosphino)-ferrocene) addition of triphenylphosphine is required. ^{19}F-NMR monitoring of the reaction revealed that, after 22 hours the conversion of **20** in **35d** is about 63% with 23% of unreacted starting material and some minor side products. If the reaction is kept for another 12 hours the starting material is consumed (in fact it drops to 9%), but at the same time the amount of **35d** does not increase and new signals appear, showing the increase in the amounts of side products instead. The addition of LiCl[71] did not improve the yield of the reaction, but a grey precipitate was noticed from the beginning of the reaction.

20 is reactive also towards benzoyl chloride at room temperature using stoichiometric amount of copper salt, affording the substituted benzophenone **35b,** an excess of electrophile is used since the silyl bis(amide) ligand reacts with this electrophile as well, forming N-(2,6-diisopropylphenyl)benzamide as side product. For the same reason 3 equivalents of allyl bromide are employed in order to form 2-allyl-1,3,5-trifluorobenzne (**35c**) in 50% yield using sub-stochiometric amount of copper salt. The iodination of **20** is not very effective achieving a yield of 32% for **35e.**

Other electrophilic quenches were attempted. Using CO_2 turns to be ineffective. As well the nucleophilic addition to the nitro styrene of the aryl moiety.[72] The poor nucleophilicity of the 1,3,5 trifluoropheyl anion of **20** is demonstrate as well by its lack of reactivity with aldehydes and disulphuric compounds. The reaction with borohydrides leads to a mixture of different products.

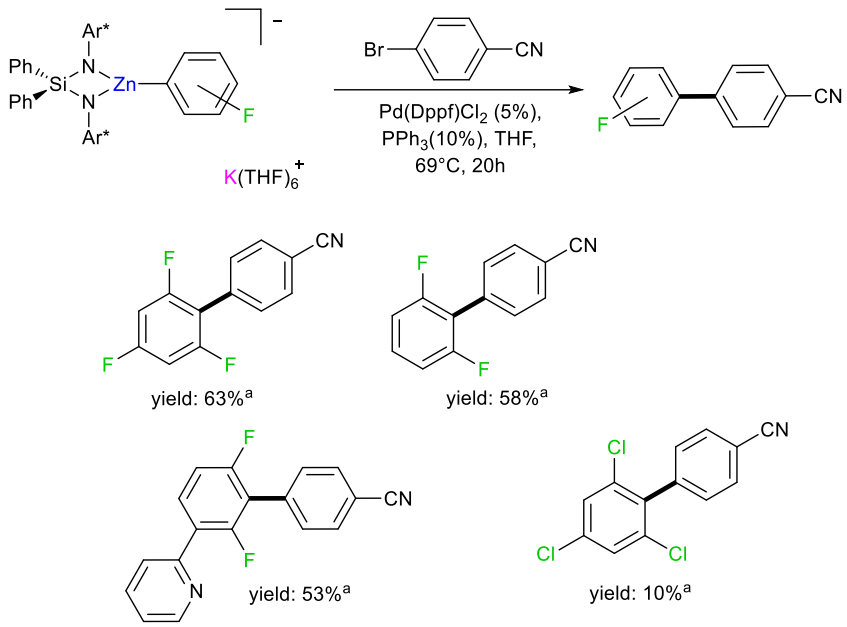

Scheme 4. 15 *Functionalization via Negishi cross coupling of **20, 21, 22** and **23**. (Dppf= 1,1'-Bis(diphenylphosphino)ferrocene). [a] Yields were calculated via ^{1}H-NMR against hexamethylbenzne as internal standard.*

In order to demonstrate the generality of the functionalization for zincates other than **20** the Negishi- type cross coupling was extended to other isolated zincates, using the same condition used in **Scheme 4. 15**. **21** and **24** demonstrated a similar reactivity to **20**, achieving similar final yields (58% and 53% respectively). Surprisingly **23** demonstrated a much sluggish reactivity, achieving only a 10% of yield.

4.4 Conclusions

The subsequent action of KR and $Zn(TMP)_2$ to amine **1** led to a formation of a new potassium zincate $[\{Ph_2Si(NAr^*)_2Zn(TMP)\}^-\{K(THF)_6\}^+]$ (**19**). Due to the high kinetic basicity of TMP anion and the steric shelter derived from the dianionic ligand $\{Ph_2Si(NAr^*)_2\}^{2-}$ it is possible to zincate fluoroarenes, variously substituted, and characterising the metalated intermediates using single crystal X-ray diffraction and multinuclear NMR spectroscopy. Observing solvent separated (or pseudo solvent separated) structures with the potassium cation located far away from the zinc centre.

It is possible to isolate the intermediate of metalation of 1,3,5 trifluorobenzene, known for the instability of its lithiated analog, without suffering of decomposition via benzyne formation. The steric bulk protection provided by the supporting silyl bis(amide) ligand enables the

isolation of the product of metalation of arenes with nitro groups, which are usually incompatible with polar organometallics. All the zincation reactions occurred in *ortho* to a fluorine atom. Optional site selectivity in metalation of **19** was demonstrate with 3-fluoropirydine where the metalation was achieved in C2 position, preferred over the thermodynamical favoured C4 position.

With more activated substrate such as pentafluorobenzene and 1,2,4,5-tetrafluorobenzene, after an initial delay, dianionic ligand $\{Ph_2Si(NAr^*)_2\}^{2-}$ participated to the metalation affording the tris-aryl zincate products $[K(THF)_yZn(C_6H_xF_{5-x})_3]$ (x= 0 or 1 respectively). Moreover with tetrafluorobenzene the product of the first deprotonation, the potassium zincate 30, is still reactive for a second deprotonation using an excess of base, achieving the di-metalation of the tetrafluororobenzene.

The metalate fluoroaryls, will be then further functionalised forming new carbon-carbon bond via acylation copper-mediated or Negishi cross-coupling catalysed by palladium.

4.5 Experimental Section

Synthesis of $[\{Ph_2Si(NAr^*)_2Zn(TMP)\}^-\{K(THF)_6\}^+]$ (**19**)

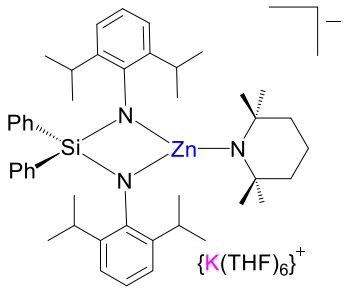

572 mg of **13** (1 mmol) and 346 mg of $Zn(TMP)_2$ (1 mmol) were solubilized in 10 mL of THF and the solution was allowed to stir at reflux overnight. Volatiles were removed under vacuum, the white residue was dissolved in 5 mL of hexane and 2 mL of THF, affording a pale-yellow solution. Storage in freezer (-33°C) for two days furnished colourless crystal of **19** (641.6 mg 67%)

^{1}H-NMR (D_8-THF; 298K; 400 MHz) δ(ppm): 7.28 [m, 4H, Ph], 6.93 [m, 4H, Ar*], 6.71 [m, 6H, Ph], 6.45 [t, 2H, Ar*], 4.14 [sept., 4H, CH ^{i}Pr], 3.61 [m, 10H, O-CH_2 THF], 1.77 [m, 10H, CH_2 THF], 1.55[m, 2H, γ-CH_2 TMP], 1.17 [m, 4H,β-CH_2 TMP], 0.97 [s, 12H, CH_3 TMP] It should be noted that around 4 molecules of the solvating THF present in **19** were removed under vacuum when drying the crystals **^{13}C{^{1}H}-NMR** (D_8-THF; 298K, 100 MHz) δ(ppm): 152.6, 148.2, 145.7 [$C_{quaternary}$ Ar* and Ph], 136.3, 126.5, 122.4, 117.5 [CH, Ar* and Ph], 68.4 [O-CH_2 of THF], 53.2 [$C_{quaternary}$ TMP], 42.0[β-CH_2 TMP], 37.0 [CH_3 TMP], 28.2 [CH ^{i}Pr], 26.5 [CH_3 ^{i}Pr], 20.8 [γ-CH_2 TMP]

Elemental analysis: analytical calculated: $C_{61}H_{94}KN_3O_4SiZn$ C 68.73, H 8.89, N 3.94. Found: C 68.51, H 8.72, N 3.94

Synthesis of [{$Ph_2Si(NAr^*)_2Zn(TMP)$}$^-${$Na(THF)_6$}$^+$] (**19b**)

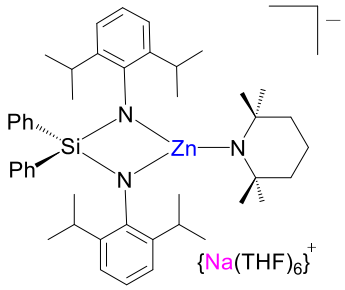

278 mg of **2** (0.5 mmol) and 176 mg of $Zn(TMP)_2$ (0.5 mmol) were solubilized in 5 mL of THF and the solution was allowed to stir at reflux overnight. Volatiles were removed under vacuum, the white residue was dissolved in 2.5 mL of hexane and 1 mL of THF, affording a pale-yellow solution. Storage in freezer (-33°C) for two days furnished colourless crystal of **19b** (541.5 mg 65%)

^{1}H-NMR (D_8-THF; 298K; 400 MHz) δ(ppm): 7.29 [m, 4H, Ph], 6.93 [m, 4H, Ar*], 6.72 [m, 6H, Ph], 6.45 [t, 2H, Ar*], 4.14 [sept., 4H, CH ^{i}Pr], 3.62 [m, 5H, O-CH_2 THF], 1.78 [m, 5H, CH_2 THF], 1.55[m, 2H, γ-CH_2 TMP], 1.17 [m, 4H,β-CH_2 TMP], 0.97 [s, 12H, CH_3 TMP] It should be noted that around 5 molecules of the solvating THF present in **19b** were removed under vacuum when drying the crystals **^{13}C{^{1}H}-NMR** (D_8-THF; 298K, 100 MHz) δ(ppm): 152.5, 148.2, 145.7 [$C_{quaternary}$ Ar* and Ph], 136.3, 126.6, 126.4,122.4, 117.4 [CH, Ar* and Ph], 68.4 [O-CH_2 of THF], 53.2 [$C_{quaternary}$ TMP], 42.0[β-CH_2 of TMP], 37.0 [CH_3 TMP], 28.2 [CH ^{i}Pr], 26.5 [CH_3 ^{i}Pr], 20.8 [γ-CH_2 TMP]

Elemental analysis: analytical calculated: $C_{61}H_{90}NaN_3O_4SiZn$ C 70.05, H 8.67, N 4.02. Found: C 69.13, H 8.94, N 4.09

Synthesis of [{$Ph_2Si(NAr^*)_2Zn(C_6H_2F_3)$}$^-${$K(THF)_6$}$^+$] (**20**):

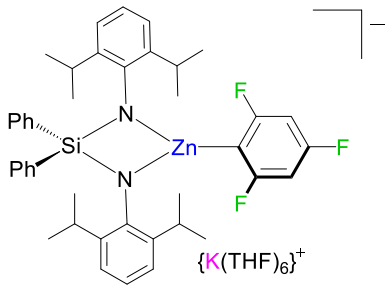

procedure A: 388 mg of **19** (0.5 mmol) was solubilized in 5 mL of THF, 0.05 mL of 1,3,5 trifluorobenzene (0.5 mmol) were added. The resulting yellow solution was allowed to stir at room temperature for 48 h. All the volatiles were removed under reduced pressure. The white solid was solubilized with 2.5 mL of hexane and 1.5 mL of THF. Overnight storage in freezer (-33°C) furnished colourless crystal of **20.**

procedure B: 388 mg of **19** (0.5 mmol) was solubilized in 5 mL of THF, 0.05 mL of 1,3,5 trifluorobenzene (0.5 mmol) were added. The resulting yellow solution was allowed to stir at reflux for 3 h. All the volatiles were removed under reduced pressure. the white solid was solubilized with 2.5 mL of hexane and 1.5 mL of THF. Overnight storage in freezer (-33°C) furnished colourless crystals of **20**. To maximize the yield the product could be obtained as powder, the solid obtained after the removing of the volatiles was suspended in 10 mL of hexane and filtered through celite. (676.6 mg, 85%)

^{1}H-NMR (D_8-THF; 298K; 400 MHz) δ(ppm): 7.34 [m, 4H, Ph], 6.99 [m, 6H, Ph], 6.72 [d, 4H, Ar*], 6.46 [t, 2H, Ar*], 6.33 [m, 2H, $C_6H_2F_3$] 4.20 [sept., 4H, CH ^{i}Pr], 0.82 [d, 24H, CH_3 ^{i}Pr] It should be noted that around 6 molecules of the solvating THF present in **3a** were

removed under vacuum when drying the crystals **^{13}C{^{1}H}-NMR** (D_8-THF; 298K, 100 MHz) δ(ppm): 171.1, 168.0, 165.2 [m, *C*-F $C_6H_2F_3$], 162.0 [C_{ipso} $C_6H_2F_3$] 152.2, 146.8, 144.7 [$C_{quaternary}$ Ar* and Ph], 135.8, 126.6, 126.2 [CH Ph] 121.8, 117.4 [CH Ar*], 98.01 [CH, $C_6H_2F_3$] 28.1 [CH ^{i}Pr], 24.3 [CH_3 ^{i}Pr] **^{19}F-NMR** (D_8-THF; 298K; 400 MHz) δ(ppm): -83.45 [m, 2F], -116.0 [m, 1F]

Elemental analysis: analytical calculated: $C_{104}H_{127}F_6K_2N_4O_5Si_2Zn_2$ C 66.01, H 6.77, N 2.96. Found: C 65.78, H 7.11, N 2.99

Synthesis of [{$Ph_2Si(NAr^*)_2Zn(C_6H_2F_3)$}$^-${$Na(THF)_5$}$^+$] (**20b**):

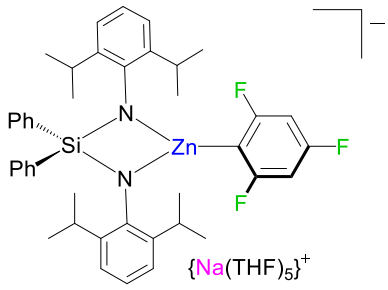

523 mg of **5** (0.94 mmol) was solubilized in 5 mL of THF, 0.097 mL of 1,3,5 trifluorobenzene (0.94 mmol) were added. The resulting yellow solution was allowed to stir at reflux for 5 h. All the volatiles were removed under reduced pressure. the white solid was solubilized with 5 mL of hexane and 3 mL of THF, that was gently heated until a yellow solution was obtained. Colourless crystals of **20b** were obtained after slow cooling of this solution (474 mg, 53%)

^{1}H-NMR (D_8-THF; 298K; 400 MHz) δ(ppm): 7.33 [m, 4H, Ph], 6.97 [m, 6H, Ph], 6.71 [d, 4H, Ar*], 6.45 [t, 2H, Ar* J=7.5 Hz], 6.32 [m, 2H, $C_6H_2F_3$] 4.19 [sept., 4H, CH ^{i}Pr], 3.62 [m, 10H, O-CH_2 THF], 1.77 [m, 10H, CH_2 THF], 0.82 [d, 24H, CH_3 ^{i}Pr] It should be noted that around 4 molecules of the solvating THF present in **20a** were removed under vacuum when drying the crystals **^{13}C{^{1}H}-NMR** (D_8-THF; 298K, 100 MHz) δ(ppm): 152.5, 147.2, 145.0 [$C_{quaternary}$ Ar* and Ph], 136.1, 127.0, 126.6 [CH Ph] 122.2, 117.7 [CH Ar*], 98.36 [CH, $C_6H_2F_3$], 68.4 [O-CH_2 THF], 28.5 [CH ^{i}Pr], 26.5 [CH_2 THF] 24.7 [CH_3 ^{i}Pr] Relevant signals for the C_{ipso} and for the *C*-F of the $C_6H_2F_3$ group were not detected, due to the dilution of the sample. **^{19}F{^{1}H}-NMR** (D_8-THF; 298K; 400 MHz) δ(ppm): -83.4 [d, 2F], -116.1 [t, 1F]

Elemental analysis: analytical calculated: $C_{58}H_{74}F_3N_2NaO_4SiZn$ C 67.20, H 7.20, N 2.70. Found: C 66.36, H 7.65, N 2.79

Synthesis of [{$Ph_2Si(NAr^*)_2Zn(C_6H_3F_2)$}$^-${$K(THF)_6$}$^+$] (**21**):

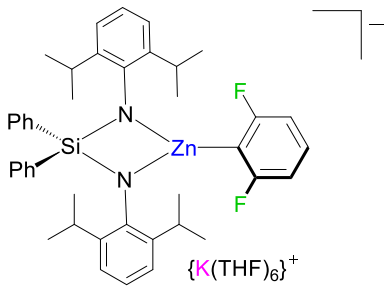

388 mg of **19** (0.5 mmol) was solubilized in 5 mL of THF, 0.1 mL of 1,3 difluorobenzene (0.5 mmol) were added. The resulting yellow solution was allowed to stir at reflux for 5 h. All the volatiles were removed under reduced pressure. The white solid was solubilized with 2.5 mL of Hexane and 1.5 mL of THF. Overnight storage in freezer (-33°C) furnished colourless crystals of **21**. (448 mg, 54%)

^{1}H-NMR (D_8-THF; 298K; 400 MHz) δ(ppm): 7.35 [m, 4H, Ph], 6.98 [m, 6H, Ph], 6.92 [m, 1H, $C_6H_3F_2$] 6.71 [d, 4H, Ar*], 6.5 [m, 2H, $C_6H_3F_2$], 6.45 [t, 2H, Ar*], 4.21 [sept., 4H, CH ^{i}Pr], 0.83 [d, 24H, CH_3 ^{i}Pr] It should be noted that most of molecules of the solvating THF present in **21** were removed under vacuum when drying the crystals **^{13}C{^{1}H}-NMR** (D_8-THF; 298K, 100 MHz) δ(ppm): 152.7, 147.4, 145.1 [$C_{quaternary}$ Ar*, $C_6H_3F_2$ and Ph], 136.2, 126.9, 126.6, 122.2, 117.6 [CH, Ar* and Ph], 109.9, 109.5 [CH, $C_6H_3F_2$] 28.5 [CH ^{i}Pr], 24.7 [CH_3 ^{i}Pr]] Relevant signals for the C_{ipso} and for the *C*-F of the $C_6H_3F_2$ group were not detected, due to the dilution of the sample. **^{19}F{^{1}H}-NMR** (D_8-THF; 298K; 400 MHz) δ(ppm): -85.75 [s, 2F]

Elemental analysis: analytical calculated: $C_{46}H_{54}F_2KN_2OSiZn$ C 67.25, H 6.63, N 3.41. Found: C 67.22, H 6.31, N 3.73

Synthesis of [{$Ph_2Si(NAr^*)_2Zn(C_6H_2Cl_3)$}$^-$ {$K(THF)_6$}$^+$] (**23**):

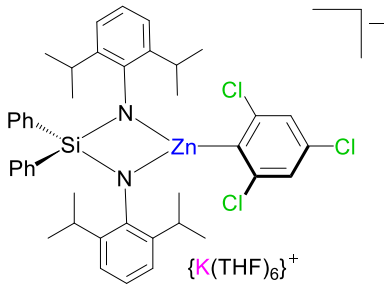

388 mg of **19** (0.5 mmol) was solubilized in 5 mL of THF, 90 mg of 1,3,5 trichlorobenzene (0.5 mmol) were added. The resulting yellow solution was allowed to stir at reflux for 21 h. All the volatiles were removed under reduced pressure. The white solid was solubilized with 3 mL of hexane and 1.5 mL of THF. Overnight storage in freezer (-33°C) furnished colourless crystals of **23** (265mg, 65%).

^{1}H-NMR (D_8-THF; 298K; 400 MHz) δ(ppm): 7.36 [m, 4H, Ph], 6.97 [m, 8H, Ph and $C_6H_2Cl_3$], 6.72 [d, 4H, Ar*], 6.46 [t, 2H, Ar*], 4.19 [sept., 4H, CH ^{i}Pr], 3.61 [m, 9H, O-CH_2 THF], 1.77 [m, 9H, CH_2 THF], 0.79 [d, 24H, CH_3 ^{i}Pr] It should be noted that around 4 molecules of the solvating THF present in **23** were removed under vacuum when drying the crystals **^{13}C{^{1}H}-NMR** (D_8-THF; 298K, 100 MHz) δ(ppm): 152.5, 147.3, 145.8, 145.1[$C_{quaternary}$ Ar*, $C_6H_2Cl_3$ and Ph], 136.3, 126.9, 126.6, 125.5, 122.3, 117.7 [CH, Ar*, Ph and $C_6H_2Cl_3$], 68.4 [O-CH_2 THF], 28.4 [CH ^{i}Pr], 26.5 [CH_2 THF], 25.0 [CH_3 ^{i}Pr] Relevant signals for the C_{ipso} and for the *C*-Cl of the $C_6H_2Cl_3$ group were not detected, due to the dilution of the sample.

Elemental analysis: analytical calculated: $C_{134}H_{152}Cl_9K_3N_6O_2Si_3Zn_3$ C 62.01, H 5.90, N 3.24. Found: C 61.81, H 6.04, N 3.25

Synthesis of [{$Ph_2Si(NAr^*)_2Zn(C_6H_2F_2NO_2)$}$^-${$K(THF)_3$}$^+$] (**24**):

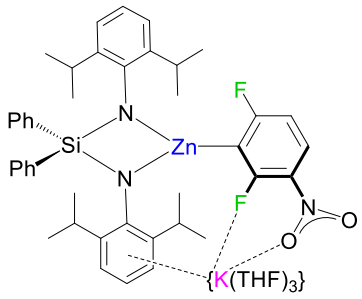

778 mg of **19** (1 mmol) was solubilized in 3.6 mL of THF in a Schlenk bottle wrapped in tin foil to prevent the contact with light. 0.11 mL of 2,4 difluoronitrobenzene (1 mmol) were added. The resulting deep red solution was allowed to stir at room temperature for 30 minutes. 6 mL of hexane were slowly added to the solution and then the mixture was stored overnight in freezer (-33°C) furnishing yellow crystals of **24** (520mg 55%).

^{1}H-NMR (D_8-THF; 298K; 300 MHz) δ(ppm): 7.79 [m, 1H, CH $C_6H_2F_2NO_2$], 7.35 [m, 4H, Ph], 6.99 [m, 6H, Ph], 6.74 [m, 5H, Ar* and $C_6H_2F_2NO_2$], 6.48 [t, 2H, Ar*], 4.19 [sept., 4H, CH ^{i}Pr], 3.62 [m, 9H, O-CH_2 THF], 1.77 [m, 9H, CH_2 THF], 0.82 [d, 24H, CH_3 ^{i}Pr] It should be noted that most of molecules of the solvating THF present in **24** were removed under vacuum when drying the crystals **^{13}C{^{1}H}-NMR** (D_8-THF; 298K, 75 MHz) δ(ppm): 152.7, 147.4, 145.1 [$C_{quaternary}$ Ar* and Ph], 136.2, 126.9, 126.6, [CH Ph] 122.2, 117.6 [CH Ar*], 109.9, 109.5 [CH, $C_6H_2F_2NO_2$] 28.5 [CH ^{i}Pr], 24.7 [CH_3 ^{i}Pr] Relevant signals for the C_{ipso} and for the *C*-F of the $C_6H_2F_2NO_2$ group were not detected, due to the dilution of the sample.**^{19}F-NMR** (D_8-THF; 298K; 300 MHz) δ(ppm): -85.75 [s, 2F]

Elemental analysis: analytical calculated: $C_{50}H_{62}F_2KN_3O_4SiZn$ C 63.61, H 6.65, N 4.47. Found: C 63.26, H 6.91, N 4.12

Synthesis of [{$Ph_2Si(NAr^*)_2Zn(C_6H_3FNO_2)$}$^-${$K(THF)_6$}$^+$] (**25**):

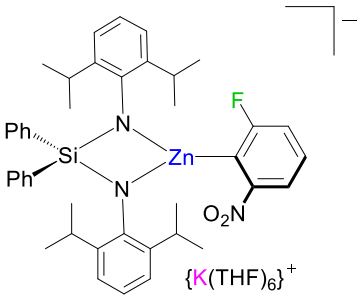

398 mg of **19** (0.5 mmol) was solubilized in 5 mL of THF. 0.05 mL of 3-fluoronitrobenzene (0.5 mmol) were added. The resulting deep red solution was allowed to stir at room temperature for 16 h. All the volatiles were removed under reduced pressure. The resulting red waxing solid was washed with 10 mL of hexane. The red solid was solubilized in 1 mL of THF and 3 mL of Hexane. Overnight storage in freezer (-33°C) furnishing red crystals of **25** (205mg 46%).

^{1}H-NMR (D_8-THF; 298K; 300 MHz) δ(ppm): 7.94 [m, 1H, CH $C_6H_3FNO_2$], 7.48 [m, 4H, Ph], 7.16 [m, 1H, CH $C_6H_3FNO_2$] 6.97 [m, 6H, Ph], 6.67 [d, 4H, Ar*], 6.40 [t, 2H, Ar*], 4.36 [sept., 4H, CH ^{i}Pr], 3.62 [m, 6H, O-CH_2 THF], 1.77 [m, 6H, CH_2 THF], 0.79 [d, 24H, CH_3 ^{i}Pr] It should be noted that most of molecules of the solvating THF present in **25** were removed under vacuum when drying the crystals **^{13}C{^{1}H}-NMR** (D_8-THF; 298K, 75 MHz) δ(ppm): 147.6, 144.9 [$C_{quaternary}$ Ar* and Ph], 136.3, 129.4, 126.3, 126.1 121.9, 117.1 [CH, Ar*, $C_6H_3FNO_2$ and Ph], 68.0 [O-CH_2 THF], 28.0 [CH ^{i}Pr], 26.2 [CH_2 THF], 24.6 [CH_3 ^{i}Pr] Relevant signals for the C_{ipso} and for the *C*-F of the $C_6H_3FNO_2$ group were not detected, due to the dilution of the sample.**^{19}F-NMR** (D_8-THF; 298K; 300 MHz) δ(ppm): -82.26 [s, 1F]

Due to the sensitivity of **25** it was not possible to obtain satisfactory elemental analysis

Synthesis of [{$Ph_2Si(NAr^*)_2Zn(C_{11}H_6F_2N)$}$^-${$K(THF)_x$}$^+$] (**26**):

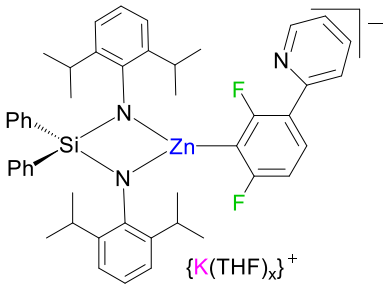

338 mg of **19** (0.44 mmol) was solubilized in 5 mL of THF, 99.5 mg of 2-(2,4-difluorophenil)pyridine (0.5 mmol) were added. The resulting yellow solution was allowed to stir at reflux for 3 h. All the volatiles were removed under reduced pressure. 10 mL of hexane was added affording a white suspension. The suspension was filtered through celite and a white solid of **26** was isolated (195 mg, 54%)

^{1}H-NMR (D_8-THF; 298K; 400 MHz) δ(ppm):8.51 [m, 1H, CH $C_{11}H_6F_2N$], 7.78 [m, 1H, CH $C_{11}H_6F_2N$], 7.74 [m, 1H, CH $C_{11}H_6F_2N$], 7.64 [m, 1H, CH $C_{11}H_6F_2N$], 7.36 [m, 4H, Ph], 7.08 [dd, 1H, CH $C_{11}H_6F_2N$], 6.99 [m, 6H, Ph], 6.72 [d, 4H, Ar*], 6.65 [m, 1H, $C_{11}H_6F_2N$], 6.46 [t, 2H, Ar*], 4.24 [sept., 4H, CH ^{i}Pr], 0.84 [d, 24H, CH_3 ^{i}Pr] It should be noted that most of molecules of the solvating THF present in **26** were removed under vacuum when drying the crystals **^{13}C{^{1}H}-NMR** (D_8-THF; 298K, 100 MHz) δ(ppm): 152.7 [$C_{quaternary}$ Ar*, Ph, $C_{11}H_6F_2N$], 150.1 [CH $C_{11}H_6F_2N$],147.3, 145.1 [$C_{quaternary}$ Ar*, Ph, $C_{11}H_6F_2N$], 136.2, 131.6 [CH Ph and $C_{11}H_6F_2N$], 126.7 [$C_{quaternary}$ Ar*, Ph, pyr or $C_{11}H_6F_2N$], 126.6, 125.0, 122.3, 122.0 117.7, 110.6 [CH Ar*, Ph, $C_{11}H_6F_2N$], 28.5 [CH ^{i}Pr], 24.8 [CH_3 ^{i}Pr] **^{19}F{^{1}H}-NMR** (D_8-THF; 298K; 400 MHz) δ(ppm): -85.32 [d, 1F], -87.31 [d, 1F]

Synthesis of [{$Ph_2Si(NAr^*)_2Zn(C_5H_3FN)$}$^-${$K(THF)_x$}$^+$] (**27**)

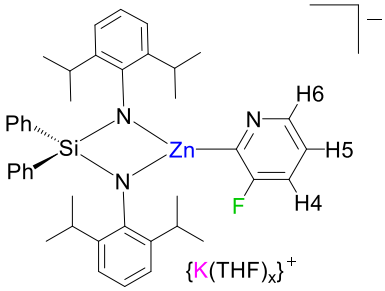

38.8 mg of **19** (0.05 mmol) were solubilised in 0.45 mL of D8-THF affording a yellow solution, 4.3 µL of 3-Fluoropyridine (0.75 mmol). The mixture was heated at 69°C for 16h. Due to the instability of the final product its clean isolation was not possible.

^{1}H-NMR (D_8-THF; 298K; 400 MHz) δ(ppm): 7.96 [d, 1H, H6], 7.92 [t, 1H, H5], 7.32 [m, 4H, Ph], 7.23 [dd, 1H, H4], 6.99 [m, 6H, Ph], 6.75 [d, 4H, Ar*], 6.50 [t, 2H, Ar*], 4.20 [sept., 4H, CH ^{i}Pr], 0.86 [d, 24H, CH_3 ^{i}Pr] **^{13}C{^{1}H}-NMR** (D_8-THF; 298K, 75 MHz) δ(ppm): 168.3, 152.2, 146.8, 144.5 [$C_{quaternary}$ Ar*, Ph, C_5H_3FN], 143.8 [CH C6 C_5H_3FN], 135.9 [CH Ph], 135.2 [CH C5 C_5H_3FN], 134.9 [CH C4 C_5H_3FN], 126.4 [CH Ph], 122.0, 117.5 [CH Ar*],49.9 [$C_{quaternary}$ TMP(H)], 38.9 [β-CH_2 TMP(H)], 32.2 [CH_3 TMP(H)], 28.1 [CH ^{i}Pr], 24.2 [CH_3 ^{i}Pr], 19.4 [γ-CH_2 TMP(H)] Relevant signals for the C_{ipso} and for the $C_{quaternary}$ of the C_5H_3FN group were not detected, due to the dilution of the sample. **^{19}F{^{1}H}-NMR** (D_8-THF; 298K; 400 MHz) δ(ppm): -102.2 [s, 1F]

Synthesis of [{$Ph_2Si(NAr^*)_2Zn(C_6F_5)\}^-\{K(THF)_x\}^+$] (**28**)

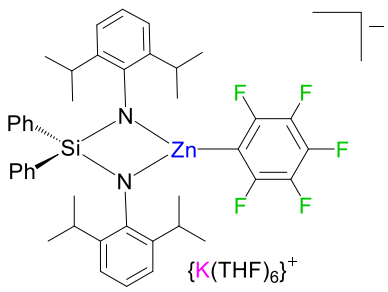

493 mg of **19** (0.46 mmol) were solubilized in 5mL of THF. The solution was cooled down to -40°C. 0.05 mL of pentafluorobenzene (0.5 mmol) were added. The mixture was allowed to stir for 30 minutes at room temperature. All the volatiles were removed under reduced pressure. The resulting waxy solid was suspended in 10 mL of hexane and the suspension was filtered through celite. The remaning yellow-white solid was solubilized in 3 mL of hexane and 0.8 mL of THF. Overnight storage in the freezer (-15°C) furnishing yellow crystals of **28**. Any attempt in isolating the pure product was unsuccessful.

^{1}H-NMR (D_8-THF; 298K; 300 MHz) δ(ppm): 7.33 [m, 4H, Ph], 6.99 [m, 6H, Ph], 6.73 [d, 4H, Ar*], 6.48 [t, 2H, Ar*], 4.16 [sept., 4H, CH ^{i}Pr], 3.61 [m, 6H, O-CH_2 THF], 1.77 [m, 6H, CH_2 THF], 0.81 [d, 24H, CH_3 ^{i}Pr] It should be noted that most of molecules of the solvating THF present in **28** were removed under vacuum when drying the crystals **^{13}C{^{1}H}-NMR** (D_8-THF; 298K, 75 MHz) δ(ppm): 151.7, 146.3 144.7 [$C_{quaternary}$ Ar* and Ph], 135.8, 126.8, 126.4[CH Ph] 122.0, 117.8 [CH Ar*], 68.0 [O-CH_2 THF], 28.2 [CH ^{i}Pr], 26.2 [CH_2 THF], 24.3 [CH_3 ^{i}Pr] Relevant signals for the C_{ipso} and for the *C*-F of the C_6F_5 group were not detected, due to the dilution of the sample.**^{19}F-NMR** (D_8-THF; 298K; 300 MHz) δ(ppm): -114.4 [m, 2F], -160.5 [t, 1F], -164.4 [m, 2F]

Due to the impurities that co-crystalize with **28** was not possible to obtain satisfactory elemental analysis

Synthesis of [{$Ph_2Si(NHAr^*)$ $(NAr^*)Zn(C_6F_5)_2\}^-\{K(THF)_1\}^+$] (**29**):

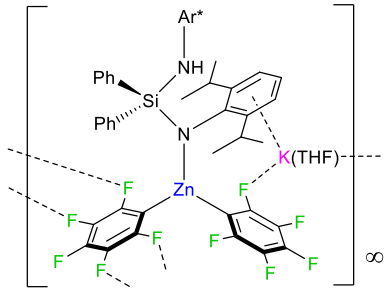

398 mg of **19** (0.5 mmol) were solubilized in 5 mL of THF. The solution was cooled down to -40°C. 0.17 mL of pentafluorobenzene (1.5 mmol) were added. The mixture was allowed to stir for 1h at room temperature. All the volatiles were removed under reduced pressure. The resulting yellow solid was solubilized in 1 mL of fluorobenzene and 1.2 mL of hexane. Overnight storage in fridge (4°C) furnishing red crystals of **29.** Due to the presence of multiple species crystalizing together was not possible obtained a crystalline yield of **29**

^{1}H-NMR (D_8-THF; 298K; 300 MHz) δ(ppm): 7.67 [m, 4H, Ph], 7.05 [m, 6H, Ph], 6.92 [d, 2H, Ar*], 6.76 [t, 1H, Ar*], 6.72 [d, 2H, Ar*], 6.59 [t, 1H, Ar*], 4.13 [sept., 2H, CH ^{i}Pr], 3.61 [m, 6H, O-CH_2 THF], 2.55 [sept., 2H, CH ^{i}Pr], 1.77 [m, 6H, CH_2 THF], 0.88 [d, 12H, CH_3 ^{i}Pr], 0.55 [d, 12H, CH_3 ^{i}Pr] It should be noted that the resonance for the NH is overlapping with the residual signal of the solvent.**^{19}F-NMR** (D_8-THF; 298K; 300 MHz) δ(ppm): -115.5 [m, 2F], -163.5 [t, 1F], -165.2 [m, 2F]

Due to the presence of $[K(THF)_xZn(C_6F_6)_3]$ and $Ph_2Si(NHAr^*)_2$ in the sample where not possible to obtain a meaningful $^{13}C\{^1H\}$-NMR spectrum.

Synthesis of $[\{Ph_2Si(NAr^*)_2Zn(C_5HF_4)\}^-\{K(THF)_x\}^+]$ (**30**)

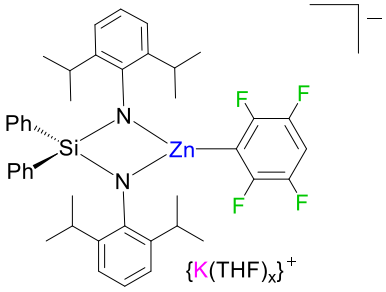

34.2 mg of **1** (0.05 mmol), were solubilised in 0.45 mL D_8-THF affording a light yellow mixture, 4 µL of α,α,α trifluorotoluene (0.032 mmol) and 10.1 mg of hexamethylbenzene (0.06 mmol) were added as internal standards. The tube was placed in cold bath at -40°C and 5 µL of 1,2,4,5 tetrafluorobenzene (0.05 mmol, 1 eq.) were added to the mixture. The yield determined using hexamethylbenzene as internal standard was 89%.

^{1}H-NMR (D_8-THF; 298K; 400 MHz) δ(ppm): 7.37 [m, 4H, Ph], 7.00 [m, 6H, Ph], 6.80 [m, 1H, C_5HF_4] 6.75 [d, 4H, Ar*], 6.50 [t, 2H, Ar*], 4.20 [sept., 4H, CH ^{i}Pr], 0.84 [d, 24H, CH_3 ^{i}Pr]

^{13}C{^{1}H}-NMR (D_8-THF; 298K, 75 MHz) δ(ppm): 151.9, 146.6, 144.7 [$C_{quaternary}$ Ar* and Ph], 135.9, 126.4 [CH Ph], 122.0, 117.7 [CH Ar*], 104.2 [CH C_5HF_4] 28.2 [CH ^{i}Pr], 24.3 [CH_3 ^{i}Pr] Relevant signals for the C_{ipso} and for the *C*-F of the C_5HF_4 group were not detected, due to the dilution of the sample.

^{19}F{^{1}H}-NMR (D_8-THF; 298K; 400 MHz) δ(ppm): -116.4 [m, 2F], -142.1 [m, 2F]

Synthesis of $[(THF)_6K_2Zn_2\{Ph_2Si(NAr^*)_2\}_2(C_6F_4)]$ (**34**):

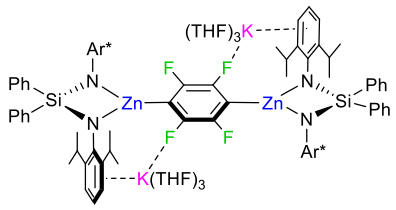

397 mg of **19** (0.39 mmol) were solubilised in 5 mL of THF. The solution was cooled down to -40°C and 0.02 mL of 1,2,4,5 tetrafluorobenzne (0.1 mmol) were added dropwise. The resulting solution was allowed to stir at room temperature for 30 minutes. The solution was then left to stir at reflux for 16h. The next day all the volatiles were removed under reduced pressure. The obtained white solid was washed with 6 mL of hexane and solubilized in 2 ml of THF. Layering 1.5 mL of hexane on the yellow solution furnished colourless crystals of **34** (59 mg, 11%)

^{1}H-NMR (D_8-THF; 298K; 300 MHz) δ(ppm): 7.29 [m, 8H, Ph], 6.97 [m, 12H, Ph], 6.74 [d, 8H, Ar*], 6.48 [t, 4H, Ar*], 4.13 [sept., 8H, CH ^{i}Pr], 3.61 [m, 10H, O-CH_2 THF], 1.77 [m, 10H, CH_2 THF], 0.78 [d, 48H, CH_3 ^{i}Pr] It should be noted that most of molecules of the solvating THF present in **33** were removed under vacuum when drying the crystals **^{13}C{^{1}H}-NMR** (D_8-THF; 298K, 100 MHz) δ(ppm): 152.5, 146.4 144.9 [$C_{quaternary}$ Ar*, C_6F_4 and Ph], 135.7, 126.8, 126.3, 122.0, 117.3 [CH, Ar*, C_6F_4 and Ph], 68.0 [O-CH_2 THF], 28.1 [CH ^{i}Pr], 26.2 [CH_2 THF], 24.2 [CH_3 ^{i}Pr] **^{19}F-NMR** (D_8-THF; 298K; 300 MHz) δ(ppm): -119.0 [s, 4F]

Elemental analysis: analytical calculated: $C_{106}H_{137}F_4K_2N_4O_7Si_2Zn_2$ C 66.3, H 7.19, N 2.92. Found: C 65.17, H 7.41, N 3.03

Organic Products

2,4,6-trifluoro-1,1'-biphenyl (**35a**)

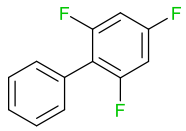

768 mg of 20 (1mmol) were solubilized in 5 mL of THF. 0.11 mL (1 mmol) of iodobenzene and 58 mg of Pd(PPh3)4 (0.05 mmol, 5%) were added to the solution. The mixture was let stir for 18h at 69°C. The reaction was quenched with a saturated solution NH_4Cl and extract with Et_2O. The combined organic layers were washed with HCl, dried with $MgSO_4$ and concentrated. 10.4 mg of ferrocene were added as internal standard (NMR yield 0.45 mmol, 45%). ^{1}H-NMR and ^{19}F-NMR agreed with the one reported in literature[73]

Phenyl(2,4,6-trifluorophenyl)methanone (**35b**)

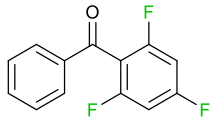

384 mg of **20** (0.5mmol) were solubilized in 5 mL of THF. The mixture was cooled down to –20°C. 286 mg of CuI (1.5 mmol) and 0.18 mL of benzoylchloride (1.5 mmol) were added. The flask was removed from the bath and the mixture was allowed to reach the room temperature. The mixture was let stir for 16h, affording a red-brown solution. The reaction was quenched with a saturated solution NH_4Cl and extract with Et_2O. The combined organic layers were washed with HCl, dried with $MgSO_4$ and concentrated. 10.2 mg of Hexamethylbenzene were added as internal standard (NMR yield 0.35 mmol, 70%).^{1}H-NMR and ^{19}F-NMR agreed with the one reported in literature.[26]

2-allyl-1,3,5-trifluorobenzene (**35c**)

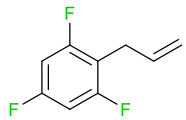

384 mg of **20** (0.5mmol) and 58.5 mg of CuI (0.3 mmol, 60%) were solubilized in 10 mL of THF. 0.13 mL of allylbromide (1.5 eq.) were added. The mixture was let stir for 6h at 66°C. The reaction was quenched with a saturated solution NH_4Cl and extract with Et_2O. The combined organic layers were washed with HCl, dried with $MgSO_4$ and concentrated. 12.1 mg of Hexamethylbenzene were added as internal standard (NMR yield 0.25 mmol, 50%). %).^{1}H-NMR and ^{19}F-NMR agreed with the one reported in literature.[74]

2',4',6'-trifluoro-[1,1'-biphenyl]-4-carbonitrile (**35d**)

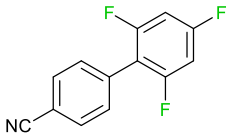

384 mg of **20** (0.5 mmol), 18.3 mg of [1,1′-Bis(diphenylphosphino)ferrocene]dichloropalladium(II) ($Pd(dppf)Cl_2$) (0.025 mmol, 5%), 13 mg of triphenylphosphine (0.05 mmol, 10%) and 82 mg of 4-Bromobenzonitrile (0.45 mmol) were solubilized in 10 mL of THF. The mixture was let stir for 20h at 66°C. The reaction were quenched with a saturated solution NH_4Cl and extract with Et_2O. The combined organic layers were washed with HCl, dried with $MgSO_4$ and concentrated. 11.7 mg of hexamethylbenzene were added as internal standard (NMR yield 0.28 mmol, 63%).^{1}H-NMR and ^{19}F-NMR agreed with the one reported in literature.[75]

1,3,5-trifluoro-2-iodobenzene (**35e**)

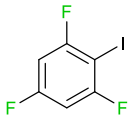

235 mg of **20** (0.3 mmol) were solubilized in 3 mL of THF. The resulting yellow solution was cooled at -78°C. A solution of 466 mg of I_2 (1.8 mmol, 6eq.) in 6 mL of THF was added dropwise. The mixture was allowed to reach the room temperature and let stirring for 16h. The reaction was quenched with Brine and a saturated solution of $Na_2S_2O_3$ and extract with Et_2O. The combined organic layers were washed with HCl, dried with $MgSO_4$ and concentrated. 10 mg of Hexamethylbenzene was added as internal standard. (NMR yield 0.1 mmol, 32%). ^{1}H-NMR and ^{19}F-NMR agreed with the one reported in literature.[76]

General procedure for the Negishi-type cross coupling of metalated fluoroarenes

0.5 mmol of the metalated fluoroaryles (**20-24**), 18.3 mg of $Pd(dppf)Cl_2$ (0.025 mmol, 5%), 13 mg of triphenylphosphine (0.05 mmol, 10%) and 82 mg of 4-Bromobenzonitrile (0.45 mmol) were solubilized in 10 mL of THF. The mixture was let stir for 20h at 69°C. The reaction was quenched with a saturated solution NH_4Cl and extract with Et_2O. The combined organic layers were washed with HCl, dried with $MgSO_4$ and concentrated. The product was not isolated, but the NMR yield was calculated against hexamethylbenzene as internal standard, using the spectra reported in literature. [75,77–79]

4.6 References

[1] D. O'Hagan, *J. Fluor. Chem.* **2010**, *131*, 1071–1081.

[2] J. Wang, J. Luis, C. Pozo, A. E. Sorochinsky, S. Fustero, V. A. Soloshonok, H. Liu, *Chem. Rev.* **2014**, 2432–2506.

[3] Y. Zhou, J. Wang, Z. Gu, S. Wang, W. Zhu, J. L. Acenã, V. A. Soloshonok, K. Izawa, H. Liu, *Chem. Rev.* **2016**, *116*, 422–518.

[4] C. Zhang, K. Yan, C. Fu, H. Peng, C. J. Hawker, A. K. Whittaker, *Chem. Rev.* **2021**, DOI 10.1021/acs.chemrev.1c00632.

[5] S. Purser, P. R. Moore, S. Swallow, V. Gouverneur, *Chem. Soc. Rev.* **2008**, *37*, 237–432.

[6] D. O'Hagan, *Chem. Soc. Rev.* **2008**, 308–319.

[7] H. Amii, K. Uneyama, *Chem. Rev.* **2009**, 2119–2183.

[8] J. Weaver, S. Senaweera, *Tetrahedron* **2014**, *70*, 7413–7428.

[9] A. D. Sun, J. A. Love, *Dalton Trans.* **2010**, *39*, 10362–10374.

[10] T. W. Butcher, W. M. Amberg, J. F. Hartwig, *Angew. Chem. Int. Ed.* **2021**, DOI 10.1002/anie.202112251.

[11] A. E. Shilov, G. B. Shul'pin, *Chem. Rev.* **1997**, *97*, 2879–2932.

[12] L. Pauling, *J. Am. Chem. Soc.* **1932**, *54*, 3570–3582.

[13] M. Schlosser, *Angew. Chem., Int. Ed.* **1998**, *110*, 1496–1513.

[14] F. Mongin, M. Schlosser, *Tetrahedron Lett.* **1996**, *37*, 6551–6554.

[15] C. Heiss, F. Leroux, M. Schlosser, *European J. Org. Chem.* **2005**, 5242–5247.

[16] F. Mongin, R. Maggi, M. Schlosser, *Chimia (Aarau).* **1996**, *50*, 650–652.

[17] O. Tai, R. Hopson, P. G. Williard, *Org. Lett.* **2017**, *19*, 3966–3969.

[18] A. C. Pöppler, H. Keil, D. Stalke, M. John, *Angew. Chem. Int. Ed.* **2012**, *51*, 7843–7846.

[19] M. Schlosser, L. Guio, F. Leroux, *J. Am. Chem. Soc.* **2001**, *123*, 3822–3823.

[20] G. Wittig, G. Pieper, G. Fuhrmann, *Berichte der Dtsch. Chem. Gesellschaft (A B Ser.* **1940**, *73*, 1193–1197.

[21] G. Wittig, *Naturwissenschaften* **1942**, *30*, 696–703.

[22] M. Schlosser, H. C. Jung, S. Takagishi, *Tetrahedron* **1990**, *46*, 5633–5648.

[23] M. Schlosser, G. Katsoulos, S. Takagishi, *Synlett* **1990**, 747–748.

[24] A. N. Chernega, A. J. Graham, M. L. H. Green, J. Haggitt, J. Lloyd, C. P. Mehnert, N. Metzler, J. Souter, *J. Chem. Soc., Dalt. Trans.* **1997**, 2293–2303.

[25] A. Seggio, G. Priem, F. Chevallier, F. Mongin, *Synthesis* **2009**, 3617–3632.

[26] R. McLellan, M. Uzelac, A. R. Kennedy, E. Hevia, R. E. Mulvey, *Angew. Chem. Int. Ed.* **2017**, *56*, 9566–9570.

[27] M. Baenziger, S. Eswaran, Y. Jiang, G. Kasinathan, *Synthesis* **2019**, *51*, 1649–1654.

[28] M. selective metalations of pyridines and related heterocycles using new frustrated lewis pairs or tmp-zinc and tmp-magnesium bases with bf 3·oet2 Jaric, B. A. Haag, A. Unsinn, K. Karaghiosoff, P. Knochel, *Angew. Chem. Int. Ed.* **2010**, *49*, 5451–5455.

[29] H. Awad, F. Mongin, F. Trécourt, G. Quéguiner, F. Marsais, F. Blanco, B. Abarca, R. Ballesteros, *Tetrahedron Lett.* **2004**, *45*, 6697–6701.

[30] L. Davin, R. McLellan, A. R. Kennedy, E. Hevia, *Chem. Commun.* **2017**, *53*, 11650–11653.

[31] X. Wang, K. Hirano, D. Kurauchi, H. Kato, N. Toriumi, R. Takita, M. Uchiyama, *Chem. Eur. J.* **2015**, *21*, 10993–10996.

[32] Y. Kondo, M. Shilai, M. Uchiyama, T. Sakamoto, *J. Am. Chem. Soc.* **1999**, *121*, 3539–3540.

[33] M. Uchiyama, T. Miyoshi, Y. Kajihara, T. Sakamoto, Y. Otani, T. Ohwada, Y. Kondo, *J. Am. Chem. Soc.* **2002**, *124*, 8514–8515.

[34] M. Uchiyama, Y. Kobayashi, T. Furuyama, S. Nakamura, Y. Kajihara, T. Miyoshi, T. Sakamoto, Y. Kondo, K. Morokuma, *J. Am. Chem. Soc.* **2008**, *130*, 472–480.

[35] J. M. Hammann, D. Haas, P. Knochel, *Angew. Chem. Int. Ed.* **2015**, *54*, 4478–4481.

[36] M. Mosrin, G. Monzon, T. Bresser, P. Knochel, *Chem. Commun.* **2009**, 5615–5617.

[37] M. Mosrin, P. Knochel, *Org. Lett.* **2009**, *11*, 1837–1840.

[38] M. Garçon, N. W. Mun, A. J. P. White, R. M. Crimmin, *Angew. Chem. Int. Ed.* **2021**, *60*, 6145–6153.

[39] Z. Livingstone, A. Hernán-Gómez, S. E. Baillie, D. R. Armstrong, L. M. Carrella, W. Clegg, R. W. Harrington, A. R. Kennedy, E. Rentschler, E. Hevia, *Dalton Trans.* **2016**, *45*, 6175–6182.

[40] V. L. Blair, W. Clegg, A. R. Kennedy, Z. Livingstone, L. Russo, E. Hevia, *Angew. Chemie* **2011**, *123*, 10031–10034.

[41] D. R. Armstrong, W. Clegg, A. Hernán-Gómez, A. R. Kennedy, Z. Livingstone, S. D. Robertson, L. Russo, E. Hevia, *Dalton Trans.* **2014**, *43*, 4361–4369.

[42] Y. C. Tsai, D. Y. Lu, Y. M. Lin, J. K. Hwang, J. S. K. Yu, *Chem. Commun.* **2007**, 4125–4127.

[43] M. L. Hlavinka, J. R. Hagadorn, *Organometallics* **2007**, *26*, 4105–4108.

[44] W. S. Rees, O. Just, H. Schumann, R. Weimann, *Polyhedron* **1998**, *17*, 1001–1004.

[45] L. C. H. Maddock, T. Nixon, A. R. Kennedy, M. R. Probert, W. Clegg, E. Hevia, *Angew. Chemie* **2018**, *130*, 193–197.

[46] J. Hicks, P. Vasko, J. M. Goicoechea, S. Aldridge, *J. Am. Chem. Soc.* **2019**, *141*, 11000–11003.

[47] T. X. Gentner, R. E. Mulvey, *Angew. Chem. Int. Ed.* **2020**, *60*, 9247–9262.

[48] L. C. H. Maddock, M. Mu, A. R. Kennedy, M. García-Melchor, E. Hevia, *Angew. Chem. Int. Ed.* **2021**, *60*, 15296–15301.

[49] D. R. Armstrong, L. Balloch, W. Clegg, S. H. Dale, P. García-Álvarez, E. Hevia, L. M. Hogg, A. R. Kennedy, R. E. Mulvey, C. T. O'Hara, *Angew. Chemie* **2009**, *121*, 8831–8834.

[50] G. Bartoli, G. Palmieri, M. Bosco, R. Dalpozzo, *Tetrahedron Lett.* **1989**, *30*, 2129–2132.

[51] M. Bosco, R. Dalpozzo, G. Bartoli, G. Palmieri, M. Petrini, *J. Chem. Soc., Perkin Trans. 2* **1991**, 657–663.

[52] M. Schlosser, *Organometallics in Synthesis: Third Manual*, Wiley-VCH, **2013**.

[53] M. Ketels, M. A. Ganiek, N. Weidmann, P. Knochel, *Angew. Chem. Int. Ed.* **2017**, *56*, 12770–12773.

[54] M. Balkenhohl, H. Jangra, I. S. Makarov, S. M. Yang, H. Zipse, P. Knochel, *Angew. Chem. Int. Ed.* **2020**, *59*, 14992–14999.

[55] W. Clegg, B. Conway, D. V. Graham, E. Hevia, A. R. Kennedy, R. E. Mulvey, L. Russo, D. S. Wright, *Chem. Eur. J.* **2009**, *15*, 7074–7082.

[56] M. R. Cargill, G. Sandford, A. J. Tadeusiak, D. S. Yufit, J. A. K. Howard, P. Kilickiran, G. Nelles, *J. Org. Chem.* **2010**, *75*, 5860–5866.

[57] S. Zhang, Z. Zhang, H. Fu, X. Li, H. Zhan, Y. Cheng, *J. Organomet. Chem.* **2016**, *825–826*, 100–113.

[58] A. Barbanente, N. Margiotta, C. Pacifico, F. P. Intini, G. Natile, *Eur. J. Inorg. Chem.* **2020**, 1018–1026.

[59] H. Na, T. S. Teets, *J. Am. Chem. Soc.* **2018**, *140*, 6353–6360.

[60] T. Zhou, L. Li, B. Li, H. Song, B. Wang, *Organometallics* **2018**, *37*, 476–481.

[61] A. S. K. Hashmi, T. D. Ramamurthi, F. Rominger, *J. Organomet. Chem.* **2009**, *694*,

592–597.

[62] L. Davin, R. McLellan, A. Hernán-Gómez, W. Clegg, A. R. Kennedy, M. Mertens, I. A. Stepek, E. Hevia, *Chem. Commun.* **2017**, *53*, 3653–3656.

[63] M. Hedidi, G. Bentabed-Ababsa, A. Derdour, Y. S. Halauko, O. A. Ivashkevich, V. E. Matulis, F. Chevallier, T. Roisnel, V. Dorcet, F. Mongin, *Tetrahedron* **2016**, *72*, 2196–2205.

[64] K. Shen, Y. Fu, J. N. Li, L. Liu, Q. X. Guo, *Tetrahedron* **2007**, *63*, 1568–1576.

[65] F. Marsais, G. Queguiner, *Tetrahedron* **1983**, *39*, 2009–2021.

[66] G. Shi, S. Takagishi, M. Schlosser, *Tetrahedron* **1994**, *50*, 1129–1134.

[67] K. Pang, Y. Rong, G. Parkin, *Polyhedron* **2010**, *29*, 1881–1890.

[68] R. J. Schwamm, M. P. Coles, C. M. Fitchett, *Organometallics* **2015**, *34*, 2500–2507.

[69] G. Schnee, C. Fliedel, T. Avilés, S. Dagorne, *Eur. J. Inorg. Chem.* **2013**, 3699–3709.

[70] S. Garratt, A. Guerrero, D. L. Hughes, M. Bochmann, *Angew. Chem. Int. Ed.* **2004**, *43*, 2166–2169.

[71] P. Eckert, S. Sharif, M. G. Organ, *Angew. Chem. Int. Ed.* **2021**, *60*, 12224–12241.

[72] M. Dell'Aera, F. M. Perna, P. Vitale, A. Altomare, A. Palmieri, L. C. H. Maddock, L. J. Bole, A. R. Kennedy, E. Hevia, V. Capriati, *Chem. Eur. J.* **2020**, *26*, 8742–8748.

[73] Y. Wei, J. Kan, M. Wang, W. Su, M. Hong, *Org. Lett.* **2009**, *11*, 3346–3349.

[74] K. F. Pfister, M. F. Grünberg, L. J. Gooßen, *Adv. Synth. Catal.* **2014**, *356*, 3302–3306.

[75] J.-J. Dai, J.-H. Liu, D.-F. Luo, L. Liu, *Chem. Commun.* **2011**, *47*, 677–679.

[76] R. F. Leroux, R. Simon, N. Nicod, *Lett. Org. Chem.* **2006**, *3*, 948–954.

[77] T. Yan, C. B. Bheeter, H. Doucet, *European J. Org. Chem.* **2013**, *2013*, 7152–7163.

[78] L. Zhao, T. Yan, C. Bruneau, H. Doucet, *Catal. Sci. Technol.* **2014**, *4*, 352–360.

[79] R. Boyaala, R. Touzani, T. Roisnel, V. Dorcet, E. Caytan, D. Jacquemin, J. Boixel, V. Guerchais, H. Doucet, J.-F. Soulé, *ACS Catal.* **2019**, *9*, 1320–1328.

Chapter 5: Alkali-metal Manganates and their Applications in Homocoupling Processes

Part of this Chapter is adapted with permission from: M. Uzelac, P. Mastropierro, M. de Tullio, I. Borilovic, M. Tarrés, A. R. Kennedy, G. Aromí, E. Hevia Tandem Mn-I Exchange and Homocoupling Process Mediated by a Synergistically Operative Lithium Manganate *Angew. Chem. Int. Ed.* **2021**, *60*, 3247-3253. DOI: 10.1002/anie.202013153. Copyright 2020 Wiley-VCH GmbH.

Contributing authors to the manuscript and their role:

Marina Uzelac: Conceived the project, performed the synthesis of all the organometallics compounds presented in the paper (with the exception of **39**), measured and solved the crystal structure of compounds **37**, **39**, **41**, **42**, [$(THF)_4MgCl_2MnPh_2$], measured the EPR spectra for the reaction with 3-iodopyridine.

Pasquale Mastropierro: Accessed manganese-iodine exchange processes of selected substrates and investigated role of additives for the success of exchange and C-C bond forming processes, performed the synthesis of compound **40,** carried out the EPR reaction monitoring studies.

Marco de Tullio: Optimised the homocoupling reaction, performed the organic substrate scope of the paper, isolated and characterized all the organic substrate.

Ivana Borilovic: Analysed the data of the EPR spectra and created the simulated EPR spectra

Màrius Tarrés: organic characterization of some homocoupling products

Alan R. Kennedy: Checked the accuracy of X-Ray diffraction data processing

Guillem Aromí: Supervised the accuracy of EPR data processing

Eva Hevia: Principal Investigator, conceived the project, secured the funding, directed the work, and wrote the final version of the manuscript with contributions from all authors

The second part is currently a manuscript in preparation. The authors and their contribution are the following:

Pasquale Mastropierro: Conceived the project, performed all the experimental work, analyzed the data.

Marina Uzelac: wrote the first draft of the paper and the supporting information, measured and solved the crystal structure of compounds **43** and [$(PMDETA)_2K_2Mn(CH_2SiMe_3)_4$].

Alan Kennedy: Checked the accuracy of X-Ray diffraction data processing

Eva Hevia: Principal Investigator, conceived the project, secured the funding, directed the work, and wrote the final version of the manuscript with contributions from all authors

5.1 General introduction to this chapter

Symmetrical biaryls compounds are important building blocks in organic synthesis present in numerous molecules with applications in medicinal and material chemistry. Some examples included Mastingophorene A and B (molecules with neuroprotective activity and stimulator of nerve growing factor) or Euphorbetin (that has found to have anticoagulant activity). They are also applied in synthetic chemistry as chiral ligand (R-BINOL and R-P-PPHOS) (see **Figure 5. 1** for some example).[1–5] In addition the 1,3-diynes are used in optical material, organic conductors, conducting polymer and liquid crystals.[6,7] Many synthetic approaches to access these compounds involves the use of transition metal catalysis employing a variety of metals (i.e. palladium, gold, copper etc.) [4,8–14]

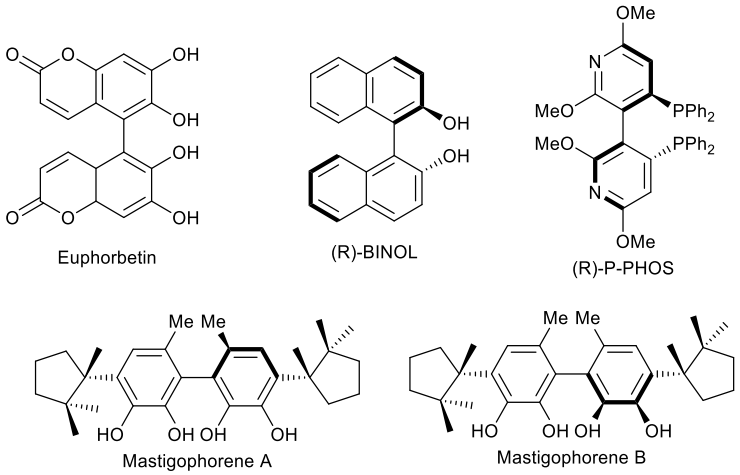

Figure 5. 1 *Representative ligands and biological active products with a symmetric biaryl moiety (BINOL= 1,1'-Bi-2-naphthol, P-PHOS= (+)-2,2',6,6'-Tetramethoxy-4,4'-bis(diphenylphosphino)-3,3'-bipyridine)*

In search of a more environmentally friendly and sustainable approaches manganese has appeared as a appealing alternative, being cheap, relatively benign toxicologically and abundant on the earth crust.[15] Seminal work by Cahiez has shown that $MnCl_2 \cdot LiCl$ was able to catalyse the homocoupling of aryl Grignard reagent at room temperature, in short time using the oxygen contained in the dry air as oxidant (**Scheme 5. 1**).[16]

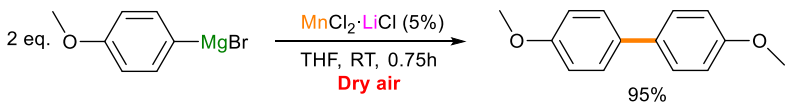

Scheme 5. 1 *Homocoupling of Arylmagnesium bromide using $MnCl_2 \cdot LiCl$ as catalyst and dry air as oxidant.*[16]

The mechanism of this oxidative homocoupling process has remained concealed for over 14 years, with limited experimental evidence on the constitution of the organometallic species

involved in these reactions. The existence of a Mn^{II}/Mn^{IV} redox manifold in the catalytic cycle has been proposed based on DFT calculations.[17] The proposed cycle (**Figure 5. 2**) involves a transmetallation step external to the cycle, forming a diaryl manganese species $MnAr_2$, which is proposed to be the active species. $MnAr_2$ can be then oxidized by O_2 to form a Mn^{IV} species, which undergoes to reductive elimination, affording the product of homocoupling and manganese epoxide. Reaction of Mn(O-O) with an excess of ArMgX regenerates $MnAr_2$, eliminating magnesium oxide (**Figure 5. 2**).[17] Notably, even if the calculations were performed in the presence of THF, the participation of the inorganic salts and the possibility to have mixed-metal species was not considered.

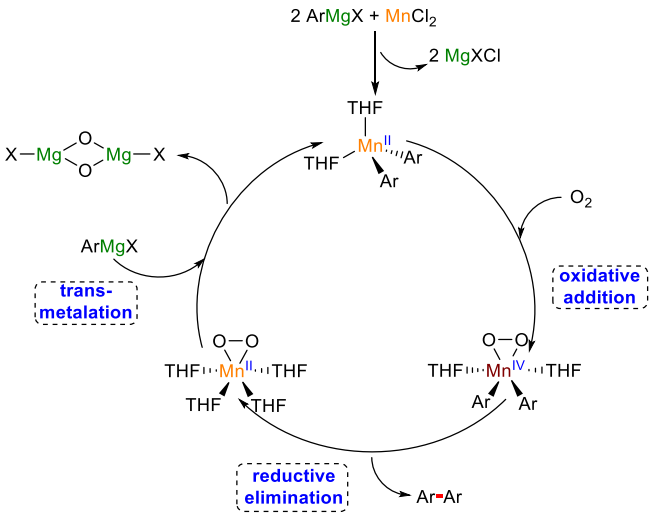

Figure 5. 2 *Proposed catalytic cycle for the oxidative homocoupling of arylmagnesium halides catalysed by Mn(II) (X= Cl or Br; Ar= aryl)*[17]

These coupling reactions do work for C(sp)-C(sp) bond formations, thus using phenylacethylenemagnesium bromide it was possible to achieve the correspondent 1-3 diynes.[18]

Steric and electronic factors affects the reactivity, this was exemplified by the failed attempt to use as substrates very sterically encumbered Grignard reagents like mesytil magnesium bromide or very electron poor aryls, such as pentafluoroaryl magnesium bromide.[17,18] This has been attributed to the stability of the Mn intermediate prior to the the reductive elimination step. Sterically encumbered aryls could increase the energy barrier for the reductive elimination. On the other hand electron poor aryls (such as pentafluorobenzene) would not have enough electron density on the *ispo*-carbons to promote the formation of a new C-C bond.[17]

Taking advantages of these effects and carefully choosing the organomagnesium halides partner, the oxidative heterocoupling catalysed by manganese was achieved. Having together an alkynyl Grignard reagent together with a sterically encumbered organomagnesium halide disfavours the homocoupling reaction, heterocoupling between the two different Grignard reagents (**Figure 5. 3**).[18]

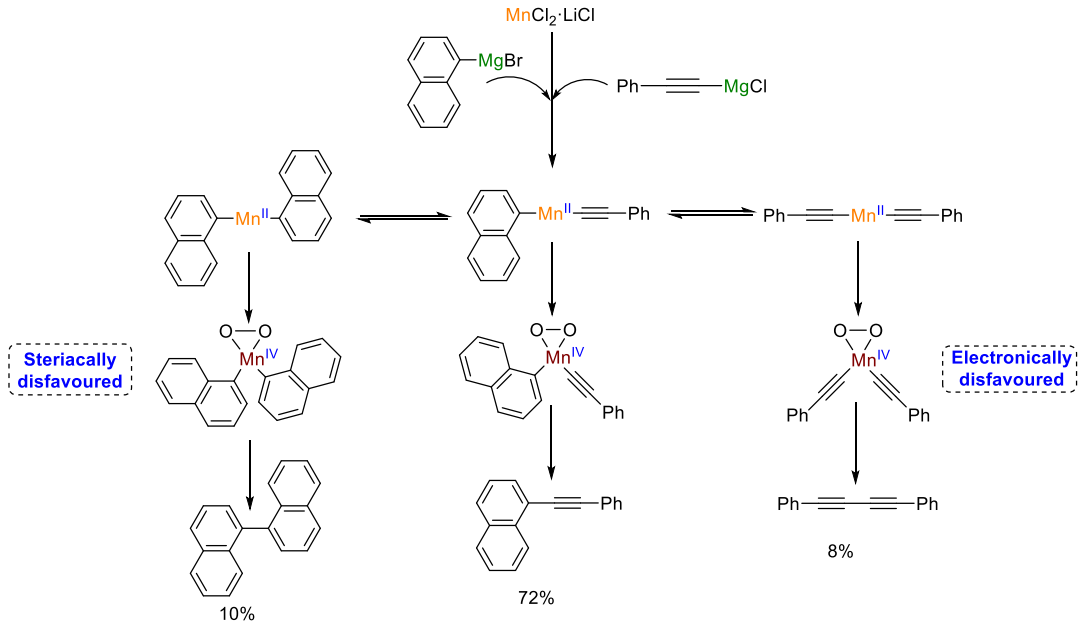

Figure 5. 3 *Proposed mechanism for the oxidative cross-coupling of Grignard reagents catalysed by manganese.*

In 2019, Taillifer and coworkers expanded the substrate scope of the homocoupling reaction demonstrating that also the organolithium could be used as starting material for manganese-catalysed homocoupling. The aryllithium species were prepared *in-situ* via metal-halogen exchange or deprotonation using ^{t}BuLi (**Scheme 5. 2**).[19]

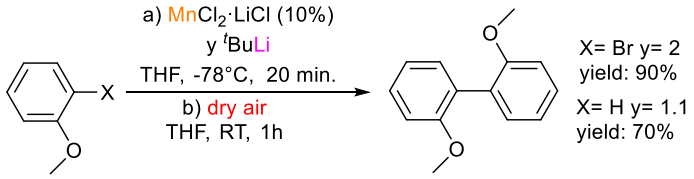

Scheme 5. 2 *Oxidative homocoupling of 2-anisolylithium catalysed by $MnCl_2$ The organolithium reagent can derived from a metal/halogen exchange or from a deprotonation.*

5.1.2 The Chemistry of Alkali-metal Manganates

The organomanganese species active in the homocoupling are usually prepared *in-situ* via salt metathesis with organolthium or organomagnesium and manganese halides. A different approach is the direct manganation of the organic substrates using reactive alkali-metal manganates. In fact, Mn(II) shares some similarities with the magnesium, which is extensively used in this chemistry.[20–22] In particular carbon manganese (II) bonds have a very ionic character,[23] moreover Mn^{2+} is similar to Mg^{2+} both in terms of size and electronegativity and therefore they show similar behaviour in coordination chemistry affording very similar structure such as $[(TMEDA)_2Li_2Mg(Me)_4]$[24] and $[(TMEDA)_2Li_2Mn(Me)_4]$[25] (**Figure 5. 4**).

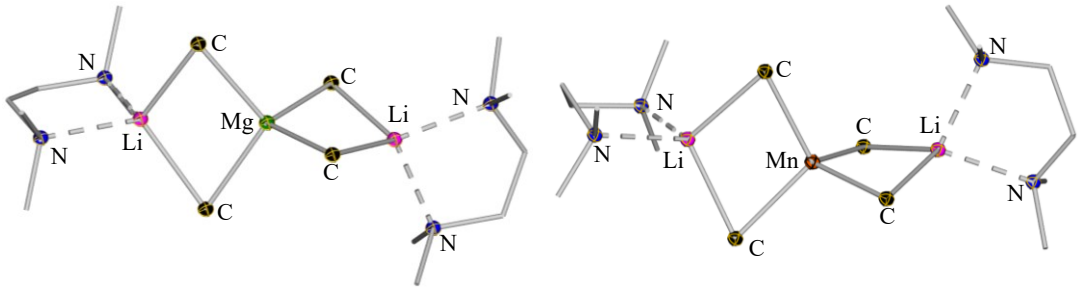

Figure 5. 4 *Crystal structure of a) [(TMEDA)$_2$Li$_2$MgMe$_4$] and b) [(TMEDA)$_2$Li$_2$MnMe$_4$]. Hydrogen atoms are omitted and carbon atom of TMEDA anions shown as wireframe for clarity. The thermal ellipsoids are rendered with 50% probability. (TMEDA= N,N,N',N'-tetramethylethylenediamine)*

Alkali-metal manganates have found applications in deprotonative metalation.[26] Thus Mulvey has shown that pairing Li and Mn(II) in the same molecule to form [(TMEDA)Li(TMP)Mn(CH$_2$SiMe$_3$)$_2$], it was possible to di-manganate ferrocene, with a great atom economy, demonstrating both, amido basicity and alkyl basicity at the heterobimetallic base with all three arms used in the metalation process, affording [(TMEDA)$_2$Li$_2$Mn$_2${Fe(C$_5$H$_4$)$_2$}$_3$] (**Figure 5. 5**).[27]

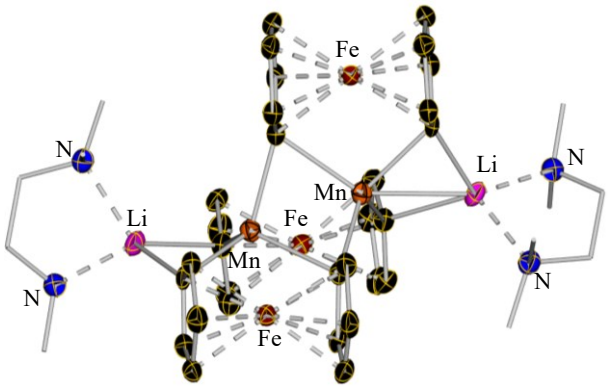

Figure 5. 5 *Crystal structure of [(TMEDA)$_2$Li$_2$Mn$_2${Fe(C$_5$H$_4$)$_2$}$_3$] product of deprotonation ferrocene using [(TMEDA)Li(TMP)Mn(CH$_2$SiMe$_3$)$_2$]. Hydrogen atoms are omitted and carbon atom of TMEDA anions are shown as wireframe for clarity. The thermal ellipsoids are rendered with 50% probability. Symmetry operations used to generate symmetrical atoms 2-x, y, 3/2-z*

Sodium manganate [(TMEDA)NaMn(TMP)$_2$(CH$_2$SiMe$_3$)] has also displayed high versatility for the deprotonation of activated and non-activated arenes (see **Figure 5. 6** for an overview of the metalated substrates).[28–30] While none of those compounds was further studied in homocoupling reactions, [(TMEDA)Na(TMP)(*o*-C$_6$H$_4$OMe)Mn(TMP)] and [(TMEDA)Na(TMP){*o*-[C(O)N-(^{i}Pr)$_2$]C$_6$H$_4$}Mn(R)] (R= CH$_2$SiMe$_3$) showed peculiar reactivity. They were able to react with iodobenzene affording the correspondent cross-coupling product in 32 and 47% yield respectively. The yields is improved with the aid of the palladium catalyst [PdCl$_2$-(dppf)] (dppf = 1,1'-bis(diphenylphosphino)ferrocene), affording 98 and 66% respectively.[31]

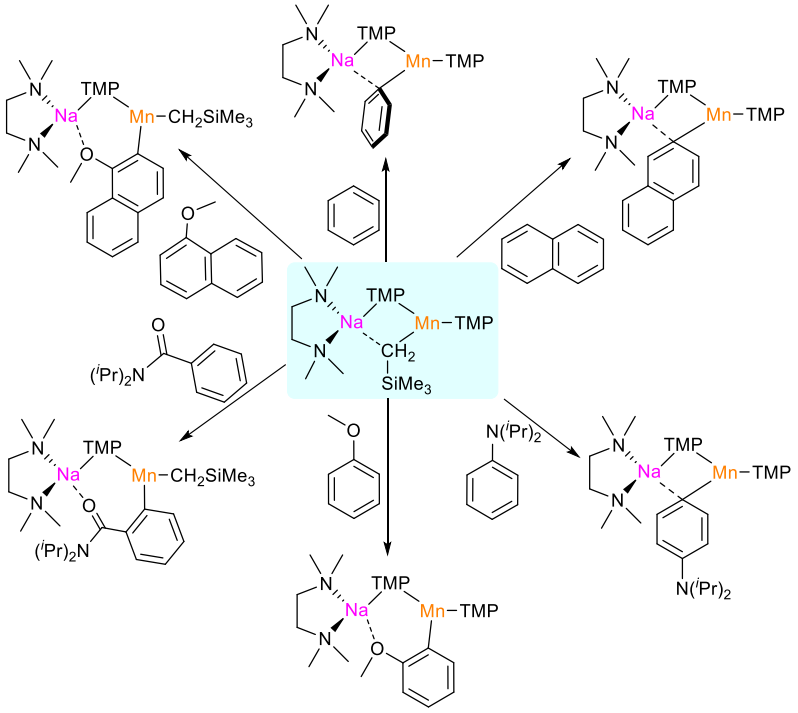

Figure 5. 6 *Overview of the substrates metalated by [(TMEDA)NaMn(TMP)$_2$(CH$_2$SiMe$_3$)]*

The template reactivity already observed in magnesium chemistry,[32] could be mimicked with sodium manganates dimetalated benzene and toluene giving a rise to supramolecular "inverse crown" motif, affording [(TMP)$_6$Na$_4$(1,4-Mn$_2$C$_6$H$_4$)][28] and [(TMP)$_6$Na$_4$(3,5-Mn$_2$C$_6$H$_3$CH$_3$)][29] which was perfectly isostructural with their magnesium analogue obtained in the same conditions (**Figure 5. 7**). [29,32] These compounds host a two-fold metalated molecule of benzene at its sterically optimum 1,4 positions. This di-anion is trapped by a cationic 12 member ring [{NaNMNNa}$^+$]$_2$ (M= Mg or Mn).

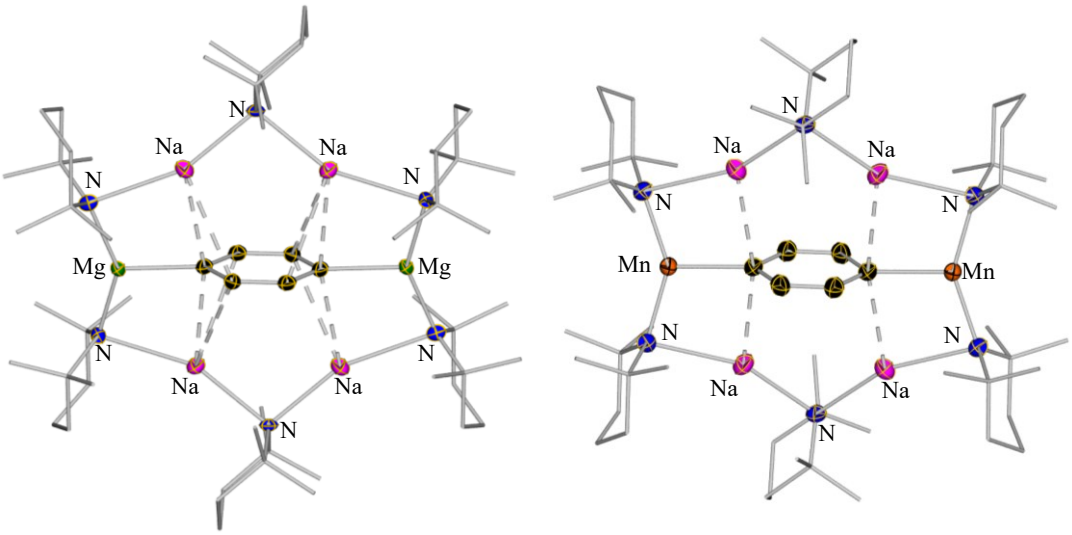

Figure 5. 7 *Crystal structure of a) [(TMP)$_6$Na$_4$(1,4-Mg$_2$C$_6$H$_4$)] and b) [(TMP)$_6$Na$_4$(1,4-Mn$_2$C$_6$H$_4$)]. Hydrogen atoms are omitted and carbon atom of TMP anions are shown as wireframe for clarity. The thermal ellipsoids are rendered with 50% probability. Symmetry operations used to generate symmetrical atoms in a) 1-x, 1-y, 1-z; in b) 2-x. 1-y, -z (TMP= 2,2,6,6-tetramethylpiperidide)*

In parallel to this works Knochel has developed [$(TMP)_2Mn{\cdot}2MgCl_2{\cdot}4LiCl$] for arene metalation. The relevant intermediates underwent oxidative homocoupling when using an external oxidant (chloranil), or heterocoupling when using electrophiles with the aid of another transition metal such as palladium or copper (**Scheme 5. 3**).[33,34]

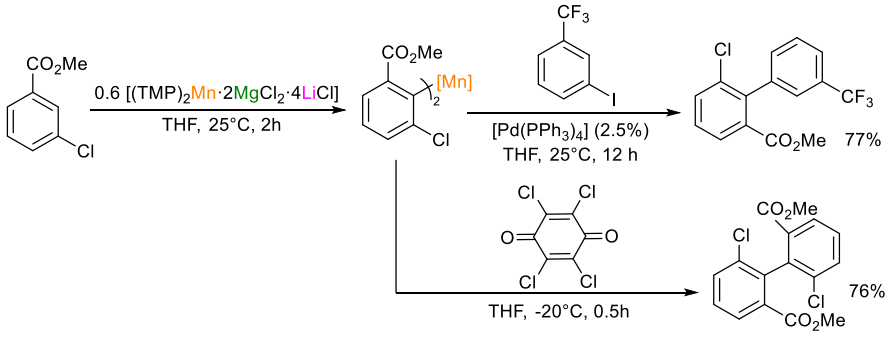

Scheme 5. 3 *Metalation of methyl-3-chlorobenzoate with [$(TMP)_2Mn{\cdot}2MgCl_2{\cdot}4LiCl$], followed by the cross-coupling catalysed by [$Pd(PPh_3)_4$] or by homocoupling in presence of chloranil as oxidant without the aid of any other transition metal. ([Mn]= $Mn{\cdot}2MgCl_2{\cdot}4LiCl$)*

Alkali-metal manganate have also been employed in Mn-Br exchange reactions with allylic substrates. Hosomi *et al.* that demonstrated how higher and lower order manganates (prepared in situ via salt-metathesis) exchanged the bromine of allylic and prop-2-ynyllic bromides generating the correspondent nucleophilic organomanganese species (**Scheme 5. 4**).[35]

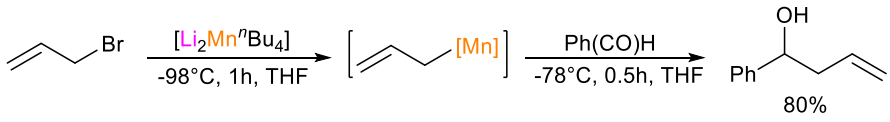

Scheme 5. 4 *Generation of allyl-manganate via metal-halogen exchange and subsequent trapping with benzaldehyde. [Mn]= [$Li_2Mn(^nBu)_3$]*

Trialkylmanganese compounds (deriving from alkyl-lithium or alkyl-Grignard and $MnCl_2$) were found active in manganese-bromine exchange towards geminal dibromo compounds, affording the product of the formal dehalogenation and alkyl-addition, Oshima and coworkers proposed a mechanism that involved first metal-halogen exchange, followed by the Br^- elimination and alkyl migration. Interestingly the same reaction was performed using a catalytic amount of $MnCl_2$ and alkyl-Grignard. Notably when $MnCl_2$ was not used and alkyl-Grignard were used alone with *gem*-dibromo-cyclopropane the product of dehalogenation was the only afforded (**Scheme 5. 5**).[36,37]

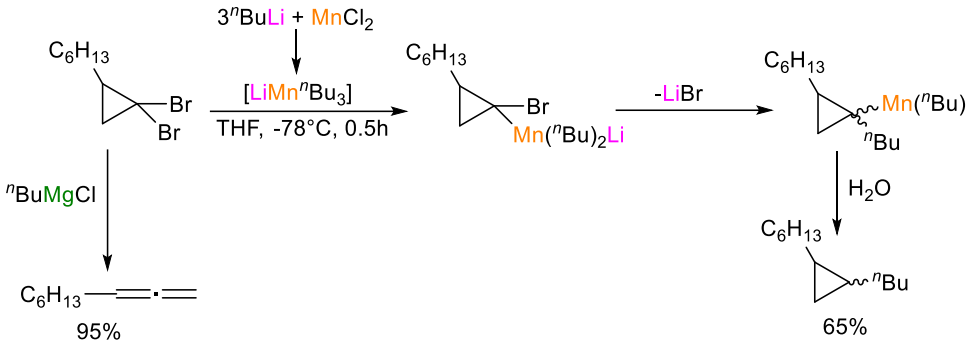

Scheme 5. 5 *Reaction of gem-dibromocyclopropanes with trialkylmanganate and with alkylmagnesium chloride*

Trialkylmanganates were also found efficient reagents in metal-halogen exchange reactions in aryliodides, [LiMnMe$_3$] was able to react with allyl-2-iodophenyl ether, exchanging the iodine quantitatively. Moreover using the *n*-Butyl group as alkyl group in the manganate with the same substrates (or N,N-diallyl-2-iodoanilines) led to the product of cyclization, to explain the phenomenon a radical mechanism was invoked (**Scheme 5. 6**).[37,38]

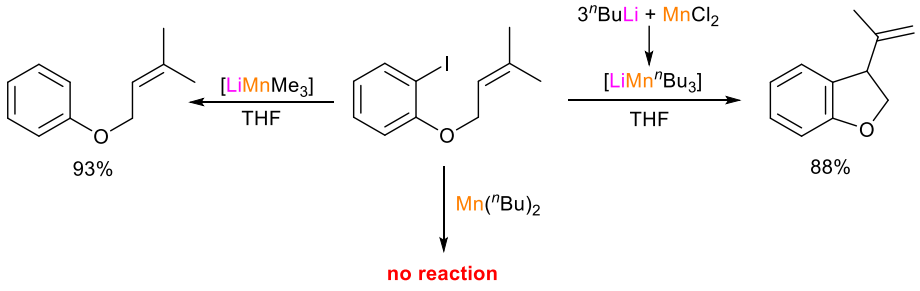

Scheme 5. 6 *Reactions of 2-iodophenyl prenyl ether with organomanganese species. On the left hand side, the product of metal-halogen exchange and on the right hand side, the product of cyclization*

5.2 Aims

Building on the precedents mentioned above, this chapter aim to uncover the constitution and reactivity of alkali-metal manganate of the constitution AM$_2$MnR$_4$ (AM= alkali-metal, R= CH$_2$SiMe$_3$). Applications of these heterobimetallic systems in Mn-I exchange and alkyne metalation have been investigated. Focusing on homocoupling of arenes and acetylides, this chapter also aims to shed light on the mechanism involved in these transformations.

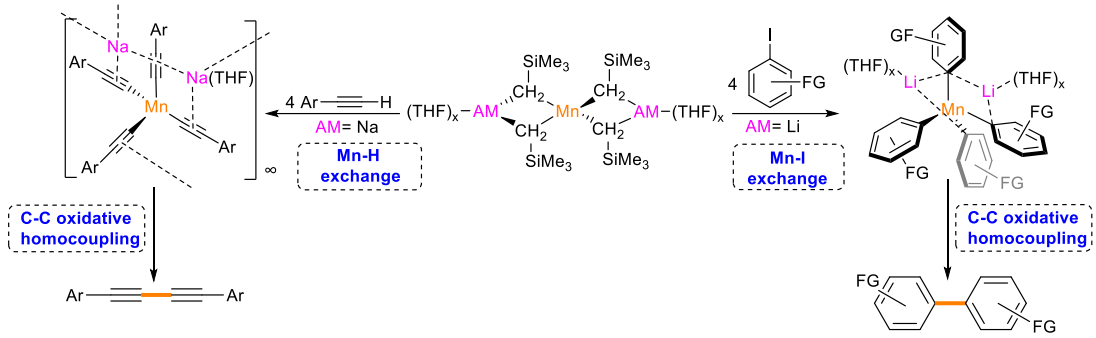

Scheme 5. 7 *Direct Manganation of unsaturated substrates via metal/halogen exchange or deprotonation using as metalating agent the higher order manganate [$AM_2Mn(CH_2SiMe_3)_4$] (AM= lithium or sodium)*

5.3 Introduction from the paper

Metal-halogen exchange constitutes one of the most powerful and widely used methods for regioselective functionalization of aromatic halides. Represented usually as an equilibrium, these kinetic processes are driven by the formation of the more stabilised aryl organometallic intermediates.[39] For decades this methodology has been essentially the exclusive domain of the classical highly polar organometallic reagents organolithium RLi or Grignard reagents RMgX. However more recent reports have shown that pairing a lower polarity metal M such as Zn, La, Sm or Ce with Li, can also promote low polarity metal-halogen exchange to access M-aryl intermediates that can in turn be employed in CC bond forming processes, usually with the aid of transition metal catalysis.[40–43] While Mn(II) organometallic compounds have shown considerable promise in organic synthesis, with seminal contributions from Cahiez and Normant on their applications in acylation, addition and other C-C bond forming processes,[15] their ability to promote Mn-halogen exchange with aromatic halides has not yet been established. This is somehow surprising considering the comparable electronegativities and sizes of Mg and Mn(II) as well as the reactivity patterns mentioned above for which these high spin Mn(II) reagents have been previously described as soft Grignard reagents.[44] Earlier work by Oshima[36–38] and Hosomi[35] has shown that lithium manganates can undergo metal-halogen exchange with allylbromides and other activated substrates such as gem-dibromocyclopropanes although the constitutions of the organometallic intermediates and the exchange reagent have remained concealed.

In parallel to these studies, early seminal work by Cahiez has shown that mixed salts such as $MnCl_2 \cdot 2LiCl$ can catalyse the homocoupling of aryl Grignard reagents using atmospheric oxygen,[16,44] providing a sustainable route to synthetically relevant symmetrical bis(aryl) molecules.[1–3] More recent work by Taillefer has also proposed that in situ generated ArLi species can undergo homocoupling in the presence of catalytic amounts of $MnCl_2$.[19] Supported by computational studies,[17,19] these reactions have been proposed to occur via formation of putative $MnAr_2$ intermediate species which in turn can undergo oxidative homocoupling in the presence of oxygen. However, limited tangible experimental evidence is

available on the actual formation of these compounds which are hypothesised to form by salt-metathesis in the presence of a large excess of the polar organometallic aryl reagent.

Merging these two fundamental types of transformations reactions, here we describe the first examples of direct Mn halogen exchange reactions of aryliodides based on aryl manganate species that in turn can undergo oxidative homocoupling to access synthetically valuable symmetrical bis(aryl) compounds in good yields. In addition, structural and spectroscopic studies on the organometallic intermediates involved in this tandem protocol uncover some of the hitherto unknown constitution of the intermediates involved in these reactions.

5.4 Results and Discussion

5.4.1 Assessing Mn-I Exchange of Iodoarenes

Considering that an important limitation to the stability of alkylmanganese compounds is their tendency to undergo β-hydride elimination,[45] we started our studies probing the reactivity of 4-iodoanisole (**36**) with MnR_2 (R= CH_2SiMe_3).[46,47] Containing bulky monosilyl substituents with no protons in the β-position, this bis(alkyl) Mn(II) species has previously been used as a precursor to access sodium and potassium alkali-metal manganates and has shown remarkable thermal stability.[48] Our reactions were initially carried out at -78 °C in THF (**Table 5. 1**), to trap and characterize anisole, the product of Mn-I exchange. In those cases, where reactions were allowed to stir at room temperature the homocoupling product (4,4'-dimethoxy-1,1'-biphenyl, **38a**) was formed and only small amounts of anisole were present.

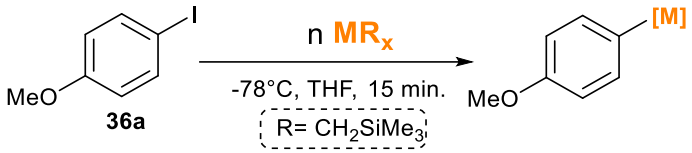

entry	n	MRx	Yield[a]
1	1	MnR_2	0%[b]
2	1	LiR	62(71)[c]%
3	1	$LiMnR_3$	56%[d]
4	1	Li_2MnR_4 (**37**)	95%
5	0.25	Li_2MnR_4 (**37**)	86%
6	0.33	Li_2MnR_4 (**37**)	94%
7	0.33	Li_2MgR_4	82%
8	0.33	4 MgRCl + $MnCl_2$	0[d] (18)[e]%
9	0.33	4 MgRCl + $MnCl_2$·LiCl	0[d] (83)[e]%
10	0.33	Li_2MnR_4 (**37**) + 2 TMEDA	93%
11	0.33	Li_2MnR_4 (**37**) + 4 12-crown-4	0%

Table 5. 1 *Optimization of the reaction conditions for the Mn-I exchange using manganese reagent containing CH_2SiMe_3 ligands [a] Yields have been determined by GC analysis of reaction aliquots after an aqueous quench using hexamethylbenzene as internal standard. Formation only of anisole and unreacted **36a** were observed. [b] 20°C. [c] -20°C. [d] reaction allowed to stir at room temperature for 5h, while only homocoupled product **38a** was detected along with starting material **36***

Under these conditions homometallic MnR_2 failed to promote Mn-I exchange of **36a** even when the temperature was increased to 20 °C (entry 1). Building on previous work in s-block organometallic chemistry which has shown that ate activation can enable effective Mg- and Zn-halogen exchange reactions,[49] we next reacted equimolar amounts of **36a** with triorganomanganate $LiMnR_3$ (prepared in situ by reaction of 3 equivalents of LiR and $MnCl_2$) leading to a 53% conversion after 15 min at -20 °C (entry 3). This conversion could then be enhanced almost quantitatively when using in-situ prepared lithium-rich manganate Li_2MnR_4 (**37**) (95%, entry 4) even at -78 °C. Furthermore, the exchange also works using substoichiometric amounts of **37** showing conversions of 86 and 94% when 0.25 and 0.33 equivalents of **37** were employed respectively, supporting the view that the four alkyl groups present in **37** engage in the exchange, making the process atom economical (entries 5 and 6). It is significant that under the conditions studied these conversions were higher than using LiR on its own (entry 2) or using the magnesium analogue of **37**, Li_2MgR_4 (entry 7) revealing that under these reaction conditions Mn-I exchange occurs more efficiently than Li-I or Mg-I exchange.

Since **37** is prepared *in-situ* by salt metathesis with $MnCl_2$, we next pondered if this approach could also work using 4 equivalents of the Grignard reagent RMgCl as a precursor. Surprisingly, no exchange was observed at lower temperatures (from -78 to -20 °C) while allowing the reaction mixture to stir at room temperature for 5 h showed a modest 18% conversion (entry 8). The latter can then be boosted to 83% when adding 2 equivalents of LiCl, hinting at a crucial role for Li to facilitate this transformation (entry 9). Further evidence was

found when assessing the influence of Lewis donors as additives when combined with **36**. While bidentate TMEDA showed no observable effect, 12-crown-4 which has the ability to coordinate and sequester the lithium cations, completely shuts down the exchange process, suggesting that the cooperation and/or close proximity between Li and Mn may also be a key factor (entries 10 and 11). Allowing the reaction of **36a** with 0.33 equivalents of **37** to reach room temperature and to stir for a further 5h formed bis(aryl) **38a** in an 87% isolated yield, indicating that as the temperature is raised, in addition to the Mn- I exchange taking place, a C-C bond forming homocoupling process occurs (**Scheme 5. 8**). This approach can be also extended to a range of substituted aromatic iodides, bearing electrondonating or electron-withdrawing groups, affording the relevant symmetric bis(aryls) **38a-38o** in good to excellent yields (33-87% yields, **Scheme 5. 8**). Steric effects seem to play a detrimental role as indicated by the contrasting yields obtained when using different iodotoluene substrates. Thus, **38c** with the methyl group located at the C4 position is furnished in a 74% yield, whereas a modest 33% is obtained for **38m** when starting with 2-iodotoluene. The same trend is observed for the homocoupled anisole derivatives **38a**, **38j**, and **38l** (87, 68, and 60% yield respectively); whereas no reaction is observed at all when 2-iodomesitylene was employed. This method is also compatible with electron withdrawing groups such as CF_3 or F furnishing bis(aryls) **38e**, **38f** and **38i** in 73, 68, and 69% yields respectively, although in the case of **38g** containing a CO_2Et substituent a significantly lower yield was observed (30%). Interestingly, **37** also reacts with 3-iodopyridine affording homocoupled product **38o** (63%), along with 3-monosilylpyridine **38o'**. The latter is a minor product (20%) resulting from the coupling between the $C(sp^2)$ of the substrate and the $C(sp^3)$ center of a CH_2SiMe_3 group.

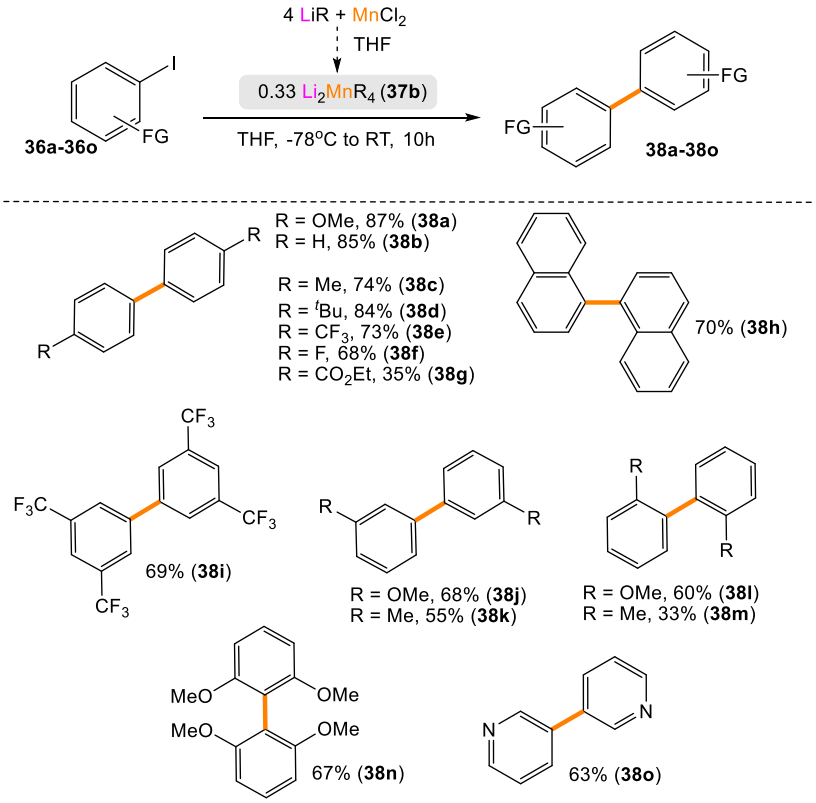

Scheme 5. 8 *Reaction of various iodoarenes with Li_2MnR_4 (**37**) prepared in situ by addition of LiR to $MnCl_2$ in 4:1 ratio in THF (R = CH_2SiMe_3). Yields of isolated products are given for **38a-38o***

Prompted by these intriguing observations we next set out to identify the constitution of bimetallic intermediates formed in these mixtures. Lithium manganate **37·2TMEDA** could be isolated as a crystalline solid in two different ways: co-complexation of 2 equivalents of LiR and TMEDA with MnR_2 in hexane or by salt metathesis using a 4:1 mixture of LiR and $MnCl_2$ in THF in the presence of 2 equivalents of TMEDA (**Figure 5. 8 a**)[50]. It should be noted that while the synthesis and EPR characterisation of **37** has been reported by Wilkinson in a seminal paper from 1976,[46] its structure in the solid state has remained concealed.

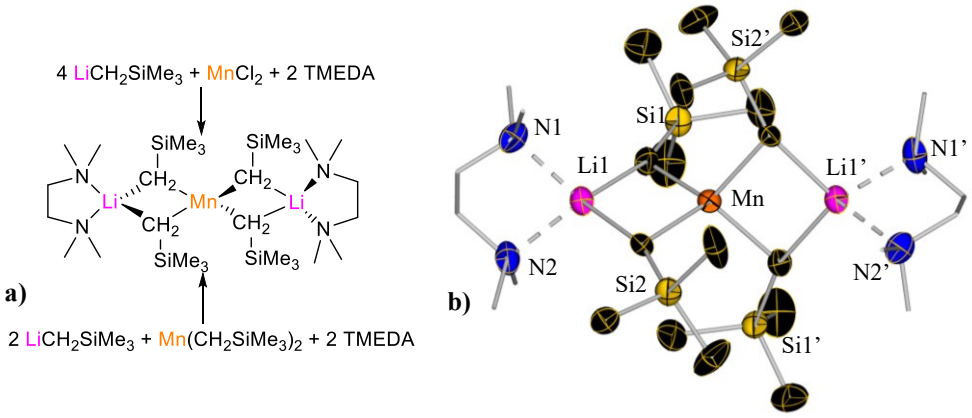

Figure 5. 8 *a) Synthesis of **37·2TMEDA** via salt metathesis of $MnCl_2$ and $LiCH_2SiMe_3$ or for co-complexation of $Mn(CH_2SiMe_3)_2$ and $LiCH_2SiMe_3$ b) Crystal structure of **37·2TMEDA**. Hydrogen atoms are omitted and carbon atoms of TMEDA ligand are shown as wireframe for clarity. The thermal ellipsoids are rendered with 50% probability. Symmetry operations used to generate symmetrical atoms x-, y+1, -z+2 (TMEDA = N,N,N',N'-tetramethylethylenediamine)*

Single crystal X-ray diffraction studies confirmed the bimetallic constitution of **37·2TMEDA**, exhibiting the same classical "Weiss motif" previously reported for its Mg analogue $[(TMEDA)_2Li_2MgR_4]$.[51] It comprises a C4-coordinated Mn atom flanked by two TMEDA-solvated Li cations, displaying a nearly linear Li···Mn···Li arrangement [176.082(2)°]. Each alkyl group in the structure bridges Mn with a Li centre with an average Mn-C distance of 2.275 Å (**Figure 5. 8 b**). These structural features are typical of high-spin Mn(II) centre and this magnetic state was confirmed by SQUID magnetometry and EPR spectroscopy.[50] **37·2TMEDA** is also isostructural with a series of lithium manganates reported by Girolami[25,52] containing Me, Et or $CH_2CH_2{}^tBu$ alkyl groups although as far as we can ascertain the reactivity of these compounds has barely been studied. Contrastingly, showing the complexity of some metathetical approaches, when 4 equivalents of RMgCl are reacted with $MnCl_2$ in THF, heteroleptic mixed-metal $[(THF)_4MgCl_2MnR_2]$ (**39**) was obtained as a crystalline solid along with variable amounts of the adduct $[(THF)_2MgCl_2]$ (**Figure 5. 9 a**). Established by single crystals X-ray diffraction, the molecular structure of **39**[50] (**Figure 5. 9 b**) displays Mn and Mg connected by two Cl bridges with Mn completing its distorted tetrahedral geometry with two terminal monosilyl groups; whereas Mg is solvated by four molecules of THF giving rise to a distorted octahedral environment. Thus, compound **39** can be envisaged as a co-complex between $MgCl_2$ and MnR_2.[53,54]

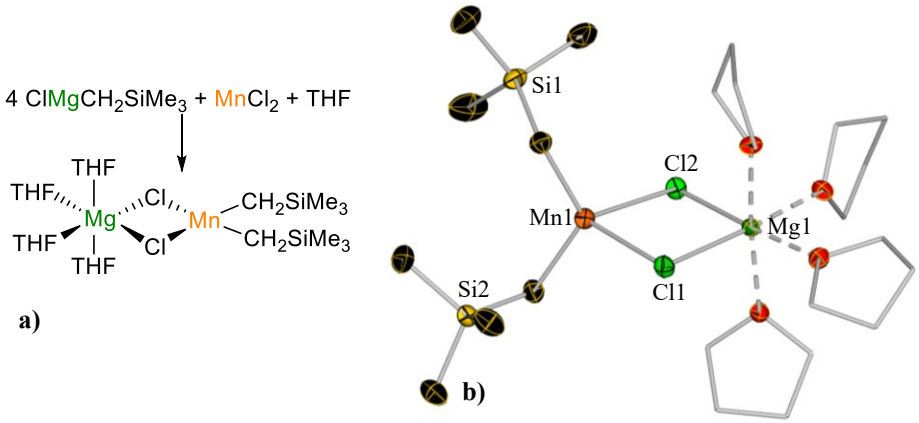

Figure 5. 9 *a) Synthesis of **39** via salt metathesis of $MnCl_2$ and $ClMgCH_2SiMe_3$ b) Crystal structure of **34**. Hydrogen atoms are omitted and carbon atoms of THF are shown as wireframe for clarity. The thermal ellipsoids are rendered with 50% probability. The unit cell of **38** contains two crystallographically independent molecules with identical connectivity, only one is shown here*

The contrasting constitutions of **37·2TMEDA** and **39** when both are prepared by reacting 4 equivalents of either RLi or RMgCl with $MnCl_2$ can help explain their different reactivity towards Mn-I exchange (**Table 5. 1**, entries 8 and 10), since **37·2TMEDA** in having a Mn centre attached to four alkyl groups can be expected to be significantly more reactive than **39** which possesses two such anions. Consistent with this, previous work in s-block bimetallic chemistry has shown the excellent ability of lithium tri- and tetraalkyl magnesiates and zincates to promote direct metal-halogen exchange.[49]

5.4.2 Manganate-Mediated Aryl-Aryl Oxidative Homocouplings

Germane to the formation of bis(aryls) **38a-38o**, work on Mn(II)-catalysed homocoupling of ArM (M= Li, MgX) has shown that atmospheric oxygen is required in order to facilitate the Csp^2-Csp^2 bond forming process.[16,17,19] Since our experiments were carried out under strict inert atmosphere conditions, it should then be the alkyl iodide Me_3SiCH_2I, concomitantly generated during the Mn-I exchange process, acts as an oxidant of putative in situ generated lithium aryl manganates Li_2MnAr_4 (**I**), facilitating the homocoupling process (**Scheme 5. 9**). Previous work by Zhou has also shown that $MnCl_2$ can catalyse homocoupling of Grignard reagents using dichloroethane (DCE) as an external oxidant.[55] Interestingly in our case, the C-C bond forming step seems to occur very quickly as soon as the temperature raises from -78 °C to RT, thus all attempts to trap and characterize intermediates **I** led to the isolation of the relevant homocoupling product as well as to variable amounts of LiI which in the presence of TMEDA crystallises as $[\{(TMEDA)LiI\}_2]$.

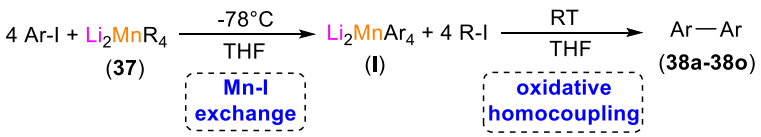

Scheme 5. 9 *Proposed ate-mediated reaction sequence for the formation of symmetrical bis(aryls) **37a-37o** from iodoarenes. (R = CH_2SiMe_3)*

Aiming to advance the understanding of the homocoupling process we next attempted to prepare Li_2MnAr_4 (**I**) via an indirect route using a salt-metathesis approach in order to probe its reactivity towards ICH_2SiMe_3. Reacting 4 equivalents of aryl lithium Li(2-OMe-C_6H_4) with $MnCl_2$ in diethyl ether produced pale orange crystals of [Li_2Mn(2-OMe-C_6H_4)$_4$(OEt_2)] (**39**) (**Scheme 5. 10**).[29–31]

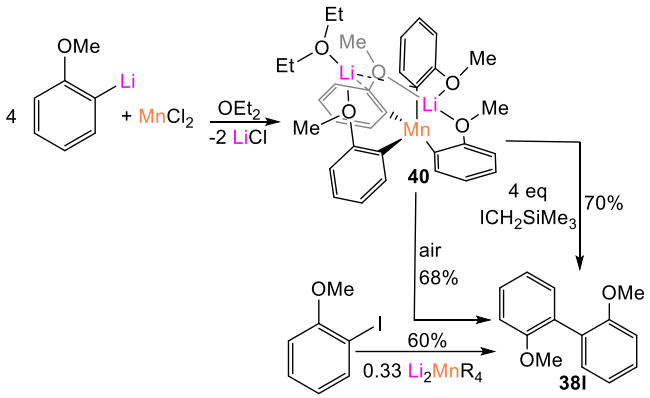

Scheme 5. 10 *Indirect synthesis of **40** via salt-metathesis and formation of **38l***

Exhibiting a contacted ion pair manganate structure in which distorted tetrahedral Mn is bonded to four ortho-metalated molecules of anisole by short (strong) bonds [average Mn-C distance: 2.111 Å]. Each lithium has a different coordination environment. Li1 binds to the O donors of three OMe substituents from the aryl fragments, whereas Li2 coordinates to the remaining OMe group as well as to the ortho-C's of two other aryls, adopting a perpendicular disposition with respect to the aromatic rings. The distinct bonding modes of the Li atoms must contribute towards the marked nonlinearity of the Li···Mn···Li vector [91.09(15)°] which contrasts with the nearly linear arrangement found in **37b·2TMEDA** (Li···Mn···Li, 176.082(2)°, **Figure 5. 10**) and other related lithium manganates.[25,52]

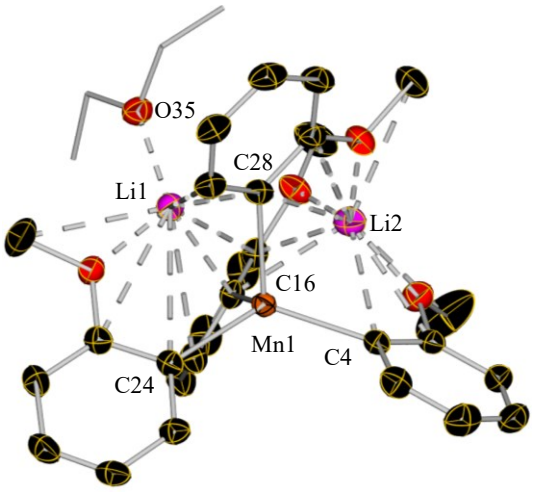

Figure 5. 10 *Crystal structure of **40** with thermal ellipsoids drawn at 50% probability. All the hydrogen atoms are omitted and carbon atoms of diethyl ether are drawn as wireframe for clarity Selected distances (Å) and angles (°) Mn1-C24 2.1543(18), Mn1-C4 2.172(2), Mn1-C28 2.2279(18), Mn1-C16 2.2973(19), Li1-C_{aryl} ranging from 2.361(4) to 3.290(3), Li1-O35 1.949(3), Li1-O18 1.997(3), Li2-O_{metoxy} ranging from 1.901(4)-1.917(4), Li2-C_{aryl} ranging from 2.595(4)-2.907(4), Li2-C_{metoxy} 2.952(4)-3.019(4), C24-Mn1-C16 100.45(6), C24-Mn1-C28 106.69(7), C24-Mn1-C4 125.24(7), C16-Mn1-C28 106.77(6), C16-Mn1-C4 108.07(7), C28-Mn1-C4 108.22(7), Li1-Mn1-Li2 91.09(15)*

Interestingly, while **40** is stable at room temperature in solution under inert atmosphere conditions, it rapidly proceeds to form bis(aryl) **38l** when reacted with ICH_2SiMe_3 or by being exposed to air. The yields observed for **38l** (70 and 68% respectively) are comparable with those seen when **37** is reacted with 2-iodoanisole (**Scheme 5. 8**). Furthermore, the EPR spectrum of **40** in THF at 80 K is identical to that observed for a mixture of **37** and 4 equivalents of 2-iodoanisole at 80 K (**Figure 5. 13 b**), offering further credence to the view that **40** is an intermediate in the homocoupling processes. Illustrating the crucial role of Mn in order to facilitate the Csp^2-Csp^2 bond forming process, the reaction of aryl lithium Li(2-OMe-C_6H_4) with ICH_2SiMe_3 failed to form **38l**, yielding instead the relevant 2-monosilyl-substituted anisole in a modest 14% resulting from electrophilic interception. In previous $MnCl_2$-catalysed homocoupling studies of ArLi and ArMgX under air, it has been proposed that reactions take place via a Mn(IV) bis(aryl)oxo complex where the O_2 is η2-bonded to Mn.[16,17,19] However, taking into account that the polar aryl reagent ArM (M= Li, MgX) is present in a large excess in comparison to the $MnCl_2$ catalyst (10-20 mol%), we ponder whether a more accurate scenario may involve lithium (or magnesium) manganate intermediates. In an attempt to further understand the fate of Mn during the homocoupling process when atmospheric oxygen is used as an oxidant, an in-situ prepared solution of **36** was exposed to dry air for 15 min at -78 °C using a drying tube charged with oven-dried $CaCl_2$. This led to the isolation of unusual bimetallic clusters $[(THF)Li_4Mn_2Ar_6(\mu_6\text{-}O)]$ (**41**) and $[(THF)_4Li_4Mn_2Ar_4Cl_2(\mu_4\text{-}O)_2]$ (**42**) (**Scheme 5. 11** and **Figure 5. 11**) containing reduced oxide anions which co-crystallised with variable amounts of homocoupling product bis(aryl) **37l**.

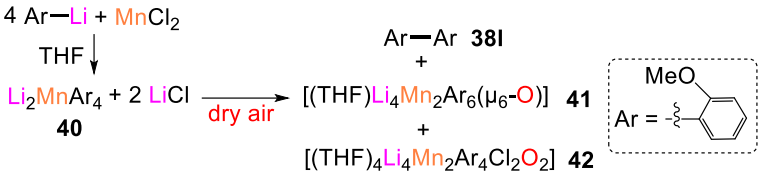

Scheme 5. 11 *Formation of the oxygen insertion products **41** and **42***

Though both **41** and **42** are dimers, Mn in **41** exhibits the +2 oxidation state, while in **42** the oxidation state is +3. In **41** μ_6-oxide is trapped in the core of a dicationic $\{Li_4Mn_2Ar_6\}^{2+}$ cage where the metals are connected by ambidentate 2-anisolyl anions that bind to Mn exclusively via their C atoms and to Li by a combination of Li-O and Li-C bonds (Figure 3, LHS). The central μ_6-oxide exhibits a distorted octahedral geometry with the two tetrahedrally coordinated Mn atoms occupying the axial positions [mean Mn-O, 2.072 Å; Mn-O-Mn, 175.7(2)°]; whereas the equatorial positions are filled by the four Li atoms [mean Li-O, 1.91 Å; sum of LiOLi angles, 360.2°].

In contrast, **42** incorporates LiCl in its constitution (present in the reaction media as co-product of the synthesis of the Li_2MnAr_4 precursor) (**Figure 5. 11 a**). It comprises two antiferromagnetically coupled Mn(III) centres connected/bridged by two oxo and two chloride anions. In addition, 4 anisolyl ligands coordinate through their ortho C and the O of the OMe group to Mn and Li, respectively. Each Li atom present in the structure completes its coordination sphere by bonding to a THF molecule. As far as we can ascertain **41** and **42** constitute the first structurally defined potential intermediates from Mn(II) mediated homocoupling processes in the presence of air. Providing the first insights into the possible fate of Mn during these transformations, their bimetallic constitutions along with the structure of **40** supports that, unlike previously proposed,[16,17,19] manganate intermediates generated by salt-metathesis may actually be more representative of the species active in literature catalytic studies combining ArM (M= Li, MgX) and substoichiometric amounts of $MnCl_2$.

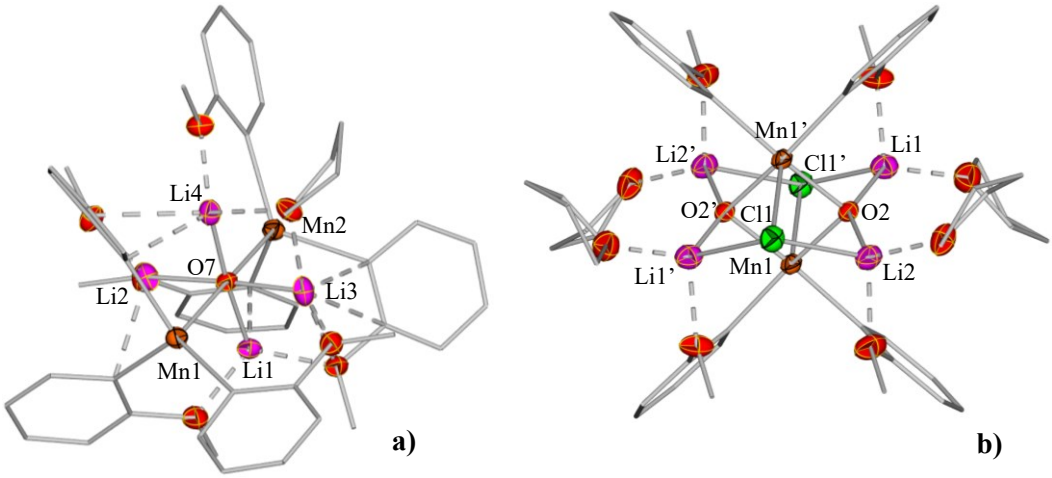

Figure 5. 11 *Crystal structure of a) **41** and b) **42**. Thermal ellipsoids are rendered at 50% probability. Hydrogen atoms are omitted, and all the carbon atoms are drawn as wireframe for clarity. Symmetry operations used to generate symmetrical atoms in b)-x, 2-y, 1-z*

Furthermore, even under stoichiometric conditions, when treating two equivalents of PhMgCl with $MnCl_2$ in THF the mixed-metal complex $[(THF)_4MgCl_2MnPh_2]$ was isolated in 51% yield (**Figure 5. 12**). Crystallographic characterisation of $[(THF)_4MgCl_2MnPh_2]$ revealed a structure almost identical to that of **39** (*vide supra*), when replacing the CH_2SiMe_3 alkyls by Ph groups, showing that co-complexation of $(THF)_4MgCl_2$ to MnR_2 reagents is likely to be a general phenomenon. $[(THF)_4MgCl_2MnPh_2]$ can be interpreted as a di-anionic manganate with a tetrahedral Mn(II) centre formally bonded to four anionic ligands (2Cl, 2Ph). Interestingly, exposure of mixed Mg/Mn complex $[(THF)_4MgCl_2MnPh_2]$ to air or reaction with two equivalents of RI led to the formation of biphenyl in 88 and 74% respectively (**Figure 5. 12**)

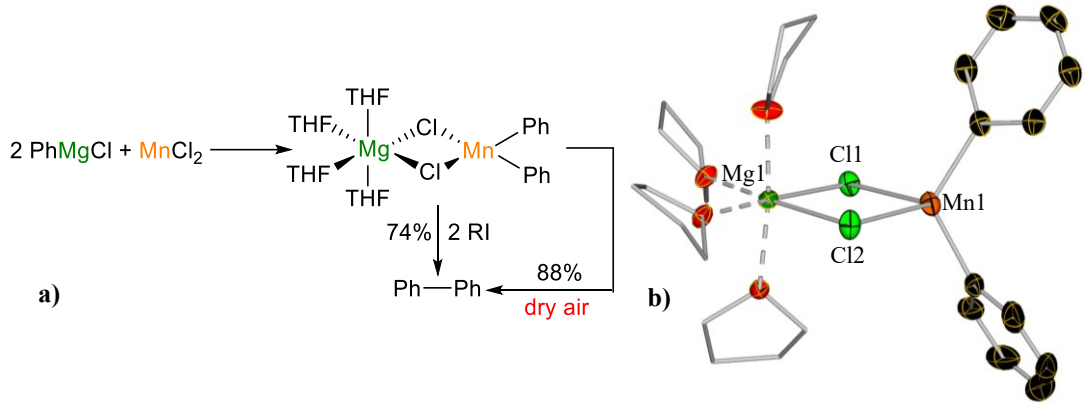

Figure 5. 12 *a) Salt metathesis reaction of $MnCl_2$ with two equivalents of PhMgCl to give $[(THF)_4MgCl_2MnPh_2]$ and homocoupling reaction to give biphenyl. b) Crystal structure of $[(THF)_4MgCl_2MnPh_2]$, thermal ellipsoids are rendered at 50% probability. Hydrogen atoms are omitted, and carbon atoms of THF are drawn as wireframe for clarity*

Regarding previously proposed mechanisms for the homocoupling of aryls using an alkylhalide as an external oxidant, Zhou's initial reports for DCE-driven (DCE= 1,2-dichloroethane) Mn-catalysed homocoupling of ArMgX tentatively proposed the involvement of $MnAr_2$ species undergoing reductive elimination to furnish the relevant bis(aryl) and a Mn(0) reactive intermediate that can react in turn with DCE to regenerate $MnCl_2$.[55] However, more recently Valyaev and Lugan have suggested an alternative mechanism via a Mn(II)/Mn(IV) redox manifold, with the initial formation of a tris(aryl) magnesium manganate. The latter can react with DCE to form an unstable Mn(IV) intermediate which subsequently could undergo reductive elimination to give the homocoupling product and $MnAr_2$ that via co-complexation with the excess of ArMgCl can regenerate the reactive manganate species.[15] A similar mechanism could be envisaged for our stoichiometric studies with the initial formation of $[Li_2MnAr_4]$ (**I**) followed by a sequence of oxidative addition/reductive elimination steps (**Scheme 5. 12**) involving Mn(II)/Mn(IV) species with concomitant elimination of LiI, along with $Me_3SiCH_2CH_2SiMe_3$ (whose formation could be detected by GC-MS spectrometry).

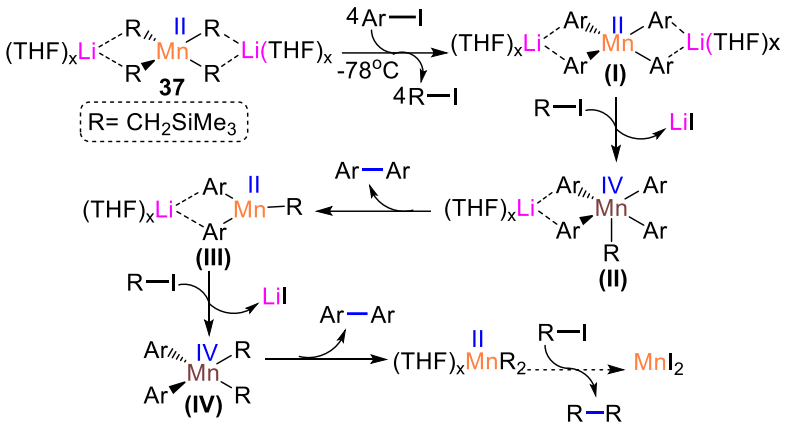

Scheme 5. 12 *Proposed mechanism for oxidative homocoupling of Li_2MnAr_4 (**I**) driven by ICH_2SiMe_3 which is generated by Mn-I exchange of ArI with **37***

This proposal could also explain the formation of 3-monosilylpyridine **38o'** as a side product when **37** is reacted with 3-iodopyridine, resulting from heterocoupling of the pyridyl fragment with a monosilyl group. Interestingly if **37** is reacted with 2-iodobenzothiazole, only the relevant heterocoupling product is obtained in a 64% yield (**Scheme 5. 13 i** and **ii**). While SET-dehalogenation reactions induced by magnesium manganates have been reported in the literature,[15,56] this scenario seems to be unlikely here, as suggested by carrying the reaction of **36** with **37** in the presence of radical scavengers such as TEMPO or galvinoxyl which allowed the isolation of bis(aryl) **38a** in yields comparable to those reported in **Table 5. 1** (**Scheme 5. 13 iii**).

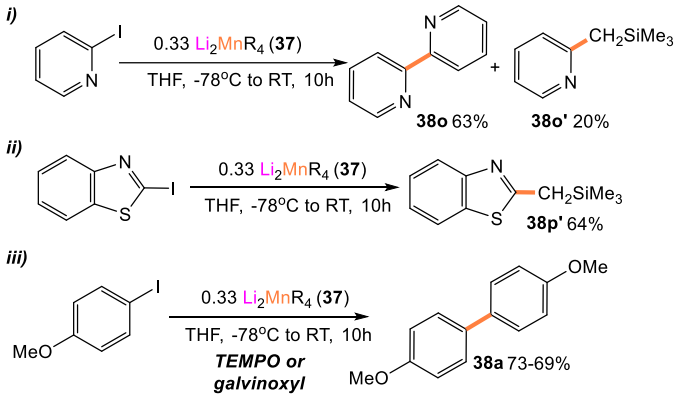

Scheme 5. 13 *Reactive studies of **37** with **i)** 3-iodopyridine and **ii)** 2-iodobenzothiazole. **iii)** Homocoupling of 4-iodoanisole in the presence of TEMPO or galvinoxyl.*

Finally, in order to gain further understanding on this tandem Mn-I exchange/C-C coupling process we monitored the reaction of **37** and 2-iodoanisole by X-band cw EPR at 80 K. Initial spectra of **37** in a frozen THF solution confirm the presence of an axially anisotropic high-spin S=5/2 Mn(II) species (D=0.20 cm−1, E=0 cm−1), as seen previously for related tetra-alkyl Mn(II) compounds reported by Girolami and Wilkinson (**Figure 5. 13 a**).[46,52]

In situ addition of 2-iodoanisole to **37** at low temperature produces the more rhombic Mn(II) species which can be identified confidently as compound **40** by comparison of its EPR spectrum with that of a frozen solution of isolated crystals of **40** in THF (D=0.18 cm−1, E=0.042 cm−1, **Figure 5. 13 b**). Thus, the Mn(II) oxidation state is maintained during the Mn-I exchange of all four alkyl groups. By allowing the in situ generated solution of **40** to warm up at room temperature new drastic modifications of EPR spectrum are detectable (**Figure 5. 13 c**). This includes a significantly decrease in intensity and the generation of a complex pattern which can be attributed to the mixture of an anisotropic mononuclear RMnI (D=0.47 cm−1, E=0.16 cm−1) and a MnIx species and/or to heteroleptic Mn(II) iodide and alkyl oligomers. In the latter case, dominant antiferromagnetic interactions populate the S=0 ground state at low temperatures which causes the decrease of intensity.[47,57,58] It should also be noted that the same changes in the EPR spectra are observed if 4 molar equivalents of RI are added at room temperature to a solution of isolated crystals of **40**.

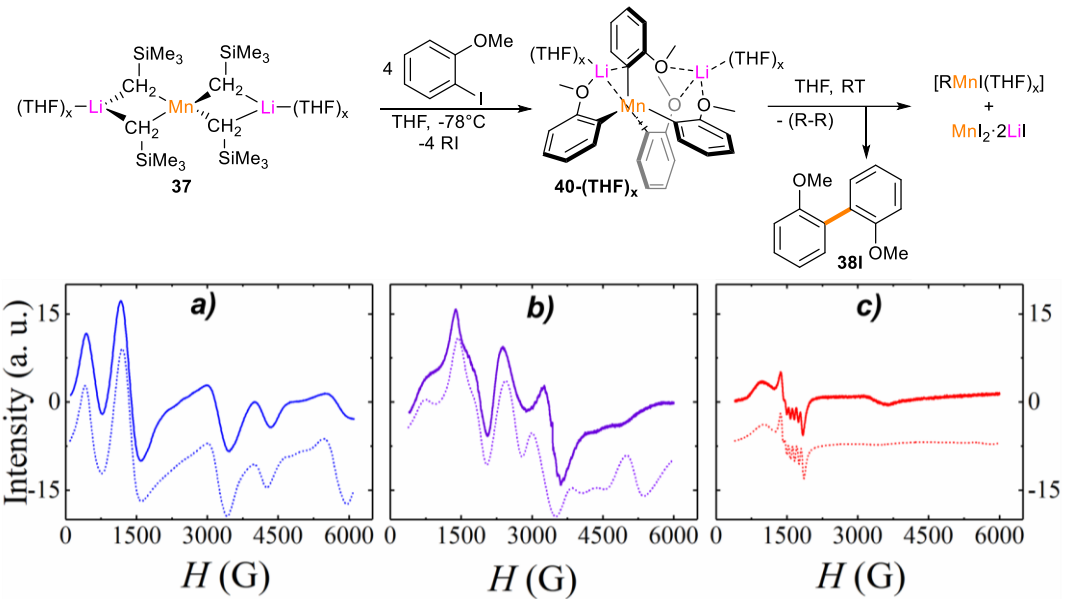

Figure 5. 13 *EPR monitoring (X-band, f= 9.412 GHz) of the reaction of **37** with four equivalents of 2-iodoanisole acquired in frozen THF solution at 80 K (full line in the EPR spectra represents experimental data while simulated spectra are shown using dashed line).*

These findings were additionally corroborated by studying the reaction of **37** and **37·2TMEDA** with 3-iodopyridine. Here, the initial addition of substate at low temperature generates one broad isotropic resonance (D=0.03 cm−1, E=0 cm−1) centered at g=2.00 attributed to the formed $Li_2Mn^{II}Ar_4$ (**I**) species formed of nearly Td symmetry which precludes any possibility of SET-induced radical intermediates. Allowing the reaction mixture to reach room temperature induces the homocoupling process causing significant reduction of intensity of the EPR signals, giving rise to a poorly resolved rhombic spectrum originating from the previously identified alkyl and iodo Mn(II) compounds as final products. Further support to this interpretation and to the proposed mechanism was found when analyzing the mixture in the end reaction products using mass spectrometry (MALDI-TOF negative mode), which

unveiled the presence of several LiI and Mn(II) iodide species with $\{MnI_3\}^-$ being predominant. The absence of any formed alkyl Mn(II) oligomers among the products is likely due to fragmentation and their sensitivity to air and moisture, as reported previously by Godfrey and McAuliffe. They indeed isolated $[HNMe_3][MnI_3(NMe_3)]$ from its parent diiodo compound for which a dimeric structure is established in THF with a series of amines.[59] In addition, detection of Mn(III) species in the positive mode of MALDI-TOF hints the possibility of partial oxidation of the resulting Mn(II) products to their Mn(III) analogues at the expense of the reduction of the remaining RI species to the coupled R-R product, as detected by GC-MS.

5.4.3 C(sp)-C(sp) homocoupling reactions mediated by $[AM_2MnR_4]$ reagents (AM= Li, Na, K)

Building on the reactivity of **37**, we next ponder if higher order AM_2MnR_4 (AM= Li, Na, K) manganate could also promote deprotonative metalation reactions. In this regards $KMn(CH_2SiMe_3)_3$, has already shown to be able to deprotonate dioxane at its α-positions followed by ring opening reaction (see section **3.1** of this thesis).[48]

We focused our attention on alkyne substrates due to the enhanced activity of their C-H group. We speculated that if successful, these compounds could grant access to 1,3-diynes,[6,7] via Glaser homocoupling.[9,60] The Glaser coupling reaction was known from 1869. In its classical formulation, involved the coupling of two terminal alkynes using copper (I) salt, oxygen as oxidant and ammonium hydroxide in ethanol; affording the correspondant1,3-diyne.[9]

The Glaser coupling reaction was evolved trough the time. In particular copper (II) salts was used as well[61] with Cu (II) being able to mediate these transformations under stochiometric and catalytic regimes[10] and with the realization that basic reaction conditions accelerate the reaction.[62–66] For the homocoupling step different oxidant can be used apart from oxygen.[62,67]

While the precise mechanism of the reaction has not been fully elucidated yet, different proposals have been reported with the aid of DFT calculations.[60,68–70] Thus it is proposed that initially the coordination of the copper to the triple bond takes place to enhance the acidity of the terminal proton, shifting of the copper oxidation state from I to III passing through II. [68,70]

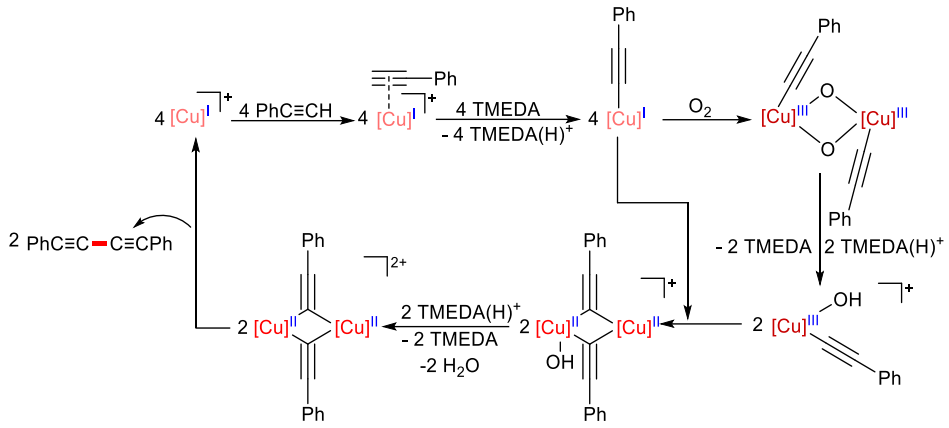

Figure 5. 14 *Simplified mechanism for Hay-Glaser homocoupling of phenylacetylene proposed by Maseras et al.*[68] *([Cu]= TMEDA·Cu*$^{+}$*, TMEDA= N,N,N',N'-tetramethylethylenediamine)*

The Glaser coupling is not limited to the acetylene substrates, in fact wisely choosing the base it is possible to abstract the protons also from activated aryls and, in presence of copper to obtain the correspondent organocopper intermediate, which in presence of oxygen undergoes to homocoupling.[71] The same methodology can be also extended to other first row transition metals such as nickel, cobalt, manganese and iron accessing to a wide range of di-arenes (**Scheme 5. 14**).[72] In this contents could be inserted the work of Taillefer who introduce ^{t}BuLi as base for the deprotonation of terminal alkynes and activated aryles, followed by manganese-catalysed oxidative homocoupling, using dry air as oxidant. [19]

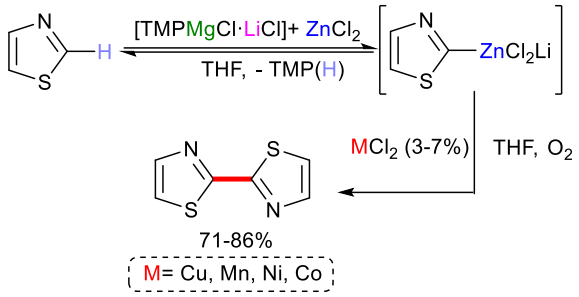

Scheme 5. 14 *Aromatic Glaser reaction using different metals as catalyst*

Considering the metalating of alkali-metal manganates, we envisaged first the deprotonation of alkyne followed by aerobic oxidation to promote the homocoupling reaction. The addition of the alkyne was made at -78°C, subsequentially the reaction was moved at room temperature, before the exposure to dry air. Notably no external base was added and the metalation was carried only by the oranomanganese species selected. Commercially available phenylacetylene was used as substrate to benchmark the reaction.

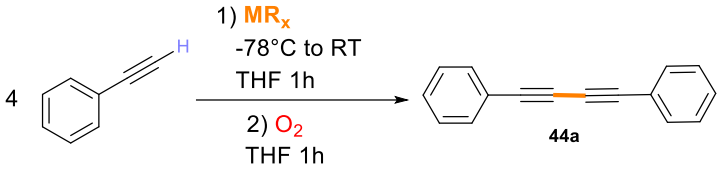

entry	MR_x	Yield[a] (%)
1	$Mn(CH_2SiMe_3)_2$	16 [b]
2	$Mn(CH_2SiMe_3)_2$+LiCl	20[b]
3	$Li_2Mn(CH_2SiMe_3)_4$	88
4	$Na_2Mn(CH_2SiMe_3)_4$ (**43**)	97
5	$K_2Mn(CH_2SiMe_3)_4$	74
6	$NaMn(CH_2SiMe_3)_3$	63[c]
7	$NaCH_2SiMe_3$ +$MnCl_2$ (6%)	17%
8	$Na_2Mg(CH_2SiMe_3)_4$	0%

Table 5. 2 *Optimization of the reactions of metallation following by homocoupling of phenylacetylene [a] The yield was determined by ^{1}H-NMR against hexamethylbenzene as internal standard [b] 2 equivalents of phenylacetylene were used*

Using the condition mentioned above the neutral species $Mn(CH_2SiMe_3)_2$[47] (entry 1) achieved yield of homocoupling of 16%. Since in literature is well known the ability of manganese to catalyse the facile homocoupling of unsaturated hydrocarbons in presence of oxygen (or an oxidant)[16,19,44,73] we argued on the possibility that the low yield of the final product was due to the low yield of metalation. Consistently with this interpretation we found that using LiC≡CPh with 0.5 eq. of $MnCl_2$ to yield in-situ $Mn(C{\equiv}CPh)_2$, lead to the efficient homocoupling to give **44a** in a 80% yield.

In order to prove this point we decide to enhance the reactivity of the neutral species with the complexation with an alkali metal.[20–22,26,74,75] A first attempt with addition of 1 equivalent of LiCl did not provide any benefit (the yield was 20%, entry 2). We then tested the higher order lithium manganate **37** (prepared *in-situ* mixing MnR_2 and the correspondent organolithium). With our delight the yield of homocoupling product was substantially improved (entry 3), achieving an 88% of NMR yield. Taking in account the enhancement of the metallation ability using a larger alkali-metal[76] we decided to evaluate the alkali-metal effect in this reaction. The use of $Na_2Mn(CH_2SiMe_3)_4$ (**43**)[50] (entry 4) improve the outcome of the reaction raising the yield of homocoupling product to 97%. An apparent inversion of the trend could be observed when the higher order potassium analogue[50] was used, dropping the yield to 74% (entry 5). However, in this case, the product of metalation of phenylacetylene was very insoluble even in bulk THF. The solubility of the species involved seems to be a key factor, in fact when the insoluble sodium phenylacetylide (prepared *in-situ* reacting $NaCH_2SiMe_3$ and phenylacetylene) was used to test the catalytic use of $MnCl_2$ for the homocoupling, poor yield was achieved (entry 7). On the other hand, the more soluble lithium phenylacetylide in similar conditions was quantitively converted into the product of homocoupling.[19]

The lower order manganate $NaMn(CH_2SiMe_3)_3$[48] had a yield of 63% (entry 6) indicating that only 2/3 of the substrate was led towards the homocoupling products.

The presence of manganese proved to be fundamental to achieve the homocoupling. This is based on the fact that the same could not be achieved when the potassium magnesiate analogue $Na_2Mg(CH_2SiMe_3)_4$ (entry 8), despite the fact that this organomagnesium is able to successfully metalate phenylacetylene affording the tetralkynil magnesiate $[Na_2Mg(C{\equiv}CPh)_4(THF)_n]$.[77]

This approach has been extended to different alkynes substrates (**Scheme 5. 15**)

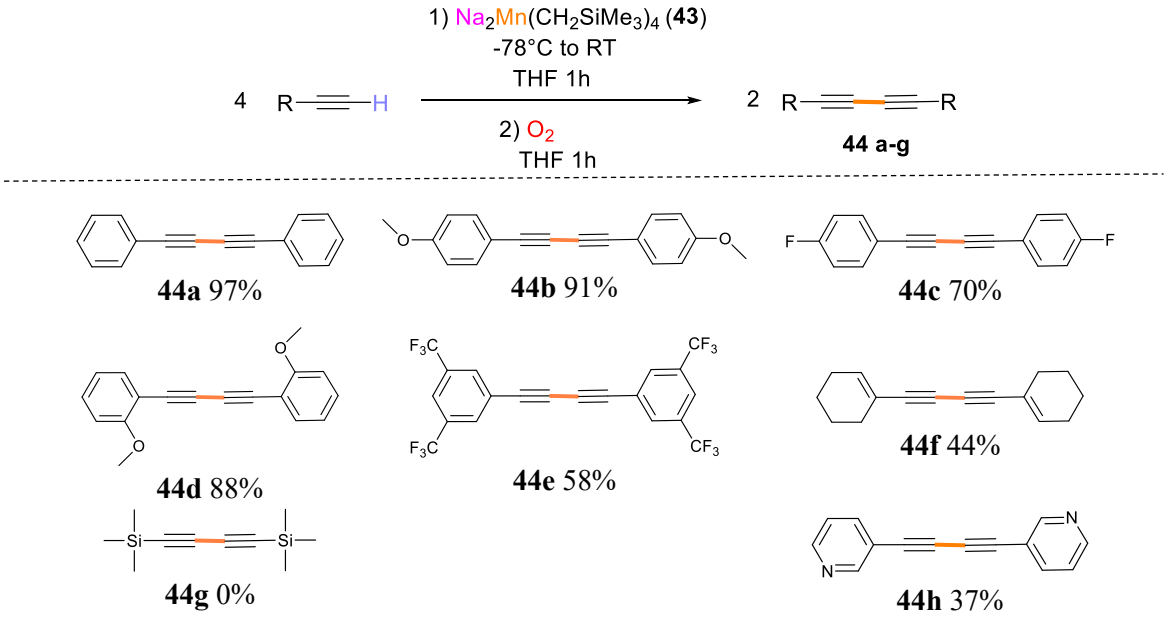

Scheme 5. 15 *Reaction of **43** with various alkynes, the yields have been determined by ^{1}H-NMR using hexamethylbenzene as internal standard*

The approaches is compatible with aromatic alkynes containing both electron withdrawing and electron donating groups (**44a-e** yields 97-58%), even if the electron withdrawing groups reducing the efficiency of homocoupling. Aliphatic alkynes such as 1-ethynylcyclohex-1-ene and ethynyltrimethylsilane lower the yields (**43f-g)** where ethynyltrimethylsilane even failed to undergo homocoupling. Pyridine substituted, 3-ethynylpyridine, gave **44g** in 37% yield.

In order to gain more insights into the ongoing mechanism and prove the atom economy of the metalation, we decided to prepare and isolate the intermediate product of metalation before the homocoupling step. Reacting 4 equivalents of phenylacetylene with **43,** formed *in-situ* mixing $NaCH_2SiMe_3$ and $Mn(CH_2SiMe_3)_2$, affording the tetraenyl-manganate $[(THF)_4Na_4Mn_2(C{\equiv}CPh)_8]$ (**45**) in 42% crystalline yield (**Scheme 5. 16**).

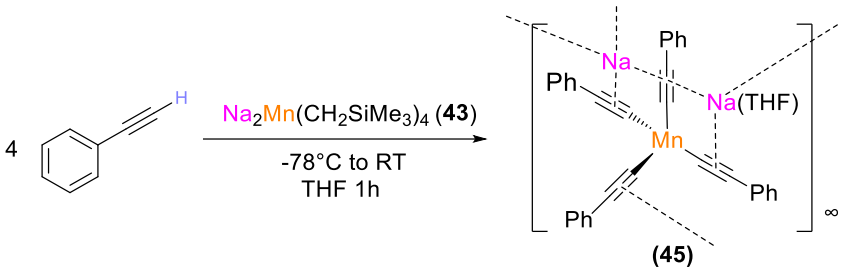

Scheme 5. 16 *Synthesis of **45** via deprotonation of phenylacetylene, the isolated yield of **45** is 44%*

The crystal structure of **45** shows the formation of a polymer by the interactions between sodium cations and the π-electrons of the triple bonds of adjacent manganese anions creating 1D chain structure, along the b crystallographic axis. Despite the presence of bulk donating solvent (THF), this motif does not disaggregate in smaller monomeric units.

Manganese displays tetracoordinated environment with a distorted tetrahedral geometry (C-Mn-C ranging from 102.07(5)° to 119.15(5)°) with a mean value of 109.45°.Manganese is coordinated by four carbons form the phenylacetylene anion and the Mn-C distances ranging from 2.1011(13) to 2.1573(13) Å. Those distances are elongated than the Mn-C distances found in the neutral diphenilacetylide manganese species, that ranged between 1.953(11) and 1.970(11) Å.[78]

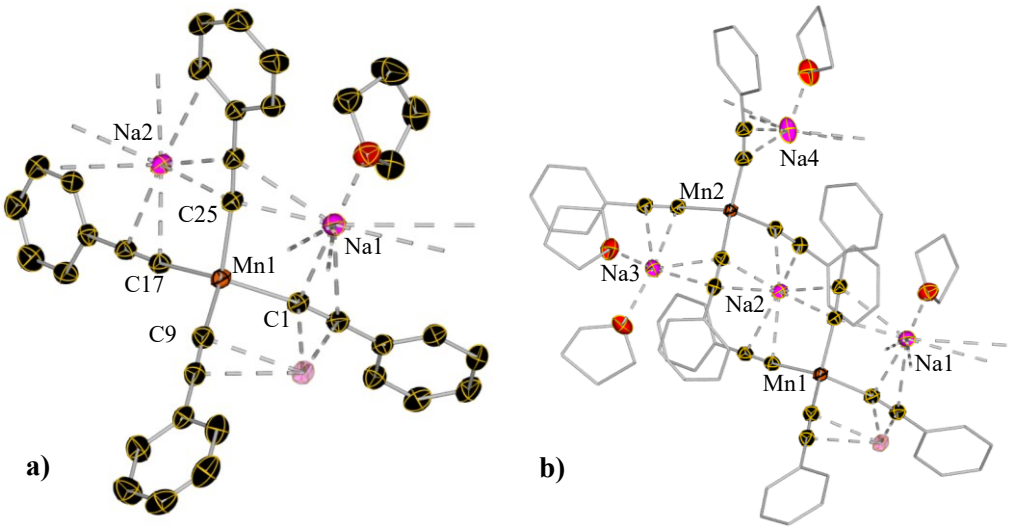

Figure 5. 15 ***a)*** *molecular fragment and* ***b)*** *polymeric crystal structure of **45**, thermal ellipsoids are rendered at 50% probability. Hydrogen atoms and disorder elements in THF are omitted for clarity. In* ***b)*** *carbon atoms not involved in triple bonds are drawn as wire frame for clarity. Selected distances (Å) and angles (°) Mn1-C9 2.1266(15), Mn1-C17 2.1390(14), Mn1-C1 2.1485(15), Mn1-C25 2.1573(13), Mn2-C53 2.1011(13), Mn2-C45 2.1433(15), Mn2-C61 2.1441(14), Mn2-C37 2.1451(14),), Na-$C_{alkynyl}$ ranging from 1.432(2) to 3.5958(16), C9-Mn1-C1 102.07(5), C37-Mn2-C45 102.19(5), C25-Mn1-C17 102.27(5), C37-Mn2-C61 103.97(5), C25-Mn1-C1 105.65(5), C45-Mn2-C61 109.57(5), C53-Mn2-C45 111.44(5), C25-Mn1-C9 111.96(5), C53-Mn2-C61 112.66(5), C17-Mn1-C9 115.59(5), C53-Mn2-C37 116.25(5), C1-Mn1-C17 119.15(5).*

In contrast sodium atoms in **45** are coordinate to C≡C of acetylides via π-electrostatic interactions. Thus, Na1 and Na4 (**Figure 5. 15**) π-engages three acetylide units (Na···C

distances are ranging from 2.6369(14) to 3.5100(14) Å). and one molecule of THF, when Na2 interacts with 4 acetylides (with distances ranging from 2.5257(14) to 3.5240(15)Å) and finally Na3 satisfies its coordination sphere with two molecules of THF and π-engaging two acetylide units (Na···C distances are ranging from 2.6095(14) to 3.5958(16) Å). The π-electrostatic interactions of sodium atoms often involve C≡C of neighbouring acetylide units, giving the rise to the polymeric motif observed in the solid state (see **Figure 5. 15 b**).

A very similar structure could be found for the higher order sodium magnesiate phenylacetylide, published recently by our group.[77] In this structure the anions $\{Mg(C{\equiv}CPh)_4\}^{2-}$ are connected by sodium cations to form a Weiss motifs.[79] As in **45** the sodium atoms have slightly different coordination environments between each other. In fact they have η^2-π-coordination with the C≡C triple bonds of two or more acetylide units (up to four) and one or two molecules of THF to complete the coordination sphere.

Despite its poor solubility, we were also able to isolate and characterize, the potassium analogue of **45,** $[(THF)_6K_4Mn_2(C{\equiv}CPh)_8]$ (**46**). In contrast to **45**, **46** was obtained via salt metathesis using four equivalent of potassium phenylacetylide (prepared *in-situ* deprotonating phenylacetylene with KCH_2SiMe_3) and one equivalent of $MnCl_2$ in THF (**Scheme 5. 17**). The poor solubility led to a crystalline yield of only 5%. Interestingly exposing the same mixture of potassium phenylacetylide and $MnCl_2$ to oxygen, the 1,3 diyne **44a** was obtained in 80% yield.

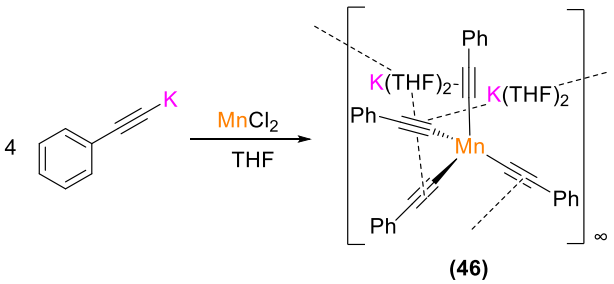

(46)

Scheme 5. 17 *Synthesis of **46** via salt metathesis of potassium phenylacetylide and $MnCl_2$, the isolated yield of **45**was 5%*

The crystal structure of **46** is very similar to **45**, in fact the structure of **46** is also a chain polymer made by the secondary interactions of potassium with π electrons (**Figure 5. 16**). Manganese is tetra-coordinated with a distorted tetrahedral geometry, the angles around Mn ranging between 102.54(8)° and 111.89(9)° with a mean value of 109.45° like in **45**. Every atom of manganese is coordinated by 4 phenylacetylide anions, the average Mn-C distance is 2.131 Å, very similar to the one observed for **45** (2.138 Å)**.**

Potassium, like sodium in **45,** is coordinated by THF molecules and triple bonds, but also from the π electrons of the phenyl. All the K atoms are coordinated by three triple bonds and two molecules of THF, except for K3 that instead fill its coordination sphere with the π electrons of the phenyl ring in a η^4 fashion. The interactions of potassium cations with the acetylene units, involving neighbouring C≡C triple bonds give rise to a polymeric 1D chain structure. In

accordance with the larger size of the cation, the K-C distances (average value 3.226 Å) are longer than the one observed for the Na-C in **45**.

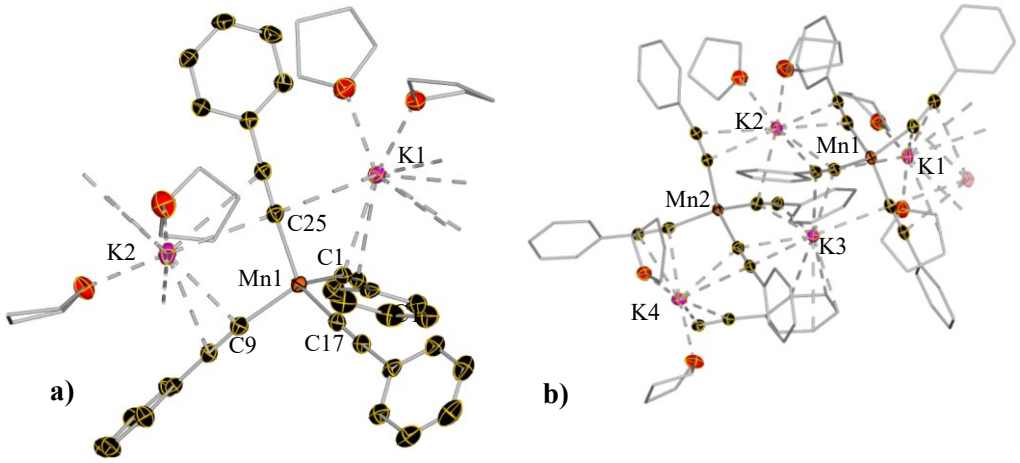

Figure 5. 16 ***a)*** *molecular fragment and* ***b)*** *polymeric structure of* ***46****, thermal ellipsoids are rendered at 50% probability. Hydrogen atoms and disorder elements in THF are omitted for clarity. In* ***b)*** *carbon atoms not involved in triple bonds are drawn as wire frame. Selected distances (Å) and angles (°) Mn1-C9 2.120(3), Mn1-C1 2.121(2), Mn1-C1 72.131(2), Mn1-C25 2.140(3), Mn2-C33 2.121(2), Mn2-C41 2.136(3), Mn2-C49 2.139(2), Mn2-C57 2.144(2), K-$C_{alkynyl}$ ranging from 2.7076(19) to 3.598(2), K-C_{aryl} from 3.182(2) to 3.543(3) ranging from C9-Mn1-C17 111.89(9), C9-Mn1-C1 102.54(8), C9-Mn1-C25 111.01(8), C1-Mn1-C25 108.64(8), C17-Mn1-C1 111.60(8), C17-Mn1-C25 110.85(8), C41-Mn2-C33 111.07(8), C41-Mn2-C49 109.89(8), C41-Mn2-C57 107.85(8), C33-Mn2-C49 107.22(8), C33-Mn2-C57 110.06(8), C49-Mn2-C57 110.78(8).*

Interestingly the polymeric structure found in **45** and **46** is not shared by the similar higher order lithium manganate $[(THF)_2Li_2Mn(2,6\text{-}(Me_3Si)_2PhC{\equiv}C)_4]$.[80] This compound, which was prepared via salt metathesis using four equivalent of $Li(2,6\text{-}(Me_3Si)_2PhC{\equiv}C)$ and $MnCl_2$, presents a monomeric structure. In fact, despite the lithium cations can π-engage 2 acetylene units each, they belong to the same monomer. Moreover, their coordination sphere is satisfied by a single THF molecule that prevents the coordination from neighbouring units.

5.5 Conclusion

To conclude, a new Mn-mediated protocol to access symmetrical bis(arenes) or 1,3 diyenes has been uncovered, which relies on the synergistic partnership between alkali metals and Mn(II). Higher order lithium manganate AM_2MnR_4 (AM= Li, Na, K) promotes direct Mn-I exchange reactions of aryliodides (AM= Li) or Mn-H exchange of terminal acetylene (AM=Na, K). These types of reactivity are typically considered as exclusive domain of polar RLi or RMgX reagents. Those exchanges occur with an excellent atom economy, forming the relevant AM_2MnAr_4 intermediates which in the presence of RI (concomitantly generated in the Mn-I exchange) or oxygen undergo oxidative homocoupling furnishing a range of symmetrical bis(aryl) and 1,3-diynes in excellent yields. Structural and magnetic insights on the constitution of the mixed Li/Mn organometallic intermediates involved in these reactions revealed that the formation of contacted ion pair alkali-metal manganates has a key role for the reactivity of the manganates. These studies also improve our understanding on how Mn(II)

aryl complexes promote homocoupling processes in the presence of atmospheric oxygen, a type of reactivity previously noted in the literature but for which the constitution of the organomanganese intermediates involved had hitherto proved elusive.

5.6 Experimental Section

Compound **37·2TMEDA**, **39** were prepared according the literature procedure.[50] The general procedure for the manganese-iodine exchange and the homocoupling of iodoarenes was previously reported together with the characterization of the organic products.[81]

General procedure for the metal/halogen exchange

An oven dried Schlenk tube was charged with the appropriate amount of $LiCH_2SiMe_3$ and $MnCl_2$, THF (5 mL) was added. The reaction was left stirring at ambient temperature (20 °C) for 15 minutes, the orange solution obtained was then cooled down to -78 °C (isopropanol/dry ice). A different oven dried Schlenk tube was charged with the selected amount of 4-iodoanisole and 16 mg of hexamethylbenzene, THF (3 mL) was added and the solution again cooled to -78 °C (isopropanol/dry ice). The two solutions were mixed via cannula and the mixture was stirred for 15 minutes at -78°C. The reaction was quenched with brine and extracted three times with 5mL of Et_2O. The combined organic layer was dried over magnesium sulphate and filtered. The sample for the GC injection was prepared using 0.5 mL of the solution of the crude product which was diluted with 4 mL of fresh Et_2O.

Synthesis of $[(Et_2O)Li_2Mn(C_6H_4\text{-}OMe)_4]$ (**40**)

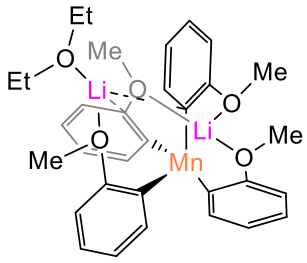

An oven-dried Schlenk tube was charged with 106 mg $MnCl_2$ (0.84mmol) and 384 mg 2-anisolyllithium (3.36 mmol) to which 15 mL of dry diethyl ether was added. The suspension was allowed to stir at room temperature overnight. LiCl was removed by filtration affording a clear solution. Solvent and all volatiles were removed under vacuum and the yellow residue was dissolved in 2 mL of hot toluene. Slow cooling of solution afforded orange, X-ray single quality crystals (80 mg, yield: 17%).

Elemental analysis: analytical calculated for $C_{32}H_{38}Li_2MnO_5$: C 67.26, H 6.70. Found: C 66.86, H 6.64.

Synthesis of [(THF)$Li_4Mn_2Ar_6(\mu_6\text{-}O)$] (**41**)

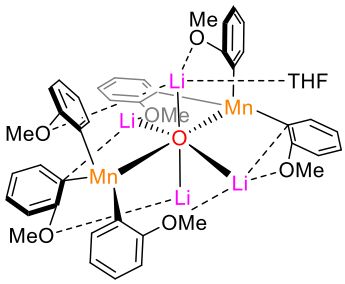

An oven-dried Schlenk was charged with 63 mg $MnCl_2$ (0.5 mmol) and 228 mg of 2-anisolyllithium (2 mmol) to which 10 mL of dried THF was added and the suspension stirred for 15 min. The yellow solution obtained was cooled on an ice bath to 0 °C and exposed to dry air (fitted with a drying tube containing oven-dried $CaCl_2$) for 15 min. The solution was then returned to inert atmosphere and stirred for another hour. The resulting orange solution was layered with hexane and placed at -33 °C for crystallization affording single crystals of **41** and **42**.

Synthesis of [$(THF)_4Li_4Mn_2Ar_4Cl_2(\mu_4\text{-}O)_2$] (**42**)

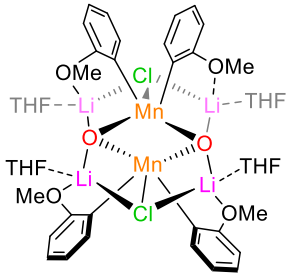

An oven-dried Schlenk was charged with 63 mg $MnCl_2$ (0.5 mmol) and 228 mg of 2-anisolyllithium (2 mmol) to which 10 mL of dried THF was added and the suspension stirred for 15 min. Obtained yellow solution was cooled on an ice bath to 0 °C and exposed to dry air (fitted with a drying tube containing oven-dried $CaCl_2$) for 15 min. The solution was then returned to inert atmosphere and stirred for another hour. Obtained orange solution was layered with hexane and placed at -33 °C for crystallization affording single crystals of **41** and **42**. A second crystallisation of filtrate afforded pure sample of **42** (97 mg, 35%) which was subjected to SQUID measurement and elemental analysis.

Elemental analysis: analytical calculated for $C_{48}H_{68}Cl_2Li_4Mn_2O_{11}$: C, 56.00; H, 6.66; found C 54.10; H, 5.37 corresponding to **42** losing two molecules of THF upon drying in vacuo (analytical calculated for $C_{40}H_{52}Cl_2Li_4Mn_2O_9$: C 54.26; H, 5.92).

Synthesis of [$(THF)_4MgCl_2MnPh_2$]

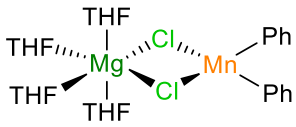

To a THF suspension of 126 mg of $MnCl_2$ (1 mmol in 10 mL THF), 2.67 mL of freshly prepared and titrated THF solution of PhMgCl (0.75 M, 2 mmol) was added dropwise. After stirring for 2 hours at room temperature, the orange solution was layered with hexane and placed at -33 °C to precipitate $MgCl_2$ which was removed by filtration. The filtrate was returned at -33 °C and after several days a crop of orange, X-ray quality crystals were isolated (300 mg, 51 %).

Elemental analysis: analytical calculated for $C_{28}H_{42}Cl_2MgMnO_4$: C, 56.73; H, 7.14; found C, 56.26; H, 7.13

General procedure for the metalation and coupling of alkynes (**44a-44h**)

An oven dried Schlenk tube was charged with 110 mg of $NaCH_2SiMe_3$ (1 mmol) and 115 mg of $Mn(CH_2SiMe_3)_2$, hexane (5 mL) was added and the suspension was allowed to stir for 30 minutes at room temperature. Volatiles were removed under vacuum, the white residue was solubilized in 5 mL of dried THF. The solution was cooled down to -78°C and 4 mmol of the selected alkynes was added dropwise. The solution was removed from the cold bath, and it was allowed to stir for 1 h at room temperature. The solution was exposed to dry air (fitted with a drying tube containing oven-dried $CaCl_2$) for 1 h, affording a black mixture. The reaction was quenched with brine and HCl (1M) and extracted with ethyl acetate three times. The combined organic layers were dried with magnesium sulphate and the volatiles were removed under reduced pressure. The yield of the product was calculated by ^{1}H-NMR against hexamethylbenzene as internal standard, based on the resonances reported in the literature for the products.[63,82–84]

Synthesis of $[(THF)_4Na_4Mn_2(C{\equiv}CPh)_8]$ (**45**)

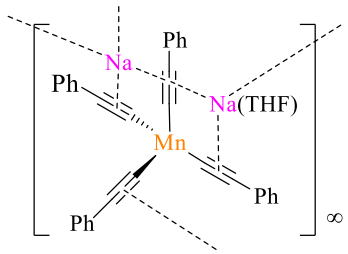

The higher order sodium manganate (**43**) was prepared in situ. 110 mg (1 mmol) of $NaCH_2SiMe_3$ and 115 mg (0.5 mmol) of $Mn(CH_2SiMe_3)_2$ were mixed together for 30 minutes in 5 mL of hexane affording a light grey suspension. The volatiles were removed under vacuum and the white solid left was then solubilized with 2 mL of THF affording an orange solution. The mixture was cooled down to -78°C and 0.22 mL (2 mmol) of phenylacetylene was added dropwise, affording a red solution. The mixture was removed from the cold bath and let stirring at room temperature for 1h. 3 mL of hexane were layered on the solution. Slow diffusion of the hexane in the solution of THF afforded single crystals of **45** (146 mg, yield: 44%).

Elemental analysis: analytical calculated $C_{52}H_{55}MnNa_2O_5$ C 72.55, H 6.44 Found: C 72.62, H 6.60.

Synthesis of $[(THF)_6K_4Mn_2(C{\equiv}CPh)_8]$ (**46**)

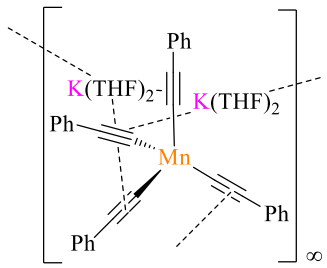

252 mg (2 mmol) of KCH_2SiMe_3 were suspended in 10 mL of Hexane, the mixture was cooled down to -78°C and 0.22 mL (2mmol) of phenylacetylene were added dropwise. The afforded suspension was removed from the cold bath and let to stir at room temperature for 30 minutes. All the volatiles were removed under vacuum and the residue was re-dissolved in 10 mL of diethyl ether. 63 mg (0.5 mmol) of $MnCl_2$ were added to the yellow solution and the mixture was let stir for 16h at room temperature, affording a light-yellow suspension. All the volatiles were removed, and the residue was suspended in 10 mL of THF affording a yellow suspension. The suspension was filtrated via canula and glass fibre filter. The mother liquor was concentrated under vacuum until almost 1 mL and 0.8 mL of

hexane were carefully added. The mixture was then stored in the freezer (-33°C) for 24 hours, furnishing a crop of orange single crystals of **46** (38 mg; yield: 5%)

5.7 References

[1] J. Hassan, M. Sévignon, C. Gozzi, E. Schulz, M. Lemaire, *Chem. Rev.* **2002**, *102*, 1359–1469.

[2] M. Kertesz, C. H. Choi, S. Yang, *Chem. Rev.* **2005**, *105*, 3448–3481.

[3] G. Bringmann, T. Gulder, T. A. M. Gulder, M. Breuning, *Chem. Rev.* **2011**, *111*, 563–639.

[4] J. Buter, D. Heijnen, C. Vila, V. Hornillos, E. Otten, M. Giannerini, A. J. Minnaard, B. L. Feringa, *Angew. Chem. Int. Ed.* **2016**, *55*, 3620–3624.

[5] D. Parmar, E. Sugiono, S. Raja, M. Rueping, *Chem. Rev.* **2014**, *114*, 9047–9153.

[6] M. B. Nielsen, F. Diederich, *Chem. Rev.* **2005**, *105*, 1837–1868.

[7] J. M. Tour, *Chem. Rev.* **1996**, *96*, 537–554.

[8] S. Mondal, *ChemTexts* **2016**, *2*, 1–11.

[9] C. Glaser, *Berichte der Dtsch. Chem. Gesellschaft* **1869**, *2*, 422–424.

[10] A. S. Hay, *J. Org. Chem.* **1962**, *27*, 3320–3321.

[11] F. Ullmann, J. Bielecki, *Berichte der Dtsch. Chem. Gesellschaft* **1901**, *34*, 2174–2185.

[12] J. H. Li, Y. Liang, X. D. Zhang, *Tetrahedron* **2005**, *61*, 1903–1907.

[13] J. H. Li, Y. Liang, Y. X. Xie, *J. Org. Chem.* **2005**, *70*, 4393–4396.

[14] A. Corma, A. Leyva-Pérez, A. Doménech-Carbò, *Nat. Commun.* **2015**, 6703–6711.

[15] D. A. Valyaev, G. Lavigne, N. Lugan, *Coord. Chem. Rev.* **2016**, *308*, 191–235.

[16] G. Cahiez, A. Moyeux, J. Buendia, C. Duplais, *J. Am. Chem. Soc.* **2007**, *129*, 13788–13789.

[17] A. Bottoni, G. Cahiez, M. Calvaresi, A. Moyeux, P. Giacinto, G. Pietro Miscione, *J. Organomet. Chem.* **2016**, *814*, 25–34.

[18] G. Cahiez, C. Duplais, J. Buendia, *Angew. Chem. Int. Ed.* **2009**, *48*, 6731–6734.

[19] Y. Liu, J. Bergès, Y. Zaid, F. O. Chahdi, A. Van Der Lee, D. Harakat, E. Clot, F. Jaroschik, M. Taillefer, *J. Org. Chem.* **2019**, *84*, 4413–4420.

[20] R. E. Mulvey, *Acc. Chem. Res.* **2009**, *42*, 743–755.

[21] S. D. Robertson, M. Uzelac, R. E. Mulvey, *Chem. Rev.* **2019**, *119*, 8332–8405.

[22] F. Mongin, A. Harrison-Marchand, *Chem. Rev.* **2013**, *113*, 7563–7727.

[23] R. A. Layfield, *Chem. Soc. Rev.* **2008**, *37*, 1098–1107.

[24] T. Greiser, J. Kopf, D. Thoennes, E. Weiss, *Chem. Ber.* **1981**, *114*, 209–213.

[25] R. J. Morris, G. S. Girolami, *J. Am. Chem. Soc.* **1988**, *110*, 6245–6246.

[26] R. E. Mulvey, F. Mongin, M. Uchiyama, Y. Kondo, *Angew. Chem. Int. Ed.* **2007**, *46*, 3802–3824.

[27] J. Garcia-Álvarez, A. R. Kennedy, J. Klett, R. E. Mulvey, *Angew. Chem. Int. Ed.* **2007**, *46*, 1105–1108.

[28] L. M. Carrella, W. Clegg, D. V. Graham, L. M. Hogg, A. R. Kennedy, J. Klett, R. E. Mulvey, E. Rentschler, L. Russo, *Angew. Chem. Int. Ed.* **2007**, *46*, 4662–4666.

[29] V. L. Blair, L. M. Carrella, W. Clegg, B. Conway, R. W. Harrington, L. M. Hogg, J. Klett, R. E. Mulvey, E. Rentschler, L. Russo, *Angew. Chem. Int. Ed.* **2008**, *47*, 6208–6211.

[30] V. L. Blair, W. Clegg, R. E. Mulvey, L. Russo, *Inorg. Chem.* **2009**, *48*, 8863–8870.

[31] V. L. Blair, W. Clegg, B. Conway, E. Hevia, A. Kennedy, J. Klett, R. E. Mulvey, L. Russo, *Chem. Eur. J.* **2008**, *14*, 65–72.

[32] D. R. Armstrong, A. R. Kennedy, R. E. Mulvey, R. B. Rowlings, *Angew. Chem. Int. Ed.* **1999**, *38*, 131–133.

[33] S. H. Wunderlich, M. Kienle, P. Knochel, *Angew. Chem. Int. Ed.* **2009**, *48*, 7256–7260.

[34] D. Haas, J. M. Hammann, A. Moyeux, G. Cahiez, P. Knochel, *Synlett* **2015**, *26*, 1515–1519.

[35] M. Hojo, H. Harada, H. Ito, A. Hosomi, *Chem. Commun.* **1997**, 2077–2078.

[36] R. Inoue, H. Shinokubo, K. Oshima, *Tetrahedron Lett.* **1996**, *37*, 5377–5380.

[37] K. Oshima, *J. Organomet. Chem.* **1999**, *575*, 1–20.

[38] J. Nakao, R. Inoue, H. Shinokubo, K. Oshima, *J. Org. Chem.* **1997**, *3263*, 1910–1911.

[39] A. Music, D. Didier, *Synlett* **2019**, *30*, 1843–1849.

[40] A. D. Benischke, L. Anthore-Dalion, G. Berionni, P. Knochel, *Angew. Chem. Int. Ed.* **2017**, *56*, 16390–16394.

[41] A. D. Benischke, L. Anthore-Dalion, F. Kohl, P. Knochel, *Chem. Eur. J.* **2018**, *24*, 11103–11109.

[42] L. Anthore-Dalion, A. D. Benischke, B. Wei, G. Berionni, P. Knochel, *Angew. Chem. Int. Ed.* **2019**, *58*, 4046–4050.

[43] A. Music, C. Hoarau, N. Hilgert, F. Zischka, D. Didier, *Angew. Chem. Int. Ed.* **2019**,

58, 1188–1192.

[44] G. Cahiez, C. Duplais, J. Buendia, *Chem. Rev.* **2009**, *109*, 1434–1476.

[45] M. Tamura, J. Kochi, *J. Organomet. Chem.* **1971**, *29*, 111–129.

[46] B. R. A. Andersen, E. Carmona-guzman, J. F. Gibson, G. Wilkinson, *J. Chem. Soc. Dalt. Trans.* **1976**, 2204–2211.

[47] A. Alberola, V. L. Blair, L. M. Carrella, W. Clegg, A. R. Kennedy, J. Klett, R. E. Mulvey, S. Newton, E. Rentschler, L. Russo, *Organometallics* **2009**, *28*, 2112–2118.

[48] M. Uzelac, I. Borilovic, M. Amores, T. Cadenbach, A. R. Kennedy, G. Aromí, E. Hevia, *Chem. Eur. J.* **2016**, *22*, 4843–4854.

[49] D. Tilly, F. Chevallier, F. Mongin, P. C. Gros, *Chem. Rev.* **2014**, *114*, 1207–1257.

[50] M. Uzelac, *New Frontiers on Cooperative Chemistry of Rarely Employed Metals*, University Of Strathclyde, PhD Thesis, Glasgow, **2016**.

[51] S. E. Baillie, W. Clegg, P. García-Álvarez, E. Hevia, A. R. Kennedy, J. Klett, L. Russo, *Organometallics* **2012**, *31*, 5131–5142.

[52] R. J. Morris, G. S. Girolami, *Organometallics* **1989**, *8*, 1478–1485.

[53] R. Fischer, H. Görls, M. Friedrich, M. Westerhausen, *J. Organomet. Chem.* **2009**, *694*, 1107–1111.

[54] A. D. Sutton, T. Ngyuen, J. C. Fettinger, M. M. Olmstead, G. J. Long, P. P. Power, *Inorg. Chem.* **2007**, *46*, 4809–4814.

[55] Z. Zhou, W. Xue, *J. Organomet. Chem.* **2009**, *694*, 599–603.

[56] G. Cahiez, D. Bernard, J. F. Normant, *J. Organomet. Chem.* **1976**, *113*, 99–106.

[57] P. Crewdson, S. Gambarotta, G. P. A. Yap, L. K. Thompson, *Inorg. Chem.* **2003**, *42*, 8579–8584.

[58] E. Solari, F. Musso, E. Gallo, C. Floriani, N. Re, A. Chiesi-Villa, C. Rizzoli, *Organometallics* **1995**, *14*, 2265–2276.

[59] H. P. Lane, S. M. Godfrey, R. G. Pritchard, C. A. McAuliffe, *J. Chem. Soc., Dalt. Trans.* **1995**, 701–706.

[60] K. S. Sindhu, G. Anilkumar, *RSC Adv.* **2014**, *4*, 27867–27887.

[61] R. Eglinton, G; Galbraith, A, *J. Chem. Soc.* **1959**, 889–890.

[62] D. Li, K. Yin, J. Li, X. Jia, *Tetrahedron Lett.* **2008**, *49*, 5918–5919.

[63] K. Yin, C.-J. Li, J. Li, X.-S. Jia, *Appl. Organomet. Chem.* **2011**, *25*, 16–20.

[64] L. Li, J. Wang, G. Zhang, Q. Liu, *Tetrahedron Lett.* **2009**, *50*, 4033–4036.

[65] Q. Zheng, R. Hua, Y. Wan, *Appl. Organomet. Chem.* **2010**, *24*, 314–316.

[66] H. A. Stefani, A. S. Guarezemini, R. Cella, *Tetrahedron* **2010**, *66*, 7871–7918.

[67] P. Siemsen, R. C. Livingston, F. Diederich, *Angew. Chem. Int. Ed.* **2000**, *39*, 2632–2657.

[68] J. Jover, P. Spuhler, L. Zhao, C. McArdle, F. Maseras, *Catal. Sci. Technol.* **2014**, *4*, 4200–4209.

[69] F. Bohlmann, H. Schönowsky, E. Inhoffen, G. Grau, *Chem. Ber.* **1964**, *97*, 794–800.

[70] L. Fomina, B. Vazquez, E. Tkatchouk, S. Fomine, *Tetrahedron* **2002**, *58*, 6741–6747.

[71] H. Do, O. Daugulis, *Journal of the American Chemical Society* **2009**, 17052–17053.

[72] T. Truong, J. Alvarado, L. D. Tran, O. Daugulis, *Org. Lett.* **2010**, *12*, 1200–1203.

[73] M. Uzelac, P. Mastropierro, M. de Tullio, I. Borilovic, M. Tarres, A. Kennedy, G. Aromì, E. Hevia, *Angew. Chem. Int. Ed.* **2021**, *60*, 3247–3253.

[74] T. X. Gentner, R. E. Mulvey, *Angew. Chem. Int. Ed.* **2020**, *60*, 9247–9262.

[75] A. Harrison-Marchand, F. Mongin, *Chem. Rev.* **2013**, *113*, 7470–7562.

[76] S. E. Baillie, T. D. Bluemke, W. Clegg, A. R. Kennedy, J. Klett, L. Russo, M. de Tullio, E. Hevia, *Chem. Commun.* **2014**, *50*, 12859–12862.

[77] M. De Tullio, A. M. Borys, A. Hernán-Gómez, A. R. Kennedy, E. Hevia, *Chem Catal.* **2021**, 1–14.

[78] V. V Krivykh, I. L. Eremenko, D. Veghini, I. A. Petrunenko, D. L. Pountney, D. Unseld, H. Berke, *J. Organomet. Chem.* **1996**, *511*, 111–114.

[79] E. Weiss, *Angew. Chem., Int. Ed. Engl.* **1993**, *32*, 1501–1523.

[80] G. M. Yee, K. Kowolik, S. Manabe, J. C. Fettinger, L. A. Berben, *Chem. Commun.* **2011**, *47*, 11680–11682.

[81] M. de Tullio, *Advancing Stoichiometric and Catalytic Applications of Cooperative Bimetallics in Organic Synthesis*, University Of Strathclyde, PhD Thesis, Glasgow, **2017**.

[82] V. Kumar, A. Chipeleme, K. Chibale, *European J. Org. Chem.* **2008**, *2008*, 43–46.

[83] S. Adimurthy, C. C. Malakar, U. Beifuss, *J. Org. Chem.* **2009**, *74*, 5648–5651.

[84] F. Yang, X. Cui, Y. nan Li, J. Zhang, G. Ren, Y. Wu, *Tetrahedron* **2007**, *63*, 1963–1969.

Chapter 6: Conclusions and Outlook

Exploiting chemical cooperativity between two different metals and also between distinct types of ligand sets, the work presented in this thesis advances the development of new protocols for arene functionalization (via deprotonative metalation or metal-halogen exchange) and C-C bond forming protocols. A connecting thread between the different chapters is the use of heterobimetallic reagents which combine an alkali-metal with an earth abundant divalent metal, namely, Zn, Mg and Mn. Adopting a metal-focused perspective, with special emphasis in the isolation and characterization of the organometallic species involved in these transformations, these findings provide new mechanistic insights into how these alkali-metal ate complexes operate and shed some light into their unique reactivity.

Chapters 2, **3**, and **4** provide new applications for sily(bis)amine $Ph_2Si(NHAr^*)_2$ as a precursor for the synthesis of heterobimetallic compounds containing a chelating silyl(bis)amide ligand. Using a stepwise deprotonative co-complexation approach a family new alkali-metal magnesiate, zincate and manganate compounds has been prepared and structurally characterized. Reactivity studies towards a selection of substrates including ketones, amines and acetylenes have revealed that depending on the nature of the divalent metal the silyl(bis)amide group can act as a steric stabilizer or alternative become involved in the metallation reaction acting as base.

The combination of this bulky silyl(bis)amide ligand and a kinetically activated TMP group within the framework of a potassium zincate has uncovered a new type of heterobimetallic base which can regioselectivly promote direct Zn-H exchange of a wide range of fluoroarenes including hypersensitive fluoro substituted nitrobenzenes. Demonstrating the metalating power of this bimetallic approach selective 3,6-dizincation of 1,2,4,5-tetrafluorobenzene can be accomplished. 1H NMR reaction monitoring studies combined with structural studies have shown the instrumental role of the bulky silyl(bis)amide ligand which coordinates to zinc in a chelating fashion providing a protective steric shelter for the sensitive fluoroaryl fragment. Key for the success of this approach is the special Zn/ligand cooperativity in these complexes whereas the alkali-metal seems to take have a secondary role.

Chapter 5 explores the reactivity of tetra(alkyl) manganates, uncovering a unique Li/Mn(II) bimetallic partnership for the synthesis of symmetric bis(aryl) via tandem Mn-I/oxidative homocoupling reactions of iodoarenes. Isolation of key reaction intermediates combined with EPR monitoring studies have revealed that initially Mn-I exchange occurs, with the lithium manganate mirroring the reactivity previously reported to lithium magnesiates. However the redox flexibility of this earth abundant transition metal enables the C-C bond forming process by reacting with the concomitant alkyliodide formed during the exchange processes which acts as an internal oxidant. Interestingly these reactions take place via the formation of contacted ion pair species which maximizes bimetallic communication between the Li and Mn centers. This seems to be a crucial aspect for the success of this tandem process since on the addition of a macrocyclic Lewis donor completely suppresses the exchange reaction. This work can

also be extended to alkynes to access 1,3-enynes via initial deprotonation of the terminal alkynes and aerobic oxidation. For this type of tandem process the influence of the alkali-metal has been investigated, showing that the Na/Mn pairing appears to be the most effective.

Building on the knowledge accrued from these thesis and the current research lines in our research group several new future directions for this work can be envisaged. This includes upgrading some of the stoichiometric successes into catalytic regimes. Alkali-metal magnesiates have shown promise as catalysts hydroelementation reactions whereas potassium zincates can catalyse benzylation of styrenes. The presence of the bulky silyl(bis)amide ligand in the new ates included in this thesis can allow for the fine tuning of the catalytic ability of these heterobimetallic systems. The steric bulk of the $\{Ph_2Si(NAr^*)_2\}^{2-}$ can be modulated by changing the Ar* substituents. These systems can be particularly interesting for hydroboration or hydrosilylation reactions favouring the formation of monomeric highly nucleophilic intermediates. Extension to catalytic hydrophosphination and hydrophosphinylation of styrenes and alkynes will lead to the development of new methods to access valuable organophosphorus compounds in a atom economical way, minimizing waste and avoiding the use of toxic PCl_3.

The full potential of potassium zincate $[\{Ph_2Si(NAr^*)_2Zn(TMP)\}^-\{K(THF)_6\}^+]$ (**19**) as a regioselective base for the zincation of other organic substrates different to fluoroarenes remains untapped. Initial studies could focus on the use of this TMP-activated base for the metallation of diazines such as pyrimidine which are well known for their fragility and poor control of the regioselectivity when metallation is attempted with traditional organolithium or lithium amide reagents. Mechanistic studies with the aid of DFT calculations may also contribute towards understanding how this base operates and which is the specific role (if any) of the alkali-metal. Further work in this field should also include extending the studies on the onward reactivity of the relevant potassium zincate products containing the metalated fluoroarenes.

The work on alkali-metal tetra(alkyl) manganates opens a new line of research in terms of promoting direct manganese-halogen exchange processes and their subsequent involvement in C-C bond forming reactions. Further work in this area can be envisaged on the development of a protocol that can enable cross-coupling reactions to access non-symmetric bis(aryls). Similarly, by changing the ligands on Mn, the basic capabilities of these bimetallic systems towards deprotonative metallation can be optimized. Last but not least, further work should assess if these type of processes are exclusive to manganates or if other divalent transition metals such as Fe, Co or Ni can also promote similar transformations. Advances in this area will involve the isolation and characterization of key reaction intermediates which can provide valuable insights into the stability and coordination preferences of these heterobimetallic systems.

Chapter 7: General Experimental Techniques and Procedures

7.1 Schlenk Techniques

The polar organometallics compounds are notoriously sensitive towards the air and the moisture, moreover some of those substances they can be even pyrophoric. Therefore, all the experimental work described in this thesis was performed in argon atmosphere to reduce to minimum the amount of moisture and oxygen. All the manipulation were doing using a Schlenk line (**Figure 7. 1**), [1] a well-known piece of glassware firstly developed by Schlenk.[2]

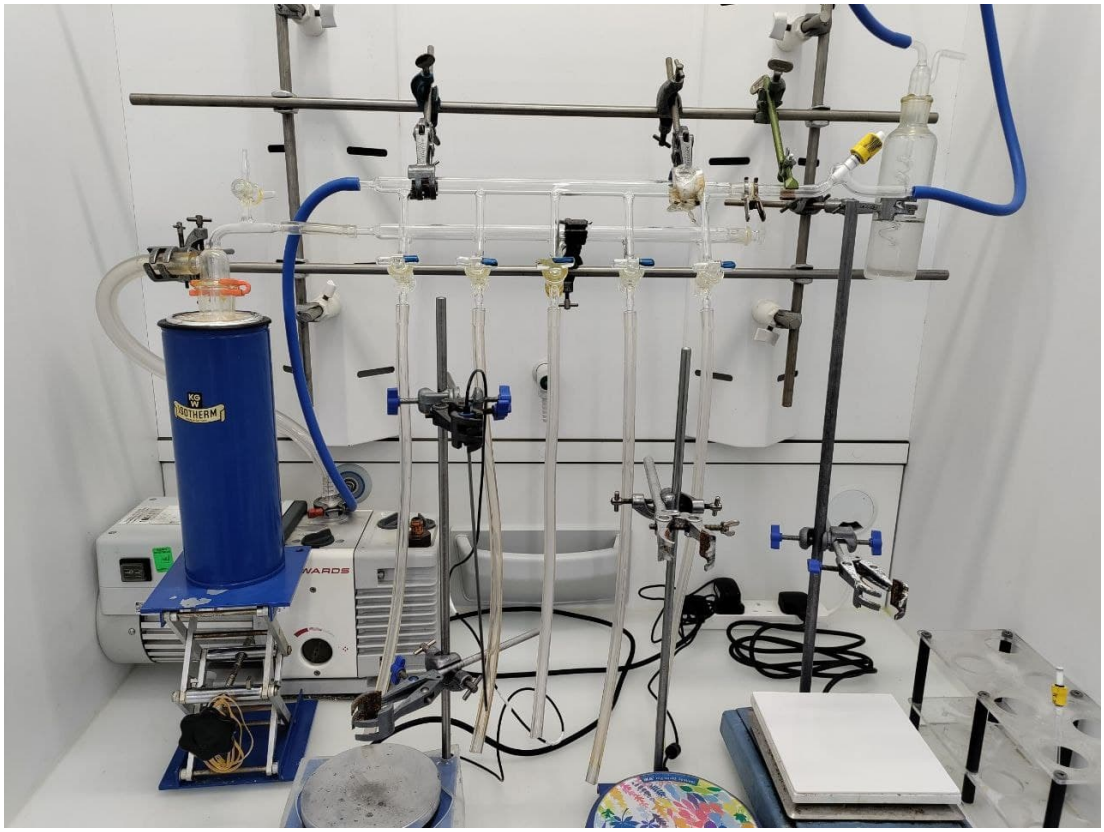

Figure 7. 1 *Typical Schlenck line set-up*

The Schlenk line used is made by two compartments, one for the vacuum and one to provide argon. The section reserved to argon is connected to an argon cylinder by an inlet and with an outlet with an oil bubbler. The vacuum manifold is connected to a vacuum pump. Before the pump is placed a trap cooled down with liquid nitrogen to stop any volatilise. The Schlenk line is equipped with 5 two-ways tap to apply alternatively vacuum or argon gas to the attached glassware.

Before the use all the glassware were cleaned dried in oven at 175°C. On all the ground-glass jointure were applied a thin layer of vacuum grease (Dow-Corning or similar) to maintain the seal. Glassware equipped with j-Young's tap can be used to avoid the use of grease. The air inside the glassware were removed under vacuum for 15 minutes, after which the glassware is

refilled by argon. This procedure was repeated at least 3 times to ensure the presence of inert atmosphere.

A positive flow of argon is always maintained to prevent air in entering in the system. the liquid or the solvent are transferred using needles or cannulae that are flushed with argon before the use.

7.2 Glovebox

A glovebox is routinely used to store reagents and products which are sensitive to air and moisture and for handling solid chemicals under argon atmosphere. The glovebox is composed a large chamber filled with argon and equipped by a gas recirculation and purification system to ensure the minimal level of oxygen and moisture. The manipulations were made using two gloves of semi-impermeable materials. The glovebox is equipped with 2 antechambers (or "port"), which allow the transfer of chemicals and glassware inside and outside the glovebox without a direct connection with the external atmosphere. After the glassware or the chemicals are loaded in the antechamber vacuum is applied for 5 minutes (15 minutes if the large port is used) than the antechamber is filled with argon and the process is repeated for other two times before opening the antechamber to the main body of the glovebox.

Figure 7. 2 *MBraun UNIlab pro glovebox*

7.3 Solvent Purification

Hexane, diethyl ether, toluene and benzene were dried over alumina column of Solvent Purification System (a MBraun MBSPS 5). The system is equipped with a pump and a nitrogen gas line to dispense solvent under nitrogen and in negative pressure. After the collection it was stored over activated 4 Å molecular sieves and argon atmosphere.

Tetrahydrofuran was dried over sodium and benzophenone ketyl and purified by distillation under argon atmosphere, metallic sodium reacts with the trace of water forming sodium hydroxide and hydrogen gas. The presence of benzophenone ketyl (generated by mono-electron reduction with sodium) give to the mixture a blue colour, which indicate the minimum level of water in the solvent. After the collection it was stored over activated 4 Å molecular sieves and argon atmosphere.

All the deuterated solvents for NMR (with exception of $CDCl_3$) were dried over $NaK_{2.8}$ for a night, degassed with the *freeze-pump-thaw* technique, consisting in removing all the volatilise under vacuum while the solvent was frozen. The solvents were distilled over static vacuum and stored over activated 4 Å molecular sieves and argon atmosphere.

7.4 Commercial Reagents

The commercially available reagents were purchased from Sigma-Aldrich, Fluorochem or Agros Chem.

When appropriate the liquid reagent were dried with CaH_2 and distilled under argon atmosphere, before being stored over activated 4 Å molecular sieves and argon atmosphere.

The metal halides salts were dried for 3 days under vacuum at 180°C and stored in the glovebox.

7.5 Standardization of the organometallic solutions

Grignard reagents were used in form of THF or Et_2O solutions and their exact concentration were determined by iodometric titration.[3] The solution of Grignard was added dropwise to a solution of iodine (exactly weighted) in THF saturated with LiCl until the solution became colourless. From the volume of Grignard reagents used it is possible to calculate the concentration.

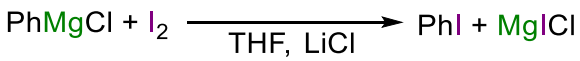

Scheme 7. 1 *Example of iodometric titration of Phenilmagnesium chloride*

The concentration of organolithium solutions were determined by titration against L-menthol with 2,2'-bipyridine as indicator. An exact amount of L-menthol was dissolved in THF

together with 5 mg of 2,2'-bipyridine. The organolithium solution were added dropwise until a deep red colour is persistent. The colour is due to the product of alkylation of the 2,2'-bipyridine by the excess of organolithium.[4]

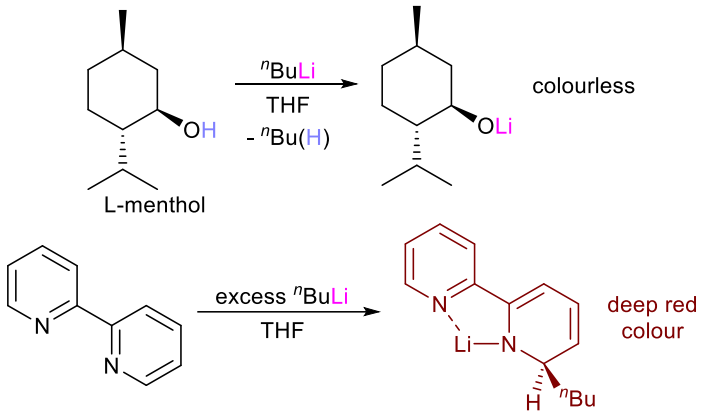

Scheme 7. 2 *Titration of ^{n}BuLi using L-Menthol and 2,2'-bipyridine as indicator*

7.6 Analytical procedures

NMR spectra were performed in J. Young's NMR tube, prior oven dried and flushed with argon. NMR spectra were recorded using a Bruker AV 400 spectrometer operating at 400.13 MHz for ^{1}H and ^{19}F, 100.62 MHz for ^{13}C{^{1}H} or a Bruker AV 400 spectrometer operating at 300 MHz for ^{1}H and ^{19}F, 75 MHz for ^{13}C{^{1}H} .^{1}H and ^{13}C{^{1}H} NMR spectra were calibrated against the appropriate solvent signal. All the 1D and 2D spectra were analysed with the software Topsin. The multiplicity of the signals was indicated with the following abbreviation: singlet (s), doublet (d), triplet (t), septet (sept.), multiplet (m).

Elemental analyses (C, H and N) were conducted with a Perkin Elmer 2400 Analyser or a Flash 2000 Organic Elemental Analyser (Thermo Scientific). Samples were prepared in the glovebox under argon atmosphere and sealed in an air-tight container prior to analyses. All results were obtained in triplicate to ensure consistency.

GC spectra were obtained using Agilent Technologies 8860 GC System [Agilent NX 8860 FID w/EPE detector], Agilent Technologies7693A Autosampler and Agilent J&W GC Column (30 m, 0.32 mm i.d., 0.25 µ).

Continuous-wave X-Band (9.42 GHz) EPR spectra of powdered samples and frozen solutions were collected in the temperature range 5-195 K on Bruker ESP300E spectrometer equipped with liquid helium cryostat. Samples were prepared in the glovebox and immediately transferred to Wilmad quartz EPR sample tube (4 mm thin wall, 25 cm long tube) which was closed under inert N2 atmosphere with a tip-off manifold (4 mm). Obtained spectra were processed with WINEPR Bruker software (version 2.11.0.0). Simulations of the spectra were preformed using the EasySpin software (version 5.2.28) and functions 'pepper' and esfit.[5]

All measurements were made on a RIGAKU Synergy S area-detector diffractometer or Oxford Diffraction Xcalibur E [6] using mirror optics monochromated Cu Kα radiation (λ = 1.54184 Å) or Mo Kα (λ = 0.71073 Å).

Data reduction was performed using the *CrysAlisPro* program[6]. The intensities were corrected for Lorentz and polarization effects, and an absorption correction based on the multi-scan method using SCALE3 ABSPACK in *CrysAlisPro*[6] was applied.

The structures were solved by direct methods using *SHELXT*[7], which revealed the positions of all non-hydrogen atoms of the title compound. All non-hydrogen atoms were refined anisotropically. H-atoms were assigned in geometrically calculated positions and refined using a riding model where each H-atom was assigned a fixed isotropic displacement parameter with a value equal to 1.2Ueq of its parent atom (1.5Ueq for methyl groups).

refinement of the structures was carried out on F^2 using full-matrix least-squares procedures, which minimized the function $\Sigma w(F_o^2 - F_c^2)^2$. The weighting scheme was based on counting statistics and included a factor to downweight the intense reflections. All calculations were performed using the *SHELXL-2014/7*[8] program in OLEX2.4[9]

7.4 Synthesis of Common Starting Materials

Synthesis of $Zn(HMDS)_2$

$Zn(HMDS)_2$ was prepared modifying the procedure reported by Hartwig *et al.*[10] 3.41 g of $ZnCl_2$ (25 mmol) and 8.36 g of Li(HMDS) (50 mmol) were placed in an Ar flushed and flame dried Schlenk tube. 50 mL of Et_2O was added affording a cloudy white suspension. The suspension was allowed to stir for 5h at 50°C. After, the suspension was cooled down to room temperature and then the solid was removed by filtration through celite. The light orange solution obtained was concentrated under vacuum affording a light orange suspension. 50 mL of hexane was then added and the solid was removed by cannula filtration. The resulting colorless solution was concentrated under vacuum affording $ZnHMDS_2$ as colorless oil (8.3 g; 86%). The spectra are consistence with the reported literature.[10]

^{1}H-NMR (300.1 MHz, C_6D_6, 298 K) δ(ppm):0.20 (s, 36H, CH_3)

Synthesis of $Zn(TMP)_2$

2.72 mL of 2,2,6,6-tetramethylpiperidine (16 mmol) were solubilized in 10 mL of THF and then 10 mL of ^{n}BuLi solution (1.6 M in hexane) were added drop by drop affording a yellow solution. 1.09 g of $ZnCl_2$ (8 mmol) were added, instantaneously a white precipitate was formed. The mixture was allowed to stir at room temperature for 1h. All the volatiles were removed under reduced pressure affording a yellow waxy solid. 30 mL of Hexane were added affording a white suspension. The suspension was filtered through celite and the mother liquor

was evaporated furnishing $Zn(TMP)_2$ as white solid (2.7 g 98%). The solid can be further purified via sublimation as reported in the literature.[11]

^{1}H-NMR (300.1 MHz, D_8-THF, 298 K) δ(ppm):1.68 (m, 4H, γ-C*H*$_2$), 1.32 (m, 8H, β-C*H*$_2$), 1.22 (s, 24H, α-C*H*$_3$)

Synthesis of $[Ph_2Si(NHAr^*)_2]$ (**1**)[12]

5.8 mL of 2,6-diisopropylanyline (NH_2Ar^*) (30 mmol) and 40 mL of diethylether (Et_2O) were added to an oven dried Schlenk. The solution was cooled to –78°C, using an isopropanol and liquid Nitrogen bath, and 18.75 mL of ^{n}BuLi was then slowly added (1.6 M solution in hexane, 30 mmol). The reaction mixture was allowed to reach room temperature then re-cooled to -78°C and 3.15 mL of dichlorodiphenylsilane (Ph_2SiCl_2) were introduced (15 mmol). A white suspension formed that was allowed to stir over-night. The resulting LiCl was filtered through a celite filled filter stick. The filtrate was removed by vacuum until a solid began to precipitate. The suspension was then gently heated until a clear solution was obtained which was then placed in the freezer. A large crop of colourless crystals was obtained, and isolated by filtration and stored in the glove box (typical yield 7.5 g, 94%). **^{1}H-NMR** (300.1 MHz, D_8-THF, 298 K) δ(ppm):7.59 (d, 4H, Ph), 7.30 (m, 2H, Ph), 7.22 (m, 4H, Ar*), 6.93 (m, 6H, Ph and Ar*), 3.72 (s, 2H, NH), 3.28 (sept., 4H, CH, ^{i}Pr, Ar*), 0.88 (d, 24H, CH_3, ^{i}Pr, Ar*)

Synthesis of $Mg(CH_2SiMe_3)_2$ (**MgR_2**)[13]

4 g of Mg (167 mmol) turnings were added to a round bottom flask, equipped with a water condenser, along with 100 ml of Et_2O. A solution of 19 mL of Me_3SiCH_2Cl (150 mmol) in 50 mL of Et_2O was then added dropwise to the Mg turnings. The solution was stirred for 2 hour. A solution of 10 mL of dioxane in 80 mL of Et_2O was then added dropwise to the Grignard solution to give a viscous grey suspension. The suspension was stirred for 16 hours at ambient temperature. The suspension was then filtered through Celite and glasswool and washed with 20 mL of Et_2O. The solvent was removed in vacuo and the resulting solid was purified by sublimation under reduced pressure at 165 °C to give the final product as a white microcrystaline powder (typical yield 9g, 60%)

Synthesis of $Mn(CH_2SiMe_3)_2$ (**MnR_2**)[14]

3 g of $Mg(CH_2SiMe_3)_2$ (15 mmol) and 1.91 g of $MnCl_2$ (15 mmol) were suspended in 60 mL of Et_2O.The suspension was allowed to stir at room temperature for 4 days. All the volatiles were removed under vacuum to give a dull orange solid. Subsequently, 160 mL of dried toluene was introduced, and with vigorous heating to boiling an orange solution with a white precipitate ($MgCl_2$) was observed. The suspension was filtered hot and the bright orange filtrate allowed to cool to room temperature. Part of the solvent were removed under reduced pressure. The mixture were stored in the freezer (-27 °C) where crystallization occurred. Thin

orange needle crystals were observed, the solvent was removed via cannula, and the resultant orange crystals were dried under vacuum for 2 h (2g, 60%)

Synthesis of $NaCH_2SiMe_3$ (**NaR**)[15]

1.92 g of NaO^tBu (20 mmol) was suspended in 40 mL of dry hexane to which 20 mL of $LiCH_2SiMe_3$ (1 M in pentane, 20 mmol) was added dropwise at 0°C. The resulting suspension was stirred overnight at room temperature, and then filtered and washed with 20 mL hexane twice. The resulting white solid was dried *in vacuo* and isolated (typical yield 1.8 g, 82 %).

Synthesis of KCH_2SiMe_3 (**KR**)[16]

2.24 g of KO^tBu (20 mmol) was suspended in 40 mL of dry hexane to which 20 mL of $LiCH_2SiMe_3$ (1 M in pentane, 20 mmol) was added dropwise at 0°C. The resulting suspension was stirred overnight at room temperature, and then filtered and washed with 20 mL hexane twice. The resulting white solid was dried *in vacuo* and isolated (typical yield 2.2 g, 87 %).

7.5 References

[1] D. F. Shriver, M. A. Drezdon, *The Maniplulation of Air-Sensitive Compounds*, Wiley & Sons Ltd, **1986**.

[2] T. T. Tidwell, *Angew. Chem. Int. Ed.* **2001**, *40*, 331–337.

[3] A. Krasovskiy, P. Knochel, *Synthesis* **2006**, *2006*, 890–891.

[4] S. C. Watson, J. F. Eastham, *J. Organomet. Chem.* **1967**, *9*, 165–168.

[5] S. Stoll, A. Schweiger, *J. Magn. Reson.* **2006**, *178*, 42–55.

[6] Oxford-Diffraction, *CrysAlisPro (Version 1.171.40.37a).*, Oxford Diffraction Ltd., Yarnton, Oxfordshire, UK, **2018**.

[7] G. M. Sheldrick, *Acta Crystallogr. Sect. A Found. Crystallogr.* **2015**, *71*, 3–8.

[8] G. M. Sheldrick, *Acta Crystallogr. Sect. C Struct. Chem.* **2015**, *71*, 3–8.

[9] O. V Dolomanov, L. J. Bourhis, R. J. Gildea, J. A. K. Howard, H. Puschmann, *J. Appl. Crystallogr.* **2009**, *42*, 339–341.

[10] D. Y. Lee, J. F. Hartwig, *Org. Lett.* **2005**, *7*, 1169–1172.

[11] W. S. Rees, O. Just, H. Schumann, R. Weimann, *Polyhedron* **1998**, *17*, 1001–1004.

[12] V. L. Blair, W. Clegg, A. R. Kennedy, Z. Livingstone, L. Russo, E. Hevia, *Angew. Chemie* **2011**, *123*, 10031–10034.

[13] C. Yeardley, A. R. Kennedy, P. C. Gros, S. Touchet, M. Fairley, R. McLellan, A. J. Martínez-Martínez, C. T. O'Hara, *Dalton Trans.* **2020**, *49*, 5257–5263.

[14] A. Alberola, V. L. Blair, L. M. Carrella, W. Clegg, A. R. Kennedy, J. Klett, R. E. Mulvey, S. Newton, E. Rentschler, L. Russo, *Organometallics* **2009**, *28*, 2112–2118.

[15] A. J. Hart, D. H. O'brien, C. R. Russell, *J. Organomet. Chem.* **1974**, *72*, C19–C22.

[16] B. Conway, D. V. Graham, E. Hevia, A. R. Kennedy, J. Klett, R. E. Mulvey, *Chem. Commun.* **2008**, 2638–2640.